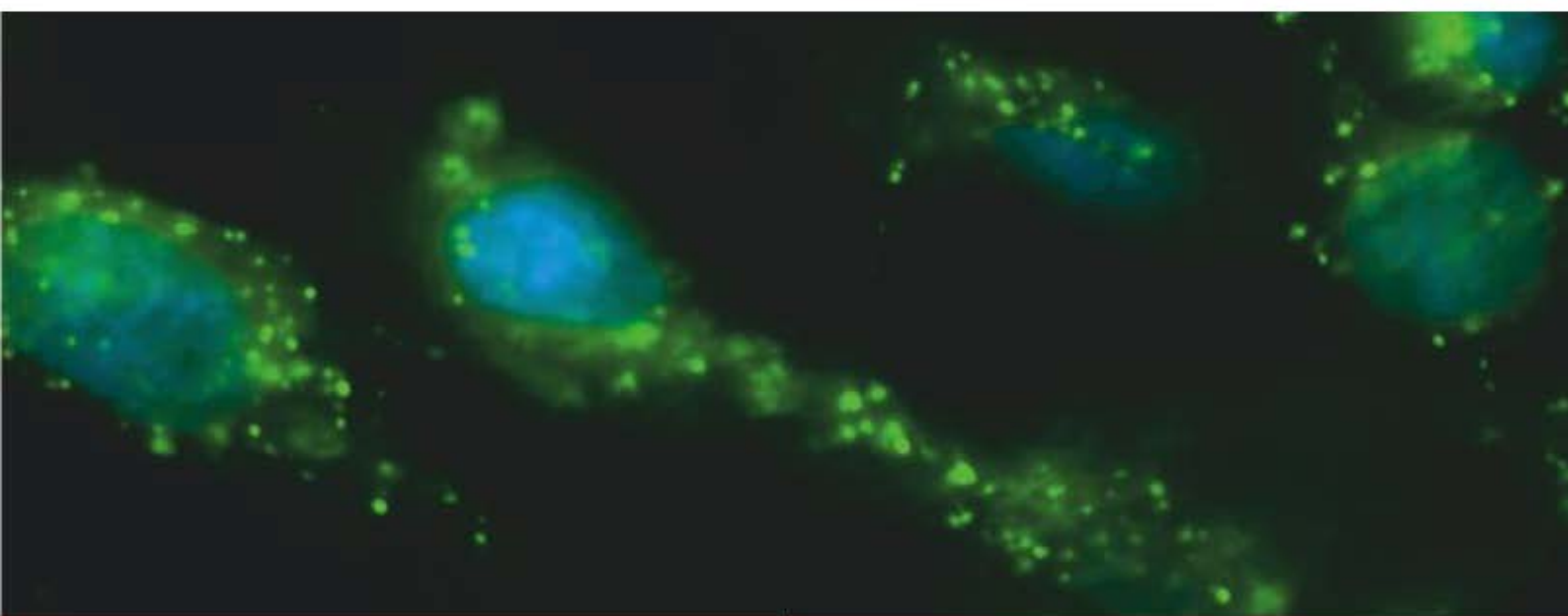# Universität Bremen

Cerium oxide nanoparticles: antioxidative potential and effects on the metabolism of glial cells

Carmen Osorio Navarro

Cerium oxide nanoparticles: antioxidative potential and effects on the metabolism of glial cells

Dissertation

zur Erlangung des akademischen Grades *Doctor rerum naturalium* (Dr. rer. nat.) des Fachbereichs 2 (Biologie/Chemie) an der Universität Bremen

María del Carmen Osorio Navarro

Verteidigungsdatum: 22.03.2024

Erster Gutachter: Professor Dr Michael Koch
Universität Bremen (Germany)

Zweite Gutachterin: Dr Ana Teresa Lemos Reis
National Institute of Health Doutor Ricardo Jorge, Porto (Portugal)

Versicherung an Eides Statt

Ich, María del Carmen Osorio Navarro versichere an Eides Statt durch meine Unterschrift, dass ich die vorstehende Arbeit selbständig und ohne fremde Hilfe angefertigt und alle Stellen, die ich wörtlich dem Sinne nach aus Veröffentlichungen entnommen habe, als solche kenntlich gemacht habe, mich auch keiner anderen als der angegebenen Literatur oder sonstiger Hilfsmittel bedient habe. Ich versichere an Eides Statt, dass ich die vorgenannten Angaben nach bestem Wissen und Gewissen gemacht habe und dass die Angaben der Wahrheit entsprechen und ich nichts verschwiegen habe. Die Strafbarkeit einer falschen eidesstattlichen Versicherung ist mir bekannt, namentlich die Strafandrohung gemäß § 156 StGB bis zu drei Jahren Freiheitsstrafe oder Geldstrafe bei vorsätzlicher Begehung der Tat bzw. gemäß § 161 Abs. 1 StGB bis zu einem Jahr Freiheitsstrafe oder Geldstrafe bei fahrlässiger Begehung.

_____   _____
Ort, Datum   Unterschrift

Table of contents

I. Acknowledgements

I would like to express my sincere gratitude to Prof. Dr Ralf Dringen for providing me with the opportunity to pursue my doctorate under his supervision. I greatly appreciate your encouragement, scientific insights and constructive feedback thorough my thesis. During my time in your group, I have been able to learn from your strong work ethic, consistent reliability and excellent organisational skills. I am deeply grateful for your commitment to adapt the lab during my first pregnancy and during the pandemic, allowing me to complete this thesis. I also treasure the relaxed treatment and the lively discussions in the seminar room.

I would also like to extend my gratitude to Prof. Dr Michael Koch and Dr Ana Teresa Lemos Reis for reviewing my thesis. I deeply appreciate your dedication, time and expertise.

In addition, I would like to thank the *Hans-Böckler-Stiftung* for the financial support of my PhD fellowship, granted through the graduate school NanoCompetence. Additionally, I also wish to acknowledge Ms. Iris Henkel-Wehseler, Ms. Christiane Francavilla, Dr Gudrun Löhrer and Dr Patrick Tschirner within the organization for their invaluable assistance in navigating this thesis.

I would like to extend my gratitude to Prof. Dr Christina Wege, for agreeing to be the external supervisor for my PhD fellowship. I am truly thankful for your altruistic dedication and your enjoyable, warming and encouraging emails. You always found the time, even if I sent it in short notice, to review my work in progress and to send me your feedback. Though we have not met in person, your support has consistently made me feel valued.

Also thank you to all the members of the graduate school NanoCompetence for the great collaboration and the stimulating discussions. To all the Professors and senior scientists, thanks for the relaxing atmosphere and the interest in this thesis. To my peers, thanks for the talks and for sharing the ups and downs of writing a "nano-thesis".

Thank you to all the former and current members of AG Dringen for making me a part of the group, for your cooperation and also for your scientific inputs, especially in the early hours of Monday´s Seminars. *Muchas* g*racias*, Yvonne for your expertise and help in the lab. Thanks for sharing our mutual personal growth and many important life experiences along these years. Thanks Ingo for gladly help with the daily matters of the AG and Gabi for all the amusing conversations (also about horses) in the breaks of writing this dissertation. Thanks Chris, for attending my last-minute questions and the refreshing and comforting

conversations about balancing the thesis with parenthood. Eric, thanks for the *buenos días* and all the football talks that made me feel more at home; Johann, thanks for your disposition to help with any lab stuff, for the vivid conversations or the comments about the victories of Atlético de Madrid. Your *excelente* made always my days and I can only wish you many more to come. Aru, thanks for all the support inside and outside the lab, for being the "non-German resistance", for the laughs, and for all the advice on how to finish this thesis. Patrick and Nico, thanks for the funny moments and the company during the very long days full of never-ending incubations; Nadine, thanks for your optimism, for being a great team player and for sharing your ketchup. Antonia, a big thank you for your acid but also sweet sense of humour, for being a great office-mate and for sharing the ups and downs of the PhD life. I didn´t get the "bla, bla, bla" into the thesis (but almost ;). Kathrin, I am deeply grateful for our past conversations and those to come about anything and everything: science, politics, women empowering and much of personal stuff. For welcoming me to the group and to NanoCompetence and for the mutual encouragement to achieve the impossible: finishing our theses and ultimately for your friendship.

Lastly, I would like to thanks the unconditional: my closest friends and family. There is no success without an excellent team, and this thesis would simply not have been without you. Thank you all for your sincere interest on the CeONPs, for your support during the unusual development of my PhD, for your understanding when I couldn´t be there for you because I was working hard, and for always being part of Team Mentxu. Thank you for sharing precious moments and creating new wonderful memories during (and despite) these busy years. I sure owe you all many missed calls, messages and toasts. But now it is finally the time to celebrate.

I would like to show my gratitude to my little group of friends here in the beautiful and hanseatic Bremen:

Yure & Toni, Nitu, Florence & Julius and Sanja & Nils: you made and, at least some still make, this city a home to me. Thanks David, for all the *Flammkuchen*, the talks and your fondness, it was great to have you around. Thanks Silvia, for your positivity, for your sincere encouragement to push this thesis forward and for the "survival-kit" for the last months. Nur, walking together along our PhDs and our new role as mums have definitely made these incompatible tasks way more bearable, real and human. Thanks for the talks, the plans and the "times-out" of the thesis, thanks for sharing all the troubles and the victories. Gonzalo, thanks for your readiness to help from baby-sitting to your graphical abilities, and especially

II. Structure of the thesis

The present thesis comprises five chapters: Introduction (1), Experimental Results (2), Summarizing Discussion (3), Conclusions (4) and Future Perspectives (5).

Chapter 1: Introduction.

The general introduction aims to present the state of the art and the most important scientific findings on the two main topics of the research: nanomaterials and brain cells. The nanotechnology section provides an insight into the history of nanotechnology and outlines the properties and applications of engineered nanoparticles, with a special focus on the current understanding of biomedical applications of cerium oxide nanoparticles. The following section describes the major roles of astrocytes within the brain and details some aspects of their metabolism and pathological states. Such factors are critical in the comprehension of the findings reported in this thesis. Additionally, this section discusses the characteristics of the immortalized C6 glioma cell line and its use as a model for astrocytes.

Chapter 2: Experimental Results.

The central chapter of this thesis contains the presentation and discussion of novel experimental results obtained on cerium oxide nanoparticles and their effects on cultured astrocytes and C6 glioma cells. It has been divided into three chapters:

2.1. Coating, functionalization and characterization of cerium oxide nanoparticles to study cellular accumulation and biocompatibility in astrocyte primary cultures and C6 glioma cells.

2.2. Cerium oxide nanoparticles and $CeCl_3$ stimulates the glycolytic flux in astrocyte primary cultures.

2.3. Scavenging of reactive oxygen species by DMSA-coated cerium oxide nanoparticles and ionic cerium in cultured glial cells.

These three chapters have been organized with the formal structure of scientific manuscripts. Therefore, each chapter comprises an abstract and a comprehensive introduction to the pertinent topic, supported by relevant literature. The section detailing the specific materials and methods used is followed by a presentation and description of the results, which are subsequently interpreted and contextualized alongside previous findings and hypothesis. All data presented have been obtained and elaborated by the author of this

thesis, unless stated otherwise within the chapter. None of these chapters have been submitted for peer-review or publication so far.

Chapter 3: Summarizing Discussion

The most relevant results and the key-findings from the experimental data obtained in Chapter 2 are consolidated and a broader picture of their meaning and their repercussions regarding the potential of cerium oxide nanoparticles as therapeutic agents in brain cells is sketched.

Chapter 4: Conclusions

The key findings of this thesis are formulated and compelled in eleven conclusions, as a summary. They cover the topics addressed in Chapter 2, including the proposed coating of CeONPs with DMSA, the impact on the metabolism of astrocytes and the scavenging properties of reactive oxygen species extra- and intracellularly.

Chapter 5: Future Perspectives

Lastly, the thesis provides an overview of possible future research directions and unsolved questions.

III. Summary

Cerium oxide nanoparticles (CeONPs) are considered a solid candidate for the new generation of antioxidants due to their protective potential against oxidative stress demonstrated *in vitro* and *in vivo* and their self-regeneration potential. Cellular or systemic CeONPs protection against radical-induced toxicity is based on their redox cycling capacity coupled with oxygen buffering. However, their antioxidant capacity as well as the side-effects of their application strongly depend on their synthesis and the cells targeted. In this line, previous studies have demonstrated protective effects of CeONPs against neuro-pathologies with a strong background of oxidative stress, such as Alzheimer´s disease, Parkinson´s disease or ischemia. However, despite this growing scientific evidences, the non-acute effects of CeONPs in glial cells remain a vast unexplored area of research. Therefore, it is of utmost importance to explore the novel formulations and the particular cellular interactions of CeONPs.

In the presented thesis, the coating with dimercaptosuccinate (DMSA) of commercial CeONPs was tested to obtain a colloidally stable DMSA-CeONPs dispersion. These nanoparticles (NPs) were thoroughly analyzed for their physicochemical properties such as size, shape and zeta potential. In addition, DMSA-CeONPs were fluorescence functionalized with the Oregon Green dye (OG), allowing the microscopical observation of their time- and temperature-dependent cellular uptake by rat C6 glioma cells and astrocytes. Cell viability and the effects on glucose metabolism was also investigated in astrocytes after incubation with DMSA-CeONPs. Different experimental conditions revealed that astrocytes remained viable over time and accumulated cerium in a concentration-dependent manner. However, the glycolytic flux was stimulated and thus, the extracellular concentration of lactate was significantly increased in astrocytes treated with DMSA-CeONPs. Comparison to astrocytes exposed to ionic cerium showed that the stimulation of the glycolytic flux depends on the presence of cerium, independently of the form in which it was presented. However, the intracellular cerium accumulation was significantly enhanced after exposure to DMSA-CeONPs compared to cells treated with ionic cerium. Incubations with hypoxia inducible 1 α (Hif-1α) stabilizers revealed that such stimulation of the glycolytic flux showed similarities to the stimulation observed when astrocytes were incubated with DMSA-CeONPs and therefore, it is concluded that cerium may interfere with the intracellular oxygen availability.

Two different approaches were taken to assess the potential antioxidative capacity of DMSA-CeONPs against reactive oxygen species (ROS): 1) the removal of exogenous H_2O_2 and the scavenging of cellularly formed superoxide was tested extracellularly and 2) intracellularly, by pre-incubating glial cells with these DMSA-CeONPs and then incubating them in the presence of exogenous H_2O_2 or under the cellular formation of superoxide. The results demonstrate that DMSA-CeONPs have only a limited extracellular ROS scavenging capacity. Internalized DMSA-CeONPs did not act as antioxidants in glial cells, nor did they show catalyst activities under the conditions tested.

In conclusion, the coating and fluorescence functionalization of CeONPs presented in this thesis are suitable tools to study the uptake, intracellular fate and accumulation in glial cells. However, these NPs cannot be applied as antioxidants due to their limited ROS scavenging capacities. DMSA-CeONPs did not affect the viability of glial cells but altered glucose metabolism, most likely via Hif-1α stabilization. In this line, this thesis highlights the importance of the investigation of the cellular effects beyond cell viability and under non-pathological conditions of CeONPs treatments.

IV. Zusammenfassung

Ceroxid-Nanopartikel (CeONPs) gelten aufgrund ihres in *vitro* und *in vivo* nachgewiesenen Schutzpotenzials gegen oxidativen Stress und ihres Selbstregenerationspotenzials als gute Kandidaten für eine neue Generation von Antioxidantien. Der zelluläre oder systemische Schutz von CeONPs vor radikalinduzierter Toxizität beruht auf ihrer Fähigkeit zum Redoxzyklus in Verbindung mit Sauerstoffpufferung. Ihre antioxidative Kapazität und die Nebenwirkungen ihrer Anwendung hängen jedoch stark von ihrer Synthese und den Zielzellen ab. In diesem Zusammenhang haben frühere Studien die schützende Wirkung von CeONPs gegen Neuropathologien mit starkem Hintergrund von oxidativem Stress gezeigt, wie z.B. Alzheimer, Parkinson oder Ischämie. Trotz dieser zunehmenden wissenschaftlichen Evidenz sind die nicht akuten Wirkungen von CeONPs auf Gliazellen noch ein weitgehend unerforschtes Gebiet. Daher ist es von größter Bedeutung, neue Formulierungen und spezifische zelluläre Interaktionen von CeONPs zu untersuchen.

In der vorliegenden Dissertation wurden kommerzielle CeONPs mit Dimercaptosuccinat (DMSA) beschichtet, um eine kolloidal stabile DMSA-CeONPs-Dispersion zu erhalten, und ihre physikalisch-chemischen Eigenschaften wie Größe, Form und Zetapotenzial eingehend analysiert. Darüber hinaus wurden die DMSA-CeONPs mit dem Farbstoff Oregon Green (OG) fluoreszenzfunktionalisiert, was die mikroskopische Beobachtung ihrer Zeit- und Temperaturabhängigen zellulären Aufnahme durch C6-Gliomzellen und Astrozyten der Ratte ermöglichte. Die Lebensfähigkeit der Zellen und die Auswirkungen auf den Glukosestoffwechsel wurden ebenfalls in Astrozyten nach Inkubation mit DMSA-CeONPs untersucht. Unterschiedliche experimentelle Bedingungen zeigten, dass CeONPs-exponierte Astrozyten über einen längeren Zeitraum lebensfähig blieben und Cerium konzentrationsabhängig anreicherten. Allerdings wurde der glykolytische Fluss stimuliert, so dass die extrazelluläre Laktatkonzentration in den mit DMSA-CeONPs behandelten Astrozyten signifikant erhöht war. Der Vergleich mit Astrozyten, die ionischem Cerium ausgesetzt waren, zeigte, dass die Stimulation des glykolytischen Flusses von der Anwesenheit von Cerium abhängt, unabhängig davon, in welcher Form es vorliegt. Allerdings war die intrazelluläre Ceriumakkumulation nach Exposition mit DMSA-CeONPs im Vergleich zu Zellen, die mit ionischem Cerium behandelt wurden, signifikant erhöht. Inkubationen mit Hypoxie-induzierbaren 1 α (Hif-1α)-Stabilisatoren zeigten, dass diese Stimulation des glykolytischen Flusses der Stimulation ähnelte, die beobachtet wurde, wenn Astrozyten mit DMSA-CeONPs inkubiert wurden.

Die potentielle antioxidative Kapazität von DMSA-CeONPs gegen reaktive Sauerstoffspezies (ROS) wurde mit zwei verschiedenen Ansätzen untersucht: 1) die Entfernung von exogenem H_2O_2 und das Abfangen von zellulär gebildetem Superoxid wurde extrazellulär getestet und 2) intrazellulär, indem Gliazellen mit diesen DMSA-CeONPs vorinkubiert und dann in Gegenwart von exogenem H_2O_2 oder unter zellulärer Superoxidbildung inkubiert wurden. Die Ergebnisse zeigen, dass DMSA-CeONPs nur eine begrenzte Fähigkeit besitzen, extrazelluläre ROS einzufangen. Internalisierte DMSA-CeONPs wirkten in Gliazellen nicht als Antioxidantien und zeigten unter den getesteten Bedingungen keine Nanozyme-Aktivität.

Zusammenfassend ist festzuhalten, dass die in dieser Dissertation vorgestellte Beschichtung und Fluoreszenzfunktionalisierung von CeONPs geeignet ist, die Aufnahme, das intrazelluläre Schicksal und die Akkumulation in Gliazellen zu untersuchen. Allerdings können diese NPs aufgrund ihrer begrenzten ROS-Fängerkapazität nicht als Antioxidantien eingesetzt werden. DMSA-CeONPs hatten keinen Einfluss auf die Lebensfähigkeit der Gliazellen, veränderten aber den Glukosemetabolismus, wahrscheinlich über die Stabilisierung von Hif-1α. In diesem Sinne unterstreicht diese Arbeit die Bedeutung der Untersuchung zellulärer Effekte von CeONPs-Behandlungen über die Zellviabilität hinaus und unter nicht-pathologischen Bedingungen.

V.Abbreviations and symbols

$	American dollar
α	alpha
β	beta
λ	wavelength
ζ	zeta
%	percent
°C	degree Celsius
T°	temperature
µL	microliter
µm	micrometer
µM	micromolar
a.u.	arbitrary units
AA	antimycin A
AD	Alzheimer´s disease
ALS	amyotrophic lateral sclerosis
ANOVA	analysis of variance
APCs	astrocyte primary cultures
ATP	adenosine-5´-triphosphate
BBB	blood brain barrier
BC	before Christ
BSA	bovine serum albumin
CAT	catalase
CE	current era
CNS	central nervous system
CeONPs	cerium oxide nanoparticles
CLSM	confocal laser scanning microscopy
D	dimensions
d	day(s)
DAPI	4', 6-diamino-1-phenylindole
DFx	deferoxamine
D_H	Hydrodynamic diameter
DLS	dynamic light scattering

DMSA	2', 3' meso-dimercaptosuccinate
DMSA-CeONPs	DMSA-coated cerium oxide nanoparticles
DMEM	Dulbecco´s modified Eagle´s medium
DMOG	dimethyloxaloylglycine
EDX	energy dispersive X-ray
ELS	electrophoretic light scattering
etc.	*et cetera* (from Latin, and the rest)
EU	European Union
FCS	fetal calf serum
Fig.	Figure
GABA	gamma-aminobutyric acid
GFAP	glial fibrillary acidic protein
Glc-6-P	glucose 6 phosphate
GPx	glutathione peroxidase
GSH	glutathione
h	hour(s)
H33342	Hoechst 3342
HEPES	4-(2-hydroxyethyl)-1-piperazine ethane sulfonic acid
IB	incubation buffer
IB-BSA	incubation buffer containing bovine serum albumin
ICP-OES	inductively coupled plasma optical emission spectrometry
ICP-MS	inductively coupled plasma mass spectrometry
i.e.	*id est* (from Latin, that is)
IgG	immunoglobulin G
kV	kilovolt(s)
LDH	lactate dehydrogenase
MCT	monocarboxylate transporter
min	minute(s)
mL	milliliter
mM	millimolar
MTT	3-(4,5-dimethylthiazol-2-yl)-2,5-diphenyltertrazolium bromide
mV	millivolt(s)
NAD/NADH	nicotinamide adenine dinucleotide
n.d.	not determined
nm	nanometer(s)

NMs	nanomaterials
NPs	nanoparticles
NQO1	NAD(P)H: quinone- acceptor oxidoreductase 1
Nrf2	nuclear factor erythroid 2-related factor 2
OG	Oregon green
OG-DMSA-CeONPs	Oregon green labeled DMSA-coated CeONPs
OSC	oxygen storage capacity
PAA	poly(acrylic acid)
PBS	phosphate buffer saline
PD	Parkinson´s disease
PEG	polyethylene glycol
PFK1	6-phosphofructo-1-kinase
PHDs	prolyl hydroxylase domain containing enzymes
PPP	pentose phosphate pathway
PI	propidium iodide
Pi	polydispersity index
ROS	reactive oxygen species
RT	room temperature
s	second(s)
SE	standard error
SD	standard deviation
SOD	superoxide dismutase
SEM	scanning electron microscopy
sp-ICP-MS	single particle inductively coupled plasma mass spectroscopy
STEM	scanning electron microscope
TCA	tricarboxylic acid cycle
TEM	transmission electron microscopy
Tris	Tris(hydroxymethyl)-aminomethane
UK	United Kingdom
Un-CeONPs	uncoated cerium oxide nanoparticles
USA	United States of America
UV-Vis	ultraviolet-visible
vs.	*versus*
VHL	von Hippel Lindau protein
v/v	volume/volume

| **WST1** | water-soluble tetrazolium salt 1 |
| **w/v** | weight/volume |

1 Introduction

1.1 Nanotechnology: Milestones, applications and socioeconomical impact

The term nanotechnology was coined by the scientist Norio Taniguchi at a conference in Tokyo (1974) describing it as the "[...] separation, consolidation and deformation of materials by one atom or one molecule". However, the study of matter at the nanoscale (1 nm= 10^{-9} m) had already started at the beginning of the twentieth century. The development of high-resolution microscopy techniques, transmission electron microscopy (1932) and scanning electron microscopy (1937), was crucial to reveal the atomic structure of the matter. These important scientific advances together with his own work in quantum electrodynamics, allowed the Nobel laureate Richard Feynman to anticipate the possibility of manipulating matter at the atomic level in 1959 in his famous speech *There´s Plenty of Room at the Bottom* (Feynman, 1959)*.* He even challenged the scientific community to write the entire Encyclopedia Britannica in the head of a pin, which was accomplished by Tom Newman in 1985 by using nanotechnology (Feynman, 1960; Dietrich, 1986). The definitive impulse to nanotechnology as a field of research occurred in the 1980s. At the beginning of this decade, Gerd Binning and Heinrich Rohrer presented the scanning tunneling microscope, which permitted to resolve molecular structures and atomic bonds and awarded them with the Nobel Prize in Physics in 1986 (Baratoff, 1986). Short time after, the buckminsterfullerenes were isolated by Kroto, Smalley and Curl, who were also awarded with the Nobel Prize in Chemistry (Curl Jr et al.; Kroto et al., 1985). Almost at the same time, the scientist Eric Drexler published his book titled *Engines of Creation: The Coming Era of Nanotechnology* (Drexler, 1987). Another significative advance in the field were the studies of carbon nanotubes by the physicist Iijima (Iijima and Ichihashi, 1993). The interest in nanotechnology continued growing in the twenty-first century and translated into economic and legislative initiatives worldwide. For instance, in 2003 the USA government signed the *Twenty-first Century Nanotechnology Research and Development Act*, which turned nanotechnology into a national priority (Roco, 2011). In 2023 the Nobel Prize in Chemistry was awarded to Bawendi, Brus and Yekimov for the discovery and synthesis of quantum dots (Liz-Marzán et al., 2023).

Although unintentionally, the use of nanotechnology started early in the history of human civilization. The chemical analysis of ancient pieces of red glass manufactured by the Egyptians and Mesopotamians during the fourteenth century BC have revealed the presence

of copper oxide nanoparticles (NPs), which might have been formed by the use of copper in the presence of antimony (Schaming and Remita, 2015). The most charismatic example of early use of the properties of metal NPs is the *Lycurgus Cup* dated from the fourth century AD and preserved in the British Museum (London, UK). In this piece of Roman glass-work the color observed, green or red, depends on which side of the cup is illuminated. Modern studies have determined that this dichroism is due to the scattering and absorption of the light produced by silver and gold NPs, respectively (Barber and Freestone, 1990). Some other examples of use of the nanotechnology have been found along the centuries, e.g., in mosaics, ceramics or Damascus steel (Reibold et al., 2009; Sciau, 2012).

Since the understanding of the fundamentals of the nanoscale, its use has dramatically expanded. In the last two decades, the applications of nanotechnology have exponentially increased, and are now present in almost all technical or industrial fields. Industries as electronics (Gong and Cheng, 2017), transportation (Mathew et al., 2019), agri-food sector (Prasad et al., 2017; Gilbertson et al., 2020), cosmeceuticals (Fytianos et al., 2020), water remediation (Ghadimi et al., 2020), and renewable energy (Ahmadi et al., 2019) exploit the advantages of using nanomaterials (NMs) to improve the efficacy of their manufacturing, the quality of their products or their endurance. The use of NMs is astonishingly diverse. For example iron nanoparticles have been used as a fertilizer to increase soybean biomass (Liu and Lal, 2015) or have been used in humans as contrast agents in magnetic resonance imaging to diagnose cancer (Vu-Quang et al., 2019). Some of the most exciting developments are probably happening in the field of biomedicine. Applications in this area can be grouped into three main clusters: i) nanotherapeutics, ii) imaging and diagnostics and iii) regenerative medicine. Regarding nanotherapeutics, different nanomaterials have been evaluated as drug carriers. Iron and gold NPs are now together with liposomes, polymeric capsules, micelles and exosomes the most frequently chosen tools for controlled drug release (Acebes-Fernández et al., 2020). In 2013, a survey identified 155 nanoproducts which were in the clinical phase or were already commercialized. Interestingly, about two-thirds of the investigational applications identified were focused on cancer treatment (Etheridge et al., 2013).

NMs have also been useful for *in vivo* diagnosis when used as contrast agents to delimit pathological tissues or *ex vivo* as biosensors which identify different compounds in fluids of patients. For this porpoise, gold NPs, quantum dots, silica NPs or intelligent NPs have been used in high-standing diagnose-techniques such as computed tomography, magnetic resonance imaging or positron emission tomography (Woźniak et al., 2022). To illustrate

the versatility of these materials, in a recent study, D´Hollander and colleagues (2020) designed gold nanostars, which first helped to localize the tumor *in vitro* and then, when injected to mice, significantly reduced its size. As mentioned before, nanotechnology also aims to repair or replace damaged tissues and organs. In this sense, carbon nanostructures show a high biocompatibility and support the growth and proliferation of different cells types. Just to mention some examples, diamond polymer composites have been developed as support of multifunctional tissues (Pelaz et al., 2017) and carbon nanotubes improve the electrical activity of neurons and as a consequence promote the growth of neuronal systems (Lorite et al., 2019).

Translating this research and the derived applications into macro-economic data is an arduous task, as there are not many open, reliable and up to date sources. In 2017, the number of international patents on nano-objects, nanotechnology and nanoproducts reached 189,000 with a net increase of 31,000 patents in comparison to 2016. The countries significantly contributing to such development were the USA, the country who has led investigation and patents in nanotechnology over the past 20 years, and China with around 85,000 patents filed respectively, followed by Japan (25,000) and South Korea (22,000). In October 2021, the USA government released the latest strategic plan for the US nanotechnology initiative, its main priority being to reinforce this leadership. The American nanotechnology market has been estimated at US $ 13.2 billion in 2021 (https://statnano.com/news/69907/Review-of-the-2021-US   Nanotechnology-Initiative-Strategic-Plan, accessed 26.01.24).

Concerning the EU, the most prolific country in patents, and the first manufacturer of commercial nanoproducts is Germany (Inshakova et al., 2020). Overall silver is the most reported nanomaterial commercialized in the EU, representing 10% of total. Remarkably, 70% of the 5,000 products registered in this database by 2020 had an unknown composition. The top three applications of nanotechnology are electronics, energy and biomedicine. Together they account for over 70% share of the global market (Inshakova et al., 2020). The majority of the nanoproducts declared to the Nanodatabase, and therefore commercialized in the EU, correspond with Health and Fitness (62%) (Inshakova et al., 2020). However, as a disclaim, these are only partial figures as not all producers declare their products to this database (Hansen et al., 2020). To illustrate the socioeconomic impact of this market, the European Commission estimated that in 2014 the nanotechnology sector directly employed between 300,000 to 400,000 people

Sociologically, in a recent study carried out by Porcari and colleagues (2019), nanotechnology was identified as a symbol of progress for more than 50% of a total of 97 participants in Denmark, Germany and Spain. It could be also inferred than the knowledge about nanotechnology positively correlated with the concern about its risks: naïve individuals, with less previous information, were less concerned. The purchase intention was greater in all three countries when nanotechnology was present in electronics or used in health monitoring, but was significantly reduced when presented in food (Porcari et al., 2019). Overall, the perception of nanotechnology is positive or neutral but stakeholders as well as general public remarked the need of clearer and more comprehensive regulations.

1.2 Nanomaterials: fundamentals

Paradoxically and despite its expansion, there is still no agreement on definition of nanomaterial. The International Organization for Standardization defines it as the "material with any external dimension in the nanoscale or having an internal structure or surface structure in the nanoscale" (ISO/TR 18401:2017, 2017). Likewise, there are also several classifications attending different criteria. Depending on the origin, nanomaterials can be generated (i) incidentally as a byproduct of industrial processes e. g. NPs produced by engines (ii) naturally produced by organisms or geological events e.g., NPs emitted by volcanoes or (iii) by designing them, i.e., the engineered nanomaterials (Jeevanandam et al., 2018).

Attending to their size and dimensionality, the engineered nanomaterials can be attributed to one of the 36 existing classes of nanostructures according to the classification suggested by Pokropivny and Skorokhod (2007). Such dimensionality results as a function of the arrangement of their elementary building units. To establish the 36 classes of nanostructures these authors first grouped the elementary building units by the number of dimensions that exceed the nanoscale. Molecules, NPs or fullerenes have all their dimensions in the nanoscale and therefore, they were considered 0 dimensions (0D), nanotubes or nanofibers 1D and nanoplates or nanolayers 2D. The spatial arrangement of these elementary building units determines to which class the nanostructure is assigned. For example, uniform NPs arrays are considered 0D0 but when these NPs form a polymer, the resulting nanostructure is classified as 1D0. Consequently, the materials which have all their dimensions above 100 nm but have different elementary building units in all

directions are considered 3D as for example tridimensional composites. In addition, nanomaterials exist in single, fused, aggregated, or agglomerated forms with spherical, tubular, ellipsoidal, irregular or amorph shapes (Sannino, 2021).

Based on its composition, NMs can be classified as single constituent or nanocomposites. In addition, they can be divided into (i) organics, which include polymers or lipids or (ii) inorganics mainly formed by metals, metalloids and their respective oxides (Saleh, 2020). Allotropes of the same nanomaterial are highly exploited in nanotechnology. The most representative example is carbon. The different crystallization of this element (i.e. fullerenes, nanotubes, graphene, graphite and diamond) lead to different features which might be useful for certain applications (Riley and Narayan, 2021)

Importantly, NMs show unique properties compared to the corresponding chemical compound in bulk. These special features derive mostly from their size. For any material that is broken down into extremely small pieces, the surface area per volume unit increases significantly and the percentage of atoms at the surface becomes more relevant (Sannino, 2021). The interior atoms of any material are more coordinated and stable as those present at the edges or corners of the surface. Therefore, materials in the nanoscale range show an enhanced reactive surface, which logically leads to a major interaction with their environment. For the same reason, nanomaterials show a lower melting point and enhanced solubility (Roduner, 2006).

Also relevant is the surface charge, which determines the dispersion stability or aggregation of the nanomaterials and its affinity towards other molecular species or even cells (Jiang et al., 2009; Huang et al., 2017). Frequently, in colloidal suspensions the surface charge is indirectly estimated by the zeta potential (ζ-potential). The ζ-potential measures the electric potential in the interfacial double layer at the location of the slipping plane relative to a point in the fluid away from the interface (Predota et al., 2016). The absolute value of the ζ-potential increases in well dispersed solutions and decreases when aggregation takes place. The ζ-potential can either be positive or negative, indicating mostly the character of the solute, and it is greatly influenced by the size of the NMs and the composition and pH of the medium (Predota et al., 2016).

Another key factor to explain the singularity of NMs is the quantum confinement. Such confinement is due to an increase in the band gap of the material due to the limitation of the random movement of electrons which can now move in discrete energy levels (Ramalingam et al., 2020). The increase in the band gap is inversely correlated to the size of the material. However, at what size a material undergoes quantum confinement varies depending on the

composition and the quantum mechanical nature of the electron and holes present in the material (Edvinsson, 2018). This effect is translated into chemical changes, mainly in the electrical and optical properties of the material in contrast to their bulk counterpart (Roduner, 2006; Loss, 2009). NMs which undergo quantum confinement usually show luminescence. Colloidal CdSe-CdS core-shell NPs nicely illustrate this phenomenon. By slowly incrementing the particle size form 1.7 nm to 6 nm, a full pallet of luminescent colors from blue to red can be observed (Talapin et al., 2004).

NMs, and particularly NPs, also show differences in magnetism in comparison to their respective bulk materials. NPs of iron, nickel or cobalt present enhanced magnetism. Moreover, Mn and Cr bulk materials possess an antiferromagnetic ground state, however, when synthesized as NPs, they instead might display ferromagnetic attraction. Ferromagnetic behavior has been observed in otherwise non-magnetic materials such as Au, Ag, TiO_2, ZnO or CeO_2 when present as NMs (Sundaresan et al., 2006). Different investigations have attributed this effect to the appearance of quantum-size effects and defects in the surface as vacancies, substitutions or interstitial atoms (Gao et al., 2010). In theoretical studies, this magnetism has been attributed to the unpaired electrons in *s*- or *p*-bands in contrast to the conventional magnetism which arises from unpaired electrons in *d*- or *f*-orbitals (Singh, 2013).

Another chemical property which appears affected in the nanoscale is the catalysis. In 1987, Haruta and colleagues discovered that gold NPs could act as catalyst mediating the transformation of CO_2 to CO by O_2 when their size was below 5 nm. Until then, gold was considered an inert metal. Since then, there has been an increased interest in using nanomaterials as heterogenous catalysts. The catalyst reactivity of certain NMs seems to be determined by a combination of factors as the size and the quantum effects deriving from it, the presence of higher densities of low coordinated atoms, an excess of electronic charge and the interaction between the nanomaterials and their support (Cuenya, 2010). Catalytic studies investigating the different contributions of the NMs have been prolific in the recent years (Astruc, 2020).

In biological systems, enzymes are natural and efficient catalysts which have resulted from evolution. Some enzymes increase reaction rates by up to one million times. Reactions, which in the absence of the enzyme would take years, occur in fractions of seconds (Cooper, 2000; Wolfenden and Snider, 2001). Despite such competition, NMs have also been investigated as "nanozymes". The NMs with enzyme-like activity have the advantage of working under dysregulated physiological conditions (pH or T°) and being resistant to the

digestion by proteases (Singh, 2019). In this line, Gao et al. (2007) demonstrated the peroxidase-like activity of magnetite NPs. Afterwards, the catalytic properties of other metallic NPs based on cerium, copper, platinum, gold or cobalt have been intensively investigated. This research has mainly focused in finding nanozymes with redox activities similar to peroxidases, oxidases, catalases or superoxidase dismutases and recently also to hydrolase mimic activities (Karakoti et al., 2010; Pirmohamed et al., 2010; Singh, 2016; Karim et al., 2018; Wang et al., 2018; Wu et al., 2019).

1.3 Nanoparticles

NPs can be defined as nano-objects with three external dimensions in the nanoscale (0D). They possess a nucleus formed by the core material which can be a single component or an alloy of different elements and provides the NPs with their physical properties such as plasmonic resonance, magnetism or optical features (Feliu et al., 2016; Heuer-Jungemann et al., 2019). The persistence of the physical properties of the core in a biologic environment is usually fundamental for their use.

The second layer of the NPs is commonly an engineered coating which is intentionally added to the NP during or just after their synthesis. The high reactivity of the native surface of the NPs usually facilitates the coating. The tailor-made coating material are usually designed to provide colloidal stability and, particularly in the field of nanomedicine, biocompatibility but also to gain some other functionality e. g. traceability (Bhirde et al., 2011; Rastedt et al., 2017), drug transportation (Naeem et al., 2021) or responsiveness to pH (Xu et al., 2020; Yan and Ding, 2020), temperature (Abulateefeh et al., 2013) or light (Wang et al., 2017; Zhang et al., 2017). Surface coatings have been seen to have a great impact on the fate of the NPs, including cell adhesion, uptake and distribution within the organism, tissue or cell compartments (Zhu et al., 2013; Meng et al., 2018). These engineered coatings are mostly polar oligomeric or polymeric compounds that can either be organic or inorganic (Chanana and Liz-Marzan, 2012). Attending to their origin there are two mayor classes, synthetic and natural coatings (Schubert and Chanana, 2018). The formers are so far, the most common in nanomedicine research, especially the polymer polyethylene glycol (PEG). Several PEG-NPs are commercially available and therapeutically used in the USA and EU (Alconcel et al., 2011; Suk et al., 2016). PEG has been considered an inert material which does not cause immunogenicity or antigenicity at least in short term studies (Chanana and Liz-Marzan, 2012), although some studies have demonstrated that PEG- conjugated substances cause an immune reaction known as accelerated blood clearance (Abu Lila et al., 2013). The NPs

coated with PEG show an enhanced colloidal stability due to the prevention in great extent of non-specific protein adsorption (Sebak, 2018). The main disadvantages are the enlargement of the particle´s size, possible abrupt release of the cargo when interfering with the reticuloendothelial system, lower cellular uptake and non-biodegradability (Sebak, 2018). Organic thiols containing one or multiple charged groups, such as mercaptosuccinic acid, dimercaptosuccinic acid, mercaptopropionic acid or penicillamine have been broadly used as coating agents for NPs as well (Bertorelle et al., 2006; Luther et al., 2013; Petters et al., 2016; Rastedt et al., 2017). These compounds also enhance the colloidal stability of the NPs, and in contrast to PEG, allow to further functionalize them, which usually does not result in a drastic change in size (Karakoti et al., 2011). However, these NPs are sensitive to the pH and the ionic strength of the medium, which may cause reversible aggregation (Taladriz-Blanco et al., 2011).

Natural coatings, on the other hand, are characterized by their high biocompatibility and exhibit a well-known structure. The most employed biopolymers are the polynucleotides (DNA and RNA), polysaccharides (dextran and chitosan) or polypeptides (Schubert and Chanana, 2019). Charged polysaccharides such as chitosan or hyaluronic acid have lately been investigated to overcome the stability problems of dextran in serum (Schubert and Chanana, 2019). Protein coatings have risen a great interest because of their high stability under physiological conditions (Chanana and Liz-Marzan, 2012) and due to the chemical versatility derived from the twenty-one different amino acids which could be present in their structure (Jeong et al., 2018).

The third and most external layer of the corona of the NPs is formed by biomolecules such as lipids, metabolites, sugars and especially proteins adsorbed from the environment. This external layer is usually denominated as "soft corona" in the literature (Mohammad-Beigi et al., 2020). So far, the research in this field has mainly been focused in the interaction between proteins and NPs (Hadjidemetriou and Kostarelos, 2017). Proteins bind to the surface of the NPs mediated by different forces, such as van der Waals, electrostatic, hydrogen bonding or salt bridge formation and critically affect the features and behavior of the NPs in the biological environment (Chen et al., 2017). These bonds are transient and vary over time. For example, for the protein corona it has been measured that low-abundance proteins were present at the beginning and the end of a 480 min incubation of NPs in plasma whereas at intermediate timepoints high-abundance proteins were adsorbed (Tenzer et al., 2013). The protein corona is dramatically influenced by the size and nature of the core as well as the surface charge hydrophobicity (Osorio-Blanco et al., 2019;

Richtering et al., 2020). As a generalization, in different *in vivo* studies it has been observed that the protein corona is mainly formed by albumin, fibrinogen and immunoglobulin G (IgG) (Winzen et al., 2015; Breznica et al., 2020). Reciprocally, the protein corona determines at great extent the fate of the NPs in the system. Importantly, when the NPs are intravenous administered, opsonins such as IgG or fibrinogen have been seen to promote their uptake by macrophages and are the cause for the rapid clearance of NPs from the blood circulation (Kotagiri and Kim, 2014). On the contrary, bovine serum albumin (BSA) precoating has been observed to significantly increase *in vivo* half-life of luminescent porous silicon NPs. Such effect might be attributed to a decrease in non-specific binding (Xia et al., 2013). However, BSA presence have been also considered as responsible of a greater NP aggregation under certain conditions (Dominguez-Medina et al., 2016). Several *in vitro* studies have shown varying protein corona conformation depending on the serum to which the NPs are exposed. For instance, in the study carried out by Schöttler et al. (2016), polystyrene NPs exposed to fetal bovine serum or human serum not only showed different composition within the six most abundant proteins representing about the 70% of the protein corona but also a different relative amount in the albumin, which was in both cases the most abundant protein in the corona.

In conclusion, the NPs protein corona is particle identity-dependent, cell type-dependent and environment-dependent. In addition, there are major difficulties for its study as it evolves over time and the bonds are transient and might be affected by the analysis employed. However, it is worth to remark that the soft protein corona crucially determines the fate of the NPs in a biological environment.

As a result of all these factors previously discussed, an overwhelming number of singular NPs with different properties and for diverse purposes have been developed and investigated (Harish et al., 2022). However, the scope of this thesis is concentrated on investigating the characteristics and effects of cerium oxide nanoparticles on brain cells and therefore, the next section is exclusively focused on these interesting NPs.

1.4 Cerium-based nanoparticles

Cerium-based NPs have been long exploited in the automotive industry as catalyzers for fuel oxidation and gas exhaust treatment as these NPs efficiently catalyze the oxidation of CO into CO_2 in the presence of O_2 (Dey and Dhal, 2019) and reduce the particulate matter emissions in diesel engines (Sajith et al., 2010). They are also widely used as abrasive in chemical mechanical polishing/planarization (Feng et al., 2003; Abiade et al., 2005; Son et

al., 2021), corrosion protection (Harb et al., 2020) and solar cells (Hajjiah et al., 2018; Mehmood et al., 2020). Lately their catalyst and redox properties have also been investigated for biomedical uses.

1.4.1 Physical and chemical characteristics

Cerium belongs to the group of lanthanides or "rare earth elements" and it is the most abundant element of this series. Concentration in the earth´s crust has been estimated at 66.5 ppm (Balaram, 2019) with an occurrence similar to copper (Migaszewski and Galuszka, 2015). For industrial purposes, it is mainly extracted from the minerals bastnäsite, monazite, allanite and cerite (Ramos et al., 2016; Dey and Dhal, 2019).

Cerium is the first element in the periodic table with a partially occupied f orbital. In fact, the electronic configuration of cerium, i.e., [Xe] $4f^1$ $5d^1$ $6s^2$, shows two partially filled orbitals, $4f$ and $5d$, with several excited sub-states predicted (Allen et al., 1986). It is remarkable that after years of study to solve the actual localization of this $4f$ electron in the cerium oxide, it still remains open to discussion whether it is fully or partially delocalized. Such question might seem trivial but is crucial to define and control the performance of cerium derivatives as redox catalysts (Huang and Lu, 2019; Herper et al., 2020).

Based in quantum theoretical modelling (i.e. density functional theory in combination with others), which aim at reproducing and explaining experimental observations, in CeO_2, also denominated ceria, the cerium atom possesses an electron in the $4f$ orbital which behaves as an ordinary valence electron, thus, it is at some extent delocalized (valence band model) (Skorodumova et al., 2002; Zhou et al., 2019). In consequence, in the bonding with oxygen, the four valence electrons leave the cerium atom to the p bands of oxygen atoms (Skorodumova et al., 2002). CeO_2 is thermodynamically stable at ambient conditions. However, as oxide, cerium can also be fully reduced to Ce_2O_3. In this formulation, the $4f$ electron has been calculated to be mainly localized in the cerium atom and, therefore, does not behave as a valence electron but as a core electron (core state model) (Wuilloud et al., 1984; Gangopadhyay et al., 2014). Ce_2O_3 is not as stable as ceria at normal conditions and get easily oxidized to CeO_2 in the presence of oxygen (Hamm et al., 2014).

Importantly, on bulk but especially at the nanoscale, ceria naturally presents a significant number of native surface defects, oxygen vacancies being the most stable ones (Skorodumova et al., 2002). Such vacancies have been described under a wide range of conditions. In the formation of neutral oxygen vacancies, an oxygen anion O^{2-}, leaves the lattice as a neutral species, formally ½ O_2 (g), and the two electrons in play get "localized"

in f-level on two Ce^{4+} atoms, which finally get reduced to Ce^{3+} (Equation 1) (Skorodumova et al., 2002).

$$O^{2-}+2Ce^{4+} \rightarrow 2Ce^{3+} + \tfrac{1}{2} O_2 \text{ (g)} \qquad \text{(Equation 1)}$$
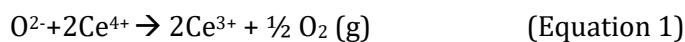
As a result, ceria exists in a non-stochiometric formulation, which can be notated as CeO_{2-x}, where x is the non-stoichiometric oxygen and which values range between $0 \leq x \leq 0.5$ (Schmitt et al., 2020). The formation of non-stoichiometric ceria is generally favored at high formation temperature and low oxygen partial pressure. In general, the number of Ce^{3+} atoms present are inversely correlated to the particle size (Chen et al., 2010). Additionally, different cations of similar size as Ce^{4+} but different valence (dopants) can be added during the synthesis to intentionally create surface defects. The most effective ones are trivalent cations as samarium and gadolinium where the loss of positive charge is compensated by the formation of one oxygen vacancy per two dopant elements (Schmitt et al., 2020).

The quantum process of localization/delocalization of the $4f$ electrons, mentioned above, coupled with the formation or presence of oxygen vacancies explain the redox capacity of ceria (Herper et al., 2020). Cerium can act as an oxygen buffer, under reducing conditions, the oxygen vacancies proliferate and Ce^{4+} atoms switch or flip-flop to Ce^{3+}. Reversibly, under oxidizing conditions, Ce^{3+} atoms get rapidly oxidized back to Ce^{4+}. Skorodumova and colleagues (2002) modelized this flip-flop and demonstrated that there is a substantial energy gain when the two remaining electrons of a newly created oxygen vacancy occupy the localized f states of two closer cerium atoms. As a result, the oxygen storage capacity (OSC) of a particular ceria sample can be calculated. The OSC is defined as the amount of oxygen that can be trapped and, therefore, released from the sample during a controlled red-ox cycle (Kullgren et al., 2013).

All these quantum models to establish the location of the $4f$ electrons consider the tridimensional arrangement of the atoms in ceria for their computations. Moreover, understanding how and where the oxygen vacancies are formed is crucial in material engineering to optimize the catalysis which takes place in the surface of the material. For this purpose, an insight into the crystallography of ceria is required. Basically, CeO_2 shows a face centered cubic fluorite structure, which contains four cerium atoms per unit cell (Conesa, 1995; Skorodumova et al., 2001; Dey and Dhal, 2019) (Fig. 1.1a). In the unit cell, every cerium atom is coordinated with eight oxygen anions with each oxygen tetrahedrally coordinated to the nearest four cerium atoms (Skorodumova et al., 2001; Dey and Dhal, 2019). In contrast, Ce_2O_3 presents a typical A-type rare earth sesquioxide crystal structure (Bärnighausen and Schiller, 1985), more typical for the lanthanide series.
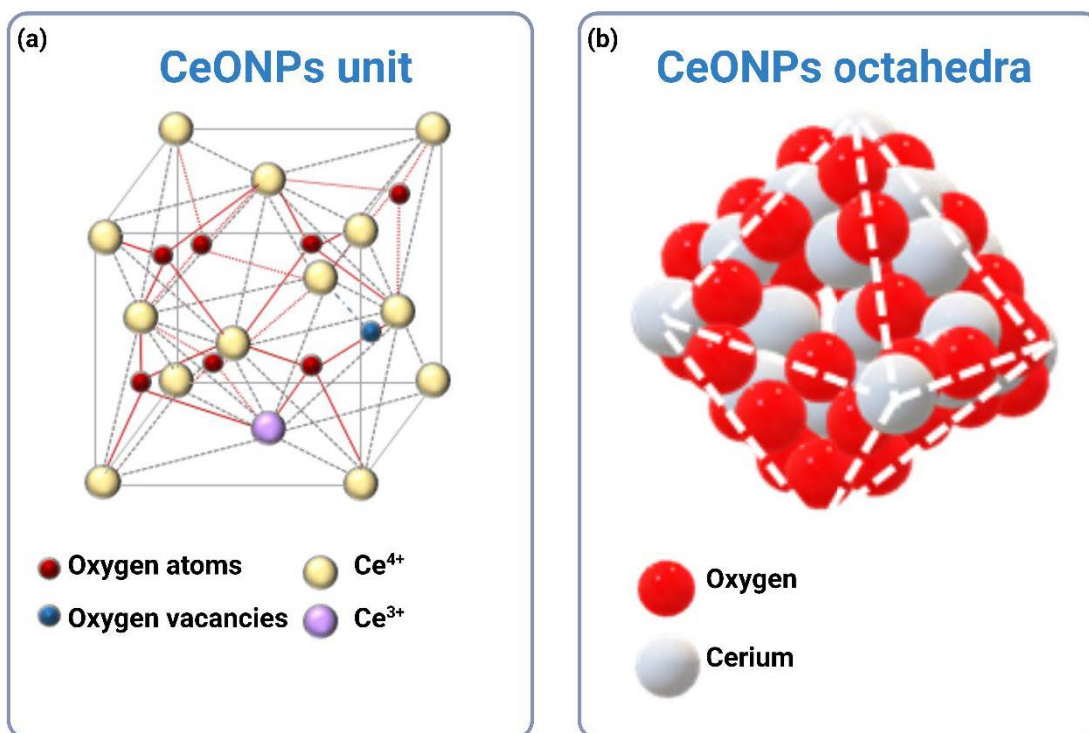
Figure 1.1. Schematic representation showing a non-stoichiometric unit cell of CeONPs (a) and the CeONPs as octahedron (b). Modified from Parwaiz et al. (2019) and Gao et al. (2023)

Ceria presents three main thermodynamically stable surfaces ordered as 111> 110 >100 by increasing surface energy (Zhang et al., 2002; Gangopadhyay et al., 2014). The different layers have different ionic exposure; for instance, the most stable (111) surface family have a three-layer structure O-Ce-O with exposition of the oxygen. This layer possesses one single coordinatively unsaturated site (Zhang et al., 2002; Gangopadhyay et al., 2014). The (110) surface family exposes both ions and oxygen and cerium has, respectively, one and two unsaturated sites. The less stable surface family (100) consists of an O-Ce-O-Ce unit which lead to the formation of a dipole, which is avoided by exposing the oxygen to the outside. In this facet, both Ce and O have two coordinative unsaturated sites. However, the disposition of the atoms in the (100) layer is still under debate and seems to be highly influenced by parameters such as temperature or pressure during the synthesis (Trovarelli and Llorca, 2017).

Early studies about ceria showed that the formation of oxygen vacancies, is strongly surface dependent, meaning that different nanocrystals with different exposed facets might possess a different redox activity (Loschen et al., 2008; Della Mea et al., 2017). Later studies showed that each facet presents different OSC. CeO usually crystallize in polyhedral shapes enclosed mainly within low energy surfaces (Sayle et al., 1994; Zhang et al., 2011; Schilling et al.,

2018). The models based in quantum calculations cited above have also established the increasing energy required to form an oxygen vacancy depending on the type of facet, resulting in (110)>(100)>(111) (Conesa, 1995; Yang et al., 2004; Hao et al., 2021). Typical nanocrystals of ceria are octahedra or truncated octahedra (Fig 1.1b). However, it is also possible to crystallize ceria in other shapes as nanocubes, nanospheres and even in 1D or 2D structures by using surface capping agents, which blocks certain crystallographic growth direction, and/or by controlling synthesis parameters (Sun et al., 2012). The typical octahedral nanoparticle shows externally (111) as the major facet while the truncated octahedra presents (111) and (100). More prone to contain oxygen vacancies are the nanocubes. Ideally, these NPs are formed by six (100) surfaces but they can also be crystallized as truncated nanocubes or nanocubes with round edges which in addition expose (111) and (110) surfaces, respectively (Wang and Feng, 2003).

Skorodumova et al. (2002) also showed by studying the formation energy of oxygen vacancies at different positions that it is more favorable to create these close to two Ce^{3+} atoms in the CeO_2 matrix. Later quantum studies have thoroughly investigated the position of these vacancies within the surface, whether they aggregate or not and tested for the effect in the fluorite structure by turning Ce^{4+} to Ce^{3+}. Electrons left by the oxygen, apparently do not localize on the nearest cerium atoms close to the vacancies, but on the next nearest cerium neighbors (Ganduglia-Pirovano et al., 2009; Shoko et al., 2010).

1.4.2 Synthesis and coating

Two main approaches exist for the synthesis of NPs: top-down or bottom-up procedures (Abid et al., 2022). The former consists in physical methods to decompose larger materials into NPs. Grinding, physical vapor deposition and chemical etching belong to this group (Fu et al., 2018). The bottom-up approach, in contrast, produces NPs from precursors and by controlling synthesis parameters such as pH, temperature and pressure. Some commonly used methods in this category are chemical precipitation, hydrothermal, sonochemical or green synthesis (Jamkhande et al., 2019). To a great extent, the synthesis determines the physical and chemical features of cerium oxide NPs (CeONPs) (Nyoka et al., 2020; Kontham et al., 2021).

The most extended method to synthesize CeONPs in research is the chemical precipitation and the most frequently precursors used are cerium chloride heptahydrate or cerium nitrate hexahydrate in combination with ammonia solutions (Suresh et al., 2013; Kalashnikova et al., 2017; Thakur et al., 2019; Nosrati et al., 2023). Chemical industries offer

a great variety of ceria nanopowders for investigation. In this case, the synthesis process is not specified.

As previously explained, most of the NPs are stabilized and further functionalized by adding a coating. In the case of CeONPs, it is also crucial to check that their redox properties are not altered by the coating. There are two main coating methods: one-step synthesis and functionalization process or two-step post-synthesis process (Spiridonov et al., 2023). In the former, low molecular weight ligands or polymers are added at the same time with the cerium precursors. In the second method, the coating materials are bound to the nanoceria surfaces after their synthesis. An advantage of this last method is that the effect/contribution of the coating to the CeONPs features can be more easily inferred (Lord et al., 2021).

1.4.3 Characterization

The interactions of NPs with biological media, in culture or in vivo, are driven by the nature of the NPs and the system. As it has been described in previous sections, the properties of NPs vary extraordinarily depending on the synthesis, the size, the form, the crystallography, the coating, the soft-corona, the ambient conditions etc. To succeed in the application of such NPs it is mandatory to characterize their particular physicochemical features in as much detail as possible. The challenge is usually the small size of the materials and, in the case of CeONPs, to quantify the ratio of Ce^{3+}/Ce^{4+} and the oxygen vacancies. A practical limitation for most of the laboratories is the high cost of these techniques (acquisition and maintenance) and, in cases, their complex operability. Table 1.1 lists the methods and techniques that have been used to characterize CeONPs.

1.4.4 Biomedical applications and toxicity of CeONPs

The initial idea of using CeONPs as therapeutics arose from a serendipitous observation made by Professor Rzigalinski and co-workers when investigating CeONPs as drug carriers. They observed that CeONPs prolonged the life-span of brain cell cultures for periods of 6 to 8 months (Rzigalinski, 2005).

Table 1.1. Tools for the characterization of CeONPs

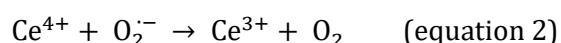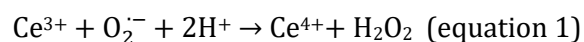| Method/ Technique	Physicochemical parameter analyzed
I. Microscopy	
- Transmission Electron Microscopy (TEM)	Core size, shape, localization in cells, detection of NPs
- High Resolution TEM	Single particle crystal structure, structural defects
- Scanning Electron Microscope	Size, morphology (three-dimensional)
- Scanning Transmission Electron Microscope (STEM)	Atomic structures and interfaces, detection of NPs
- Atomic Force Microscope	Size and morphology (three dimensional)
- Confocal Laser Scanning Microscope (CLSM)	Localization in biological systems
II. X-Ray based	
- X-Ray Diffraction	Size, crystal structure, elemental composition
- Energy-Dispersive X-Ray spectroscopy (EDX)	Elemental composition
- X-Ray Absorption Spectroscopy	Chemical oxidation-state of the species
III. Spectroscopy /Spectrometry	
- Inductive Coupled Plasma Optical Emission Spectroscopy (ICP-OES)	Elemental composition, concentration
- Inductive Coupled Plasma Mass Spectrometry (ICP-MS)	Elemental composition, concentration
- UV-Vis Spectroscopy	Optical properties, concentration
- Fourier Transform Infrared Spectroscopy	Functional groups, surface composition (coating)
IV. Others	
- Dynamic Light Scattering (DLS)	Size and size distribution in dispersion
- Electrical light Scattering (ELS)	Surface charge (ζ-potential), colloidal stability

The information for the elaboration of this table was obtained from Mourdikoudis et al. (2018); Modena et al. (2019)

ROS/RNS scavenging and nanozyme-mimicking behavior of CeONPs

The reactive oxygen species (ROS) are generated as natural by-products of normal cell activity, including aerobic respiration. Members of this group are hydrogen peroxide (H_2O_2), superoxide anion ($O_2^{\cdot-}$) and hydroxyl radicals (OH^-). H_2O_2 and $O_2^{\cdot-}$ are also metabolites involved direct- or indirectly in cell signaling pathways and cell homeostasis (Pomatto and Davies, 2018). In hypoxic conditions, nitric oxide may also be produced during the respiratory chain reaction. This leads to the formation of reactive nitrogen species (RNS) (Sies et al., 2017).

Healthy cells are able to regulate the presence of ROS in order to avoid oxidative stress, which may cause irreversible damages in proteins, lipids or DNA and finally lead to cell death (Schieber and Chandel, 2014). However, cells allow a controlled increase in ROS when adaptation is needed as these molecules activate signaling pathways and the immunological defense. A lack of such regulation has been linked to a myriad of pathologies (e.g. cancer, Alzheimer's disease (AD), Parkinson disease (PD), diabetes) and to aging (Liguori et al., 2018; Baev et al., 2022). Antioxidant enzymes and some non-enzymatic compounds are the endogenous mechanism to eliminate ROS in cells. The most relevant antioxidant enzymes are superoxide dismutase (SOD), catalase (CAT) and glutathione peroxidase (GPx) (Sies et al., 2017) (Figure 1.2). Other antioxidants such as glutathione, uric acid, vitamin E, vitamin C or β- carotene also contribute to remove ROS from the cellular space (Pisoschi et al., 2021).

In the past decade nanoceria have been reported to show SOD (Korsvik et al., 2007), CAT (Pirmohamed et al., 2010), peroxidase (Tian et al., 2015; Guo et al., 2019) and oxidase mimetic activities (Hayat et al., 2015; Singh, 2016). SOD mimic behavior was described first in nanoceria by Korsvik et al. (2007). The mechanism proposed behind the disproportionation of $O_2^{\cdot-}$ by nanoceria was described as follows:

$$Ce^{3+} + O_2^{\cdot-} + 2H^+ \rightarrow Ce^{4+} + H_2O_2 \text{ (equation 1)}$$

$$Ce^{4+} + O_2^{\cdot-} \rightarrow Ce^{3+} + O_2 \qquad \text{(equation 2)}$$

Afterwards some follow-up experiments determined that a higher ratio of Ce^{3+}/Ce^{4+} resulted in an enhanced SOD activity (Heckert et al., 2008; Singh et al., 2011). As previously described in this introduction, there is a negative correlation between the size and the presence of Ce^{3+} in nanoceria. Therefore, NPs larger than 5 nm show a reduced or inexistent SOD activity (Korsvik et al., 2007; Dowding et al., 2013). In addition, theoretical studies on the adsorption of oxygen on surface vacancies have concluded that the reduction of Ce^{4+} to Ce^{3+} by $O_2^{\cdot-}$ (equation 2) is not feasible (Zhao et al., 2012). However, an interesting

discovery was that larger NPs could acquire superoxide scavenging activity when exposed to native CuZn-SOD or other electron donors (Li et al., 2015). Li and colleagues speculated that the CuZn-SOD or the electron donor interacts with nanoceria by transferring electrons, which results in the reduction of Ce^{4+} to Ce^{3+} getting the reactive sites of nanoceria active and thus, being able to scavenge $O_2^{\cdot-}$.
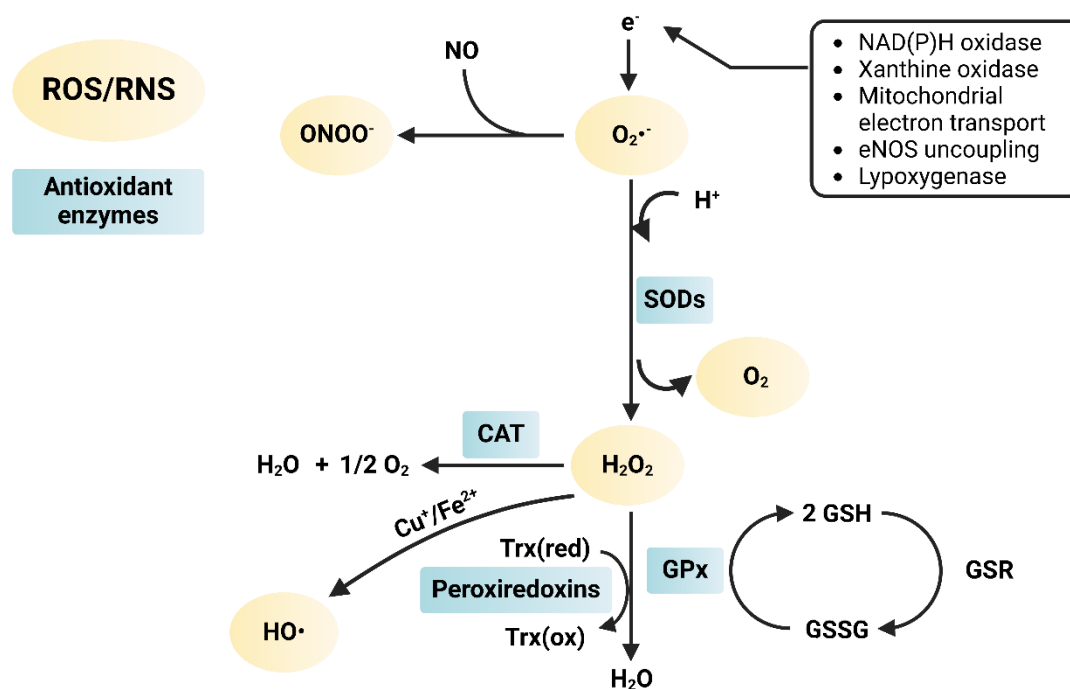
Figure 1.2. Schematic representation of ROS and RNS metabolism in mammalian cells. Superoxide is a (by-)product of NAD(P)H oxidase, xanthine oxidase, nitric oxide synthase, lipoxygenase and mitochondrial activity. SOD catalyzes the disproportionation of $O_2^{\bullet-}$ to H_2O_2, which in turns, is reduced to H_2O by CAT, GPx and/or peroxiredoxins. Superoxide can also react with nitric oxide and form the strong oxidant peroxynitrite (ONOO-). Therefore, SOD is the first line of defense against oxidative stress caused by superoxide anions. The enzyme is involved in cell signaling via regulating ROS and NO. Importantly, H_2O_2 can undergo chemical reduction to hydroxyl radical (OH•) in the presence of Cu^+ or Fe^{2+} (Fenton reaction). e-: electron; Trx(red): thioredoxin reduced; Trx(ox): thioredoxin oxidized; GSR: Glutathione disulfide reductase. Adapted from Fukai and Ushio-Fukai (2011).

Similarly, Self and colleagues demonstrated that nanoceria possess CAT-like activity, when the ratio of Ce^{3+}/Ce^{4+} is low (Pirmohamed et al., 2010; Singh et al., 2011). The reaction involves a reduction of Ce^{4+} to Ce^{3+} by H_2O_2, which in turn gets oxidized to molecular O_2. The mechanism is similar that of CAT activity and can be noted as in equations 3 and 4.

$$2Ce^{4+} + H_2O_2 \rightarrow 2Ce^{3+} + O_2 + 2H^+ \qquad \text{(equation 3)}$$

$$2Ce^{3+} + 2H^+ + H_2O_2 \rightarrow 2Ce^{4+} + 2H_2O \qquad \text{(equation 4)}$$
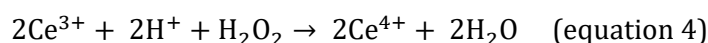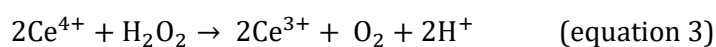
Experimental observations showed that only Ce^{3+} gets oxidized and produce peroxide when scavenging $O_2^{\cdot-}$ (equation 2) and the disproportionation of H_2O_2 only occurs when Ce^{4+} gets reduced (equation 3). However, restoring the initial state of the nanoceria is required in both cases to show authentic enzymatic behavior and for making it an interesting ROS scavenger in biological systems. Initially, it could not be fully explained how nanoceria returns to its initial oxidation state and it was stated in the literature that nanoceria could recycle "spontaneously" via unexplained mechanisms (Das et al., 2007; Heckert et al., 2008). In 2011, Celardo and colleagues suggested a plausible mechanism for the redox regeneration of nanoceria based on the coupling of the reactions with $O_2^{\cdot-}$ and H_2O_2 (equations 2 and 3). In this sense, when nanoceria reduces $O_2^{\cdot-}$, H_2O_2 is formed and Ce^{3+} is oxidized to Ce^{4+} afterwards H_2O_2 can react together to regenerate Ce^{3+} and oxidize to O_2. The same researchers also suggested as an alternative that H_2O_2 may also oxidize Ce^{3+} leading to Ce^{4+} and reducing H_2O_2 to H_2O (Figure 1.3).

The radical scavenging capacity of CeONPs has been further investigated and it was suggested that nanoceria could neutralize hydroxyl radicals too (Babu et al., 2007; Das et al., 2007). Hydroxyl radicals are characterized by their strong oxidant capacity, their high reactivity and an extremely short life time in aqueous solution. These characteristics hamper their investigation. Nevertheless, several studies have reported scavenging activity of hydroxyl radicals by CeONPs (Babu et al., 2007; Xue et al., 2011; Filippi et al., 2019; Mitchell et al., 2021). In addition, the research group of Self examined the ability of CeONPs to scavenge RNS. They demonstrated that CeONPs scavenge nitric oxide radical and accelerated the decay of peroxynitrite (Dowding et al., 2012; Dowding et al., 2013).

Thus, the flip-flop of cerium between the different redox states provides a unique opportunity of scavenging ROS and nitrating agents and potentially an endless possibility of regenerating its antioxidant capability. Compared to natural enzymes that usually present one or two active sites, nanoceria possess a large number of active sites on the surface of a single nanoparticle. Moreover, nanoceria is more resistant to changes in temperature and pH in comparison to endogenous enzymes. However, CeONPs also present some important disadvantages in contrast to natural enzymes, as the lack of specificity towards a particular ROS or RNS species, their oxidase-like activity which may cause cytotoxicity under particular circumstances (see next section) or the dependency of its biological behavior on the surface defects and morphology (Lord et al., 2021).
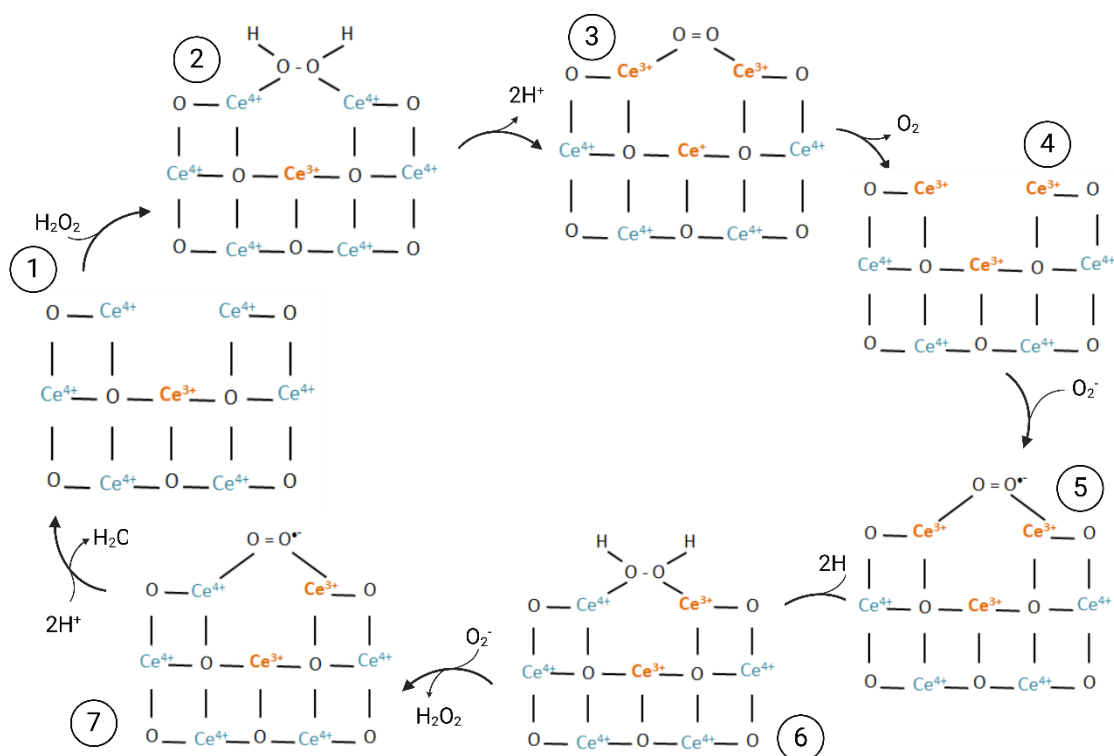
Figure 1.3. Schematic model of the flip-flop Ce³⁺/Ce⁴⁺. For the initiation of the redox cycle the presence of an oxygen vacancy on the surface of CeONPs is necessary (1). In this way, the H_2O_2 can bind to two atoms of Ce⁴⁺ (2), after the release of protons and the reduction of the two cerium ions (3), the oxygen is released (4). Subsequently superoxide can bind to this site (5). After the transfer of one single electron and the uptake of two protons from the solution (6), H_2O_2 is formed and can be released. After repeating this last step with a second superoxide molecule (7), the oxygen vacancy returns to the initial status. The distribution of the atoms does not correspond to the actual spatial arrangement of the atoms in the crystal structure but is used to illustrate the suggested model. From Celardo et al. (2011) with slight modifications.

Pro-oxidant activity of CeONPs

Several studies have remarked the potential pro-oxidant (i.e. oxidant) capacity of CeONPs, and oxidase and peroxidase mimic activities of nanoceria have been described (Pirmohamed et al., 2010; Tian et al., 2015; Guo et al., 2019). In a set of experiments, nanoceria oxidized organic dyes (3,3′,5,5′-tetramethylbenzidine and AzBTS) at low pH values without the presence of H_2O_2. To further verify its oxidant potential, the authors used dopamine in citrate buffer (pH 4.0) and nanoceria facilitated its oxidation within minutes (Asati et al., 2010). In a more recent study, the oxidase mimic activity of nanoceria was reproduced and the mechanism was elucidated (equation 5). The results suggested that $O_2^{\cdot-}$, formed at the surface of nanoceria, is the main intermediate in its oxidase-like activity. In the same investigation, the authors were able to modulate the oxidase-like activity of

nanoceria by adding adenosine triphosphate, acetylcholinesterase and urease (Cheng et al., 2016).

$$O_2 + Ce^{3+}(CeO_2) \rightarrow O_2^{\cdot-} + Ce^{4+}(CeO_2) \qquad \text{(equation 5)}$$
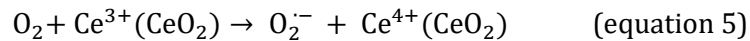
It has been also suggested that in the presence of H_2O_2 and at acidic pH, CeONPs can produce hydroxyl radicals and $O_2^{\cdot-}$ in a reaction similar to Fenton/Haber-Weiss (Heckert et al., 2008). The peroxidase like behavior of CeONPs has also been used for the detection of cancer biomarkers (Asati et al., 2011), glucose (Jiao et al., 2012) or phosphoproteins (Yıldırım et al., 2021).

Biomedical research: *in vitro* and *in vivo* studies

In 2005, Tarnuzzer and colleagues pioneered the application of CeONPs as therapeutics by demonstrating in an *in vitro* study that nanoceria protected healthy human breast cells but not a tumor cell line from radiation. Since then, CeONPs have been investigated in different *in vitro* and *in vivo* disease models, which mainly involved oxidative stress. Many authors have demonstrated the key role of oxidative stress in cancer (Reuter et al., 2010; Sosa et al., 2013; Hayes et al., 2020). A beneficial effect of CeONPs has been demonstrated against cutaneous squamous (Alili et al., 2011), melanoma (Sack et al., 2014), ovarian (Giri et al., 2013; Hijaz et al., 2016; Das et al., 2017), breast (Li et al., 2016), pancreatic (Wason and Zhao, 2013; Wason et al., 2018), colon (Jana et al., 2014) and hepatic (Fernández-Varo et al., 2020) cancers.

Short-lived inflammation is a natural defense against pathogens and is intrinsically related to oxidative stress. ROS favors inflammation by activating the expression of proinflammatory genes (Reuter et al., 2010; Hussain et al., 2016).

However, chronic inflammation is suggested to trigger pathologies such as diabetes, hypertension, cardiovascular disease, depression, neurodegenerative and autoimmune diseases or even cancer (Furman et al., 2019). Several authors have explored the anti-inflammatory effect of CeONPs in different conditions reviewed by Corsi et al. (2023). Recently it has been demonstrated that ultra-small citric-acid coated CeONPs alleviate inflammation-induced edema (Kim et al., 2021) and that functionalized CeONPs mitigate the pro-inflammatory activity associate to the portal vein endothelium of cirrhotic rats (Ribera et al., 2019).

Furthermore, CeONPs were the first nanomaterial to be tested as an antioxidant in space. The colloidal stability of nanoceria was investigated by the European Space Agency, and it

was proven to provide protection to muscle cells. The antioxidant capacity of CeONPs against the oxidative stress induced by microgravity conditions has also been tested in a later study in the International Space Station (https://www.esa.int/ESA_Multimedia/Images/2019/04/Nanoceria, accessed 26.01.2024).

Focusing now on brain-related studies, the positive effect of CeONPs have been especially relevant in vision diseases which involved neuronal dysfunction and degeneration (e.g. retinitis pigmentosa, aged-related macular degeneration) (Maccarone et al., 2020). In those conditions, oxidative stress have been also identified as a key factor (Nebbioso et al., 2022). Different *in vivo* studies showed a reduction in apoptotic cells in the retina and a reduction in microglial activation after a single intravitreal application of CeONPs (Fiorani et al., 2015; Wong et al., 2015). Based on these data, CeONPs have been suggested to be a new therapeutic approach to be tested in clinical trials to validate their benefit (Maccarone et al., 2020).

The scavenging properties of CeONPs have also contributed to alleviate neuronal toxicity caused by Aβ-induced ROS in Alzheimer´s disease (AD) models (Cimini et al., 2012; Dowding et al., 2014; Guan et al., 2016). Even an *in vivo* study reported that AD mice could restore neuronal cell viability and mitochondrial morphology and lower the expressions of astrocyte and microglia inflammatory markers after treatment with decorated CeONPs (Kwon et al., 2016).

CeONPs have also been studied as an alternative therapy against amyotrophic lateral sclerosis (ALS) (DeCoteau et al., 2016). The researchers used a common mouse model of ALS where the transgenic animals overexpress a SOD1[G93A] mutation. After the onset of the symptoms, the animals were injected with CeONPs or saline. CeONPs treated animals preserved muscle function and increased longevity in comparison to the control group.

In addition, it has been observed that a 10 nM dose of CeONPs improves the survival of neurons and blocks injury-induced aberrant glutamate signaling *in vitro*, when administered 1 h after a mild traumatic brain injury in rats (Bailey et al., 2020). Neuronal death and misfunction are usually linked to an increase in oxidative stress in a second phase of the brain injury (Rauchman et al., 2023). In the same study, researchers observed an improvement in the activity of endogenous antioxidants (SOD, CAT and GSH) in animals treated with nanoceria in comparison to animals treated with saline.

Despite the presented evidence of the antioxidative power of CeONPs *in vivo* and their potential use as therapeutics, this line of research still lacks of systemization and unequivocal characterization of the conditions under which these positive effects occur in biological system (Heckman et al., 2020). However, some references in the literature describe also negative effects of CeONPs *in vitro* and *in vivo* (Hussain et al., 2012; Mittal and Pandey, 2014; Yokel et al., 2014). Therefore, an exhaustive study of CeONPs behaviors in biological systems remains a challenge for its further translation into clinical practice.

Commercial applications

The current biomedical applications of CeONPs are still under study and no commercial formulation has been approved by any regulatory agency. However, it is to remark that their potential is outstanding against the pathologies cited above i.e. cancer, stroke, neurodegenerative illnesses (AD, ALS or retinal diseases)(Huang et al., 2023). Different *in vivo* studies have also found promising results of CeONPs against liver inflammation, hepatic ischemia, sepsis, acute kidney injury, radiation-induced tissue damage, obesity and constipation (reviewed in Stephen Inbaraj and Chen (2020)).

In contrast to biomedicine, a type of application of CeONPs that has generated several commercial patents has been the development of different type of sensors for biomolecules. Due to its characteristics, CeONPs are used to detect H_2O_2 in concentrations as low as 5 µM (Zhang et al., 2012) or glucose with a detection limit of 0.5 mM and linear range up to 100 mM and being reusable for at least ten consecutive cycles (Jiao et al., 2012). Nanoceria-based immunoassays have also been explored and developed (Tian et al., 2015; Peng et al., 2016).

Exposure and Toxicity

Currently the most common source of exposure to CeONPs is the emission of diesel engines, which use CeONPs as diesel fuel additive to reduce the generation of particulate matter (Zhang et al., 2013; Dale et al., 2017). In 2017, Dale and colleagues roughly estimated a world-wide yearly emission of 70 million metric tons of cerium into the atmosphere. Despite the exposition in daily- life to CeONPs is steadily increasing, there is a general gap of knowledge about their potential adverse effects. Investigations about the fate of CeONPs, their impact in human health and on different ecosystems must be urgently addressed. In fact, cerium is a xenobiotic and therefore there are no known natural clearance pathways. This implies that exposure to nanoceria could lead to accumulation and finally to systemic toxicity.

Regarding the potential long-term toxicity caused by a chronic exposition to CeONPs, results and data are scarce. A comprehensive 2-year combined study, assessed the genotoxicity in rat blood cells upon 3- or 6- months inhalation exposure to CeONPs (Cordelli et al., 2017). The data showed that CeONPs did not elicit changes in the DNA, gene or chromosome levels. However, contradictory studies have been published too. For example, Schwotzer et al. (2018) found that Wistar rats who inhaled CeONPs for 28 or 90 days, showed an increase in oxidative stress mediators in alveolar epithelial cells and, to a minor extend, in liver and kidneys.

At systemic level, there is a unanimous agreement that nanoceria, as almost all other NMs, ends up passively accumulating in the liver and the spleen (90% of the dose administered), followed by the kidneys (9%) (Casals et al., 2020). Some researchers have concluded that a further dissolution and bioprocessing of CeONPs takes place, observing a reduction in size of the NPs after 90 days of residence in the liver (Muhammad et al., 2014). The elimination of CeONPs via feces or urine has also been detected but mostly for orally administered CeONPs (Molina et al., 2014).

Several *in vitro* studies have concluded that CeONPs are mostly non-cytotoxic although the outcome seems to be particle-, concentration- and cell-dependent (Fisichella et al., 2014; Urner et al., 2014; Forest et al., 2017). The internalization and subcellular localization of CeONPs seem to be determine their toxicity. It has been reported that when nanoceria is localized in the cytoplasm, it does not cause toxicity while its allocation in lysosomes involve a significant decrease in cell viability (Asati et al., 2010; Li et al., 2018)

1.5 Brain cells

''*Men ought to know that from nothing else but the brain come joys, delights, laughter and sports, and sorrows, grieves, despondency, and lamentations. And by this, in an especial manner, we acquire wisdom and knowledge, and see and hear, and know what are foul and what are fair, what are bad and what are good, what are sweet, and what unsavory; some we discriminate by habit, and some we perceive by their utility''* (Hippocrates of Kos).

Hippocrates is acknowledged as the "Father of medicine" and was a pioneer in the field of neuroscience. The Greek identified the brain as the organ which integrates and process sensory information coming from the environment and starts body-wide responses via neurotransmitters or synapses (Arendt et al., 2008; Breitenfeld et al., 2014). But the brain is also the organ, at least in humans, which is responsible of higher cognitive abilities as for

example autobiographical memory, symbolic and logical thought, self-reflection, long-term planning ability, creativity or ethical beliefs (Sousa et al., 2017).

At cytological level, the brain is formed by two major types of cells: neurons and glial cells (Araque and Navarrete, 2010) (Figure 1.4). Neurons are characterized by their ability to exert action potentials which are rapid electrical signals used to transmit information through a network. Neuronal communication involves the propagation of the action potential through axonal processes, the depolarization of the presynaptic terminal followed by the release of neurotransmitters, which reach the receptors on the postsynaptic membrane of other neuron provoking a new spike in this receptor neuron to transmit the information further or inhibit the impulse (Kandel et al., 2000). Any other cell in the brain lacking the ability to produce spikes is considered glia (Araque and Navarrete, 2010). In 1827, Virchow defined glial cells as the *Zwissenmasse* or the glue, which keep the neurons together.
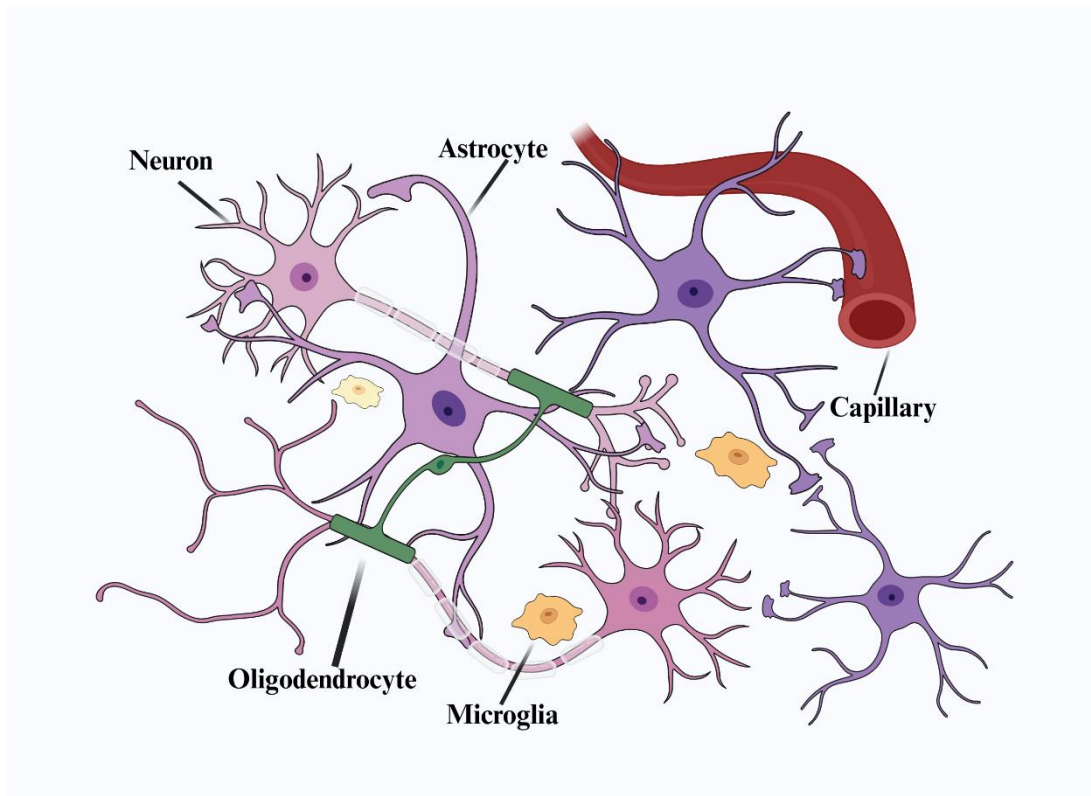

Figure 1.4. Schematic representation of major cell types and their interaction in mammal brain.

Nowadays, different types of glial cells have been identified. In mammals, glial cells comprise four major classes of cells: ependymal cells, microglia, oligodendrocytes and astrocytes (Allen and Barres, 2009). Glial cells contribute to many fundamental functions as

for example protection against damage and infection, insulation of axons to accelerate the electrical impulses, support for neurotransmission and maintenance of homeostasis in the brain (Verkhratsky and Nedergaard, 2018).

As astrocytes and cell line commonly utilized as a model for astrocytes (i.e. C6 glioma cells) are the models employed for the investigation presented in this thesis, their properties and functions are described in greater detail in the following sections.

1.5.1 Astrocytes

The term astrocyte derives from the Greek astron "star" and kytos "hollow vessel" (later, "cell") and evokes a cell with a stellate shape. This term was assumed by observing the characteristic morphology of some eye-catching subclass of astrocytes (Verkhratsky and Nedergaard, 2018). Astroglia refers to many different cell subpopulations differing in their morphology and function (Matyash and Kettenmann, 2010). A major distinction can be established between protoplasmic astrocytes present in the grey matter of the brain and fibrous astrocytes located in the white matter (Miller and Raff, 1984; Köhler et al., 2021; Köhler et al., 2023). Protoplasmic astrocytes present way more contacts at synapses (e.g. one single human protoplasmic astrocyte can contact up to 2 million neurons) (Oberheim et al., 2006), an enhanced glutamate metabolism (Köhler et al., 2023), and more intense gap junction coupling in comparison to fibrous astrocytes (Köhler et al., 2021). These differences correlate with the different functions of the grey and white matter within the brain and also with the region-specificity shown by different astrocyte types, which in turn also impact the neurogenesis (Köhler et al., 2021). However, two common hallmarks of astrocytes can be pointed out: their neuroepithelial origin and their role in the regulation of the central nervous system (CNS) homeostasis (Verkhratsky and Nedergaard, 2018). A universal marker of astroglia based on genetic expression or on morphology is still lacking. However, the intermediate filament glial fibrillary acidic protein (GFAP) (Fig. 1.5) seems to be predominant- and extensively expressed by astroglia cells in the CNS even though not all astrocytes are positive to this marker (e.g. astroglia cells in the striatum or tectum of humans) and other brain cells have also been seen to possess detectable levels of GFAP (e. g. Schwann cells, neurogenic stem cells of the sub-granular zone in the hippocampus) (Messing and Brenner, 2020).
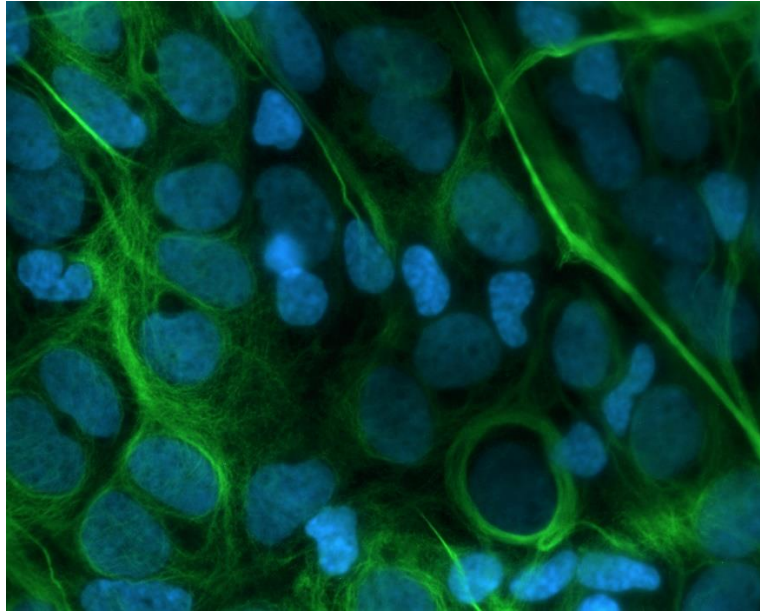
Figure 1.5. GFAP-expression in a representative astrocyte-rich primary culture used in the present thesis. Cultured astrocytes were washed twice with cold phosphate-buffered saline, fixed with 3.5% (w/v) paraformaldehyde and stained as previously described by Stapelfeldt et al. (2017) for α-tubulin (green) by using a mouse anti- α-tubulin antibody (clone DM1A) from Sigma-Aldrich (Steinheim, Germany) and Cy2-conjugated goat anti-mouse antibody form Jackson ImmunoResearch (West Grove, Pennsylvania, USA). The nuclei were stained with DAPI (blue).

Main functions of astrocytes

Astrocytes are considered major regulators within the CNS as they control the import and export of substances from plasma, the neurotransmitter and ion homeostasis, the brain pH and at great extent the presence of ROS (Verkhratsky and Nedergaard, 2018). Astrocytes interact among themselves, with neurons, microglia, and pericytes but also with brain blood vessel cells (Figure 1.4). The connection between astrocytes and the blood brain barrier (BBB) was early discovered by Camillo Golgi (Golgi, 1870; da Fano, 1926). Protoplasmic astrocytes project at least one process, their endfoot, towards nearby blood vessels (Köhler et al., 2021). Brain microvessels are almost completely covered by the endfeet of astrocytes (Mathiisen et al., 2010), which regulate the BBB function by releasing different factors, such as vascular endothelial growth factors, metalloproteinases, nitric oxide or sonic hedgehog proteins (Michinaga and Koyama, 2019). Moreover, compelling evidence suggests an active role of astrocytes in functional hyperemia. This local increase in blood flow triggered by neuronal firing has been linked to a release of metabolites derived from arachidonic acid from the endfeet of astrocytes under certain conditions (Nippert et al., 2018). Whether their endfeet are part of the physical barrier in the BBB is still under debate (Heithoff et al., 2021). However, ablation of endfeet in microvessels of the mice brain, did not impair the BBB

function but led to a re-cover of the vessels by other astrocytes within few days, indicating an important role of such connections in CNS maintenance (Kubotera et al., 2019). Thus, astrocytes control the import and export of substances into the brain as they constitute the first parenchymal brain cell type, which encounters and collects the compounds from the circulating plasma, including energetic and metabolic substrates and drugs (Verkhratsky et al., 2015).

Astrocytes are also indispensable in brain signal cascading. Astrocyte membranes express a large amount and variety of neurotransporters allowing them to take up neurotransmitters from the synaptic cleft. This function is crucial to maintain the spatial and temporal encoding of synaptic transmission and to avoid neuronal toxicity (Andersen and Schousboe, 2023). Neurotransmitters as glutamate, gamma-aminobutyric acid (GABA), adenosine and norepinephrine are taken up and recycled by astrocytes from the synaptic cleft (Andersen and Schousboe, 2023). The three-part role of astrocytes in the particular case of glutamate homeostasis is remarkable. First, astrocytes take up about 80% of glutamate released during neuron synapses modulating its timing, efficacy and outcome (Cuellar-Santoyo et al., 2023). Second, astrocytes are the only cells in the CNS, which synthesize glutamate from glucose and are also capable of converting glutamate into glutamine, which is the precursor in excitatory neurons of glutamate (Mahmoud et al., 2019). Third, glutamine and glutamate are shuttled to excitatory and inhibitory neurons from astrocytes, respectively (Hertz et al., 1999; Andersen and Schousboe, 2023). The former use glutamine to synthesize glutamate, which produce excitatory impulses while the glutamate is further converted into GABA in the cytoplasm of the presynaptic neuron. Therefore, the astroglial glutamine-glutamate shuttle is essential for the maintenance of excitatory and inhibitory neurotransmission (Verkhratsky et al., 2015; Verkhratsky and Nedergaard, 2018; Andersen and Schousboe, 2023; Cuellar-Santoyo et al., 2023). Furthermore, astrocytes are involved in the synaptogenesis (Shan et al., 2021), synaptic maturation and pruning (Bosworth and Allen, 2017).

Astrocytes also significantly influence brain metabolism by exporting an important energetic substrate to the extracellular space: lactate (for more details, see section below) (Mason, 2017; Magistretti and Allaman, 2018). Additionally, glucose can also follow an alternative path and be stored as glycogen by astroglia, being the only brain cell able to store glycogen (Magistretti and Allaman, 2018).

The importance of astrocytes within the CNS is also demonstrated by the correlation between astrocytic aberrations or malfunctioning and different neurological disorders and

neurodegenerative diseases as AD, PD and multiple sclerosis (Phatnani and Maniatis, 2015; Li et al., 2019) and more specifically in Alexander's disease, which is characterized by an accumulation of GFAP (Olabarria and Goldman, 2017; Saito et al., 2018).

Glucose metabolism and lactate release in astrocytes

Glucose has been established as the preferential and primordial energy substrate for the mammalian brain. In humans, it has been estimated that although the brain accounts for only 2% of the total body mass, it consumes around 20% of the intake of glucose, which is equivalent to approximately 100-150 g of glucose per day (Mergenthaler et al., 2013; Patching, 2017). The glucose catabolism provides the energy required for brain activities and the building blocks for neurotransmitter synthesis. The transfer of glucose from the blood stream to the brain occurs at the BBB, following a decreasing concentration gradient (Qutub and Hunt, 2005; Harris et al., 2023). Under normal physiological conditions, the concentration of glucose in the blood oscillates between 4-6 mM while in the brain it drops to 1-2 mM. Therefore, glucose molecules migrate through the basal membrane to the interstitial fluid in the brain and then, are taken up by mainly astrocytes, neurons and microglia (Patching, 2017). This transport of glucose requires specialized sodium-independent facilitative glucose transporters (GLUT) as glucose cannot just diffuse via tight junctions (Koepsell, 2020).

GLUT is present in the brain in different isoforms (i.e. hexoses transporters with different expression, substrate specificity and kinetics) (Thorens and Mueckler, 2010; Suades et al., 2023). Astrocytes predominantly express the GLUT1 isoform however, GLUT4 and GLUT7 are also present (Patching, 2017). GLUT1 transports the glucose to the cytosol of astrocytes, which subsequently undergoes rapid and irreversible phosphorylation to glucose-6-phosphate (Glc-6-P) catalyzed by hexokinase I (da Mata et al., 2023). Glc-6-P can have different metabolic fates within the astrocytes as it constitutes the common substrate for glycolysis, glycogenesis, pentose phosphate pathway (PPP) or sorbitol synthesis (Mergenthaler et al., 2013).

Glycogenesis, the transformation by which glucose is stored as glycogen, is performed under conditions where there is an excess in glucose in comparison to the demand in astrocytes (Dienel and Cruz, 2015). This glycogen can be mobilized to fuel the astrocyte, which initially stored it, or to other astrocytes coupled through gap-junction via oxidative metabolism (Walls et al., 2009), to be converted into lactate, which is generated via glycolysis and serves as an alternative substrate for neurons or astrocytes (Dringen et al.,

1993; Matsui et al., 2017) or can be used as precursor for the glutamate synthesis and contribute to memory consolidation (Gibbs et al., 2007; Gibbs and Hutchinson, 2012). Another possible fate of Glc-6P in astrocytes is to enter the PPP to regenerate nicotinamide adenine dinucleotide phosphate and produce some lactate (Dringen et al., 2007; Bouzier-Sore and Bolaños, 2015; Bolaños, 2016).

Depending on the metabolic demands of the cells, Glc-6-P can be metabolized down the glycolytic pathway to generate pyruvate that might be transported to the mitochondria to enter the tricarboxylic acid cycle (TCA) or can be reduced by LDH5 into lactate (Wiesinger et al., 1997). Importantly, the production of lactate via glycolysis yields little adenosine-5´-triphosphate (ATP) molecules but it confers an advantage when a fast energy demand is required at subcellular level or under hypoxic conditions. Lactate will then be released to the extracellular space via MCT1 or 4 (Debernardi et al., 2003; Pierre and Pellerin, 2005).

The role of lactate release by astrocytes continues to be a hot topic in astrocyte and neuron metabolism (Patel et al., 2014; Barros and Weber, 2018; Barros and Weber, 2018). Accumulating evidence led Pellerin and Magistretti to enunciate the Astrocyte Neuron Lactate Shuttle (ANLS) hypothesis in 1994. These researchers observed that the increase in glutamate release due to an increased excitatory activity of the neurons induced an up-regulation of the glycolytic flux of astrocytes, i.e. glucose consumption and lactate release. These authors postulated that if additional glucose is used up by astrocytes, neurons may receive a metabolic intermediate to complement their own energy demand from astrocytes (Fig. 1.6), and in line with the ANLS, lactate is a reasonable candidate. Neurons express MCT2 and thus, are able to take up lactate from the extracellular space, which can then be oxidized to pyruvate by LDH1 (Barros and Deitmer, 2010; Magistretti and Allaman, 2018). Subsequently, pyruvate can enter the mitochondria in neurons and be oxidized to provide energy via respiration. Over the years, many researchers have found further arguments to support the role of lactate release as an astrocytic contribution to neuron metabolism during activation. For example, several authors have observed a faster glucose consumption by astrocytes than by neighboring neurons during intense neuronal activity (Barros et al., 2009; Chuquet et al., 2010; Jakoby et al., 2014). These results also correlate with the greater presence of nicotinamide adenine dinucleotide (NADH/NAD+) in the cytosol of astrocytes than in neurons (Mongeon et al., 2016). Other experiments in which MCTs functions were impaired genetically or pharmacologically reported alterations in neuronal function and viability, and could not be rescued by supplementing with extracellular lactate, thereby demonstrating that neurons need access to lactate for their proper working (Barros and

Weber (2018) and references therein). In addition, it has been argued that the lactate shuttle from astrocytes to neurons is analog to the one taking place in the testis between Sertoli cells and germ cells, which use lactate as primordial energy substrate (Boussouar and Benahmed, 2004).

Since the ANLS hypothesis was proposed, several researchers have also expressed their doubts based on scientific findings, which do not fit into this general hypothesis (Chih et al., 2001; Díaz-García et al., 2017; Dienel, 2017). Díaz-García and Yellen (2019) postulate that excited neurons mainly oxidize glucose and perform glycolysis themselves to overcome the increased energetic demand, implying they do not consume astrocytic lactate during activation. The researchers based this change of paradigm on the increase in cytosolic NADH and maintenance of intracellular lactate level in activated neurons, which were previously treated with MCT inhibitors as showed in their lab.

Independently of the debate about the occurrence and meaning of the interchange of lactate between astrocytes and neurons, astrocytes *in vivo* and *in vitro* are considered as naturally glycolytic cells, as most of glucose taken up is transformed into lactate (Lopez-Fabuel et al., 2016). Moreover, it has been described that respiration-deficient astrocytes survived based on glycolysis for over a year (Supplie et al., 2017) In fact, the activity of pyruvate dehydrogenase is more strongly inhibited by phosphorylation in cultured astrocytes than in neurons (Halim et al., 2010). Since pyruvate dehydrogenase regulates the entry of pyruvate into TCA, this finding has been suggested as a reason why astrocytes are more prone to produce lactate (Halim et al., 2010; Zhang et al., 2014). However, most enzymes involved in the TCA cycle are found in higher activities in astrocytes than in neurons and mitochondria are thoroughly present specially in fine astrocytic processes at the synapses (Rose et al., 2020).
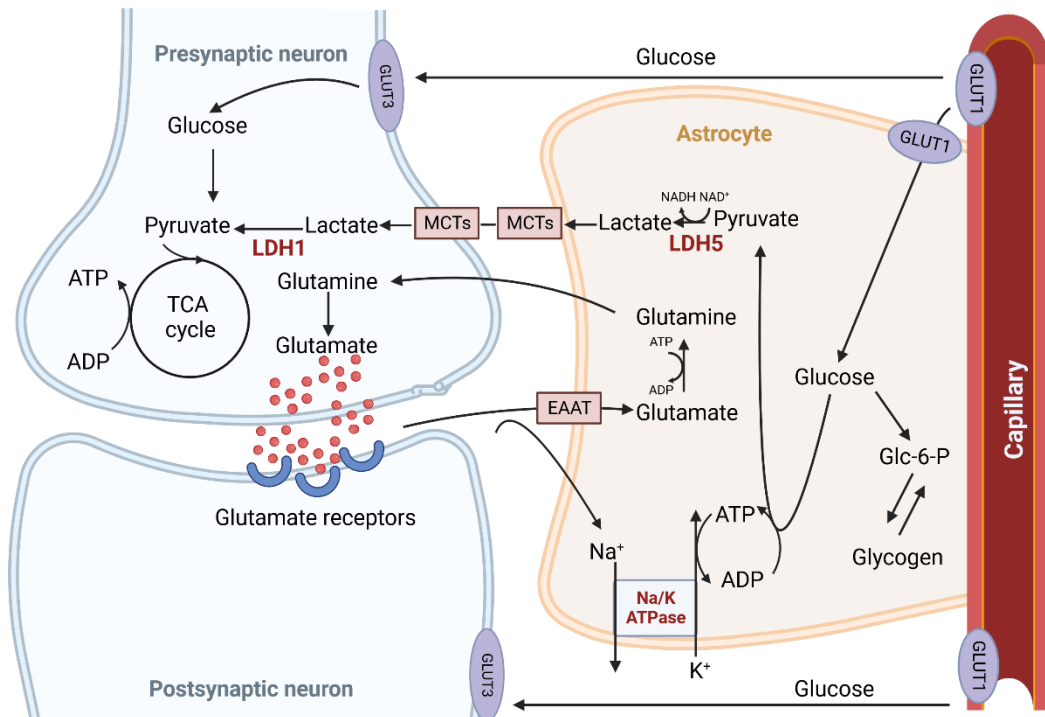
Figure 1.6. Schematic representation of metabolic interaction of astrocytes and neurons. Glucose is transported to astrocytes from the capillaries through GLUT1 transporter and then, part of the glucose enters the glycolysis and is metabolized to lactate via pyruvate by the isoenzyme lactate dehydrogenase 5 (LDH5) (Wiesinger et al., 1997). ANLS theory postulates that subsequently, the lactate is shuttled to neurons via monocarboxylate transporters (MCTs) (Pellerin and Magistretti, 1994). Once internalized by the neuron, lactate is oxidized to pyruvate by lactate dehydrogenase 1 (LDH1) and used as substrate to generate ATP in the tricarboxylic acid (TCA) cycle. Glucose may be also transported directly from the bloodstream to neuronal cells via GLUT3 (Koepsell, 2020). Astrocytes also store glucose in glycogen as energy reservoir (Dringen et al., 1993). In addition, astrocytes synthesize glutamine, which is used as precursor by neurons to generate glutamate (Hertz et al., 1999). At the same time, glutamate is retrieved from the synaptic cleft via excitatory amino acid transporters (EAAT) by astrocytes. The transport of glutamate into the astrocytes is energetically associated to the import of Na^+ into the cell and the release of K^+ via Na^+/K^+-ATPase (Rose and Verkhratsky, 2016).

Astrocytic glycolysis is compelled by 10 different enzymatic steps (Dienel, 2019; Barros et al., 2020). However, it is considered to be mainly regulated by three of these enzymes: hexokinase, 6-phosphofructo-1-kinase (PFK1) and pyruvate kinase (PK) (Bolaños, 2016). In the third step of glycolysis, PFK1 catalyzes the phosphorylation of fructose-6-phosphate to fructose-1,6-bisphosphate using ATP (Souza et al., 2019). PFK1 is considered to be the major regulator of astrocytic glycolysis as its activity can be allosterically lowered by citrate, ATP or long-chain fatty acids (Gonçalves et al., 2019) or in contrast, be increased by e.g. adenosine monophosphate or adenosine diphosphate, suggesting that the activity of PFK1 is intrinsically coupled to the energetic status of the cells. The enzyme 6-phosphofructo-2-kinase/fructose-2,6-bisphopshatase-3 produces fructose-2,6-biphosphate, which is the

main allosteric activator of PFK1 (Gonçalves et al., 2019). Interestingly, this enzyme is thoroughly expressed in astrocytes while it is constantly degraded in neurons (Herrero-Mendez et al., 2009).

PK participates in the last step of glycolysis mediating the conversion of phosphoenolpyruvate to pyruvate. The PKM2 isoform is highly expressed in astrocytes besides cancer and embryonic cells and contrary to differentiated neurons (Lee et al., 2022). Importantly, PKM2, in its dimer form, also functions as a transcriptional activator and can bind the transcriptional hypoxia inducible factor (Hif-1α), stabilizing it in the nucleus, and activating further transcription of pro-glycolytic genes including lactate-producing LDHA and GLUT1 or even PKM2 (Wang et al., 2014). Such activation has been observed under hypoxic conditions, where the glycolysis requires to be enhanced for survival and can in extreme conditions promote Warburg effect but also under normoxic environments, when some disruptors are present. An oxygen-independent mechanism of Hif-1α stabilization has therefore been described and is termed pseudohypoxia. Anyhow, as a result, lactate, the final product of normoxic glycolysis, re-enhances glycolysis by stabilization of Hif-1α (Wang et al., 2014; Lee, 2021).

Oxidative stress in astrocytes

Oxygen is an indispensable element to sustain the high-energy demand of the brain. It has been calculated that the 20% of total inhaled oxygen is used up by this organ in oxidative metabolism (Bolaños, 2016). As a consequence of this high oxygen consumption, brain cells generate a high amount of ROS. ROS damage nucleic acids, lipids and produce degradation of proteins and enzymes, when they are not readily scavenged by the endogenous antioxidant system of the cells (Schieber and Chandel, 2014). Astrocytes possess a potent antioxidative system from which even neighboring cells, including neurons, benefit. This system is highly efficient against oxidative stress, and therefore, protects neuronal function and contributes significantly to brain homeostasis (Dringen et al., 2015).

A key component in the antioxidative system of astrocytes is glutathione (GSH, γ-L-glutamyl-L-cysteinyl glycine), which is found in their cytosol in millimolar concentrations (Dringen et al., 2015). In this sense, GSH participates in three major detoxification processes: (i) direct reactions with radicals such as $O_2^{\cdot-}$ or OH^- without enzymatic involvement, (ii) as electron donor for the reduction of H_2O_2 or organic peroxides in reactions catalyzed by GPx or (iii) as a cofactor in the detoxification of formaldehyde and

methylglyoxal. Importantly, astrocytes provide neurons with a cysteine precursor (CysGly) to enable neuronal synthesis of GSH (Dringen, 2000).

The enzymatic antioxidant system of astrocytes includes other relevant enzymes besides GPx, such as SOD, CAT, peroxidases, and drug metabolizing enzymes as for example the NAD(P)H: quinone acceptor oxidoreductase 1 (NQO1) (Chen et al., 2020). NQO1 is a quinone reductase, mainly expressed in the cytosol and highly inducible when cellular adaptation to stress is needed. NQO1 can be efficiently inhibited by the anticoagulant dicoumarol and by other anti-cancer drugs (Pey et al., 2019). Several important functions have been reported but its efficiency at catalyzing the two-electron mediated reduction of quinone to hydroquinone is the best characterized (Ross and Siegel, 2017). This reduction of quinones to their respective hydroquinone prevents the formation of semiquinone radicals, which effects include redox cycling and oxidative stress (Ross et al., 1993; Rooseboom et al., 2004). However, there are cases where the instability of the generated hydroquinone leads to an enhancement of the cellular oxidative stress. This is the case of the reduction of β-lapachone by NQO1, which results in the formation of β -lapachol. β-lapachol is not chemical stable and auto-oxidizes back to β-lapachone with the formation of superoxide (Silvers et al., 2017; Steinmeier et al., 2020). Remarkably, this toxic activation seems to be the explanation to the beneficial effects observed after administration of β-lapachone in cancer studies. An extremely high expression of NQO1 in certain cancer lines and therefore, treatment with β-lapachone produces a severe oxidative stress in cancer cells, which finally leads to a reduction of the tumor (Kung et al., 2014; Li et al., 2014).

Recently, Dringen's group has demonstrated that the application of micromolar concentrations of β-lapachone to cultured astrocytes also induces severe oxidative stress and suggested this experimental setup for the study of acute oxidative stress in APCs (Steinmeier et al., 2020; Watermann and Dringen, 2023). With the results presented in this thesis, we aim at gaining insight into the ROS scavenging activity of CeONPs in astrocytes under oxidative stress conditions.

1.5.2 Glioma-cells

The C6 glioma cell-line is a rat tumor cell-line, which has been generated by exposition of rats to N-nitrosomethylurea (Benda et al., 1968). This tumor cell-line is characterized by a typical spindle-like morphology in culture, variably shaped nuclei and rapid proliferation (Giakoumettis et al., 2018) . C6 glioma cells are widely used as models for brain glioma cells (Grobben et al., 2002; Giakoumettis et al., 2018). Moreover, they are also used as an

astrocyte model system as they share common hallmarks as the expression of the astrocytic markers GFAP and S100B (although expressed in low amounts) and glutamine synthetase (Galland et al., 2019). The C6 glioma cell-line has been previously employed to assess NPs toxicity in glial cells (Joshi et al., 2019) and specifically to study their interaction with NPs (Joshi et al., 2016; Rastedt et al., 2017; Joshi et al., 2019).

The major disadvantage of using tumor cells is the uncontrolled presence of genetic aberrations, the altered metabolism and the miscommunication with other cells in comparison to healthy cells (Saeidnia et al., 2015). However, the establishment and maintenance of the cultures save an important amount of time, manpower and money. Besides, they offer more comparable results among different research groups as the cultures are homogeneous and well standardized (Zhao, 2023) .

1.5.3 Cell cultures as model systems for glial cells

Astrocyte primary cultures (APCs) constitute an isolated system to study these cells in their physiological and pathological states. Such cultures are enriched with astroglia cells *versus* other brain cells as confirmed by the immunostaining for GFAP. However, a reduced number of microglia, oligodendrocytes and neurons are usually present (Hamprecht and Löffler, 1985; Lange et al., 2012; Tulpule et al., 2014). Cultured astrocytes are most commonly prepared from brain tissue of newborn mice or rats (Hamprecht and Löffler, 1985; Tulpule et al., 2014) and grown until reaching confluence. In contrast, C6 glioma cell cultures are exclusively composed of one type of cells and duplicates their cell number within a day (Joshi et al., 2016) (Fig. 1.7).

Primary cultures as well as immortalized cell lines are a common and successful tool used to increase the knowledge about the individual functions, metabolism or physiology of the respective cells (Segeritz and Vallier, 2017) (Fig. 1.7). However, as the connection with other cell types are depleted, and therefore there are no modulating effects of neighboring cells, the results obtained reflect their individual biology. They represent a simplification of the system, which is required to gain knowledge about the individual impact of a treatment and to foresee the possible outcome in the whole system. Nevertheless, it is worthy to keep in mind that *in vitro* results obtained in cell culture models cannot be directly translated into *in vivo* systems (Lange et al., 2012)

C6 glioma cells

- Origin: rat glial tumor
- Immortalized cell line with chromosomal aberrations
- Duplication rate: 24 h
- Share morphological and metabolic hallmarks with astrocytes
- Expression of GFAP but to a lesser extent than APCs

Astrocyte-rich Primary Culture

- Origin: Brains of newborns Wistar rats (PD<24h)
- Seeding density 150,000 cells well^{-1}; confluent after ~ 10 days in 24-well plate
- ~95% of the cells express GFAP
- ~ 5% of other glial cells
- Life span for experimental porpoises: ~28 days

Figure 1.7. **Phase-contrast images of a representative C6 glioma and APCs culture used in the presented thesis.** The C6 glioma cells were allowed to proliferate for 24 hours and APCs for 16 days in cell culture medium containing fetal calf serum at 37°C and 10% CO_2 before being imaged with in the phase-contrast modus of an Eclipse TE2000-U microscope with a DS-QiMc camera and imaging software NIS-Elements BR (Nikon, Düsseldorf, Germany). The characteristics of the C6 glioma cells and APCs are listed in the corresponding box below the picture and were characterized by Joshi et al. (2016) and Tulpule et al. (2014), respectively. PD: postnatal day.

1.6 Aim of the thesis

CeONPs have been reported to show exceptional ROS scavenging potential in different *in vitro* (Cimini et al., 2012; Dowding et al., 2014; Guan et al., 2016) and *in vivo* systems (Kwon et al., 2016; Decouteau et al., 2016). This antioxidant power has also been observed to prevent or ameliorate certain specific deregulations of neurodegenerative diseases (Cimini et al., 2012; Dowding et al., 2014; Guan et al., 2016) alongside cancer (Reuter et al., 2010; Sosa et al., 2013; Hayes et al., 2020). A key feature of CeONPs is their ability to self-regenerate, which may be a significant development in antioxidant therapy. CeONPs have potential for being studied in relation to brain cells and oxidative stress. In this context, the present thesis utilizes CeONPs and ionic cerium on APCs and C6 glioma cells to explore their antioxidant activity.

To investigate the ability of CeONPs to scavenge ROS CeONPs in glial cells, in a first approach, a new functionalization of CeONPs with DMSA coating will be optimized. This coating will enable the fluorescent labeling of the NPs with Oregon Green dye (OG), allowing microscopic studies of their uptake and intracellular fate. Physicochemical properties, such as size, shape, and surface charge, will be characterized for DMSA-CeONPs and OG-DMSA-CeONPs, and compared to uncoated CeONPs. Time- and concentration-dependent studies will be conducted in C6 glioma cells and APCs to examine the biocompatibility of the new branded CeONPs. In this regard, experiments will be conducted to observe the uptake over time. The accumulation of intracellular cerium will also be determined after exploring the suitability of an ICP-OES method, which may reduce the per-sample analysis cost and the duration of the analysis compared to other techniques (e.g. ICP-MS or CLSM).

Subsequently, the effect of DMSA-CeONPs on the metabolism of APCs will be analyzed, with a particular emphasis on their glycolytic flux. Various exposure scenarios will be investigated, encompassing potential long-term effects once DMSA-CeONPs have been rinsed out. Comparative examinations will be carried out to differentiate the effects of exposing cultured astrocytes to nanoparticulate or ionic cerium (namely, $CeCl_3$ and $Ce(SO_4)_2$). Furthermore, mechanism of the cerium-induced alterations on the glucose metabolism of cultured astrocytes will be elucidated.

Lastly, the ability of DMSA-CeONPs to scavenge ROS will be investigated. To determine whether DMSA-CeONPs efficiently scavenge extracellular ROS, glial cells will be exposed to exogenous H_2O_2 or endogenous superoxide in the presence or absence of DMSA-CeONPs. and compared to the scavenging activity presented by ionic cerium, native catalase or superoxidase under identical conditions. It will be determined whether pre-incubation with DMSA-CeONPs improves protection against oxidative stress.

1.7 References

Abiade, J. T., W. Choi and R. K. Singh (2005). "Effect of pH on ceria-silica interactions during chemical mechanical polishing." Journal of Materials Research 20(5): 1139-1145.

Abid, N., A. M. Khan, S. Shujait, K. Chaudhary, M. Ikram, M. Imran, J. Haider, M. Khan, Q. Khan and M. Maqbool (2022). "Synthesis of nanomaterials using various top-down and bottom-up approaches, influencing factors, advantages, and disadvantages: A review." Advances in Colloid and Interface Science 300: 102597.

Abu Lila, A. S., H. Kiwada and T. Ishida (2013). "The accelerated blood clearance (ABC) phenomenon: Clinical challenge and approaches to manage." Journal of Controlled Release 172(1): 38-47.

Abulateefeh, S. R., S. G. Spain, K. J. Thurecht, J. W. Aylott, W. C. Chan, M. C. Garnett and C. Alexander (2013). "Enhanced uptake of nanoparticle drug carriers via a thermoresponsive shell enhances cytotoxicity in a cancer cell line." Biomaterials Science 1(4): 434-442.

Acebes-Fernández, V., A. Landeira-Viñuela, P. Juanes-Velasco, A.-P. Hernández, A. Otazo-Perez, R. Manzano-Román, R. Gongora and M. Fuentes (2020). "Nanomedicine and onco-immunotherapy: from the bench to bedside to biomarkers." Nanomaterials 10(7): 1274.

Ahmadi, M. H., M. Ghazvini, M. A. Nazari, M. A. Ahmadi, F. Pourfayaz, G. Lorenzini and T. Z. Ming (2019). "Renewable energy harvesting with the application of nanotechnology: A review." International Journal of Energy Research 43(4): 1387-1410.

Alconcel, S. N. S., A. S. Baas and H. D. Maynard (2011). "FDA-approved poly(ethylene glycol)-protein conjugate drugs." Polymer Chemistry 2(7): 1442-1448.

Alili, L., M. Sack, A. S. Karakoti, S. Teuber, K. Puschmann, S. M. Hirst, C. M. Reilly, K. Zanger, W. Stahl and S. Das (2011). "Combined cytotoxic and anti-invasive properties of redox-active nanoparticles in tumor–stroma interactions." Biomaterials 32(11): 2918-2929.

Allen, J., S. Oh, O. Gunnarsson, K. Schönhammer, M. Maple, M. Torikachvili and I. Lindau (1986). "Electronic structure of cerium and light rare-earth intermetallics." Advances in Physics 35(3): 275-316.

Allen, N. J. and B. A. Barres (2009). "Glia—more than just brain glue." Nature 457(7230): 675-677.

Andersen, J. V. and A. Schousboe (2023). "Milestone review: Metabolic dynamics of glutamate and GABA mediated neurotransmission—The essential roles of astrocytes." Journal of Neurochemistry 166(2): 109-137.

Araque, A. and M. Navarrete (2010). "Glial cells in neuronal network function." Philosophical Transactions of the Royal Society B: Biological Sciences 365(1551): 2375-2381.

Arendt, D., A. S. Denes, G. Jékely and K. Tessmar-Raible (2008). "The evolution of nervous system centralization." Philosophical Transactions of the Royal Society B: Biological Sciences 363(1496): 1523-1528.

Asati, A., C. Kaittanis, S. Santra and J. M. Perez (2011). "pH-tunable oxidase-like activity of cerium oxide nanoparticles achieving sensitive fluorigenic detection of cancer biomarkers at neutral pH." Analytical hemistry 83(7): 2547-2553.

Asati, A., S. Santra, C. Kaittanis and J. M. Perez (2010). "Surface-charge-dependent cell localization and cytotoxicity of cerium oxide nanoparticles." ACS Nano 4(9): 5321-5331.

Astruc, D. (2020). "Introduction: Nanoparticles in catalysis." Chemical Reviews 120(2): 461-463.

Babu, S., A. Velez, K. Wozniak, J. Szydlowska and S. Seal (2007). "Electron paramagnetic study on radical scavenging properties of ceria nanoparticles." Chemical Physics Letters 442(4-6): 405-408.

Baev, A. Y., A. Y. Vinokurov, I. N. Novikova, V. V. Dremin, E. V. Potapova and A. Y. Abramov (2022). "Interaction of mitochondrial calcium and ROS in neurodegeneration." Cells 11(4): 706.

Bailey, Z. S., E. Nilson, J. A. Bates, A. Oyalowo, K. S. Hockey, V. S. S. S. Sajja, C. Thorpe, H. Rogers, B. Dunn and A. S. Frey (2020). "Cerium oxide nanoparticles improve outcome after in vitro and in vivo mild traumatic brain injury." Journal of Neurotrauma 37(12): 1452-1462.

Balaram, V. (2019). "Rare earth elements: A review of applications, occurrence, exploration, analysis, recycling, and environmental impact." Geoscience Frontiers 10(4): 1285-1303.

Baratoff, A. (1986). "1986 Nobel Prizes Development of Scanning Tunnelling Microscopy." Europhysics News 17(11-12): 141-144.

Barber, D. J. and I. C. Freestone (1990). "An investigation of the origin of the color of the Lycurgus Cup by analytical transmission electron-microscopy." Archaeometry 32: 33-45.

Bärnighausen, H. and G. Schiller (1985). "The crystal structure of A-Ce_2O_3." Journal of the Less Common Metals 110(1-2): 385-390.

Barros, L., R. Courjaret, P. Jakoby, A. Loaiza, C. Lohr and J. Deitmer (2009). "Preferential transport and metabolism of glucose in Bergmann glia over Purkinje cells: a multiphoton study of cerebellar slices." Glia 57(9): 962-970.

Barros, L. and B. Weber (2018). "CrossTalk proposal: an important astrocyte-to-neuron lactate shuttle couples neuronal activity to glucose utilisation in the brain." The Journal of Physiology 596(3): 347.

Barros, L. and B. Weber (2018). "Rebuttal from LF Barros and B Weber." The Journal of Physiology 596(3): 355.

Barros, L. F. and J. W. Deitmer (2010). "Glucose and lactate supply to the synapse." Brain Research Reviews 63(1-2): 149-159.

Barros, L. F., A. San Martín, I. Ruminot, P. Y. Sandoval, F. Baeza-Lehnert, R. Arce-Molina, D. Rauseo, Y. Contreras-Baeza, A. Galaz and S. Valdivia (2020). "Fluid brain glycolysis: limits, speed, location, moonlighting, and the fates of glycogen and lactate." Neurochemical Research 45(6): 1328-1334.

Benda, P., J. Lightbody, G. Sato, L. Levine and W. Sweet (1968). "Differentiated rat glial cell strain in tissue culture." Science 161(3839): 370-371.

Bertorelle, F., C. Wilhelm, J. Roger, F. Gazeau, C. Ménager and V. Cabuil (2006). "Fluorescence-modified superparamagnetic nanoparticles: intracellular uptake and use in cellular imaging." Langmuir 22(12): 5385-5391.

Bhirde, A., J. Xie, M. Swierczewska and X. Chen (2011). "Nanoparticles for cell labeling." Nanoscale 3(1): 142-153.

Bolaños, J. P. (2016). "Bioenergetics and redox adaptations of astrocytes to neuronal activity." Journal of Neurochemistry 139: 115-125.

Bosworth, A. P. and N. J. Allen (2017). "The diverse actions of astrocytes during synaptic development." Current Opinion in Neurobiology 47: 38-43.

Boussouar, F. and M. Benahmed (2004). "Lactate and energy metabolism in male germ cells." Trends in Endocrinology and Metabolism 15(7): 345-350.

Bouzier-Sore, A.-K. and J. P. Bolaños (2015). "Uncertainties in pentose-phosphate pathway flux assessment underestimate its contribution to neuronal glucose consumption: relevance for neurodegeneration and aging." Frontiers in Aging Neuroscience 7: 89.

Breitenfeld, T., M. Jurasic and D. Breitenfeld (2014). "Hippocrates: the forefather of neurology." Neurological Sciences 35(9): 1349-1352.

Breznica, P., R. Koliqi and A. Daka (2020). "A review of the current understanding of nanoparticles protein corona composition." Medicine and Pharmacy Reports 93(4): 342.

Casals, E., M. Zeng, M. Parra-Robert, G. Fernández-Varo, M. Morales-Ruiz, W. Jiménez, V. Puntes and G. Casals (2020). "Cerium oxide nanoparticles: advances in biodistribution, toxicity, and preclinical exploration." Small 16(20): 1907322.

Celardo, I., J. Z. Pedersen, E. Traversa and L. Ghibelli (2011). "Pharmacological potential of cerium oxide nanoparticles." Nanoscale 3(4): 1411-1420.

Chanana, M. and L. M. Liz-Marzan (2012). "Coating matters: the influence of coating materials on the optical properties of gold nanoparticles." Nanophotonics 1(3-4): 199-220.

Chen, D., S. Ganesh, W. Wang and M. Amiji (2017). "Plasma protein adsorption and biological identity of systemically administered nanoparticles." Nanomedicine: Nanotechnology, Biology, and Medicine 12(17): 2113-2135.

Chen, L., P. Fleming, V. Morris, J. D. Holmes and M. A. Morris (2010). "Size-related lattice parameter changes and surface defects in ceria nanocrystals." The Journal of Physical Chemistry C 114(30): 12909-12919.

Chen, Y., C. Qin, J. Huang, X. Tang, C. Liu, K. Huang, J. Xu, G. Guo, A. Tong and L. Zhou (2020). "The role of astrocytes in oxidative stress of central nervous system: A mixed blessing." Cell Proliferation 53(3): e12781.

Cheng, H., S. Lin, F. Muhammad, Y.-W. Lin and H. Wei (2016). "Rationally modulate the oxidase-like activity of nanoceria for self-regulated bioassays." ACS Sensors 1(11): 1336-1343.

Chih, C.-P., P. Lipton and E. L. Roberts Jr (2001). "Do active cerebral neurons really use lactate rather than glucose?" Trends in Neurosciences 24(10): 573-578.

Chuquet, J., P. Quilichini, E. A. Nimchinsky and G. Buzsáki (2010). "Predominant enhancement of glucose uptake in astrocytes versus neurons during activation of the somatosensory cortex." Journal of Neuroscience 30(45): 15298-15303.

Cimini, A., B. D'Angelo, S. Das, R. Gentile, E. Benedetti, V. Singh, A. M. Monaco, S. Santucci and S. Seal (2012). "Antibody-conjugated PEGylated cerium oxide nanoparticles for specific targeting of Aβ aggregates modulate neuronal survival pathways." Acta Biomaterialia 8(6): 2056-2067.

Conesa, J. (1995). "Computer modeling of surfaces and defects on cerium dioxide." Surface Science 339(3): 337-352.

Cooper, G. M. (2000). The central role of enzymes as biological catalysts, Sinauer Associates.

Cordelli, E., J. Keller, P. Eleuteri, P. Villani, L. Ma-Hock, M. Schulz, R. Landsiedel and F. Pacchierotti (2017). "No genotoxicity in rat blood cells upon 3-or 6-month inhalation exposure to CeO_2 or $BaSO_4$ nanomaterials." Mutagenesis 32(1): 13-22.

Corsi, F., G. Deidda Tarquini, M. Urbani, I. Bejarano, E. Traversa and L. Ghibelli (2023). "The impressive anti-inflammatory activity of cerium oxide nanoparticles: more than redox?" Nanomaterials 13(20): 2803.

Cuellar-Santoyo, A. O., V. M. Ruiz-Rodríguez, T. B. Mares-Barbosa, A. Patrón-Soberano, A. G. Howe, D. P. Portales-Pérez, A. Miquelajáuregui Graf and A. M. Estrada-Sánchez (2023). "Revealing the contribution of astrocytes to glutamatergic neuronal transmission." Frontiers in Cellular Neuroscience 16: 1037641.

Cuenya, B. R. (2010). "Synthesis and catalytic properties of metal nanoparticles: Size, shape, support, composition, and oxidation state effects." Thin Solid Films 518(12): 3127-3150.

Curl Jr, R. F., H. Kroto, R. E. Smalley, R. F. Curl Jr and H. W. Kroto "The Nobel Prize in Chemistry 1996 Explore Press Release."

D'Hollander, A., G. Vande Velde, H. Jans, B. Vanspauwen, E. Vermeersch, J. Jose, T. Struys, T. Stakenborg, L. Lagae and U. Himmelreich (2020). "Assessment of the theranostic potential of gold nanostars—A multimodal imaging and photothermal treatment study." Nanomaterials 10(11): 2112.

da Fano, C. (1926). "Prof. Camillo Golgi." Nature 117(2936): 203-203.

da Mata, L. R., L. D. dos Santos and M. de Cerqueira Cesar (2023). "Hexokinase and glycolysis: between brain cells life and death." Current Chemical Biology 17(2): 91-123.

Dale, J. G., S. S. Cox, M. E. Vance, L. C. Marr and M. F. Hochella Jr (2017). "Transformation of cerium oxide nanoparticles from a diesel fuel additive during combustion in a diesel engine." Environmental Science & Technology 51(4): 1973-1980.

Das, J., Y.-J. Choi, J. W. Han, A. M. M. T. Reza and J.-H. Kim (2017). "Nanoceria-mediated delivery of doxorubicin enhances the anti-tumour efficiency in ovarian cancer cells via apoptosis." Scientific Reports 7(1): 1-12.

Das, M., S. Patil, N. Bhargava, J. F. Kang, L. M. Riedel, S. Seal and J. J. Hickman (2007). "Auto-catalytic ceria nanoparticles offer neuroprotection to adult rat spinal cord neurons." Biomaterials 28(10): 1918-1925.

Debernardi, R., K. Pierre, S. Lengacher, P. J. Magistretti and L. Pellerin (2003). "Cell-specific expression pattern of monocarboxylate transporters in astrocytes and neurons observed in different mouse brain cortical cell cultures." Journal of Neuroscience Research 73(2): 141-155.

DeCoteau, W., K. L. Heckman, A. Y. Estevez, K. J. Reed, W. Costanzo, D. Sandford, P. Studlack, J. Clauss, E. Nichols and J. Lipps (2016). "Cerium oxide nanoparticles with antioxidant properties ameliorate strength and prolong life in mouse model of amyotrophic lateral sclerosis." Nanomedicine: Nanotechnology, Biology and Medicine 12(8): 2311-2320.

Della Mea, G. B., L. P. Matte, A. S. Thill, F. O. Lobato, E. V. Benvenutti, L. T. Arenas, A. Jürgensen, R. Hergenröder, F. Poletto and F. Bernardi (2017). "Tuning the oxygen vacancy population of cerium oxide (CeO_{2-x}, $0<x<0.5$) nanoparticles." Applied Surface Science 422: 1102-1112.

Dey, S. and G. C. Dhal (2019). "Materials progress in the control of CO and CO_2 emission at ambient conditions: an overview." Materials Science for Energy Technologies 2(3): 607-623.

Díaz-García, C. M., R. Mongeon, C. Lahmann, D. Koveal, H. Zucker and G. Yellen (2017). "Neuronal stimulation triggers neuronal glycolysis and not lactate uptake." Cell Metabolism 26(2): 361-374. e364.

Díaz-García, C. M. and G. Yellen (2019). "Neurons rely on glucose rather than astrocytic lactate during stimulation." Journal of Neuroscience Research 97(8): 883-889.

Dienel, G. A. (2017). "Lack of appropriate stoichiometry: Strong evidence against an energetically important astrocyte–neuron lactate shuttle in brain." Journal of Neuroscience Research 95(11): 2103-2125.

Dienel, G. A. (2019). "Brain glucose metabolism: integration of energetics with function." Physiological Reviews 99(1): 949-1045.

Dienel, G. A. and N. F. Cruz (2015). "Contributions of glycogen to astrocytic energetics during brain activation." Metabolic Brain Disease 30(1): 281-298.

Dietrich, J. S. (1986). "Tiny tale gets grand." Engineering and Science 49(3): 25-26.

Dominguez-Medina, S., L. Kisley, L. J. Tauzin, A. Hoggard, B. Shuang, A. S. DS Indrasekara, S. Chen, L.-Y. Wang, P. J. Derry and A. Liopo (2016). "Adsorption and unfolding of a single protein triggers nanoparticle aggregation." ACS Nano 10(2): 2103-2112.

Dowding, J., W. Song, K. Bossy, A. Karakoti, A. Kumar, A. Kim, B. Bossy, S. Seal, M. Ellisman and G. Perkins (2014). "Cerium oxide nanoparticles protect against Aβ-induced mitochondrial fragmentation and neuronal cell death." Cell Death and Differentiation 21(10): 1622-1632.

Dowding, J. M., S. Das, A. Kumar, T. Dosani, R. McCormack, A. Gupta, T. X. Sayle, D. C. Sayle, L. von Kalm and S. Seal (2013). "Cellular interaction and toxicity depend on physicochemical properties and surface modification of redox-active nanomaterials." ACS Nano 7(6): 4855-4868.

Dowding, J. M., T. Dosani, A. Kumar, S. Seal and W. T. Self (2012). "Cerium oxide nanoparticles scavenge nitric oxide radical ($^{.}NO$)." Chemical Communications 48(40): 4896-4898.

Dowding, J. M., S. Seal and W. T. Self (2013). "Cerium oxide nanoparticles accelerate the decay of peroxynitrite ($ONOO^{-}$)." Drug Delivery and Translational Research 3(4): 375-379.

Drexler, E. (1987). Engines of Creation: The Coming Era of Nanotechnology, Anchor.

Dringen, R. (2000). "Metabolism and functions of glutathione in brain." Progress in Neurobiology 62(6): 649-671.

Dringen, R., M. Brandmann, M. C. Hohnholt and E.-M. Blumrich (2015). "Glutathione-dependent detoxification processes in astrocytes." Neurochemical Research 40(12): 2570-2582.

Dringen, R., R. Gebhardt and B. Hamprecht (1993). "Glycogen in astrocytes: possible function as lactate supply for neighboring cells." Brain Research 623(2): 208-214.

Dringen, R., H. H. Hoepken, T. Minich and C. Ruedig (2007). Pentose phosphate pathway and NADPH metabolism. Handbook of neurochemistry and molecular neurobiology: brain energetics. Integration of molecular and cellular processes, Springer**:** 41-62.

Edvinsson, T. (2018). "Optical quantum confinement and photocatalytic properties in two-, one-and zero-dimensional nanostructures." Royal Society Open Science 5(9): 180387.

Etheridge, M. L., S. A. Campbell, A. G. Erdman, C. L. Haynes, S. M. Wolf and J. McCullough (2013). "The big picture on nanomedicine: the state of investigational and approved nanomedicine products." Nanomedicine: Nanotechnology, Biology, and Medicine 9(1): 1-14.

Feliu, N., D. Docter, M. Heine, P. Del Pino, S. Ashraf, J. Kolosnjaj-Tabi, P. Macchiarini, P. Nielsen, D. Alloyeau and F. Gazeau (2016). "*In vivo* degeneration and the fate of inorganic nanoparticles." Chemical Society Reviews 45(9): 2440-2457.

Feng, X. D., Y. S. Her, W. L. Zhang, J. Davis, E. Oswald, J. Lu, V. Bryg, S. Freeman and D. Gnizak (2003). "CeO_2 particles for chemical mechanical planarization." Chemical-Mechanical Planarization 767: 173-183.

Fernández-Varo, G., M. Perramón, S. Carvajal, D. Oró, E. Casals, L. Boix, L. Oller, L. Macías-Muñoz, S. Marfà and G. Casals (2020). "Bespoken nanoceria: An effective treatment in experimental hepatocellular carcinoma." Hepatology 72(4): 1267-1282.

Feynman, R. P. (1959). "There's plenty of room at the bottom." Engineering and science 23(5).

Feynman, R. P. (1960). "There's plenty of room at the bottom - An invitation to enter a new field of physics." Engineering and Science 23(5): 22-36.

Filippi, A., F. Liu, J. Wilson, S. Lelieveld, K. Korschelt, T. Wang, Y. Wang, T. Reich, U. Pöschl and W. Tremel (2019). "Antioxidant activity of cerium dioxide nanoparticles and nanorods in scavenging hydroxyl radicals." RSC Advances 9(20): 11077-11081.

Fiorani, L., M. Passacantando, S. Santucci, S. Di Marco, S. Bisti and R. Maccarone (2015). "Cerium oxide nanoparticles reduce microglial activation and neurodegenerative events in light damaged retina." PloS One 10(10): e0140387.

Fisichella, M., F. Berenguer, G. Steinmetz, M. Auffan, J. Rose and O. Prat (2014). "Toxicity evaluation of manufactured CeO_2 nanoparticles before and after alteration: combined physicochemical and whole-genome expression analysis in Caco-2 cells." BMC Genomics 15(1): 1-15.

Forest, V., L. Leclerc, J.-F. Hochepied, A. Trouvé, G. Sarry and J. Pourchez (2017). "Impact of cerium oxide nanoparticles shape on their in vitro cellular toxicity." Toxicology In Vitro 38: 136-141.

Fu, X., J. Cai, X. Zhang, W.-D. Li, H. Ge and Y. Hu (2018). "Top-down fabrication of shape-controlled, monodisperse nanoparticles for biomedical applications." Advanced Drug Delivery Reviews 132: 169-187.

Fukai, T. and M. Ushio-Fukai (2011). "Superoxide dismutases: role in redox signaling, vascular function, and diseases." Antioxidants & Redox Signaling 15(6): 1583-1606.

Furman, D., J. Campisi, E. Verdin, P. Carrera-Bastos, S. Targ, C. Franceschi, L. Ferrucci, D. W. Gilroy, A. Fasano and G. W. Miller (2019). "Chronic inflammation in the etiology of disease across the life span." Nature Medicine 25(12): 1822-1832.

Fytianos, G., A. Rahdar and G. Z. Kyzas (2020). "Nanomaterials in cosmetics: recent updates." Nanomaterials 10(5).

Galland, F., M. Seady, J. Taday, S. S. Smaili, C. A. Gonçalves and M. C. Leite (2019). "Astrocyte culture models: Molecular and function characterization of primary culture, immortalized astrocytes and C6 glioma cells." Neurochemistry International 131: 104538.

Ganduglia-Pirovano, M. V., J. L. F. Da Silva and J. Sauer (2009). "Density-functional calculations of the structure of near-surface oxygen vacancies and electron localization on $CeO_2(111)$." Physical Review Letters 102(2).

Gangopadhyay, S., D. D. Frolov, A. E. Masunov and S. Seal (2014). "Structure and properties of cerium oxides in bulk and nanoparticulate forms." Journal of Alloys and Compounds 584: 199-208.

Gao, D., J. Zhang, G. Yang, J. Zhang, Z. Shi, J. Qi, Z. Zhang and D. Xue (2010). "Ferromagnetism in ZnO nanoparticles induced by doping of a nonmagnetic element: Al." The Journal of Physical Chemistry C 114(32): 13477-13481.

Gao, L., J. Zhuang, L. Nie, J. Zhang, Y. Zhang, N. Gu, T. Wang, J. Feng, D. Yang and S. Perrett (2007). "Intrinsic peroxidase-like activity of ferromagnetic nanoparticles." Nature Nanotechnology 2(9): 577-583.

Gao, S., D. Yu, S. Zhou, C. Zhang, L. Wang, X. Fan, X. Yu and Z. Zhao (2023). "Construction of cerium-based oxide catalysts with abundant defects/vacancies and their application to catalytic elimination of air pollutants." Journal of Materials Chemistry A 11(36): 19210-19243.

Ghadimi, M., S. Zangenehtabar and S. Homaeigohar (2020). "An overview of the water remediation potential of nanomaterials and their ecotoxicological impacts." Water 12(4).

Giakoumettis, D., A. Kritis and N. Foroglou (2018). "C6 cell line: the gold standard in glioma research." Hippokratia 22(3): 105.

Gibbs, M. E. and D. S. Hutchinson (2012). "Rapid turnover of glycogen in memory formation." Neurochemical Research 37(11): 2456-2463.

Gibbs, M. E., H. G. Lloyd, T. Santa and L. Hertz (2007). "Glycogen is a preferred glutamate precursor during learning in 1-day-old chick: Biochemical and behavioral evidence." Journal of Neuroscience Research 85(15): 3326-3333.

Gilbertson, L. M., L. Pourzahedi, S. Laughton, X. Y. Gao, J. B. Zimmerman, T. L. Theis, P. Westerhoff and G. V. Lowry (2020). "Guiding the design space for nanotechnology to advance sustainable crop production." Nature Nanotechnology 15(9): 801-+.

Giri, S., A. Karakoti, R. P. Graham, J. L. Maguire, C. M. Reilly, S. Seal, R. Rattan and V. Shridhar (2013). "Nanoceria: a rare-earth nanoparticle as a novel anti-angiogenic therapeutic agent in ovarian cancer." PloS One 8(1): e54578.

Golgi, C. (1870). "Sulla sostanza connettiva del cervello (nevroglia)." Rendiconti del R Instituto Lombardo di Scienze e Lettere 3: 275-277.

Gonçalves, C.-A., L. Rodrigues, L. D. Bobermin, C. Zanotto, A. Vizuete, A. Quincozes-Santos, D. O. Souza and M. C. Leite (2019). "Glycolysis-derived compounds from astrocytes that modulate synaptic communication." Frontiers in Neuroscience: 1035.

Gong, S. and W. L. Cheng (2017). "One-dimensional nanomaterials for soft electronics." Advanced Electronic Materials 3(3).

Grobben, B., P. De Deyn and H. Slegers (2002). "Rat C6 glioma as experimental model system for the study of glioblastoma growth and invasion." Cell and Tissue Research 310(3): 257-270.

Guan, Y., M. Li, K. Dong, N. Gao, J. Ren, Y. Zheng and X. Qu (2016). "Ceria/POMs hybrid nanoparticles as a mimicking metallopeptidase for treatment of neurotoxicity of amyloid-β peptide." Biomaterials 98: 92-102.

Guo, W., M. Zhang, Z. Lou, M. Zhou, P. Wang and H. Wei (2019). "Engineering nanoceria for enhanced peroxidase mimics: A solid solution strategy." ChemCatChem 11(2): 737-743.

Hadjidemetriou, M. and K. Kostarelos (2017). "Evolution of the nanoparticle corona." Nature Nanotechnology 12(4): 288-290.

Hajjiah, A., E. Samir, N. Shehata and M. Salah (2018). "Lanthanide-doped ceria nanoparticles as backside coaters to improve silicon solar cell efficiency." Nanomaterials 8(6).

Halim, N. D., T. Mcfate, A. Mohyeldin, P. Okagaki, L. G. Korotchkina, M. S. Patel, N. H. Jeoung, R. A. Harris, M. J. Schell and A. Verma (2010). "Phosphorylation status of pyruvate dehydrogenase distinguishes metabolic phenotypes of cultured rat brain astrocytes and neurons." Glia 58(10): 1168-1176.

Hamm, C. M., L. Alff and B. Albert (2014). "Synthesis of microcrystalline Ce_2O_3 and formation of solid solutions between cerium and lanthanum oxides." Zeitschrift fur Anorganische und Allgemeine Chemie 640(6): 1050-1053.

Hamprecht, B. and F. Löffler (1985). [27] Primary glial cultures as a model for studying hormone action. Methods in Enzymology, Elsevier. 109: 341-345.

Hansen, S. F., O. F. H. Hansen and M. B. Nielsen (2020). "Advances and challenges towards consumerization of nanomaterials." Nature Nanotechnology 15(12): 964-965.

Hao, X., S. Zhang, Y. Xu, L. Tang, K. Inoue, M. Saito, S. Ma, C. Chen, B. Xu and T. Adschiri (2021). "Surfactant-mediated morphology evolution and self-assembly of cerium oxide nanocrystals for catalytic and supercapacitor applications." Nanoscale 13(23): 10393-10401.

Harb, S. V., A. Trentin, T. A. C. de Souza, M. Magnani, S. H. Pulcinelli, C. V. Santilli and P. Hammer (2020). "Effective corrosion protection by eco-friendly self-healing PMMA-cerium oxide coatings." Chemical Engineering Journal 383: 123219.

Harish, V., D. Tewari, M. Gaur, A. B. Yadav, S. Swaroop, M. Bechelany and A. Barhoum (2022). "Review on nanoparticles and nanostructured materials: Bioimaging, biosensing, drug delivery, tissue engineering, antimicrobial, and agro-food applications." Nanomaterials 12(3): 457.

Harris, W. J., M.-C. Asselin, R. Hinz, L. M. Parkes, S. Allan, I. Schiessl, H. Boutin and B. R. Dickie (2023). "In vivo methods for imaging blood–brain barrier function and dysfunction." European Journal of Nuclear Medicine and Molecular Imaging 50(4): 1051-1083.

Haruta, M., T. Kobayashi, H. Sano and N. Yamada (1987). "Novel gold catalysts for the oxidation of carbon monoxide at a temperature far below 0°C." Chemistry Letters 16(2): 405-408.

Hayat, A., J. Cunningham, G. Bulbul and S. Andreescu (2015). "Evaluation of the oxidase like activity of nanoceria and its application in colorimetric assays." Analytica Chimica Acta 885: 140-147.

Hayes, J. D., A. T. Dinkova-Kostova and K. D. Tew (2020). "Oxidative stress in cancer." Cancer Cell 38(2): 167-197.

Heckert, E. G., A. S. Karakoti, S. Seal and W. T. Self (2008). "The role of cerium redox state in the SOD mimetic activity of nanoceria." Biomaterials 29(18): 2705-2709.

Heckman, K. L., A. Y. Estevez, W. DeCoteau, S. Vangellow, S. Ribeiro, J. Chiarenzelli, B. Hays-Erlichman and J. S. Erlichman (2020). "Variable in vivo and in vitro biological effects of cerium oxide nanoparticle formulations." Frontiers in Pharmacology: 1599.

Heithoff, B. P., K. K. George, A. N. Phares, I. A. Zuidhoek, C. Munoz-Ballester and S. Robel (2021). "Astrocytes are necessary for blood–brain barrier maintenance in the adult mouse brain." Glia 69(2): 436-472.

Herper, H. C., O. Y. Vekilova, S. I. Simak, I. Di Marco and O. Eriksson (2020). "Localized versus itinerant character of 4f-states in cerium oxides." Journal of Physics: Condensed Matter 32(21): 215502.

Herrero-Mendez, A., A. Almeida, E. Fernández, C. Maestre, S. Moncada and J. P. Bolaños (2009). "The bioenergetic and antioxidant status of neurons is controlled by continuous degradation of a key glycolytic enzyme by APC/C–Cdh1." Nature Cell Biology 11(6): 747-752.

Hertz, L., R. Dringen, A. Schousboe and S. R. Robinson (1999). "Astrocytes: glutamate producers for neurons." Journal of Neuroscience Research 57(4): 417-428.

Heuer-Jungemann, A., N. Feliu, I. Bakaimi, M. Hamaly, A. Alkilany, I. Chakraborty, A. Masood, M. F. Casula, A. Kostopoulou and E. Oh (2019). "The role of ligands in the chemical synthesis and applications of inorganic nanoparticles." Chemical Reviews 119(8): 4819-4880.

Hijaz, M., S. Das, I. Mert, A. Gupta, Z. Al-Wahab, C. Tebbe, S. Dar, J. Chhina, S. Giri and A. Munkarah (2016). "Folic acid tagged nanoceria as a novel therapeutic agent in ovarian cancer." BMC Cancer 16(1): 1-14.

Huang, L. and H. Lu (2019). "Electronic structure of cerium: a comprehensive first-principles study." Physical Review B 99(4): 045122.

Huang, Y.-W., M. Cambre and H.-J. Lee (2017). "The toxicity of nanoparticles depends on multiple molecular and physicochemical mechanisms." International Journal of Molecular Sciences 18(12): 2702.

Huang, Y., M. Zhang, M. Jin, T. Ma, J. Guo, X. Zhai and Y. Du (2023). "Recent advances on cerium oxide-based biomaterials: toward the next generation of intelligent theranostics platforms." Advanced Healthcare Materials 12(25): 2300748.

Hussain, S., F. Al-Nsour, A. B. Rice, J. Marshburn, B. Yingling, Z. Ji, J. I. Zink, N. J. Walker and S. Garantziotis (2012). "Cerium dioxide nanoparticles induce apoptosis and autophagy in human peripheral blood monocytes." ACS Nano 6(7): 5820-5829.

Hussain, T., B. Tan, Y. Yin, F. Blachier, M. C. Tossou and N. Rahu (2016). "Oxidative stress and inflammation: what polyphenols can do for us?" Oxidative Medicine and Cellular Longevity 2016.

Iijima, S. and T. Ichihashi (1993). "Single-shell carbon nanotubes of 1-nm diameter." Nature 363(6430): 603-605.

Inshakova, E., A. Inshakova and A. Goncharov (2020). "Engineered nanomaterials for energy sector: Market trends, modern applications and future prospects." IOP Conference Series: Materials Science and Engineering 971(3): 032031.

ISO/TR 18401:2017 (2017). "Plain language explanation of selected terms from the ISO/IEC 80004 series." International Organization for Standardization, Geneva.

Jakoby, P., E. Schmidt, I. Ruminot, R. Gutiérrez, L. F. Barros and J. W. Deitmer (2014). "Higher transport and metabolism of glucose in astrocytes compared with neurons: a multiphoton study of hippocampal and cerebellar tissue slices." Cerebral Cortex 24(1): 222-231.

Jamkhande, P. G., N. W. Ghule, A. H. Bamer and M. G. Kalaskar (2019). "Metal nanoparticles synthesis: An overview on methods of preparation, advantages and disadvantages, and applications." Journal of Drug Delivery Science and Technology 53: 101174.

Jana, S. K., P. Banerjee, S. Das, S. Seal and K. Chaudhury (2014). "Redox-active nanoceria depolarize mitochondrial membrane of human colon cancer cells." Journal of Nanoparticle Research 16(6): 1-9.

Jeevanandam, J., A. Barhoum, Y. S. Chan, A. Dufresne and M. K. Danquah (2018). "Review on nanoparticles and nanostructured materials: history, sources, toxicity and regulations." Beilstein Journal of Nanotechnology 9: 1050-1074.

Jeong, W.-j., J. Bu, L. J. Kubiatowicz, S. S. Chen, Y. Kim and S. Hong (2018). "Peptide–nanoparticle conjugates: a next generation of diagnostic and therapeutic platforms?" Nano Convergence 5(1): 1-18.

Jiang, J., G. Oberdörster and P. Biswas (2009). "Characterization of size, surface charge, and agglomeration state of nanoparticle dispersions for toxicological studies." Journal of Nanoparticle Research 11(1): 77-89.

Jiao, X., H. Song, H. Zhao, W. Bai, L. Zhang and Y. Lv (2012). "Well-redispersed ceria nanoparticles: promising peroxidase mimetics for $H2O_2$ and glucose detection." Analytical Methods 4(10): 3261-3267.

Joshi, A., W. Rastedt, K. Faber, A. G. Schultz, F. Bulcke and R. Dringen (2016). "Uptake and toxicity of copper oxide nanoparticles in C6 glioma cells." Neurochemical Research 41(11): 3004-3019.

Joshi, A., K. Thiel, K. Jog and R. Dringen (2019). "Uptake of intact copper oxide nanoparticles causes acute toxicity in cultured glial cells." Neurochemical Research 44(9): 2156-2169.

Kalashnikova, I., J. Mazar, C. J. Neal, A. L. Rosado, S. Das, T. J. Westmoreland and S. Seal (2017). "Nanoparticle delivery of curcumin induces cellular hypoxia and ROS-mediated apoptosis via modulation of Bcl-2/Bax in human neuroblastoma." Nanoscale 9(29): 10375-10387.

Kandel, E. R., J. H. Schwartz, T. M. Jessell, S. Siegelbaum, A. J. Hudspeth and S. Mack (2000). Principles of Neural Science, McGraw-Hill New York.

Karakoti, A., S. Singh, J. M. Dowding, S. Seal and W. T. Self (2010). "Redox-active radical scavenging nanomaterials." Chemical Society Reviews 39(11): 4422-4432.

Karakoti, A. S., S. Das, S. Thevuthasan and S. Seal (2011). "PEGylated inorganic nanoparticles." Angewandte Chemie International Edition 50(9): 1980-1994.

Karim, M. N., S. R. Anderson, S. Singh, R. Ramanathan and V. Bansal (2018). "Nanostructured silver fabric as a free-standing NanoZyme for colorimetric detection of glucose in urine." Biosensors and Bioelectronics 110: 8-15.

Kim, J., G. Hong, L. Mazaleuskaya, J. C. Hsu, D. N. Rosario-Berrios, T. Grosser, P. F. Cho-Park and D. P. Cormode (2021). "Ultrasmall Antioxidant Cerium Oxide Nanoparticles for Regulation of Acute Inflammation." ACS Applied Materials & Interfaces.

Koepsell, H. (2020). "Glucose transporters in brain in health and disease." Pflügers Archiv-European Journal of Physiology 472(9): 1299-1343.

Köhler, S., U. Winkler and J. Hirrlinger (2021). "Heterogeneity of astrocytes in grey and white matter." Neurochemical Research 46(1): 3-14.

Köhler, S., U. Winkler, T. Junge, K. Lippmann, J. Eilers and J. Hirrlinger (2023). "Gray and white matter astrocytes differ in basal metabolism but respond similarly to neuronal activity." Glia 71(2): 229-244.

Kontham, S., K. Mandava, S. Dosa, F. U. Mohd, O. A. Mohammed and A. U. Mohammad (2021). "Review on facile synthesis of cerium oxide nanoparticles and their biomedical applications." Inorganic and Nano-Metal Chemistry: 1-13.

Korsvik, C., S. Patil, S. Seal and W. T. Self (2007). "Superoxide dismutase mimetic properties exhibited by vacancy engineered ceria nanoparticles." Chemical Communications(10): 1056-1058.

Kotagiri, N. and J.-W. Kim (2014). "Stealth nanotubes: strategies of shielding carbon nanotubes to evade opsonization and improve biodistribution." International Journal of Nanomedicine 9(Suppl 1): 85.

Kroto, H. W., J. R. Heath, S. C. O'Brien, R. F. Curl and R. E. Smalley (1985). "C_{60}: Buckminsterfullerene." Nature 318(6042): 162-163.

Kubotera, H., H. Ikeshima-Kataoka, Y. Hatashita, A. L. Allegra Mascaro, F. S. Pavone and T. Inoue (2019). "Astrocytic endfeet re-cover blood vessels after removal by laser ablation." Scientific Reports 9(1): 1-10.

Kullgren, J., K. Hermansson and P. Broqvist (2013). Ceria chemistry at the nanoscale: effect of the environment. Solar Hydrogen and Nanotechnology VIII, International Society for Optics and Photonics.

Kung, H.-N., K.-S. Lu and Y.-P. Chau (2014). "The chemotherapeutic effects of lapacho tree extract: β-lapachone." Chemotherapy 3(2): 131-135.

Kwon, H. J., M.-Y. Cha, D. Kim, D. K. Kim, M. Soh, K. Shin, T. Hyeon and I. Mook-Jung (2016). "Mitochondria-targeting ceria nanoparticles as antioxidants for Alzheimer's disease." ACS Nano 10(2): 2860-2870.

Lange, S. C., L. K. Bak, H. S. Waagepetersen, A. Schousboe and M. D. Norenberg (2012). "Primary cultures of astrocytes: their value in understanding astrocytes in health and disease." Neurochemical Research 37(11): 2569-2588.

Lee, T.-Y. (2021). "Lactate: a multifunctional signaling molecule." Yeungnam University Journal of Medicine 38(3): 183.

Lee, Y. B., J. K. Min, J. G. Kim, K. C. Cap, R. Islam, A. J. Hossain, O. Dogsom, A. Hamza, S. Mahmud and D. R. Choi (2022). "Multiple functions of pyruvate kinase M2 in various cell types." Journal of Cellular Physiology 237(1): 128-148.

Li, C., X. Shi, Q. Shen, C. Guo, Z. Hou and J. Zhang (2018). "Hot topics and challenges of regenerative nanoceria in application of antioxidant therapy." Journal of Nanomaterials 2018.

Li, H., C. Liu, Y.-P. Zeng, Y.-H. Hao, J.-W. Huang, Z.-Y. Yang and R. Li (2016). "Nanoceria-mediated drug delivery for targeted photodynamic therapy on drug-resistant breast cancer." ACS Applied Materials & Interfaces 8(46): 31510-31523.

Li, J. Z., Y. Ke, H. P. Misra, M. A. Trush, Y. R. Li, H. Zhu and Z. Jia (2014). "Mechanistic studies of cancer cell mitochondria-and NQO1-mediated redox activation of beta-lapachone, a potentially novel anticancer agent." Toxicology and Applied Pharmacology 281(3): 285-293.

Li, K., J. Li, J. Zheng and S. Qin (2019). "Reactive astrocytes in neurodegenerative diseases." Aging and Disease 10(3): 664.

Li, Y. Y., X. He, J. J. Yin, Y. H. Ma, P. Zhang, J. Y. Li, Y. Y. Ding, J. Zhang, Y. L. Zhao, Z. F. Chai and Z. Y. Zhang (2015). "Acquired superoxide-scavenging ability of ceria nanoparticles." Angewandte Chemie-International Edition 54(6): 1832-1835.

Liguori, I., G. Russo, F. Curcio, G. Bulli, L. Aran, D. Della-Morte, G. Gargiulo, G. Testa, F. Cacciatore, D. Bonaduce and P. Abete (2018). "Oxidative stress, aging, and diseases." Clinical Interventions in Aging 13: 757-772.

Liu, R. Q. and R. Lal (2015). "Potentials of engineered nanoparticles as fertilizers for increasing agronomic productions." Science of the Total Environment 514: 131-139.

Liz-Marzán, L. M., N. Artzi, S. Bals, J. M. Buriak, W. C. Chan, X. Chen, M. C. Hersam, I.-D. Kim, J. E. Millstone and P. Mulvaney (2023). Celebrating a Nobel Prize to the "Discovery of Quantum Dots, an Essential Milestone in Nanoscience", ACS Publications. 17: 19474-19475.

Lopez-Fabuel, I., J. Le Douce, A. Logan, A. M. James, G. Bonvento, M. P. Murphy, A. Almeida and J. P. Bolaños (2016). "Complex I assembly into supercomplexes determines differential mitochondrial ROS production in neurons and astrocytes." Proceedings of the National Academy of Sciences 113(46): 13063-13068.

Lord, M. S., J. F. Berret, S. Singh, A. Vinu and A. S. Karakoti (2021). "Redox Active Cerium Oxide Nanoparticles: Current Status and Burning Issues." Small 17(51).

Lorite, G. S., L. Ylä-Outinen, L. Janssen, O. Pitkänen, T. Joki, J. T. Koivisto, M. Kellomäki, R. Vajtai, S. Narkilahti and K. Kordas (2019). "Carbon nanotube micropillars trigger guided growth of complex human neural stem cells networks." Nano Research 12(11): 2894-2899.

Loschen, C., A. Migani, S. T. Bromley, F. Illas and K. M. Neyman (2008). "Density functional studies of model cerium oxide nanoparticles." Physical Chemistry Chemical Physics 10(37): 5730-5738.

Loss, D. (2009). "Quantum phenomena in Nanotechnology." Nanotechnology 20(43): 430205.

Luther, E. M., C. Petters, F. Bulcke, A. Kaltz, K. Thiel, U. Bickmeyer and R. Dringen (2013). "Endocytotic uptake of iron oxide nanoparticles by cultured brain microglial cells." Acta Biomaterialia 9(9): 8454-8465.

Maccarone, R., A. Tisi, M. Passacantando and M. Ciancaglini (2020). "Ophthalmic applications of cerium oxide nanoparticles." Journal of Ocular Pharmacology and Therapeutics 36(6): 376-383.

Magistretti, P. J. and I. Allaman (2018). "Lactate in the brain: from metabolic end-product to signalling molecule." Nature Reviews Neuroscience 19(4): 235-249.

Mahmoud, S., M. Gharagozloo, C. Simard and D. Gris (2019). "Astrocytes maintain glutamate homeostasis in the CNS by controlling the balance between glutamate uptake and release." Cells 8(2): 184.

Mason, S. (2017). "Lactate shuttles in neuroenergetics—homeostasis, allostasis and beyond." Frontiers in Neuroscience 11: 43.

Mathew, J., J. Joy and S. C. George (2019). "Potential applications of nanotechnology in transportation: A review." Journal of King Saud University Science 31(4): 586-594.

Mathiisen, T. M., K. P. Lehre, N. C. Danbolt and O. P. Ottersen (2010). "The perivascular astroglial sheath provides a complete covering of the brain microvessels: an electron microscopic 3D reconstruction." Glia 58(9): 1094-1103.

Matsui, T., H. Omuro, Y.-F. Liu, M. Soya, T. Shima, B. S. McEwen and H. Soya (2017). "Astrocytic glycogen-derived lactate fuels the brain during exhaustive exercise to maintain endurance capacity." Proceedings of the National Academy of Sciences 114(24): 6358-6363.

Matyash, V. and H. Kettenmann (2010). "Heterogeneity in astrocyte morphology and physiology." Brain Research Reviews 63(1-2): 2-10.

Mehmood, U., S. H. A. Ahmad, A. Al-Ahmed, A. S. Hakeem, H. Dafalla and A. Laref (2020). "Synthesis and characterization of cerium oxide impregnated titanium oxide photoanodes for efficient dye-sensitized solar cells." IEEE Journal of Photovoltaics 10(5): 1365-1370.

Meng, H., W. Leong, K. W. Leong, C. Chen and Y. Zhao (2018). "Walking the line: The fate of nanomaterials at biological barriers." Biomaterials 174: 41-53.

Mergenthaler, P., U. Lindauer, G. A. Dienel and A. Meisel (2013). "Sugar for the brain: the role of glucose in physiological and pathological brain function." Trends in Neurosciences 36(10): 587-597.

Messing, A. and M. Brenner (2020). "GFAP at 50." ASN Neuro 12: 1759091420949680.

Michinaga, S. and Y. Koyama (2019). "Dual roles of astrocyte-derived factors in regulation of blood-brain barrier function after brain damage." International Journal of Molecular Sciences 20(3): 571.

Migaszewski, Z. M. and A. Galuszka (2015). "The characteristics, occurrence, and geochemical behavior of rare earth elements in the environment: a review." Critical Reviews in Environmental Science and Technology 45(5): 429-471.

Miller, R. H. and M. C. Raff (1984). "Fibrous and protoplasmic astrocytes are biochemically and developmentally distinct." Journal of Neuroscience 4(2): 585-592.

Mitchell, K. J., J. L. Goodsell, B. Russell-Webster, U. T. Twahir, A. Angerhofer, K. A. Abboud and G. Christou (2021). "Expansion of the family of molecular nanoparticles of cerium dioxide and their catalytic scavenging of hydroxyl radicals." Inorganic Chemistry 60(3): 1641-1653.

Mittal, S. and A. K. Pandey (2014). "Cerium oxide nanoparticles induced toxicity in human lung cells: role of ROS mediated DNA damage and apoptosis." BioMed research international 2014.

Modena, M. M., B. Rühle, T. P. Burg and S. Wuttke (2019). "Nanoparticle characterization: what to measure?" Advanced Materials 31(32): 1901556.

Mohammad-Beigi, H., Y. Hayashi, C. M. Zeuthen, H. Eskandari, C. Scavenius, K. Juul-Madsen, T. Vorup-Jensen, J. J. Enghild and D. S. Sutherland (2020). "Mapping and identification of soft corona proteins at nanoparticles and their impact on cellular association." Nature Communications 11(1): 4535.

Molina, R. M., N. V. Konduru, R. J. Jimenez, G. Pyrgiotakis, P. Demokritou, W. Wohlleben and J. D. Brain (2014). "Bioavailability, distribution and clearance of tracheally instilled, gavaged or injected cerium dioxide nanoparticles and ionic cerium." Environmental Science: Nano 1(6): 561-573.

Mongeon, R., V. Venkatachalam and G. Yellen (2016). "Cytosolic NADH-NAD+ redox visualized in brain slices by two-photon fluorescence lifetime biosensor imaging." Antioxidants & Redox Signaling 25(10): 553-563.

Mourdikoudis, S., R. M. Pallares and N. T. Thanh (2018). "Characterization techniques for nanoparticles: comparison and complementarity upon studying nanoparticle properties." Nanoscale 10(27): 12871-12934.

Muhammad, F., A. Wang, W. Qi, S. Zhang and G. Zhu (2014). "Intracellular antioxidants dissolve man-made antioxidant nanoparticles: using redox vulnerability of nanoceria to develop a responsive drug delivery system." ACS Applied Materials & Interfaces 6(21): 19424-19433.

Naeem, M., M. Z. Hoque, M. Ovais, C. Basheer and I. Ahmad (2021). "Stimulus-responsive smart nanoparticles-based CRISPR-Cas delivery for therapeutic genome editing." International Journal of Molecular Sciences 22(20).

Nebbioso, M., F. Franzone, A. Lambiase, V. Bonfiglio, P. G. Limoli, M. Artico, S. Taurone, E. M. Vingolo, A. Greco and A. Polimeni (2022). "Oxidative stress implication in retinal diseases— A review." Antioxidants 11(9): 1790.

Nippert, A. R., K. R. Biesecker and E. A. Newman (2018). "Mechanisms mediating functional hyperemia in the brain." The Neuroscientist 24(1): 73-83.

Nosrati, H., M. Heydari and M. Khodaei (2023). "Cerium oxide nanoparticles: Synthesis methods and applications in wound healing." Materials Today Bio: 100823.

Nyoka, M., Y. E. Choonara, P. Kumar, P. P. Kondiah and V. Pillay (2020). "Synthesis of cerium oxide nanoparticles using various methods: implications for biomedical applications." Nanomaterials 10(2): 242.

Oberheim, N. A., X. Wang, S. Goldman and M. Nedergaard (2006). "Astrocytic complexity distinguishes the human brain." Trends in Neurosciences 29(10): 547-553.

Olabarria, M. and J. E. Goldman (2017). "Disorders of astrocytes: Alexander disease as a model." Annual Review of Pathology: Mechanisms of Disease 12: 131-152.

Osorio-Blanco, E. R., J. Bergueiro, B. E. Abali, S. Ehrmann, C. Böttcher, A. J. Müller, J. L. Cuellar-Camacho and M. Calderon (2019). "Effect of core nanostructure on the thermomechanical properties of soft nanoparticles." Chemistry of Materials 32(1): 518-528.

Parwaiz, S., M. M. Khan and D. Pradhan (2019). "CeO_2-based nanocomposites: An advanced alternative to TiO_2 and ZnO in sunscreens." Materials Express 9(3): 185-202.

Patching, S. G. (2017). "Glucose transporters at the blood-brain barrier: function, regulation and gateways for drug delivery." Molecular Neurobiology 54(2): 1046-1077.

Patel, A. B., J. C. Lai, G. M. Chowdhury, F. Hyder, D. L. Rothman, R. G. Shulman and K. L. Behar (2014). "Direct evidence for activity-dependent glucose phosphorylation in neurons with implications for the astrocyte-to-neuron lactate shuttle." Proceedings of the National Academy of Sciences 111(14): 5385-5390.

Pelaz, B., C. Alexiou, R. A. Alvarez-Puebla, F. Alves, A. M. Andrews, S. Ashraf, L. P. Balogh, L. Ballerini, A. Bestetti and C. Brendel (2017). "Diverse applications of nanomedicine." ACS Nano 11(3): 2313-2381.

Pellerin, L. and P. J. Magistretti (1994). "Glutamate uptake into astrocytes stimulates aerobic glycolysis: a mechanism coupling neuronal activity to glucose utilization." Proceedings of the National Academy of Sciences 91(22): 10625-10629.

Peng, J., J. Guan, H. Yao and X. Jin (2016). "Magnetic colorimetric immunoassay for human interleukin-6 based on the oxidase activity of ceria spheres." Analytical Biochemistry 492: 63-68.

Petters, C., K. Thiel and R. Dringen (2016). "Lysosomal iron liberation is responsible for the vulnerability of brain microglial cells to iron oxide nanoparticles: comparison with neurons and astrocytes." Nanotoxicology 10(3): 332-342.

Pey, A. L., C. F. Megarity and D. J. Timson (2019). "NAD(P)H quinone oxidoreductase (NQO1): an enzyme which needs just enough mobility, in just the right places." Bioscience Reports 39(1): BSR20180459.

Phatnani, H. and T. Maniatis (2015). "Astrocytes in neurodegenerative disease." Cold Spring Harbor Perspectives in Biology 7(6): a020628.

Pierre, K. and L. Pellerin (2005). "Monocarboxylate transporters in the central nervous system: distribution, regulation and function." Journal of Neurochemistry 94(1): 1-14.

Pirmohamed, T., J. M. Dowding, S. Singh, B. Wasserman, E. Heckert, A. S. Karakoti, J. E. King, S. Seal and W. T. Self (2010). "Nanoceria exhibit redox state-dependent catalase mimetic activity." Chemical Communications 46(16): 2736-2738.

Pirmohamed, T., J. M. Dowding, S. Singh, B. Wasserman, E. Heckert, A. S. Karakoti, J. E. S. King, S. Seal and W. T. Self (2010). "Nanoceria exhibit redox state-dependent catalase mimetic activity." Chemical Communications 46(16): 2736-2738.

Pisoschi, A. M., A. Pop, F. Iordache, L. Stanca, G. Predoi and A. I. Serban (2021). "Oxidative stress mitigation by antioxidants-an overview on their chemistry and influences on health status." European Journal of Medicinal Chemistry 209: 112891.

Pokropivny, V. V. and V. V. Skorokhod (2007). "Classification of nanostructures by dimensionality and concept of surface forms engineering in nanomaterial science." Materials Science & Engineering C-Biomimetic and Supramolecular Systems 27(5-8): 990-993.

Pomatto, L. C. and K. J. Davies (2018). "Adaptive homeostasis and the free radical theory of ageing." Free Radical Biology and Medicine 124: 420-430.

Porcari, A., E. Borsella, C. Benighaus, K. Grieger, P. Isigonis, S. Chakravarty, P. Kines and K. A. Jensen (2019). "From risk perception to risk governance in nanotechnology: a multi-stakeholder study." Journal of Nanoparticle Research 21(11): 1-19.

Prasad, R., A. Bhattacharyya and Q. D. Nguyen (2017). "Nanotechnology in sustainable agriculture: recent developments, challenges, and perspectives." Frontiers in Microbiology 8: 1014.

Predota, M., M. L. Machesky and D. J. Wesolowski (2016). "Molecular origins of the zeta potential." Langmuir 32(40): 10189-10198.

Qutub, A. A. and C. A. Hunt (2005). "Glucose transport to the brain: a systems model." Brain Research Reviews 49(3): 595-617.

Ramalingam, G., P. Kathirgamanathan, G. Ravi, T. Elangovan, N. Manivannan and K. Kasinathan (2020). Quantum confinement effect of 2D nanomaterials. Quantum Dots-Fundamental and Applications, IntechOpen.

Ramos, S. J., G. S. Dinali, C. Oliveira, G. C. Martins, C. G. Moreira, J. O. Siqueira and L. R. G. Guilherme (2016). "Rare earth elements in the soil environment." Current Pollution Reports 2(1): 28-50.

Rastedt, W., K. Thiel and R. Dringen (2017). "Uptake of fluorescent iron oxide nanoparticles in C6 glioma cells." Biomedical Physics & Engineering Express 3(3): 035007.

Rauchman, S. H., A. Zubair, B. Jacob, D. Rauchman, A. Pinkhasov, D. G. Placantonakis and A. B. Reiss (2023). "Traumatic brain injury: Mechanisms, manifestations, and visual sequelae." Frontiers in Neuroscience 17: 1090672.

Reibold, M., N. Pätzke, A. Levin, W. Kochmann, I. Shakhverdova, P. Paufler and D. Meyer (2009). "Structure of several historic blades at nanoscale." Crystal Research and Technology: Journal of Experimental and Industrial Crystallography 44(10): 1139-1146.

Reuter, S., S. C. Gupta, M. M. Chaturvedi and B. B. Aggarwal (2010). "Oxidative stress, inflammation, and cancer: how are they linked?" Free Radical Biology and Medicine 49(11): 1603-1616.

Ribera, J., J. Rodriguez-Vita, B. Cordoba, I. Portolés, G. Casals, E. Casals, W. Jiménez, V. Puntes and M. Morales-Ruiz (2019). "Functionalized cerium oxide nanoparticles mitigate the oxidative stress and pro-inflammatory activity associated to the portal vein endothelium of cirrhotic rats." PloS One 14(6): e0218716.

Richtering, W., I. Alberg and R. Zentel (2020). "Nanoparticles in the biological context: Surface morphology and protein corona formation." Small 16(39): 2002162.

Riley, P. R. and R. J. Narayan (2021). "Recent advances in carbon nanomaterials for biomedical applications: A review." Current Opinion in Biomedical Engineering 17: 100262.

Roco, M. C. (2011). "The long view of nanotechnology development: the National Nanotechnology Initiative at 10 years." Journal of Nanoparticle Research 13: 427-445.

Roduner, E. (2006). "Size matters: why nanomaterials are different." Chemical Society Reviews 35(7): 583-592.

Rooseboom, M., J. N. Commandeur and N. P. Vermeulen (2004). "Enzyme-catalyzed activation of anticancer prodrugs." Pharmacological Reviews 56(1): 53-102.

Rose, C. R. and A. Verkhratsky (2016). "Principles of sodium homeostasis and sodium signalling in astroglia." Glia 64(10): 1611-1627.

Rose, J., C. Brian, A. Pappa, M. I. Panayiotidis and R. Franco (2020). "Mitochondrial metabolism in astrocytes regulates brain bioenergetics, neurotransmission and redox balance." Frontiers in Neuroscience 14: 536682.

Ross, D. and D. Siegel (2017). "Functions of NQO1 in cellular protection and CoQ_{10} metabolism and its potential role as a redox sensitive molecular switch." Frontiers in Physiology 8: 595.

Ross, D., D. Siegel, H. Beall, A. Prakash, R. T. Mulcahy and N. W. Gibson (1993). "DT-diaphorase in activation and detoxification of quinones." Cancer and Metastasis Reviews 12(2): 83-101.

Rzigalinski, B. A. (2005). "Nanoparticles and cell longevity." Technology in Cancer Research & Treatment 4(6): 651-659.

Sack, M., L. Alili, E. Karaman, S. Das, A. Gupta, S. Seal and P. Brenneisen (2014). "Combination of conventional chemotherapeutics with redox-active cerium oxide nanoparticles - a novel aspect in cancer therapy." Molecular Cancer Therapeutics 13(7): 1740-1749.

Saeidnia, S., A. Manayi and M. Abdollahi (2015). "From in vitro experiments to in vivo and clinical studies; pros and cons." Current Drug Discovery Technologies 12(4): 218-224.

Saito, K., E. Shigetomi, R. Yasuda, R. Sato, M. Nakano, K. Tashiro, K. F. Tanaka, K. Ikenaka, K. Mikoshiba and I. Mizuta (2018). "Aberrant astrocyte Ca^{2+} signals "AxCa signals" exacerbate pathological alterations in an Alexander disease model." Glia 66(5): 1053-1067.

Sajith, V., C. B. Sobhan and G. P. Peterson (2010). "Experimental investigations on the effects of cerium oxide nanoparticle fuel additives on biodiesel." Advances in Mechanical Engineering 2: 581407.

Saleh, T. A. (2020). "Nanomaterials: Classification, properties, and environmental toxicities." Environmental Technology & Innovation 20: 101067.

Sannino, D. (2021). Types and Classification of Nanomaterials. Nanotechnology, Springer: 15-38.

Sayle, T., S. Parker and C. Catlow (1994). "The role of oxygen vacancies on ceria surfaces in the oxidation of carbon monoxide." Surface Science 316(3): 329-336.

Schaming, D. and H. Remita (2015). "Nanotechnology: from the ancient time to nowadays." Foundations of Chemistry 17(3): 187-205.

Schieber, M. and N. S. Chandel (2014). "ROS function in redox signaling and oxidative stress." Current Biology 24(10): R453-R462.

Schilling, C., M. V. Ganduglia-Pirovano and C. Hess (2018). "Experimental and theoretical study on the nature of adsorbed oxygen species on shaped ceria nanoparticles." The Journal of Physical Chemistry Letters 9(22): 6593-6598.

Schmitt, R., A. Nenning, O. Kraynis, R. Korobko, A. I. Frenkel, I. Lubomirsky, S. M. Haile and J. L. Rupp (2020). "A review of defect structure and chemistry in ceria and its solid solutions." Chemical Society Reviews 49(2): 554-592.

Schöttler, S., K. Klein, K. Landfester and V. Mailänder (2016). "Protein source and choice of anticoagulant decisively affect nanoparticle protein corona and cellular uptake." Nanoscale 8(10): 5526-5536.

Schubert, J. and M. Chanana (2018). "Coating matters: Review on colloidal stability of nanoparticles with biocompatible coatings in biological media, living cells and organisms." Current Medicinal Chemistry 25(35): 4553-4586.

Schubert, J. and M. Chanana (2019). "Coating matters: Review on colloidal stability of nanoparticles with biocompatible coatings in biological media, living cells and organisms." Current Medicinal Chemistry 25(35): 4556.

Schwotzer, D., M. Niehof, D. Schaudien, H. Kock, T. Hansen, C. Dasenbrock and O. Creutzenberg (2018). "Cerium oxide and barium sulfate nanoparticle inhalation affects gene expression in alveolar epithelial cells type II." Journal of Nanobiotechnology 16(1): 1-25.

Sciau, P. (2012). Nanoparticles in ancient materials: the metallic lustre decorations of medieval ceramics, IntechOpen.

Sebak, A. A. (2018). "Limitations of PEGylated nanocarriers: unfavourable physicochemical properties, biodistribution patterns and cellular and subcellular fates." International Journal of Applied Pharmaceutics 10(5): 6-12.

Segeritz, C.-P. and L. Vallier (2017). Cell culture: Growing cells as model systems in vitro. Basic Science Methods for Clinical Researchers, Elsevier: 151-172.

Shan, L., T. Zhang, K. Fan, W. Cai and H. Liu (2021). "Astrocyte-neuron signaling in synaptogenesis." Frontiers in Cell and Developmental Biology 9: 1786.

Shoko, E., M. Smith and R. H. McKenzie (2010). "Charge distribution near bulk oxygen vacancies in cerium oxides." Journal of Physics: Condensed Matter 22(22): 223201.

Sies, H., C. Berndt and D. P. Jones (2017). "Oxidative stress." Annual Review of Biochemistry 86: 715-748.

Silvers, M. A., S. Deja, N. Singh, R. A. Egnatchik, J. Sudderth, X. Luo, M. S. Beg, S. C. Burgess, R. J. DeBerardinis and D. A. Boothman (2017). "The NQO1 bioactivatable drug, β-lapachone, alters the redox state of NQO1+ pancreatic cancer cells, causing perturbation in central carbon metabolism." Journal of Biological Chemistry 292(44): 18203-18216.

Singh, R. (2013). "Unexpected magnetism in nanomaterials." Journal of Magnetism and Magnetic Materials 346: 58-73.

Singh, S. (2016). "Cerium oxide based nanozymes: Redox phenomenon at biointerfaces." Biointerphases 11(4): 04B202.

Singh, S. (2019). "Nanomaterials exhibiting enzyme-like properties (nanozymes): current advances and future perspectives." Frontiers in Chemistry 7: 46.

Singh, S., T. Dosani, A. S. Karakoti, A. Kumar, S. Seal and W. T. Self (2011). "A phosphate-dependent shift in redox state of cerium oxide nanoparticles and its effects on catalytic properties." Biomaterials 32(28): 6745-6753.

Skorodumova, N., R. Ahuja, S. Simak, I. Abrikosov, B. Johansson and B. Lundqvist (2001). "Electronic, bonding, and optical properties of CeO_2 and Ce_2O_3 from first principles." Physical Review B 64(11): 115108.

Skorodumova, N., S. Simak, B. I. Lundqvist, I. Abrikosov and B. Johansson (2002). "Quantum origin of the oxygen storage capability of ceria." Physical Review Letters 89(16): 166601.

Son, Y. H., G. P. Jeong, P. S. Kim, M. H. Han, S. W. Hong, J. Y. Bae, S. I. Kim, J. H. Park and J. G. Park (2021). "Super fine cerium hydroxide abrasives for SiO_2 film chemical mechanical planarization performing scratch free." Scientific Reports 11: 17736.

Sosa, V., T. Moliné, R. Somoza, R. Paciucci, H. Kondoh and M. E. LLeonart (2013). "Oxidative stress and cancer: an overview." Ageing Research Reviews 12(1): 376-390.

Sousa, A. M., K. A. Meyer, G. Santpere, F. O. Gulden and N. Sestan (2017). "Evolution of the human nervous system function, structure, and development." Cell 170(2): 226-247.

Souza, D. G., R. F. Almeida, D. O. Souza and E. R. Zimmer (2019). The astrocyte biochemistry. Seminars in Cell & Developmental Biology, Elsevier.

Spiridonov, V. V., A. V. Sybachin, V. A. Pigareva, M. I. Afanasov, S. A. Musoev, A. V. Knotko and S. B. Zezin (2023). "One-step low temperature synthesis of CeO_2 nanoparticles stabilized by carboxymethylcellulose." Polymers 15(6): 1437.

Stapelfeldt, K., E. Ehrke, J. Steinmeier, W. Rastedt and R. Dringen (2017). "Menadione-mediated WST1 reduction assay for the determination of metabolic activity of cultured neural cells." Analytical Biochemistry 538: 42-52.

Steinmeier, J., S. Kube, G. Karger, E. Ehrke and R. Dringen (2020). "β-lapachone induces acute oxidative stress in rat primary astrocyte cultures that is terminated by the NQO1-inhibitor dicoumarol." Neurochemical Research 45(10): 2442-2455.

Stephen Inbaraj, B. and B. H. Chen (2020). "An overview on recent in vivo biological application of cerium oxide nanoparticles." Asian Journal of Pharmaceutical Sciences 15(5): 558-575.

Suades, A., A. Qureshi, S. E. McComas, M. Coinçon, A. Rudling, Y. Chatzikyriakidou, M. Landreh, J. Carlsson and D. Drew (2023). "Establishing mammalian GLUT kinetics and lipid composition influences in a reconstituted-liposome system." Nature Communications 14(1): 4070.

Suk, J. S., Q. G. Xu, N. Kim, J. Hanes and L. M. Ensign (2016). "PEGylation as a strategy for improving nanoparticle-based drug and gene delivery." Advanced Drug Delivery Reviews 99: 28-51.

Sun, C., H. Li and L. Chen (2012). "Nanostructured ceria-based materials: synthesis, properties, and applications." Energy & Environmental Science 5(9): 8475-8505.

Sundaresan, A., R. Bhargavi, N. Rangarajan, U. Siddesh and C. Rao (2006). "Ferromagnetism as a universal feature of nanoparticles of the otherwise nonmagnetic oxides." Physical Review B 74(16): 161306.

Supplie, L. M., T. Düking, G. Campbell, F. Diaz, C. T. Moraes, M. Götz, B. Hamprecht, S. Boretius, D. Mahad and K.-A. Nave (2017). "Respiration-deficient astrocytes survive as glycolytic cells in vivo." Journal of Neuroscience 37(16): 4231-4242.

Suresh, R., V. Ponnuswamy and R. Mariappan (2013). "Effect of annealing temperature on the microstructural, optical and electrical properties of CeO_2 nanoparticles by chemical precipitation method." Applied Surface Science 273: 457-464.

Taladriz-Blanco, P., N. J. Buurma, L. Rodríguez-Lorenzo, J. Pérez-Juste, L. M. Liz-Marzán and P. Herves (2011). "Reversible assembly of metal nanoparticles induced by penicillamine. Dynamic formation of SERS hot spots." Journal of Materials Chemistry 21(42): 16880-16887.

Talapin, D. V., I. Mekis, S. Götzinger, A. Kornowski, O. Benson and H. Weller (2004). "CdSe/CdS/ZnS and CdSe/ZnSe/ZnS Core– Shell– Shell Nanocrystals." The Journal of Physical Chemistry B 108(49): 18826-18831.

Tarnuzzer, R. W., J. Colon, S. Patil and S. Seal (2005). "Vacancy engineered ceria nanostructures for protection from radiation-induced cellular damage." Nano Letters 5(12): 2573-2577.

Tenzer, S., D. Docter, J. Kuharev, A. Musyanovych, V. Fetz, R. Hecht, F. Schlenk, D. Fischer, K. Kiouptsi and C. Reinhardt (2013). "Rapid formation of plasma protein corona critically affects nanoparticle pathophysiology." Nature Nanotechnology 8(10): 772-781.

Thakur, N., P. Manna and J. Das (2019). "Synthesis and biomedical applications of nanoceria, a redox active nanoparticle." Journal of Nanobiotechnology 17(1): 1-27.

Thorens, B. and M. Mueckler (2010). "Glucose transporters in the 21st Century." American Journal of Physiology-Endocrinology and Metabolism 298(2): E141-E145.

Tian, Z., J. Li, Z. Zhang, W. Gao, X. Zhou and Y. Qu (2015). "Highly sensitive and robust peroxidase-like activity of porous nanorods of ceria and their application for breast cancer detection." Biomaterials 59: 116-124.

Trovarelli, A. and J. Llorca (2017). "Ceria Catalysts at Nanoscale: How Do Crystal Shapes Shape Catalysis?" ACS Catalysis 7(7): 4716-4735.

Tulpule, K., M. C. Hohnholt, J. Hirrlinger and R. Dringen (2014). Primary cultures of astrocytes and neurons as model systems to study the metabolism and metabolite export from brain cells. Brain Energy Metabolism, Springer: 45-72.

Urner, M., A. Schlicker, B. R. Z'graggen, A. Stepuk, C. Booy, K. P. Buehler, L. Limbach, C. Chmiel, W. J. Stark and B. Beck-Schimmer (2014). "Inflammatory response of lung macrophages and epithelial cells after exposure to redox active nanoparticles: effect of solubility and antioxidant treatment." Environmental Science & Technology 48(23): 13960-13968.

Verkhratsky, A. and M. Nedergaard (2018). "Physiology of astroglia." Physiological Reviews 98(1): 239-389.

Verkhratsky, A., M. Nedergaard and L. Hertz (2015). "Why are astrocytes important?" Neurochemical Research 40(2): 389-401.

Vu-Quang, H., M. S. Vinding, T. Nielsen, M. G. Ullisch, N. C. Nielsen, D.-T. Nguyen and J. Kjems (2019). "Pluronic F127-folate coated super paramagenic iron oxide nanoparticles as contrast agent for cancer diagnosis in magnetic resonance imaging." Polymers 11(4): 743.

Walls, A., C. Heimbürger, S. Bouman, A. Schousboe and H. Waagepetersen (2009). "Robust glycogen shunt activity in astrocytes: Effects of glutamatergic and adrenergic agents." Neuroscience 158(1): 284-292.

Wang, H.-J., Y.-J. Hsieh, W.-C. Cheng, C.-P. Lin, Y.-s. Lin, S.-F. Yang, C.-C. Chen, Y. Izumiya, J.-S. Yu and H.-J. Kung (2014). "JMJD5 regulates PKM2 nuclear translocation and reprograms HIF-1α–mediated glucose metabolism." Proceedings of the National Academy of Sciences 111(1): 279-284.

Wang, Q., H. Wei, Z. Zhang, E. Wang and S. Dong (2018). "Nanozyme: An emerging alternative to natural enzyme for biosensing and immunoassay." TRAC Trends in Analytical Chemistry 105: 218-224.

Wang, Y. Y., Y. B. Deng, H. H. Luo, A. J. Zhu, H. T. Ke, H. Yang and H. B. Chen (2017). "Light-responsive nanoparticles for highly efficient cytoplasmic delivery of anticancer agents." ACS Nano 11(12): 12134-12144.

Wang, Z. L. and X. Feng (2003). "Polyhedral shapes of CeO_2 nanoparticles." The Journal of Physical Chemistry B 107(49): 13563-13566.

Wason, M. S., H. Lu, L. Yu, S. K. Lahiri, D. Mukherjee, C. Shen, S. Das, S. Seal and J. Zhao (2018). "Cerium oxide nanoparticles sensitize pancreatic cancer to radiation therapy through oxidative activation of the JNK apoptotic pathway." Cancers 10(9): 303.

Wason, M. S. and J. Zhao (2013). "Cerium oxide nanoparticles: potential applications for cancer and other diseases." American Journal of Translational Research 5(2): 126.

Watermann, P. and R. Dringen (2023). "β-lapachone-mediated WST1 reduction as indicator for the cytosolic redox metabolism of cultured primary astrocytes." Neurochemical Research 48(7): 2148-2160.

Wiesinger, H., B. Hamprecht and R. Dringen (1997). "Metabolic pathways for glucose in astrocytes." Glia 21(1): 22-34.

Winzen, S., S. Schoettler, G. Baier, C. Rosenauer, V. Mailaender, K. Landfester and K. Mohr (2015). "Complementary analysis of the hard and soft protein corona: sample preparation critically effects corona composition." Nanoscale 7(7): 2992-3001.

Wolfenden, R. and M. J. Snider (2001). "The depth of chemical time and the power of enzymes as catalysts." Accounts of Chemical Research 34(12): 938-945.

Wong, L. L., Q. N. Pye, L. Chen, S. Seal and J. F. McGinnis (2015). "Defining the catalytic activity of nanoceria in the P23H-1 rat, a photoreceptor degeneration model." PloS One 10(3): e0121977.

Woźniak, M., A. Płoska, A. Siekierzycka, L. W. Dobrucki, L. Kalinowski and I. T. Dobrucki (2022). "Molecular imaging and nanotechnology - emerging tools in diagnostics and therapy." International Journal of Molecular Sciences 23(5): 2658.

Wu, J., X. Wang, Q. Wang, Z. Lou, S. Li, Y. Zhu, L. Qin and H. Wei (2019). "Nanomaterials with enzyme-like characteristics (nanozymes): next-generation artificial enzymes (II)." Chemical Society Reviews 48(4): 1004-1076.

Wuilloud, E., B. Delley, W.-D. Schneider and Y. Baer (1984). "Spectroscopic evidence for localized and extended f-symmetry states in CeO_2." Physical Review Letters 53(2): 202.

Xia, B., W. Zhang, J. Shi and S.-j. Xiao (2013). "Engineered stealth porous silicon nanoparticles via surface encapsulation of bovine serum albumin for prolonging blood circulation in vivo." ACS Applied Materials & Interfaces 5(22): 11718-11724.

Xu, W. Q., L. Jiao, H. R. Ye, Z. Z. Guo, Y. Wu, H. Y. Yan, W. L. Gu, D. Du, Y. H. Lin and C. Z. Zhu (2020). "pH-responsive allochroic nanoparticles for the multicolor detection of breast cancer biomarkers." Biosensors and Bioelectronics 148: 111780.

Xue, Y., Q. Luan, D. Yang, X. Yao and K. Zhou (2011). "Direct evidence for hydroxyl radical scavenging activity of cerium oxide nanoparticles." The Journal of Physical Chemistry C 115(11): 4433-4438.

Yan, Y. F. and H. W. Ding (2020). "pH-responsive nanoparticles for cancer immunotherapy: a brief review." Nanomaterials 10(8): 1613.

Yang, Z., T. K. Woo, M. Baudin and K. Hermansson (2004). "Atomic and electronic structure of unreduced and reduced CeO_2 surfaces: A first-principles study." The Journal of Chemical Physics 120(16): 7741-7749.

Yıldırım, D., B. Gökçal, E. Büber, Ç. Kip, M. C. Demir and A. Tuncel (2021). "A new nanozyme with peroxidase-like activity for simultaneous phosphoprotein isolation and detection based on metal oxide affinity chromatography: Monodisperse-porous cerium oxide microspheres." Chemical Engineering Journal 403: 126357.

Yokel, R. A., S. Hussain, S. Garantziotis, P. Demokritou, V. Castranova and F. R. Cassee (2014). "The yin: an adverse health perspective of nanoceria: uptake, distribution, accumulation, and mechanisms of its toxicity." Environmental Science: Nano 1(5): 406-428.

Zhang, C. N., G. N. Shi, J. Zhang, J. F. Niu, P. S. Huang, Z. H. Wang, Y. M. Wang, W. W. Wang, C. Li and D. L. Kong (2017). "Redox- and light-responsive alginate nanoparticles as effective drug carriers for combinational anticancer therapy." Nanoscale 9(9): 3304-3314.

Zhang, F., S.-W. Chan, J. E. Spanier, E. Apak, Q. Jin, R. D. Robinson and I. P. Herman (2002). "Cerium oxide nanoparticles: size-selective formation and structure analysis." Applied Physics Letters 80(1): 127-129.

Zhang, J., H. Kumagai, K. Yamamura, S. Ohara, S. Takami, A. Morikawa, H. Shinjoh, K. Kaneko, T. Adschiri and A. Suda (2011). "Extra-low-temperature oxygen storage capacity of $CeO2$ nanocrystals with cubic facets." Nano Letters 11(2): 361-364.

Zhang, J., Y. Nazarenko, L. Zhang, L. Calderon, K.-B. Lee, E. Garfunkel, S. Schwander, T. D. Tetley, K. F. Chung and A. E. Porter (2013). "Impacts of a nanosized ceria additive on diesel engine emissions of particulate and gaseous pollutants." Environmental Science & Technology 47(22): 13077-13085.

Zhang, W., G. Xie, S. Li, L. Lu and B. Liu (2012). "Au/CeO$_2$–chitosan composite film for hydrogen peroxide sensing." Applied Surface Science 258(20): 8222-8227.

Zhang, Y., K. Chen, S. A. Sloan, M. L. Bennett, A. R. Scholze, S. O'Keeffe, H. P. Phatnani, P. Guarnieri, C. Caneda and N. Ruderisch (2014). "An RNA-sequencing transcriptome and splicing database of glia, neurons, and vascular cells of the cerebral cortex." Journal of Neuroscience 34(36): 11929-11947.

Zhao, C. (2023). "Cell culture: in vitro model system and a promising path to in vivo applications." Journal of Histotechnology 46(1): 1-4.

Zhao, Y., B. T. Teng, X. D. Wen, Y. Zhao, Q. P. Chen, L. H. Zhao and M. F. Luo (2012). "Superoxide and peroxide species on CeO$_2$(111), and their oxidation roles." Journal of Physical Chemistry C 116(30): 15986-15991.

Zhou, G., W. Geng, L. Sun, X. Wang, W. Xiao, J. Wang and L. Wang (2019). "Influence of mixed valence on the formation of oxygen vacancy in cerium oxides." Materials 12(24): 4041.

Zhu, M., G. Nie, H. Meng, T. Xia, A. Nel and Y. Zhao (2013). "Physicochemical properties determine nanomaterial cellular uptake, transport, and fate." Accounts of Chemical Research 46(3): 622-631.

2 Experimental Results

2.1 Coating, functionalization and characterization of cerium oxide nanoparticles to study cellular accumulation and biocompatibility in astrocyte primary cultures and C6 glioma cells.

Abstract

The synthesis of functionalized cerium oxide nanoparticles (CeONPs) suitable for biomedical investigations remains one of the major challenges in this field. In this chapter, the functionalization of CeONPs with dimercaptosuccinate (DMSA) as a coating material is investigated. Dispersed in H_2O, the DMSA-CeONPs generated had a hydrodynamic diameter of 112 ± 4.5 nm, a negative zeta potential (-27.2 mV), and remained stable for up to 30 days. In addition, DMSA-CeONPs also allowed fluorescent labelling by covalent binding of Oregon Green (OG). The size of the fluorescent OG-DMSA-CeONPs were not significantly different from those of DMSA-CeONPs, as analyzed by transmission electron microscopy (TEM) (~ 25 nm). *In vitro* incubation of C6 glioma cells and astrocyte primary cultures (APCs) with 10, 100 or 1000 µM DMSA-CeONPs or OG-DMSA-CeONPs for 72 h did not compromise membrane integrity, as demonstrated by the quantification of lactate dehydrogenase (LDH) activity and by propidium iodide (PI) staining of the cells. Fluorescence microscopy uptake studies of the OG-DMSA-CeONPs in C6 glioma cells and APCs at 37°C revealed intracellular dots of fluorescent staining, which were detectable after 15 min incubation and increased in intensity with time. In contrast, after incubation at 4°C with OG-DMSA-CeONPs, a reduced and diffuse fluorescent background was obtained, suggesting that active transport is required for the internalization of CeONPs. Quantification of cellular cerium content by inductively coupled plasma optical emission spectrometry (ICP-OES) confirmed that incubations at 37°C resulted in a higher cellular content of cerium compared to 4°C incubations. These data demonstrate that DMSA-CeONPs are biocompatible with cultured glial cells. In addition, it was shown that C6 glioma cells and APCs efficiently accumulate DMSA-CeONPs in a time- and concentration-dependent manner by a mechanism which is strongly affected by temperature.

Introduction

Ageing, cancer and neurodegenerative diseases e.g. Alzheimer's disease (AD), Parkinson's disease (PD) and Huntington disease have driven the scientific research in biomedicine during the latest years (Naz et al., 2017). As a consequence, the search and development of new compounds that cure or mitigate the onset of oxidative stress associated to these pathologies have experienced a great impulse (Gulcin, 2020; Baschieri and Amorati, 2021; Parcheta et al., 2021). In this context, CeONPs have stood out due to their physicochemical properties and the results obtained in pioneering pre-clinical studies in the field of biomedicine (Alili et al., 2011; Giri et al., 2013; Wason and Zhao, 2013; Jana et al., 2014; Sack et al., 2014; Hijaz et al., 2016; Li et al., 2016; Das et al., 2017; Wason et al., 2018; Fernández-Varo et al., 2020).

CeONPs are currently considered as nanozymes with a solid therapeutic potential due to their ability to scavenge reactive oxygen species (ROS) in biological systems under certain conditions (Wei and Wang, 2013; Wu et al., 2019; Singh et al., 2021). Ultimately, the ratio Ce^{3+}/Ce^{4+} present on the surface, intrinsically associated with their enhanced oxygen storage capacity, facilitates the neutralization of ROS in the cytosol (Rzigalinski et al., 2017). It has been demonstrated that a higher presence of Ce^{3+} favors superoxide dismutase mimic activity while a predominance of Ce^{4+} leads to catalase-like behavior (Heckert et al., 2008; Pirmohamed et al., 2010; Singh et al., 2011). This Ce^{3+}/Ce^{4+} ratio strongly depends on the physicochemical characteristics of the CeONPs (Skorodumova et al., 2002; Kullgren et al., 2013), especially on their size (Korsvik et al., 2007; Dowding et al., 2013; Li et al., 2015). Hard and soft corona coatings of the surfaces of CeONPs are also a determinant factor for the catalytic properties exhibited by CeONPs (Estevez and Erlichman, 2014). Moreover, the interaction between the coating and the medium constitutes a bottleneck for the colloidal stability of the CeONPs and therefore, for their ulterior fate. Phenomena such as agglomeration, aggregation, sedimentation and dissolution might decrease or even prevent the uptake of CeONPs in different cell lines (Ju et al., 2020) and also *in vivo* (Rzigalinski et al., 2017). Many types of CeONPs are commercially available and cover a wide range of shapes, sizes and compositions; however, not all of them seem to be suitable for the investigation in biological systems. Subsequently, the dispersion process and medium and the coating have to be individually designed and characterized to optimize their fate and behavior with biomedical purposes (Casals et al., 2020). Hence, in this study we investigate, for the first time, a method to functionalize CeONPs with dimercarptosuccinic acid (DMSA),

based on previous results obtained with iron oxide and copper oxide NPs (Geppert et al., 2011; Bulcke et al., 2014; Joshi et al., 2016; Rastedt et al., 2017).

The brain possesses an energetically demanding metabolism, that consumes about twenty percent of the total inhaled oxygen (Mink et al., 1981; Bolaños, 2016) and therefore, is associated with a relative elevated production of ROS (Sies et al., 2017; Bylicky et al., 2018). In addition, in several neurodegenerative diseases, an enhanced presence of ROS has been pointed out as a major contributor in the etiology of these conditions (Andersen, 2004; Behl et al., 2021). The catalytic properties of CeONPs have also been found to be cell-dependent (Kumar et al., 2014). Therefore, CeONPs have been previously investigated as potential ROS scavengers in brain cells (Cimini et al., 2012; Dowding et al., 2014; Fiorani et al., 2015; Wong et al., 2015; DeCoteau et al., 2016; Guan et al., 2016; Bailey et al., 2020). These studies have reported that CeONPs exerted neuroprotective effects under diverse conditions e.g. in AD, PD, ischemia or stroke models, in which also astrocytes are affected (Maragakis and Rothstein, 2006; Phatnani and Maniatis, 2015). Astrocytes are directly connected to the blood-brain barrier through their end-feet (Mathiisen et al., 2010) and selectively block the uptake and distribution of nutrients and xenobiotics to the rest of the brain (Verkhratsky et al., 2015). As astrocytes are the first parenchymal cell which the CeONPs might encounter after peripheral application and due to their key role in ROS detoxification in the brain (Dringen et al., 2015), the fate of CeONPs within these cells seems of vital importance for future biomedical applications. However, little information is available so far regarding the uptake, biocompatibility and clearance of CeONPs in astrocytes or in C6 glioma cell line, which has been also frequently used as a model for APCs research (Galland et al., 2019).

To facilitate the observation of the internalization and posterior distribution within cellular compartments *in vitro*, fluorescent labeled CeONPs were developed. In parallel, the quantification of cerium content after their administration is also essential. Hence, the development of fast, sensitive and accessible methods is also mandatory. Here we report that dispersion and coating with dimercaptosuccinate (DMSA) of commercial CeONPs (DMSA-CeONPs) can be successfully achieved, being stable in dispersion for cell investigations. The high biocompatibility of DMSA-CeONPs with brain cells was demonstrated as the proliferation of C6 glioma cells and viability of APCs after treatment with a wide range of DMSA-CeONPs concentrations were not impaired. The data presented demonstrate that the uptake of CeONPs seems to rely on active mechanisms. The microscopical observation of the uptake was confirmed by the determination of the intracellular cerium content in C6 glioma cells by ICP-OES.

Materials and methods

Materials

Cerium oxide nano-powder (<25 nm, by Brunauer-Emmett-Teller analysis), cerium (III) chloride heptahydrate, 2, 3-meso dimercaptosuccinic acid (DMSA), H_2O_2 for ultratrace analysis, nigrosine, sodium chloride, 2-amino-2 (hydroxymethyl)-1,3-propanediol (Trizma base), bisbenzimide Hoechst 33342 (H33342) and DPX mounting medium were purchased from Sigma-Aldrich (Steinheim, Germany). Dulbecco´s modified Eagle´s medium (DMEM, containing 25 mM glucose) was from Gibco (Karlsruhe, Germany). Fetal calf serum (FCS), trypsin solution and penicillin/streptomycin solution were obtained from Biochrom (Berlin, Germany). Bovine serum albumin (BSA) and nicotinamide adenine dinucleotide (NADH) were purchased from Applichem (Darmstadt, Germany). Oregon Green®488 idodoacetamide (mixed isomers) was obtained from Invitrogen (Darmstadt, Germany). Cerium dioxide standard (1000 μg mL^{-1}, v/v) for ICP-OES analysis was obtained from Inorganic Ventures (Virginia, USA). Other chemicals of the highest purity used in these investigations were purchased from Merck (Darmstadt, Germany) or Fluka (Buchs, Switzerland). 24-well cell culture plates and 96-well plates microtiter plates were purchased from Sarstedt (Nümbrecht, Germany) and black 96-well plates were acquired from VWR (Darmstadt, Germany).

Preparation of DMSA-coated CeONPs dipersions

A 100 mM dispersion of colloidal uncoated CeONPs (Un-CeONPs) was prepared as stock solution by stirring 0.172 g nano-powder in 10 mL distilled water for 15 min and twice ultrasonicating on ice for 5 minutes intervals at 50 W with a Branson B-12 sonifier (Danbury, Connecticut, USA). In parallel, a 5 mM DMSA aqueous solution was prepared at 65°C in a covered beaker under stirring for 15 min and left to cool down until reaching room temperature (RT). Afterwards, for the preparation of 20 mM DMSA-CeONPs, 5 mL of the 5 mM DMSA solution was added to 10 mL of a 29 mM dilution in H_2O of the stock CeONPs dispersion. After 15 min of additional stirring at RT the dispersion was collected and centrifuged for 10 min at 1500g and the supernatant was discarded. Subsequently two cycles of washing were completed by washing with 15 mL distilled H_2O the pellet containing the DMSA-CeONPs and discarding the washing solution after 10 min centrifugation at 1500g. The resulting CeONPs pellet was finally dispersed in 15 mL pure H_2O and sonicated

twice with the same settings mentioned before. The DMSA-CeONPs dispersion was stored at 4°C and sonicated for 5 min with the above described settings prior to any further use.

OG fluorescent labelling of DMSA-CeONPs

To microscopically assess the uptake and fate of the CeONPs within astrocytes or C6 cells, DMSA coating was previously functionalized with the OG fluorescent dye, adapting an early published method (Fauconnier et al., 1997; Luther et al., 2013; Petters et al., 2014; Rastedt et al., 2017). Briefly, fluorescence labeled DMSA was synthesized by mixing 10 μL 10 mM OG with 359 μL 47 mM DMSA solution in 359 μL 47 mM glycine/NaOH buffer at pH 10 for 30 min at room temperature (RT) in the dark. Subsequently, 187 μL 58 mM CeONPs were added to 351 μL of the fluorescence labeled DMSA solution and acidified to pH 3 by adding 1.5 μL concentrated HNO_3 (65%, v/v). The mixture was incubated under continuous shaking for 30 min at RT in the dark. To eliminate the unattached DMSA and excess of fluorescent dye, three consecutive cycles of 90 s centrifugation at 12,300g were performed in an Eppendorf MiniSpin centrifuge (Hamburg, Germany). After each centrifugation, the supernatant was discarded and the pellet was resuspended in 1.3 mL H_2O and 0.5 μL concentrated HNO_3. Finally, the nanoparticles were dispersed in 350 μL H_2O by addition of 1μL 1 mM NaOH to re-establish the pH. The final concentration of CeONPs was ~ 30 mM. The dispersion was stored at 4°C in the dark until use on the same or the next day.

Characterization of DMSA-CeONPs

Transmission electron microscopy (TEM) and Energy dispersive X-ray spectroscopy (EDX) for elemental analysis of the CeONPs dispersions was kindly carried out by Dr Karsten Thiel (Fraunhofer Institute for Manufacturing Technology and Advanced Materials, Bremen, Germany) as previously described (Bulcke et al., 2014; Joshi et al., 2019). Briefly, samples for TEM imaging were prepared by drying 10 μL of 1 mM DMSA-CeONPs onto copper grids at RT. The grid was then washed with 10 μL pure water twice before letting it air-dry. Images were taken by a FEI Tecnai F20 S-TWIN (Hilsboro, Oregon, USA) operated at 200 kV using a GATAN GIF2001 SSC-CCD camera (Pleasanton, California, USA). EDX analysis of the DMSA-CeONPs dispersion was carried out in the scanning mode of the microscope (STEM) with an EDAX r-TEM-EDX-detector with an energy resolution of 136 eV measured at Mn-Kα.

DMSA-CeONPs dispersions (1 mM) in H_2O_2 and different culture media were characterized for their hydrodynamic diameter, polydispersity index (Pi) and zeta potential. These parameters were determined by dynamic and electrophoretic light scattering (DLS, ELS) in

a Beckman Coulter (Krefeld, Germany) Delsa™ Nano C Particle analyzer at RT (Bulcke et al., 2014)

C6 glioma cell cultures

The C6 glioma cell line was cultured as previously described (Joshi et al., 2016). Briefly, C6 glioma cells (internal passage numbers between 3 and 14) were cultured in 175 cm² flasks in cell culture medium (DMEM+ 10% FCS, 90% DMEM, 10% fetal calf serum (FCS), 1 mM pyruvate, 18 U/mL penicillin G, 18 µg/mL streptomycin sulfate) at 37°C in an humified atmosphere enriched with 10% CO_2 inside a Sanyo incubator (Osaka, Japan). The cultures used in the presented experiments were sub-cultured from 80% of confluent cultures. In short, the cultures were washed twice with 10 mL of pre-warmed (37°C) sterile PBS (10 mM potassium phosphate buffer, 150 mM NaCl; pH 7,4) and treated with 10 mL 0.05% (w/v) trypsin in pre-warmed (37°C) PBS for 5 min at 37°C. The activity of trypsin was terminated by the addition of 10 mL cultured medium. The resulting 20 mL cell suspension was centrifugated for 5 min at 400g. Subsequently, the supernatant was discarded and the cell pellet resuspended in 10 mL culture medium. The cell density and cell viability was then determined by nigrosine staining (0.25%, w/v) using a Neubauer-counting chamber as described earlier (Hohnholt et al., 2011). Cells were seeded in 1 mL culture medium at a seeding density of $2x10^5$ viable cells mL^{-1}, if not stated otherwise, into wells of 24-well plates and used for experimental incubations 24 h after seeding.

Astrocyte-rich primary cultures

The preparation of the cultures was performed in accordance with the legal regulations dictated by the *Bundesministerium für Ernährung und Landwirtschaft* included in the *Tierschutzgesetz* (reissued on the 18.05.2006) and later modifications. The maintenance of the animals and their utilization with research purposes were approved and supervised by the local animal care committee, *Senatorische Behörde* of Bremen (Germany).

APCs were successfully obtained from the full brain of newborn Wistar rats within the first 24 h after birth and being naturally fed. The cultures were prepared as previously described by Hamprecht and Löffler (1985) and later slightly modified (Tulpule et al., 2014). Briefly, the full brains were extracted after decapitation and mechanically dissociated, consecutively, through two nylon meshes of 210 and 132 µm pore diameter respectively to eliminate blood vessels and singularize cells. For seeding, 1 mL culture medium containing approximately $3x10^5$ viable cells was transferred into wells of 24-well cell culture plates.

The cell culture medium was renewed every 7th day. The age of the cultures used for the experiment described in this manuscript was between 15 and 28 days.

Experimental incubations

To incubate the cells with CeONPs, the cultures were first washed twice with 1 mL of pre-warmed physiological incubation buffer (IB; 1.8 mM $CaCl_2$, 1 mM $MgCl_2$, 5.4 mM KCl, 145 mM NaCl, 20 mM HEPES, 5 mM D-glucose; pH 7.4) containing 0.5 mg mL^{-1} bovine serum albumin (IB-BSA) in the wells of 24-well cell culture plates. Subsequently, the cells were incubated for the indicated time periods at 37°C in the humified atmosphere of an incubator (without CO_2 supply) with the adequate volume of IB-BSA containing CeONPs in the concentrations given in the legends of the figures and tables. To end the incubations, the cells were washed twice with 1 mL ice cold (4°C) PBS. Dry cells were stored at -20°C until subsequent quantification of cerium and protein contents.

For the proliferation assay with C6 glioma cells, $5x10^4$ cells well^{-1} were seeded in culture medium. 24 h after seeding, the cells were washed twice with PBS at 37°C and incubated for 24, 48 or 72 h with 1 mL culture medium containing 1 mM uncoated CeONPs (Un-CeONPs), DMSA-CeONPs or $CeCl_3$ at 37 °C.

For the microscopical study of OG-DMSA-CeONPs uptake and fate, C6 glioma cells or cultured astrocytes were seeded on a sterile glass cover slides placed inside a well of a 24-well dish and then treated with the indicated concentrations of NPs over different times. The cell seeding density for C6 glioma cells was $5 x10^4$ cells well^{-1}, and treatments were started 24 h after seeding.

Viability assays

Cell vitality was assessed by quantification of the activity of the cellular LDH and by visualizing the cell membrane integrity by PI staining as described previously (Bulcke et al., 2014; Tulpule et al., 2014; Joshi et al., 2016).

LDH activity determination

Briefly, after the indicated incubation, cells were washed twice with pre-warmed (37°C) IB-BSA and lysed with 1% (v/v) Triton x-100 in 200 μL IB-BSA for 30 min at 37°C. After the lysis, 10 μL of the lysate was diluted with 170 μL LDH buffer (80 mM Tris, 200 mM NaCl, pH 7.2) in a well of a 96-well microtiter plate. The photometric determination of the LDH activity was performed at 340 nm as previously described by Tulpule et al. (2014).

To test for the proliferation of C6 glioma cells after the incubation, the cells were lysed for 30 min in 1 mL cultured medium containing 1% Triton X-100 and 40 µL of these lysates were used to determine the LDH activity after 24 and 48 h while only 20 µL was taken for the 72 h timepoint. The cellular LDH activity was determined as described previously (Dringen et al., 1998; Tulpule et al., 2014).

PI staining

The integrity of the cellular membrane was used as an indicator of cell viability and was determined by staining the cells with the membrane impermeable fluorescent dye PI as described previously by Tulpule et al. (2014). In addition, the membrane permeable dye Hoechst H33342 was applied to visualize all cell nuclei present. Images of the stained cells were captured using a fluorescence microscope (Eclipse TE-2000-U with a DS-QiMc camera and imaging software NIS-Elements BR, Nikon, Düsseldorf, Germany) using the specified filter settings (see fluorescence microscopy).

Protein determination

For the determination of cellular protein contents, cells in the 24-well dishes were lysed in 200 µL 0.5M NaOH for 60 min at RT in a humidified atmosphere. The protein content of the cultures was determined based on the Lowry method (Lowry et al., 1951), using BSA as standard protein.

Quantification of cellular cerium content

For the quantification of cellular cerium contents, cells in 24-well plates were lysed in 400 µL 500 mM NaOH, harvested and incubated with 1.2 mL of 65% HNO_3 (suprapur) and 0.2 µL of 35% H_2O_2 (suprapur) at 65°C for 60 min and then at 85°C for the necessary time ($\sim$ 24 h) until the evaporation was completed. Digestions were carried out in 2 mL Eppendorf cups which remained open to allow the samples to dry. The dry residues were resuspended in 4 mL of 2% HNO_3 (suprapur). The subsequent quantification of cerium was carried out in collaboration with Dr Fröllje (Department of Geochemistry and Hydrogeology, University of Bremen). The cerium content was measured by inductively coupled plasma–optical emission spectrometry (ICP-OES) using a Perkin Elmer Optima 7300 DV instrument. The cerium standards used for the calibration and quality controls were dissolved in extract of cells which had never been exposed to cerium but were digested following the same procedure as the samples of the different treatments. The emission wavelength chosen for cerium determination was 413.764 nm (He et al., 2017). The specific cellular cerium content

was calculated by normalizing the total cellular cerium content per well to the cellular protein content of the respective well.

Fluorescence microscopy

To allow the fluorescence microscopical observations of PI and OG-DMSA-CeONPs staining, treated cells were washed with 1 mL ice-cold (4°C) PBS. The cells were additionally incubated with 20 μL 4'-6-diamidino-2-phenylindole (DAPI) dye to visualize the nuclei and then, fixed with 250 μL 3.5% (w/v) paraformaldehyde in PBS for 15 min at RT and washed three times with ice-cold (4°C) PBS in intervals of 5 min. The cells were then embedded in DPX mounting medium. Fluorescence images were taken by using an Eclipse TE2000-U fluorescent microscope connected to a DS-QiMc camera (Nikon, Düsseldorf, Germany). For monitoring the different fluorescence signals the following filter settings were used: PI (λ_{ex}: 510-560 nm; λ_{em}: 590 nm; dichromatic mirror: 505 nm) and H33342 (λ_{ex}: 330-380 nm; λ_{em}: 435-485 nm; dichromatic mirror: 400 nm). In the case of OG-DMSA-CeONPs (λ_{ex}: 465-495 nm; λ_{em}: 505-515 nm; dichromatic mirror: 505 nm) and DAPI (λ_{ex}: 330-380 nm; λ_{em}: 420 nm; dichromatic mirror: 400 nm). All images were taken under the same light intensity and with the same exposure settings in order to allow direct comparisons between cells exposed to different incubation conditions.

Presentation of data

The quantitative data are presented as means ± standard deviation (SD) of values obtained in experiments on three independently prepared cultures, if not stated otherwise. Microscopic images were selected from a representative experiment that had been reproduced at least twice with comparable results. Statistical analysis of data from multiple sets of results was carried out by ANOVA followed by the Bonferroni *post-hoc* test. Significant differences between two sets of data was analyzed by the Student´s t-test using the software SigmaPlot (version 11.0). Values of $p > 0.05$ were considered as not significant. Fig.3 was created using BioRender.com.

Results

Dispersion, coating and fluorescent labeling of stable CeONPs

Different parameters were studied to assess the successful dispersion and coating of CeONPs and their physicochemical characteristics (hydrodynamic diameter, polydispersity index (Pi), ζ-potential) as well as the colloidal stability of the resulting dispersions. An

ultrasonic bath and a probe-type ultrasonic homogenizer were used to disperse the Un-CeONPS. Afterwards, size and Pi of the Un-CeONPs were tested by DLS. Both parameters were strongly affected by the ultrasonication technique applied. Sonication applied with the probe-type ultrasonic homogenizer delivered better results compared to water-bath ultrasonication, with particle sizes in the range of 156 to 98 nm (n=2) (data not shown). Different ultrasonication intensities and times were tried to achieve optimal dispersion of Un-CeONPS (Fig. 1). Size and Pi also decreased with longer ultrasonication time. For further experiments ultrasonication in two intervals of 5 minutes at 50 W were used.
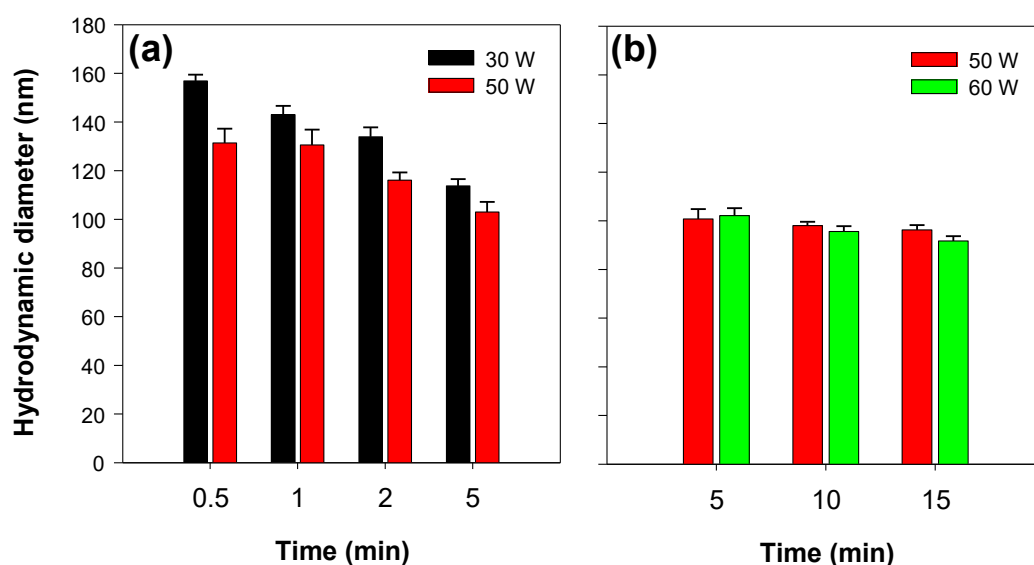
Figure 1. Effects of different ultrasonication intensities and times on the hydrodynamic diameter in Un-CeONPs. Characterization of 1 mM Un-CeONPs dispersed in H_2O with a probe-type ultrasonic homogenizer. The data represent means ± SE of values obtained for CeONPs from two independent syntheses.

After coating CeONPs with DMSA, larger aggregates formed, and two cycles of 5 min centrifugation at 1,500g, followed by two intervals of ultrasonication were needed to obtain particles with an average hydrodynamic diameter of 112 ± 4.5 nm (n=3). In detail, different coating concentrations were studied (Fig. 2) and it was observed that the stoichiometry between the CeONPs and DMSA affected in the functionalization of the particles. The addition of the coating material increased the hydrodynamic diameter in comparison to Un-CeONPs (Fig. 2a). However, when 5 mM of DMSA was added to 29 mM CeONPs, the hydrodynamic diameter of the DMSA-coated particles appeared to be slightly smaller than when 1 mM or 20 mM were used. Similarly, the coating with 10 mM DMSA resulted in NPs with a smaller hydrodynamic diameter in comparison to 1 or 20 mM. In contrast, the hydrodynamic diameter did not differ when 5 or 10 mM DMSA had been applied. The size distribution in solution was similar to that of dispersed Un-CeONPs and independent of the

DMSA concentration employed, according to the Pi (Fig. 2b). The volumetric ratios (DMSA:Un-CeONPs) tested did not seem to influence the size of the particles (data not shown). Therefore, an initial concentration of 5 mM DMSA was considered to be optimal for functionalizing the NPs. The stability of the dispersion over time for 5 mM DMSA was more than 30 days (data not shown). Finally, DMSA-CeONPs dispersion and coating procedure was established and followed for the experiments as described in the methods section.
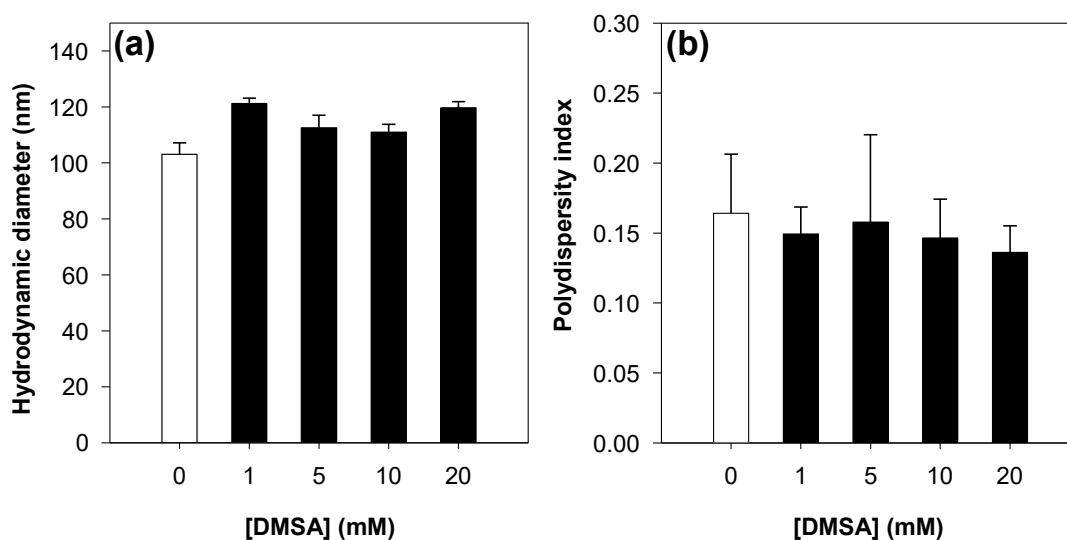
Figure 2. **Effects of coating with different initial DMSA concentrations on the hydrodynamic diameter and Pi in CeONPs dispersed in H_2O.** The hydrodynamic diameter **(a)** and Pi **(b)** of 1 mM CeONPs dispersions in H_2O were investigated and compared to those obtained for Un-CeONPs (0 mM DMSA). The data represent means ± SE of values obtained for CeONPs from two independent syntheses.

A fluorescence labeling method has been previous- and successfully used in our lab to study the fate of iron oxide nanoparticles in neural cells (Luther et al., 2013; Petters et al., 2014; Petters et al., 2016; Rastedt et al., 2017). However, this method needed to be optimized for CeONPs. Different concentrations of DMSA coating and CeONPs were evaluated as well as addition of HNO_3 (Table 1). At the same time different conditions for the synthesis, as pH and speed and time of centrifugation were successfully optimized in order to obtain a robust, reproducible and efficient labeling method (Fig. 3). The separation of OG-DMSA-CeONPs from the excess of reaction mixture is a critical step in the preparation. Iron oxide NPs can be easier sorted as they are magnetic. In the case of OG-DMSA-CeONPs, precipitation by addition of 10 times concentrated IB plus centrifugation or only centrifugation in H_2O was tested. The best results, by visual inspection, were obtained when centrifugation at 3287g for 90 s in H_2O was applied.
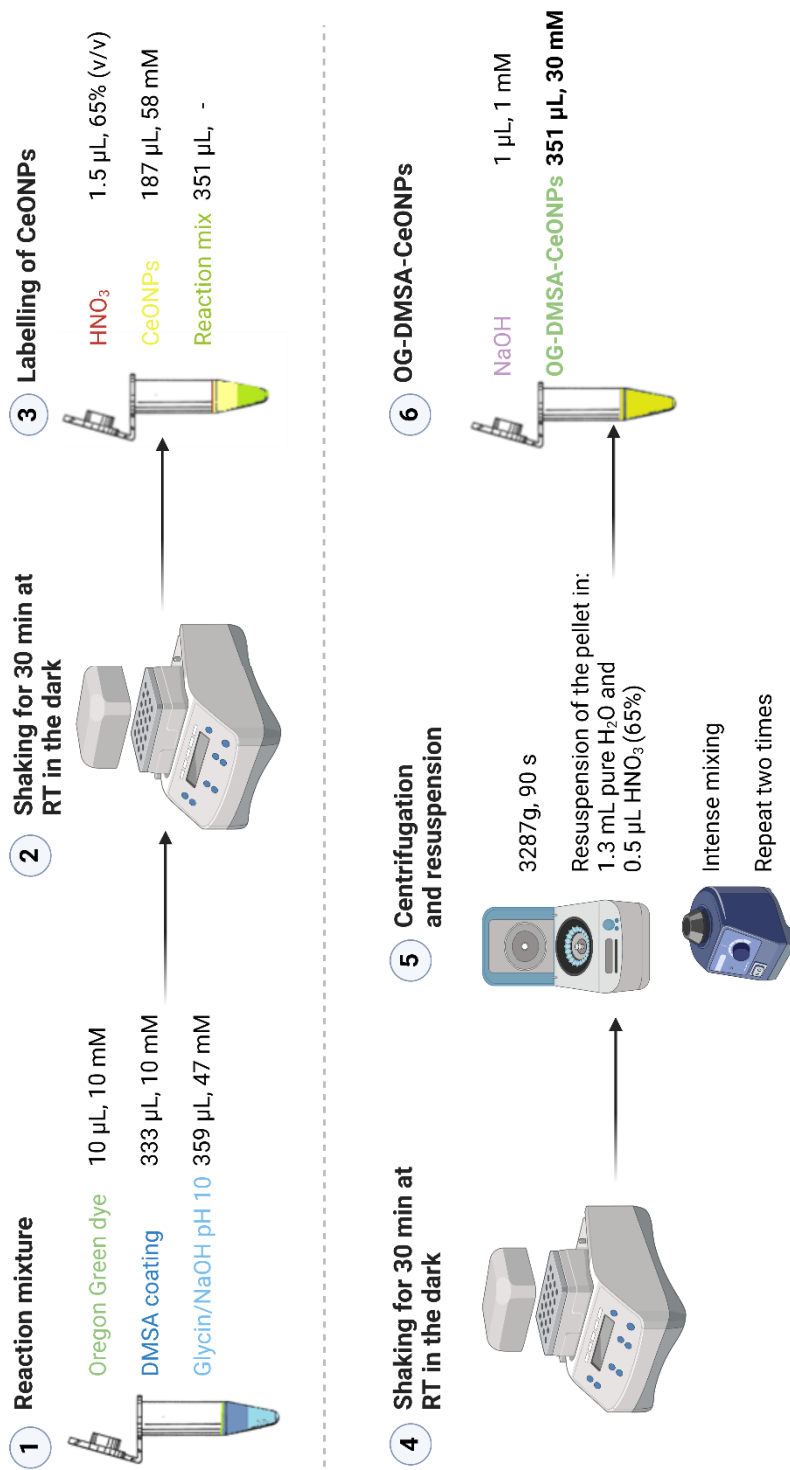
Figure 3. Method for the preparation of OG-DMSA-CeONPs. Stepwise description (1-6) of the coating and fluorescent labeling of CeONPs.

Table 1. Parameters studied for the preparation of fluorescent OG-DMSA-CeONPs.

		Alternative A		Alternative B	
		V (µL)	[C]	V (µL)	[C]
Reaction mixture	DMSA	333	10 mM	333	5 mM
	Glycin/NaOH pH 10	359	47 mM	359	47 mM
	OG	10	10 mm	10	10 mM
Un-CeONPs		187	29 mM	187	58 mM
HNO₃		0/0/0	65%	1.5/0.5/0.5	65%
NaOH		1	1 mM	1	1 mM

[V]: volume
[C]: concentration

CeONPs generated by method A (Table 1) precipitated faster (~18 h after its preparation) and showed poorer results when incubated with cells (data not shown). Alternative B had the additional advantage that the final concentration of cerium was higher and therefore allowed the preparation of more treatments from the same stock solution.

Characterization of CeONPs in H_2O and physiological media

TEM imaging of DMSA-CeONPs revealed the presence of crystalline octahedrons with an approximate size of 25 nm (Fig. 4d,e). EDX analysis of DMSA-CeONPs dispersed in water detected the specific presence of cerium (Ce), oxygen (O) and sulfur (S) (Fig. 4f). The latter element corresponds to the coating material used in the preparation of the NPs. In addition, silicon (Si) and copper (Cu) were also present, denoting the elemental composition of the TEM grid. As expected, similar results were obtained by TEM and EDX in dispersed Un-CeONPs (Fig. 4a-c) and OG-DMSA-CeONPs (Fig. 4g-i) in H_2O, indicating that the coating and labeling process did not alter the nominal size or shape of CeONPs.
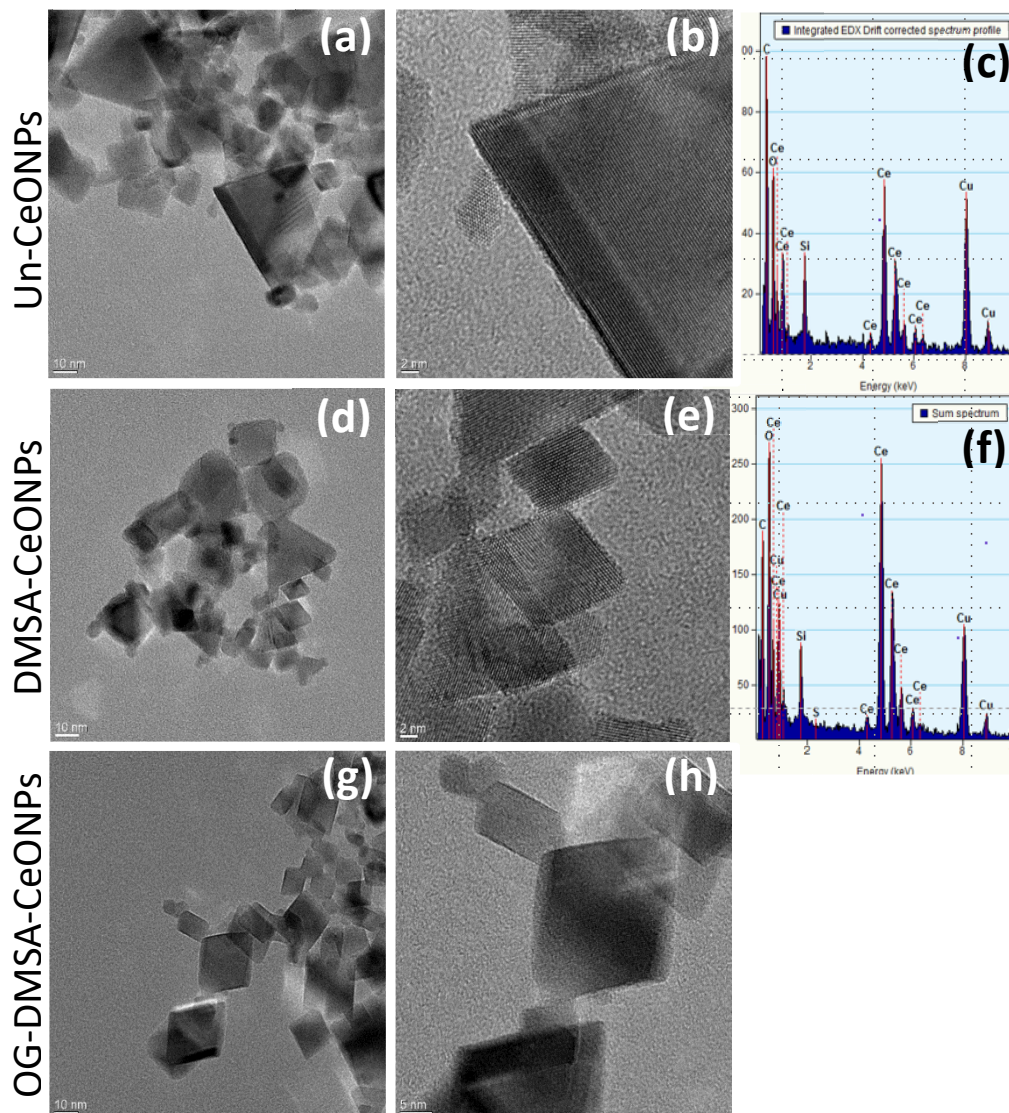
Figure 4. Characterization of Un-CeONPs, DMSA-CeONPs and OG-DMSA-CeONPs. Different CeONPs which had been dispersed in a concentration of 1 mM in pure water were applied, dried and visualised by TEM **(a, d, g)**. Higher magnifications revealed the formation of crystalline octahedrons with a size of around 25 nm **(b, e, h)**. Analysis of the elemental composition of the NPs by EDX determined the presence of Ce, O, Cu, Si as well as S derived from the DMSA coating, except for the Un-CeONPs **(c, f)**.

In order to assess the stability of CeONPs for further cell investigations, different dispersions of Un-CeONPs, DMSA-CeONPs and OG-DMSA-CeONPs in physiological media were characterized via DLS and ELS and compared with data from water dispersions. For these analyses, 1 mM of the different NPs were dispersed in IB, IB-BSA or in DMEM in the presence or absence of 10% FCS (Table 2). The results showed that Un-CeONPs and DMSA-CeONPs formed agglomerates, when dispersed in culture medium or IB in absence of proteins. The same effect has been observed in the presence of phosphate (data not shown). Therefore, the culture media had to be prepared in absence of phosphate and with the addition of BSA in the case of IB or FCS for DMEM.

Table 2. Characterization of DMSA-CeONPs.

Uncoated CeONPs (Un-CeONPs), DMSA-CeONPs were prepared and the hydrodynamic diameter (D_H), Pi and ζ- potential of 1 mM dispersions in H_2O, IB without (-BSA) or with 0.5 mg/mL BSA (+BSA) or DMEM without (-FCS) or with 10 % FCS (+FCS) were determined. For fluorescent OG-DMSA-CeONPs the D_H, Pi and ζ- potential of 1 mM dispersions only in H_2O and IB containing 0.5 mg/mL BSA were determined. The data represent means ± SD of values obtained in n =3 independent syntheses.

		H2O	IB		DMEM	
			-BSA	+ BSA	-FCS	+10% FCS
Un-CeONPs	D_H (nm)	103 ± 4	2341 ± 103	213 ± 6	2506 ± 53	212 ± 1
	Pi	0.161 ± 0.03	0.324 ± 0.12	0.230 ± 0.03	0.221± 0.15	0.200 ± 0.02
	ζ-potential (mV)	+58.1 ± 1.5	n.d.	-10 ± 1	n.d.	-13.9 ± 0.3
DMSA-CeONPs	D_H (nm)	112 ± 5	1360 ± 139	262.7 ± 1	1474 ± 117	228 ± 2
	Pi	0.150 ± 0.03	0.254 ± 0.05	0.200 ± 0.02	0.261± 0.02	0.169 ± 0.02
	ζ-potential (mV)	-27.2 ± 2.5	n.d.	-12 ±0.07	n.d.	-13.1 ± 0.8
OG-DMSA-CeONPs	D_H (nm)	133 ± 4	n.d.	152 ± 3	n.d.	n.d.
	Pi	0.15 ± 0.03	n.d.	0.196 ± 0.02	n.d.	n.d.
	ζ-potential (mV)	-10.2 ± 0.4	n.d.	-9.1 ± 0.3	n.d.	n.d.

n.d: not determined

Biocompatibility of DMSA-CeONPs and CeCl$_3$ in C6 glioma cells

To study the biocompatibility of uncoated and DMSA-coated CeONPs, a proliferation study with C6 glioma cells was performed. To investigate the difference between the potential effect of cerium when presented as NPs or as bulk material a control treatment with CeCl$_3$ and one without addition of cerium were included. The cells density at the starting of the treatments was estimated to be 1×10^5 cells well^{-1}, with a doubling rate of 24 hours. The intracellular LDH activity of control cells was 155 ± 16 nmol well^{-1} min^{-1} after the first 24 h of incubation, doubling to 359 ± 17nmol well^{-1} min^{-1} and 842 ± 83 nmol well^{-1} min^{-1} after 48 and 72 h, respectively (Fig. 5a).
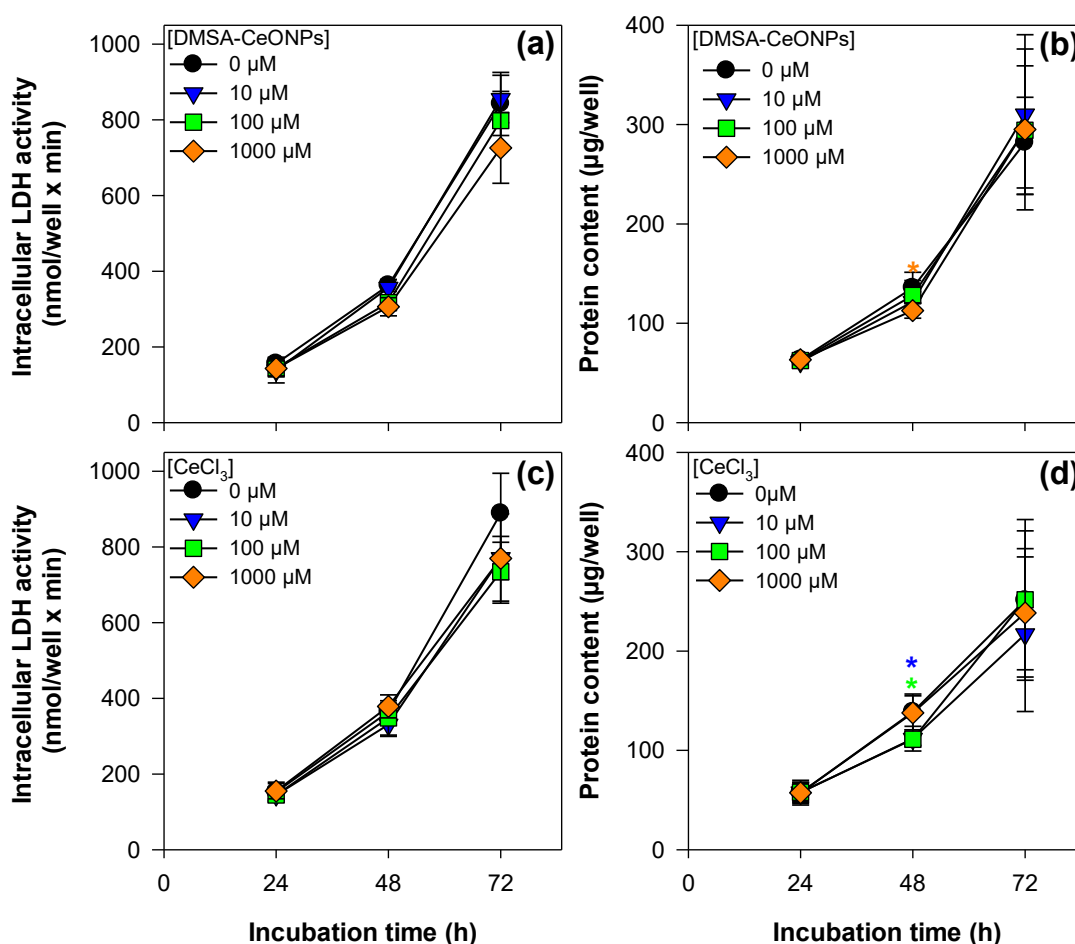
Figure 5. Time and concentration dependent effects on the proliferation of C6 glioma cells after incubation with DMSA-CeONPs or CeCl$_3$. Cells were incubated without (control; 0 µM) or with DMSA-CeONPs (a, b) or CeCl$_3$ (c, d) in DMEM+10% FCS for up to 72 h at 37°C. For the indicated timepoints, the intracellular LDH activity **(a, c)** and the protein content were determined **(b, d)**. The data shown are means ± SD of values obtained in three independent experiments (n=3). Significant differences (ANOVA) of data compared to the control are indicated by asterisks marked in the colors of the respective symbols used for the given concentrations (*p<0.05).

Treatment of cells with DMSA-CeONPs did not significantly affect the cellular LDH activity at any timepoint by comparison to the control (Fig. 5a). Under these conditions, the control had a protein content of 63 ± 5 μg well^{-1} after 24 h of incubation, increasing to 135 ± 15 μg well^{-1} and 281 ± 45 μg well^{-1} after 48 h and 72 h respectively (Fig. 5b). Similarly, the protein content of DMSA-CeONPs treated cells doubled over time for the concentrations investigated. A slight but significant decrease when treated with 1000 μM DMSA-CeONPs was observed after 48 h incubation (Fig. 5c) but not at 72 h. Moreover, exposure of C6 glioma cells to CeCl$_3$ in a concentration of up to 1000 μM did not consistently decrease the cellular LDH activity or the protein content in comparison to cells incubated in the absence of cerium (Fig. 5c,d).

APCs viability after incubation with DMSA-CeONPs

To further investigate the potential adverse effect of DMSA-CeONPs on brain cells, confluent APCs were incubated for 24, 48 and 72 h in the absence or presence of DMSA-CeONPs in culture medium at 37°C (Fig. 6).
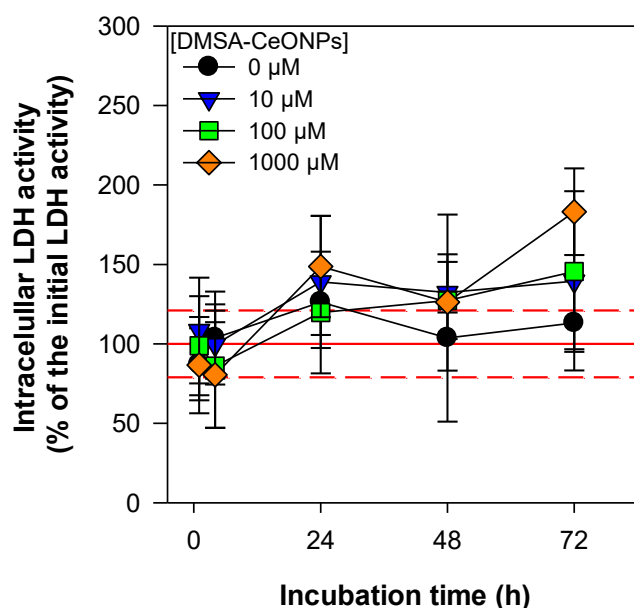
Figure 6. Test for viability of APCs after exposure to DMSA-CeONPs. Cells were incubated without (control; 0 μM) or with DMSA-CeONPs in culture medium for up to 72 h at 37°C. For the indicated timepoints, the intracellular LDH activity was determined. The data shown are means ± SD of values obtained in three independent experiments (n=3). Significant differences (ANOVA) of data compared to the control were calculated but no statistically difference was found.

The intracellular LDH activity was preserved even during the incubations for 72 h with 1000 μM DMSA-CeONPs in comparison to the control (Fig. 6). No significant differences in cellular

LDH were obtained compared to the astrocytes incubated in the absence of DMSA-CeONPs. The absence of toxicity of DMSA-CeONPs for APCs was validated by investigating their membrane integrity by staining with the fluorescent dye PI (Fig. 7).
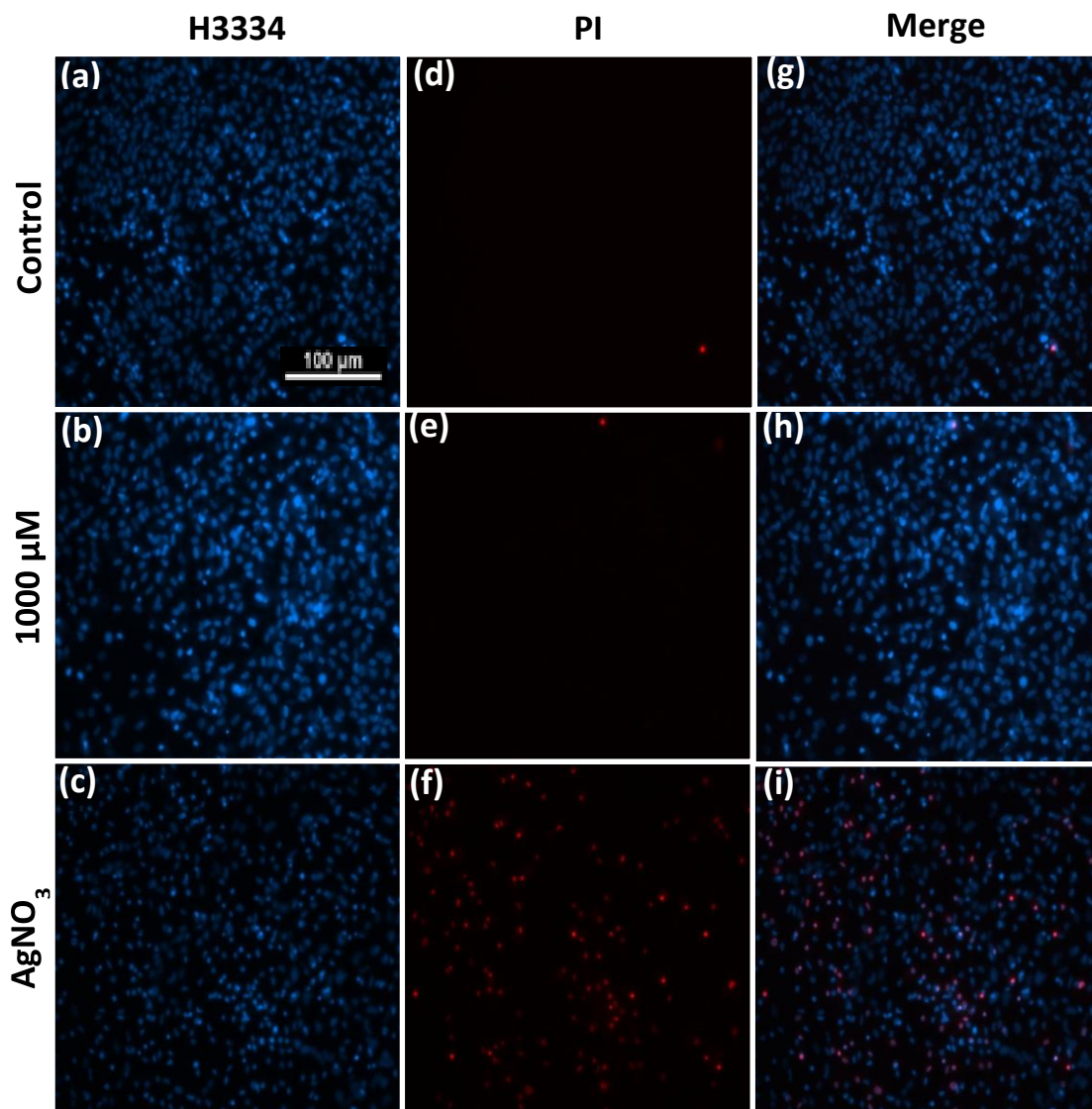
Figure 7. Membrane integrity of APCs after treatment with DMSA-CeONPs. Cells were incubated without (control) or with 1000 μM DMSA-CeONPs in culture medium for 72 h at 37°C. Subsequently, the cells were stained for membrane integrity by application of PI **(d, e)** and the cell nuclei were visualized with H33342 **(a, b)**. As positive control for the loss of cell membrane integrity cells were incubated with 200 μM AgNO$_3$ for 2 h **(c, f)**. The data shown are from a representative experiment that was replicate twice on independent prepared cultures with equivalent results. The scale bar in panel **(a)** represents 100 μm and applies to all panels

Control cultures treated in the absence of DMSA-CeONPs did not show PI positive cells (Fig. 7d,g). Similarly, the cell membrane integrity was not compromised within a 72 h incubation with 1000 μM DMSA-CeONPs as indicated by the absence of PI positive cells (Fig. 7e,h). APCs

were also treated with 200 µM AgNO$_3$. This positive control confirmed the detection of a severe loss in membrane integrity by PI staining (Fig. 7f,i).

Qualitative and quantitative uptake of OG-DMSA-CeONPs in C6 glioma cells.

As shown above, no toxic effects in brain cell cultures incubated in the presence of DMSA-CeONPs were observed. However, a demonstration of internalization of DMSA-CeONPs was required to assess their biocompatibility and possible biomedical use.

To demonstrate the uptake of DMSA-CeONP, C6 glioma cells were incubated with 1000 µM OG-DMSA-CeONPs in IB-BSA for up to 1 h at 4°C or 37°C. This treatment caused no loss of cell viability as demonstrated by the absence of any significant increase in the extracellular LDH activity (data not shown). However, a significant time-dependent uptake of OG-DMSA-CeONPs into the cells was taking place already within 15 min after the application of the OG-DMSA-CeONPs, as demonstrated by the localization of CeONPs fluorescence around stained nuclei (Fig. 8e-h). Cells that had been incubated with OG-DMSA-CeONPs at 37°C showed a more intense and localized cellular fluorescence compared to cells that had been incubated at 4°C (Fig. 8a-d). These observations suggest an uptake of OG-DMSA-CeONPs mediated by active cell mechanisms. This data also seems to indicate that the uptake continued increase over time (Fig. 8e-h).
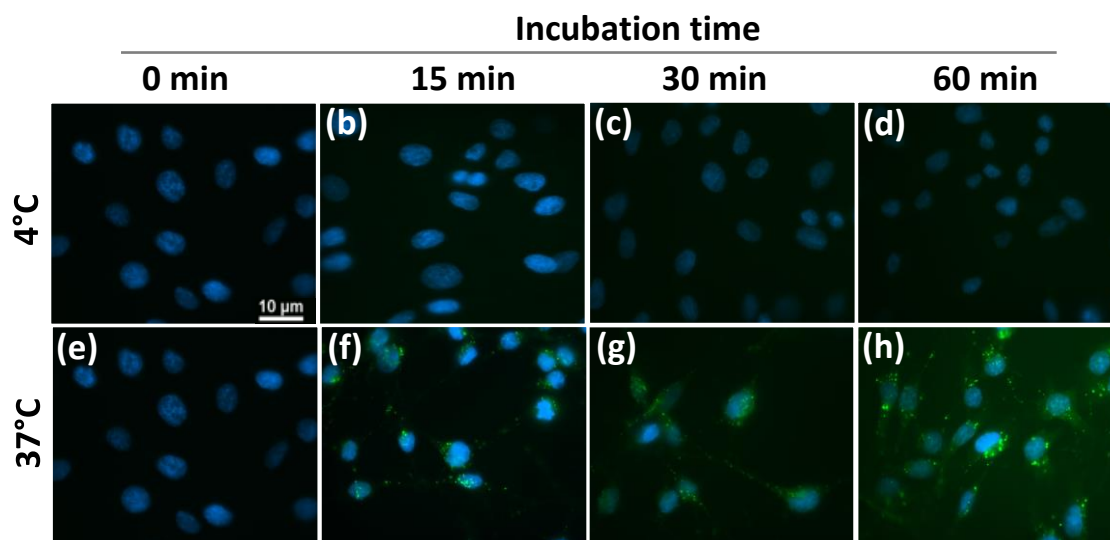
Figure 8. Microscopical study to investigate the uptake of OG-DMSA-CeONPs at a concentration of 1000 µM in C6 glioma cells. The cells were incubated in 24-well plates at 4°C or 37°C in IB containing 0.5 mg/mL BSA for the indicated time periods. Nuclei were stained with DAPI (blue) and OG-DMSA-CeONPs staining is shown in green. All images were recorded using identical microscopical settings. The data shown are from a representative experiment that was replicate twice on independent prepared cultures with equivalent results. The scale bar in **(a)** represents 10 µm and applies to all panels.

APCs were also incubated with 1000 μM OG-DMSA-CeONPs in IB-BSA at 4°C and 37°C for up to 4 h (Fig. 9). Similar to the incubation with C6 glioma cells (Fig.8), the intracellular accumulation of the NPs showed a time- and temperature dependent pattern. The uptake seemed to be faster and greater at 37°C (Fig. 9e-h) than at 4°C (Fig. 9a-d).
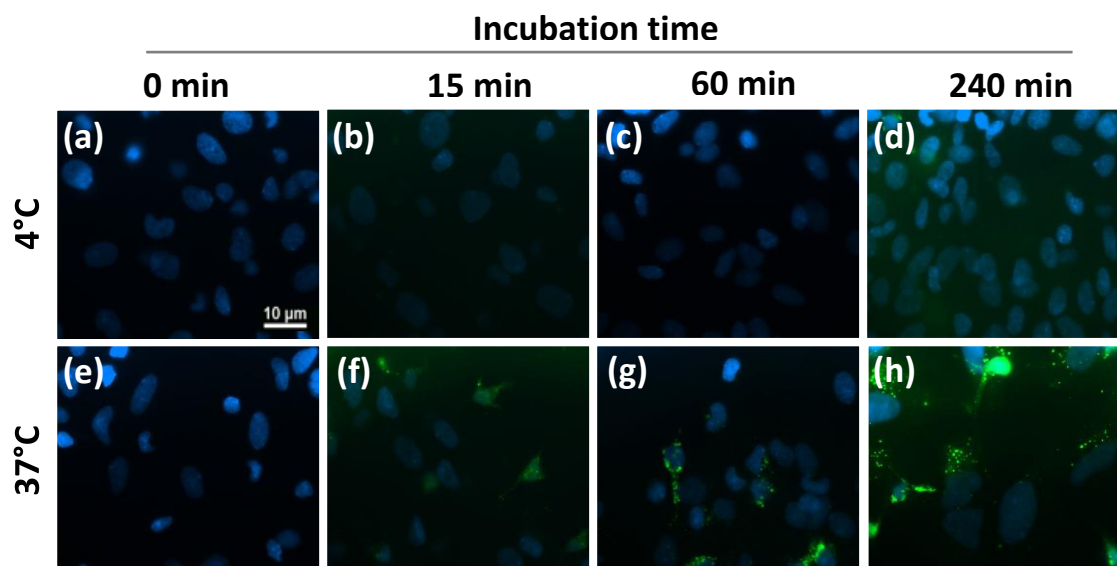
Figure 9. Microscopical study to investigate the uptake of OG-DMSA-CeONPs at a concentration of 1000 μM in APCs. The cells were incubated in 24-well plates at 4 °C or 37 °C in IB containing 0.5 mg/mL BSA for the indicated time periods. Nuclei were stained with DAPI (blue) and OG-DMSA-CeONPs staining is green. All images were recorded using identical microscopical settings. The data shown are from a representative experiment that was replicate twice on independent prepared cultures with equivalent results. The scale bar in (a) represents 10 μm and applies to all panels.

Quantification of cellular cerium content by ICP-OES in C6 glioma cells

As expected based on our previous results, the incubation of C6 glioma cells with 400 μL 1 mM DMSA-CeONPs at 4°C or 37°C for 1 h in a dedicated experiment to quantify CeONPs uptake, did not affect cell viability. Cell membrane permeability was not increased by the incubation with DMSA-CeONPs in comparison to control cells after incubations, as seen by the almost identical cellular LDH activity (Fig. 10a). Protein content was also almost identical after incubation in the absence or the presence of DMSA-CeONPs and was also not affected by the incubation temperature (Fig. 10b).

For the quantification of cerium by ICP-OES, a calibration curve was prepared (Fig. 10c). To imitate the matrix in which the samples were prepared, each standard solution containing cerium was diluted in the appropriate volume of an aqueous solution containing lysates of C6 glioma cells and 2% HNO_3 (v/v). The calibration curve, which was obtained at a

wavelength emission (λ) of 413.764 nm, showed a perfect linearity in the concentration range chosen (Fig. 10c).
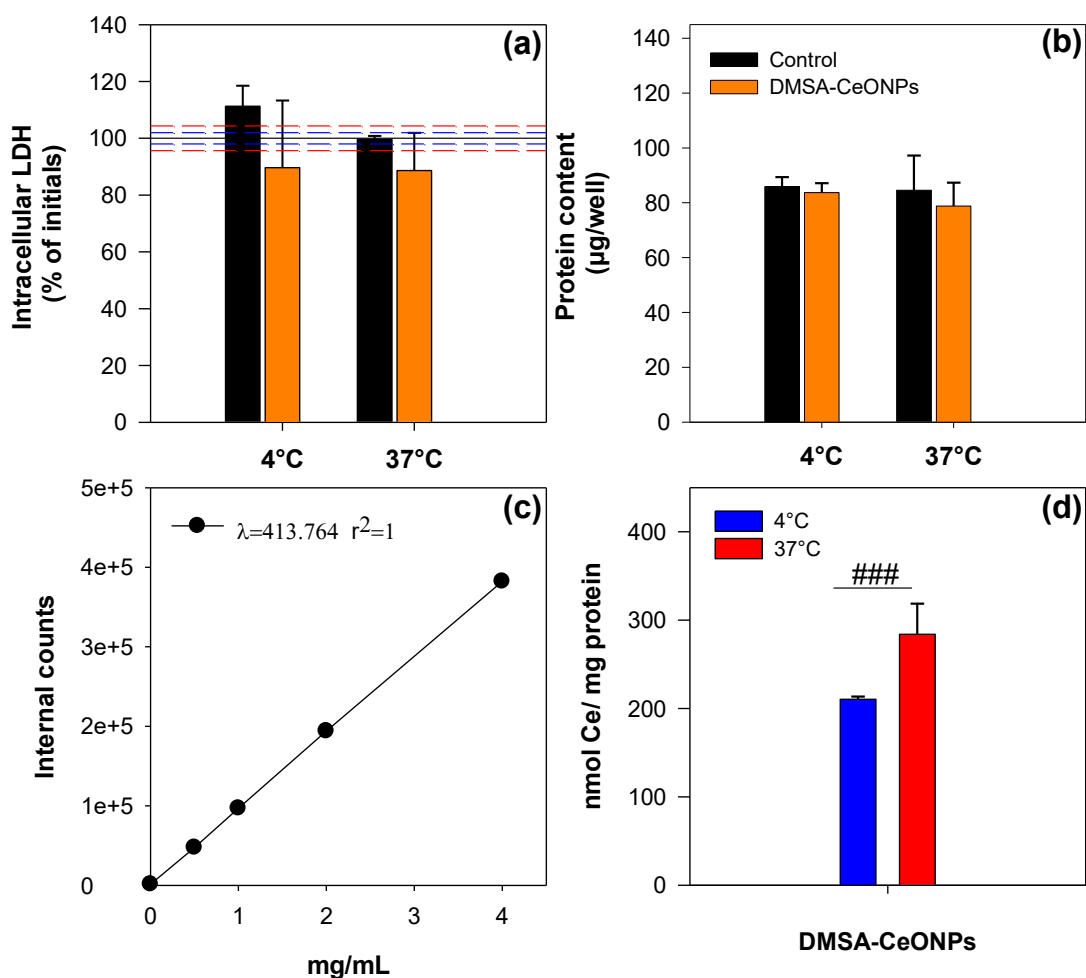
Figure 10. Uptake of DMSA-CeONPs by C6 glioma cells. The cells were incubated with 400 μL 1 mM cerium applied as DMSA-CeONPs at 4°C or 37°C for 1 h. For the different incubation-temperatures the intracellular LDH activity **(a)**, the protein content **(b)**, the calibration curve with 0, 0.5, 1, 2 and 4 mg/L cerium standards **(c)** and the cellular content of cerium (nmol) per milligram of protein **(d)** were determined. In **(a)** the black line indicates the activity of LDH in untreated cells before the incubation, the dotted lines in blue and red indicate the SD for the 4°C and 37°C experiments, respectively. In **(a)** and **(b)**: results are mean ± SD of triplicates from three experiments (n=3); in **(c)** and **(d)** the results concerning DMSA-CeONPs at 37°C are mean ± SD of triplicates of two independent experiments (n=2).

For the determination of cellular cerium, samples needed to be resuspended in 4 mL 2% HNO$_3$ (v/v) in order to reach the minimum volume which could be injected in the IPC-OES. The calculated uptake of cerium at 4°C was 210 ± 3 nmol Ce mg^{-1} protein while a significant increase occurred when the cells have been incubated at 37°C containing 314 ± 15 nmol Ce

mg^{-1} protein. This difference represented $\sim$ 33% of increase in the accumulation of cerium at the temperature which cells are considered to display normal physiological activity.

Discussion

The biocompatibility and cellular uptake of CeONPs have been previously investigated on diverse cell cultures as well as *in vivo*. These particles appear not to be toxic for many mammalian cell lines (Dhall and Self, 2018) but controversial results can also be found in the literature (Casals et al., 2020). The reported contradictory results have been attributed to differences in size, shape, colloidal distribution or the coating of the NPs (Nelson et al., 2016). Therefore, in order to potentially add a new type of functionalized CeONPs, biocompatible with primary rat astrocytes and C6 glioma cells, the parameters for a successful dispersion and a new coating were tested.

Commercial CeONPs showed promising results when the dispersion followed two cycles of ultrasonication. The resulting stock solution of Un-CeONPs had a long shelf-life (up to 60 days) and high stability in H$_2$O, standing out from many other metal NPs (Haddad et al., 2014) and also other preparations of CeONPs. Subsequently, these NPs were functionalized with DMSA, showing a high colloidal stability in H$_2$O and physiological culture media as well. To the best of our knowledge, this is the first report describing CeONPs which have been functionalized with DMSA. Common coatings already explored in the literature include poly(acrylic acid) (PAA) (Sehgal et al., 2005; Zhang et al., 2016; Ju et al., 2021), polyethylene glycol (Cimini et al., 2012; Xue et al., 2018; Hu and Ding, 2022), dextran (Perez et al., 2008; Alpaslan et al., 2015) and polyethilenimine (Hasanzadeh et al., 2019; Tian et al., 2020).

In a recent study, Ju and colleagues (2020) investigated the colloidal stability of uncoated, spherical and self-synthesized CeONPs with a nominal diameter in the range of 2-6 nm and compared the results when such NPs were coated with dextran or PAA and dispersed in H$_2$O in the absence or presence of BSA, DMEM or DMEM + 5% FCS. Although no direct comparison can be established due to the difference in nominal size with our results, their uncoated CeONPs showed a hydrodynamic diameter of 176 nm and a negative ζ-potential (-28 mV) in H$_2$O, in contrast to the here reported Un-CeONPs which presented a positive ζ-potential. The authors observed an increase in the hydrodynamic diameter in the presence of serum and a negative ζ-potential (-35 mV). Contrary to DMSA-CeONPs, the absence of proteins or serum in the culture medium did not result in a drastic agglomeration and precipitation. The authors argue that changes in stability resulted from the combination of

steric and electrostatic repulsion, deriving from the polymers and the ionic strength of the media respectively.

In the case of DMSA-CeONPs, the binding between the coating and the NPs most likely occurs through electrostatic interactions between negatively charged carboxyl groups of the DMSA molecules and the surface of the CeONPs, as previously reported for iron oxide NPs (Petters et al., 2014; Petters et al., 2016; Rastedt et al., 2017) and copper oxide NPs (Bulcke et al., 2014; Joshi et al., 2016). Un-CeONPs in H_2O revealed a net positive value of 58 mV. However, when coated with DMSA, the ζ-potential of CeONPs turned negative (-27,2 mV). It has been hypothesized that DMSA forms a cage-like structure around the core of copper oxide NPs via disulfide bridges (Geppert et al., 2011; Bulcke et al., 2014), exposing its free carboxyl groups to the outside. A similar mechanism might occur in the DMSA-CeONPs as their ζ-potential had a relatively strong negative value.

Previous studies showed that electrostatically stabilized NPs have generally shown limited stability in culture media (Asati et al., 2010). In the case of the dextran-coated CeONPs mentioned above, where a combination of steric and electrostatic forces was involved, the shelf-life was limited to 72 h even in the presence of FCS (Ju et al., 2020). In this sense, DMSA-CeONPs represent an advance as they showed a better stability with a shelf-life up to 7 days. All together implies that other factors as ionic strength, pH and soft corona formation are unequally contributing to the colloidal stability of the different CeONPs in dispersion. In fact, for the current study, to obtain DMSA-CeONPs in the nanoscale range and with a relative long shelf-life, the physiological incubation media needed to be supplemented with protein (BSA or FCS). This effect has been already reported for other metal NPs as for example copper oxide (Joshi et al., 2019), silver and iron oxide NPs (Jurašin et al., 2016; Levak et al., 2017).

In order to evaluate the actual uptake of CeONPs, a qualitative and a quantitative approach were developed. A new fluorescent labeling method of CeONPs was optimized based on a previous procedure developed for iron oxide nanoparticles (OG-DMSA-IONPs) (Rastedt et al., 2017). The fluorescent dye OG forms covalent bonds with the DMSA coating (Kaewsaneha et al., 2015) and allow the intracellular localization of internalized CeONPs. Importantly, the fluorescent labeling with OG did not alter the size distribution or the morphology of the NPs in comparison to DMSA-CeONPs. Fluorescence microscopy of C6 glioma cells and APCs after incubation with OG-DMSA-CeONPs at 37°C showed a dotted cellular staining pattern which seems to indicate that the NPs accumulated within the cells in vesicular structures. To test whether CeONPs were internalized by C6 glioma cells and

APCs or the fluorescence obtained resulted from adsorbed CeONPs to the cell membrane, the cells were exposed to OG-DMSA-CeONPs at 4°C, since the low temperature is known to slow down transport across the membrane (Luther et al., 2013; Rastedt et al., 2017). Hardly any fluorescence was recorded at 4°C neither in C6 glioma cells or APCs, suggesting an active uptake of OG-DMSA-CeONPs might occur. Previous studies have suggested that negatively charged NPs concentrate at cationic sites of adsorption along the cell membrane due to repulsive forces caused by the negatively charged domains of the cell surface. The NPs already bound to the cell membrane reduce the repulsion of other NPs by decreasing the charge density what may favour adsorption of other free NPs (Wilhelm et al., 2003). Consequently, several studies have described a faster and more efficient internalization of negatively charged CeONPs (Patil et al., 2007; Renu et al., 2012; Babu et al., 2014). However, other findings indicate that positively charged CeONPs were broadly internalized (Asati et al., 2010). The uptake can occur via several mechanism as non-specific or receptor-mediated endocytosis, pinocytosis or phagocytosis in the case of larger particles (Lorenz et al., 2006). Later studies have suggested that the uptake is a function of the ζ-potential and size of the NPs but also cell dependent (Behzadi et al., 2017; Vassie et al., 2017).

Whereas the synthesis of iron fluorescent metal NPs has been explored in the past (Lee et al., 2008; Yen et al., 2013; Petters and Dringen, 2015; Wu et al., 2015), fluorescent CeONPs have been less investigated. Patil et al. (2007) analysed the internalization of functionalized CeONPs with fluorescent carboxyfluorescein in the retina by confocal fluorescence microscopy. Xia et al. (2008) examined the uptake and cellular localization of CeONPs in macrophage and epithelial cells by using CeONPs labelled with fluorescein. The authors conclude that CeONPs were localized in a caveolin-1 positive cell compartment in epithelial cells while in the macrophages CeONPs were allocated in late endosomes after 24 h of incubation. Other study showed by fluorescence microscopy the uptake of 5 mg mL^{-1} rhodamine conjugated CeONPs in human prostate cancer cells after a 24 h incubation. The results demonstrated that negative charged fluorescent CeONPs were effectively taken up and even caused some change in cell morphology (Renu et al., 2012). OG-DMSA-IONPs incubated with C6 glioma cells accumulated in a time-, concentration- and temperature-dependent manner (Rastedt et al., 2017), similarly to the results presented here for the OG-DMSA-CeONPs and did not affect cell morphology in short time incubations. Of note OG-DMSA-IONPs also exhibited a negative ζ-potential (∼-21 mV) when dispersed in IB (Rastedt et al., 2017).

To have a further and quantitative insight in the internalization of CeONPs by C6 glioma cells, an ICP-OES method was developed and applied. After incubation, the organic phase of the samples was totally digested and the cerium was solubilized. The measurements were inside the range of the detection limit calculated as three times the standard deviation of the blank (Shemirani and Yousefi, 2007). The relatively high content of NaOH present in the samples (115 ppm) did not cause an interference with the determinations as observed by the results of the two different quality controls measured, which were diluted in the same lysate matrix as the samples. The results corroborated the increased uptake of cerium when the incubation was performed at 37°C compared to 4°C. After 1 h incubation at 37°C the uptake of Ce represented 7.8% of the total Ce added while at 4°C the cells had only internalized 5.3%. Comparisons in the uptake based on the literature are hard to establish due to the different incubation conditions (type of cells, initial concentration of CeONPs added, time of incubation, etc.). In our group, it has been shown that the cellular uptake of C6 glioma cells after incubation with 500 μM DMSA-CuONPs for 1 h at 37°C is approximately 10% and at 4°C about the 4.3% of the total Cu amount added, measured by atomic absorption spectroscopy (Joshi, 2019). The uptake of DMSA-IONPs by C6 glioma cells have also been studied in our group. C6 glioma cells strikingly internalized 50% of the total iron added (1 mM) at 37°C and after 1 h incubation (Rastedt et al., 2017). The similarities between DMSA-CeONPs and DMSA-CuONPs might indicate that the uptake of these two different NPs share a common mechanism in C6 glioma cells. Likewise, the adsorption of NPs to cells surface seem to be very similar. In contrast, in the case of DMSA-IONPs a different internalization route might be involved. In a recent report concerning the administration of CeONPs in space, it was demonstrated that the uptake of the same commercial CeONPs as used in the present study by C2C12 myoblast was ~22% after 48 h incubation with 100 μg/mL CeONPs at normal gravity (Genchi et al., 2021). Remarkably, the NPs were coated by adding 50% foetal bovine serum and allowing them to bond for certain time. The hydrodynamic diameter and ζ-potential in H_2O were very similar to DMSA-CeONPs in IB-BSA, despite the different coating.

Inductively coupled plasma mass spectrometry (ICP-MS) is the more extended method for the quantification of cerium in biomedical studies, investigating NPs (Flores et al., 2021). ICP-OES have been also used for such determinations but limited, most likely by the larger detection limit in comparison to ICP-MS. However, in the present study, data showed that ICP-OES is also suitable and reliable for *in vitro* studies. ICP-OES is more affordable and the samples analysis is significantly faster in comparison to ICP-MS.

Nevertheless, the major weakness of IPC-OES (and also ICP-MS) determinations is that the extent of the signal which corresponds with the adsorbed cerium to the cells surface and even to the plastic of the incubation wells cannot be distinguished from the effectively internalized cerium. In addition, it is unclear whether the adsorption process varies with the temperature as well. Also remarkable is the inability of ICP-OES or ICP-MS to differentiate if dissolution of the NPs occurs (Clases and Gonzalez de Vega, 2022). Some authors have tried to overcome the mentioned analytical limitations by coupling ICP-MS to single particle analysis (sp-ICP-MS). This technique also provides relevant information concerning the size, elemental composition, physicochemical states and particles concentrations in biological samples (Flores et al., 2021). However, for the complete study of the internalization of NPs by cells, qualitative microscopy techniques as SEM, TEM or confocal laser scanning microscopy (CLSM) need to be considered. CLSM stands out as it facilitates the visualization of the uptake considering the three dimensions of the cells and therefore, revealing important factors of the fate of the NPs inside the cells (Zhou et al., 2013; Abdel-Hafez et al., 2018).

In the interaction with cells, treatment with DMSA-CeONPs up to 1000 µM ($\sim$140 mg Ce L[1]) did not compromise cell membrane integrity over three days in C6 glioma cells or APCs, demonstrated by cellular LDH activity and PI staining results. This suggests a high biocompatibility of DMSA-CeONPs with cultured brain cells. The comparison between DMSA-CeONPs and $CeCl_3$ on the proliferation of C6 glioma cells revealed that under the conditions tested, the fact of presenting cerium as NPs or salt was not relevant. This is important as NPs are not just chemicals but rather entities with their own complete physicochemical features or as Rzigalinski and colleagues (2017) introduced, NPs exert as "mini-reactors".

Despite its relevance, the findings concerning the biocompatibility and uptake of CeONPs in C6 glioma cells or APCs in the literature are still scarce and have produced rather atomized knowledge. Interestingly, Fernández-Bertólez et al. (2023) investigated the cytotoxicity of the same CeONPs presented in this study in human A172 glial cells and SH-SY5Y neuronal cells in a similar concentration range and determined scarce cytotoxicity or genotoxicity, which only started to develop under longer incubation times (48 h). In a different approach, viability of CeONPs as an anticancer drug in a model of human glioma was studied, specifically in a cell line derived from anaplastic astrocytoma. It was shown that 300 µM CeONPs after 72 h were cytotoxic to the glioma cells but not toxic for healthy endothelial cells under the same conditions (Sack-Zschauer et al., 2017). In contrast, DMSA-CeONPs in

our study did not present any toxicity to C6 glioma cells after the same period and for higher concentrations. A possible explanation might be the origin of the cells, human vs. Wistar rat APCs or the size of the CeONPs. Also contrary to the present findings, Minchenko et al. (2013) showed that exposure of human immortalized astrocytes to concentrations of 0.17 and 0.34 mg mL^{-1} during 20 h significantly reduced the expression level of transcription factors which regulate proliferation and survival. On the other hand, Xu et al. (2016) demonstrated the neuroprotective effect of CeONPs by reducing astrogliosis *in vitro* and *in vivo* in a mice model for hypothalamic inflammation. Indirectly in this study, it is shown that the CeONPs in low concentrations (5-200 µg mL^{-1}) are biocompatible with mice APCs, similar to results presented here. In fact, in the mentioned study, CeONPs significantly extended the lifespan of APCs subjected to neuroinflammation (Xu et al., 2016).

With the present study we have contributed to fill the gap regarding the possibility of incorporating CeONPs by two cell models for astrocytes. Thereby we paved the way for further investigations regarding the metabolic effects and potential ROS scavenging activity of these compounds.

Future perspectives

DMSA-CeONPs present some advantages over pre-existing functionalized CeONPs, regarding for example their stability and potentially also biocompatibility. Therefore, future investigations of their physicochemical features are recommended. For instance, the quantification of the DMSA molecules adsorbed to the CeONPs could give further insights into the colloidal stability and the influence of the ionic strength of the media (Bemowsky et al., 2019). In addition, the investigation of the Ce^{3+}/Ce^{4+}, by X-ray photoelectron spectroscopy, would be necessary to predict their potential as nanozymes and to study some possible substitutions occurring in their surface when dispersed in media with the presence of BSA or FCS. The determination of the total amount of the protein adsorbed to the NPs might add relevant information about the identity in culture of the DMSA-CeONPs as well. Another important aspect to be studied concerning stability, is the potential dissolution behavior of DMSA-CeONPs over time. The release of cerium ions and the detachment of the coating need to be addressed.

As the uptake of DMSA-CeONPs in C6 glioma cells and APCs has been demonstrated a detailed investigation of their fate inside the cell could be of relevance. Such investigations could target the incorporation mechanism and a potential accumulation in lysosomes, endosomes or other structures. For that purpose, a more exhaustive time-concentration

study in combination with microscopical observations and ICP-OES quantification must be considered.

Another aspect to be investigated in the future is the effects caused by the accumulation of DMSA-CeONPs on the metabolism of C6 glioma cells and APCs and their possible ability to scavenge ROS in pathological conditions. To explore their potential as biomedical tools is the ulterior motivation of the establishment of this new coated CeONPs and their characterization.

References

Abdel-Hafez, S. M., R. M. Hathout and O. A. Sammour (2018). "Tracking the transdermal penetration pathways of optimized curcumin-loaded chitosan nanoparticles via confocal laser scanning microscopy." International Journal of Biological Macromolecules 108: 753-764.

Alili, L., M. Sack, A. S. Karakoti, S. Teuber, K. Puschmann, S. M. Hirst, C. M. Reilly, K. Zanger, W. Stahl and S. Das (2011). "Combined cytotoxic and anti-invasive properties of redox-active nanoparticles in tumor–stroma interactions." Biomaterials 32(11): 2918-2929.

Alpaslan, E., H. Yazici, N. H. Golshan, K. S. Ziemer and T. J. Webster (2015). "pH-dependent activity of dextran-coated cerium oxide nanoparticles on prohibiting osteosarcoma cell proliferation." ACS Biomaterials Science & Engineering 1(11): 1096-1103.

Andersen, J. K. (2004). "Oxidative stress in neurodegeneration: cause or consequence?" Nature Medicine 10(7): S18-S25.

Asati, A., S. Santra, C. Kaittanis and J. M. Perez (2010). "Surface-charge-dependent cell localization and cytotoxicity of cerium oxide nanoparticles." ACS Nano 4(9): 5321-5331.

Babu, K. S., M. Anandkumar, T. Tsai, T. Kao, B. S. Inbaraj and B. Chen (2014). "Cytotoxicity and antibacterial activity of gold-supported cerium oxide nanoparticles." International Journal of Nanomedicine 9: 5515.

Bailey, Z. S., E. Nilson, J. A. Bates, A. Oyalowo, K. S. Hockey, V. S. S. S. Sajja, C. Thorpe, H. Rogers, B. Dunn and A. S. Frey (2020). "Cerium oxide nanoparticles improve outcome after in vitro and in vivo mild traumatic brain injury." Journal of Neurotrauma 37(12): 1452-1462.

Baschieri, A. and R. Amorati (2021). "Methods to determine chain-breaking antioxidant activity of nanomaterials beyond DPPH•. A review." Antioxidants 10(10): 1551.

Behl, T., R. Makkar, A. Sehgal, S. Singh, N. Sharma, G. Zengin, S. Bungau, F. L. Andronie-Cioara, M. A. Munteanu and M. C. Brisc (2021). "Current trends in neurodegeneration: Cross talks between oxidative stress, cell death, and inflammation." International Journal of Molecular Sciences 22(14): 7432.

Behzadi, S., V. Serpooshan, W. Tao, M. A. Hamaly, M. Y. Alkawareek, E. C. Dreaden, D. Brown, A. M. Alkilany, O. C. Farokhzad and M. Mahmoudi (2017). "Cellular uptake of nanoparticles: journey inside the cell." Chemical Society Reviews 46(14): 4218-4244.

Bemowsky, S., A. Rother, W. Willmann, J. Köser, M. Markiewicz, R. Dringen and S. Stolte (2019). "Quantification and biodegradability assessment of meso-2, 3-dimercaptosuccinic acid adsorbed on iron oxide nanoparticles." Nanoscale Advances 1(9): 3670-3679.

Bolaños, J. P. (2016). "Bioenergetics and redox adaptations of astrocytes to neuronal activity." Journal of Neurochemistry 139: 115-125.

Bulcke, F., K. Thiel and R. Dringen (2014). "Uptake and toxicity of copper oxide nanoparticles in cultured primary brain astrocytes." Nanotoxicology 8(7): 775-785.

Bylicky, M. A., G. P. Mueller and R. M. Day (2018). "Mechanisms of endogenous neuroprotective effects of astrocytes in brain injury." Oxidative Medicine and Cellular Longevity 2018.

Casals, E., M. Zeng, M. Parra-Robert, G. Fernández-Varo, M. Morales-Ruiz, W. Jiménez, V. Puntes and G. Casals (2020). "Cerium oxide nanoparticles: advances in biodistribution, toxicity, and preclinical exploration." Small 16(20): 1907322.

Cimini, A., B. D'Angelo, S. Das, R. Gentile, E. Benedetti, V. Singh, A. M. Monaco, S. Santucci and S. Seal (2012). "Antibody-conjugated PEGylated cerium oxide nanoparticles for specific targeting of Aβ aggregates modulate neuronal survival pathways." Acta Biomaterialia 8(6): 2056-2067.

Clases, D. and R. Gonzalez de Vega (2022). "Facets of ICP-MS and their potential in the medical sciences—Part 2: nanomedicine, immunochemistry, mass cytometry, and bioassays." Analytical and Bioanalytical Chemistry 414(25): 7363-7386.

Das, J., Y.-J. Choi, J. W. Han, A. M. M. T. Reza and J.-H. Kim (2017). "Nanoceria-mediated delivery of doxorubicin enhances the anti-tumour efficiency in ovarian cancer cells via apoptosis." Scientific Reports 7(1): 1-12.

DeCoteau, W., K. L. Heckman, A. Y. Estevez, K. J. Reed, W. Costanzo, D. Sandford, P. Studlack, J. Clauss, E. Nichols and J. Lipps (2016). "Cerium oxide nanoparticles with antioxidant properties ameliorate strength and prolong life in mouse model of amyotrophic lateral sclerosis." Nanomedicine: Nanotechnology, Biology and Medicine 12(8): 2311-2320.

Dhall, A. and W. Self (2018). "Cerium oxide nanoparticles: a brief review of their synthesis methods and biomedical applications." Antioxidants 7(8): 97.

Dowding, J., W. Song, K. Bossy, A. Karakoti, A. Kumar, A. Kim, B. Bossy, S. Seal, M. Ellisman and G. Perkins (2014). "Cerium oxide nanoparticles protect against Aβ-induced mitochondrial fragmentation and neuronal cell death." Cell Death and Differentiation 21(10): 1622-1632.

Dowding, J. M., S. Das, A. Kumar, T. Dosani, R. McCormack, A. Gupta, T. X. Sayle, D. C. Sayle, L. von Kalm and S. Seal (2013). "Cellular interaction and toxicity depend on physicochemical properties and surface modification of redox-active nanomaterials." ACS Nano 7(6): 4855-4868.

Dringen, R., M. Brandmann, M. C. Hohnholt and E.-M. Blumrich (2015). "Glutathione-dependent detoxification processes in astrocytes." Neurochemical Research 40(12): 2570-2582.

Dringen, R., L. Kussmaul and B. Hamprecht (1998). "Detoxification of exogenous hydrogen peroxide and organic hydroperoxides by cultured astroglial cells assessed by microtiter plate assay." Brain Research Protocols 2(3): 223-228.

Estevez, A. Y. and J. S. Erlichman (2014). "The potential of cerium oxide nanoparticles (nanoceria) for neurodegenerative disease therapy." Nanomedicine: Nanotechnology, Biology, and Medicine 9(10): 1437-1440.

Fauconnier, N., J. Pons, J. Roger and A. Bee (1997). "Thiolation of maghemite nanoparticles by dimercaptosuccinic acid." Journal of Colloid and Interface Science 194(2): 427-433.

Fernández-Bertólez, N., A. Touzani, L. Martínez, J. Méndez, A. T. Reis, C. Costa, S. Fraga, J. P. Teixeira, E. Pásaro and B. Laffon (2023). "Neuron and Glial Cells Exposed to Cerium Dioxide Nanoparticles: Results from MTT and γH2AX Assays." Materials Proceedings 14(14).

Fernández-Varo, G., M. Perramón, S. Carvajal, D. Oró, E. Casals, L. Boix, L. Oller, L. Macías-Muñoz, S. Marfà and G. Casals (2020). "Bespoken nanoceria: An effective treatment in experimental hepatocellular carcinoma." Hepatology 72(4): 1267-1282.

Fiorani, L., M. Passacantando, S. Santucci, S. Di Marco, S. Bisti and R. Maccarone (2015). "Cerium oxide nanoparticles reduce microglial activation and neurodegenerative events in light damaged retina." PloS One 10(10): e0140387.

Flores, K., R. S. Turley, C. Valdes, Y. Ye, J. Cantu, J. A. Hernandez-Viezcas, J. G. Parsons and J. L. Gardea-Torresdey (2021). "Environmental applications and recent innovations in single particle inductively coupled plasma mass spectrometry (SP-ICP-MS)." Applied Spectroscopy Reviews 56(1): 1-26.

Galland, F., M. Seady, J. Taday, S. S. Smaili, C. A. Gonçalves and M. C. Leite (2019). "Astrocyte culture models: Molecular and function characterization of primary culture, immortalized astrocytes and C6 glioma cells." Neurochemistry International 131: 104538.

Genchi, G. G., A. Degl'Innocenti, C. Martinelli, M. Battaglini, D. De Pasquale, M. Prato, S. Marras, G. Pugliese, F. Drago and A. Mariani (2021). "Cerium oxide nanoparticle administration to skeletal muscle cells under different gravity and radiation conditions." ACS Applied Materials & Interfaces 13(34): 40200-40213.

Geppert, M., M. C. Hohnholt, K. Thiel, S. Nürnberger, I. Grunwald, K. Rezwan and R. Dringen (2011). "Uptake of dimercaptosuccinate-coated magnetic iron oxide nanoparticles by cultured brain astrocytes." Nanotechnology 22(14): 145101.

Giri, S., A. Karakoti, R. P. Graham, J. L. Maguire, C. M. Reilly, S. Seal, R. Rattan and V. Shridhar (2013). "Nanoceria: a rare-earth nanoparticle as a novel anti-angiogenic therapeutic agent in ovarian cancer." PloS One 8(1): e54578.

Guan, Y., M. Li, K. Dong, N. Gao, J. Ren, Y. Zheng and X. Qu (2016). "Ceria/POMs hybrid nanoparticles as a mimicking metallopeptidase for treatment of neurotoxicity of amyloid-β peptide." Biomaterials 98: 92-102.

Gulcin, İ. (2020). "Antioxidants and antioxidant methods: An updated overview." Archives of Toxicology 94(3): 651-715.

Haddad, Z., C. Abid, H. F. Oztop and A. Mataoui (2014). "A review on how the researchers prepare their nanofluids." International Journal of Thermal Sciences 76: 168-189.

Hamprecht, B. and F. Löffler (1985). [27] Primary glial cultures as a model for studying hormone action. Methods in Enzymology, Elsevier. 109: 341-345.

Hasanzadeh, L., M. Darroudi, N. Ramezanian, P. Zamani, S. H. Aghaee-Bakhtiari, E. Nourmohammadi and R. K. Oskuee (2019). "Polyethylenimine-associated cerium oxide nanoparticles: A novel promising gene delivery vector." Life Sciences 232: 116661.

He, M., B. Hu, B. Chen and Z. Jiang (2017). "Inductively coupled plasma optical emission spectrometry for rare earth elements analysis." Physical Sciences Reviews 2(1).

Heckert, E. G., A. S. Karakoti, S. Seal and W. T. Self (2008). "The role of cerium redox state in the SOD mimetic activity of nanoceria." Biomaterials 29(18): 2705-2709.

Hijaz, M., S. Das, I. Mert, A. Gupta, Z. Al-Wahab, C. Tebbe, S. Dar, J. Chhina, S. Giri and A. Munkarah (2016). "Folic acid tagged nanoceria as a novel therapeutic agent in ovarian cancer." BMC Cancer 16(1): 1-14.

Hohnholt, M. C., M. Geppert and R. Dringen (2011). "Treatment with iron oxide nanoparticles induces ferritin synthesis but not oxidative stress in oligodendroglial cells." Acta Biomaterialia 7(11): 3946-3954.

Hu, Z. and Y. Ding (2022). "Cerium oxide nanoparticles-mediated cascade catalytic chemo-photo tumor combination therapy." Nano Research 15(1): 333-345.

Jana, S. K., P. Banerjee, S. Das, S. Seal and K. Chaudhury (2014). "Redox-active nanoceria depolarize mitochondrial membrane of human colon cancer cells." Journal of Nanoparticle Research 16(6): 1-9.

Joshi, A., W. Rastedt, K. Faber, A. G. Schultz, F. Bulcke and R. Dringen (2016). "Uptake and toxicity of copper oxide nanoparticles in C6 glioma cells." Neurochemical Research 41(11): 3004-3019.

Joshi, A., K. Thiel, K. Jog and R. Dringen (2019). "Uptake of intact copper oxide nanoparticles causes acute toxicity in cultured glial cells." Neurochemical Research 44(9): 2156-2169.

Ju, X., A. Fučíková, B. Šmíd, J. Nováková, I. Matolínová, V. Matolín, M. Janata, T. Bělinová and M. H. Kalbáčová (2020). "Colloidal stability and catalytic activity of cerium oxide nanoparticles in cell culture media." RSC Advances 10(65): 39373-39384.

Ju, X., M. H. Kalbacova, B. Šmíd, V. Johánek, M. Janata, T. N. Dinhová, T. Bělinová, M. Mazur, M. Vorokhta and L. Strnad (2021). "Poly (acrylic acid)-mediated synthesis of cerium oxide nanoparticles with variable oxidation states and their effect on regulating the intracellular ROS level." Journal of Materials Chemistry B 9(36): 7386-7400.

Jurašin, D. D., M. Ćurlin, I. Capjak, T. Crnković, M. Lovrić, M. Babič, D. Horák, I. V. Vrček and S. Gajović (2016). "Surface coating affects behavior of metallic nanoparticles in a biological environment." Beilstein Journal of Nanotechnology 7(1): 246-262.

Kaewsaneha, C., P. Tangboriboonrat, D. Polpanich and A. Elaissari (2015). "Multifunctional fluorescent-magnetic polymeric colloidal particles: preparations and bioanalytical applications." ACS Applied Materials & Interfaces 7(42): 23373-23386.

Korsvik, C., S. Patil, S. Seal and W. T. Self (2007). "Superoxide dismutase mimetic properties exhibited by vacancy engineered ceria nanoparticles." Chemical Communications(10): 1056-1058.

Kullgren, J., K. Hermansson and P. Broqvist (2013). Ceria chemistry at the nanoscale: effect of the environment. Solar Hydrogen and Nanotechnology VIII, International Society for Optics and Photonics.

Kumar, A., S. Das, P. Munusamy, W. Self, D. R. Baer, D. C. Sayle and S. Seal (2014). "Behavior of nanoceria in biologically-relevant environments." Environmental Science: Nano 1(6): 516-532.

Lee, J. H., B. Schneider, E. K. Jordan, W. Liu and J. A. Frank (2008). "Synthesis of complexable fluorescent superparamagnetic iron oxide nanoparticles (FL SPIONs) and cell labeling for clinical application." Advanced Materials 20(13): 2512-2516.

Levak, M., P. Burić, M. Dutour Sikirić, D. Domazet Jurašin, N. Mikac, N. Bačić, R. Drexel, F. Meier, Z. e. Jakšić and D. M. Lyons (2017). "Effect of protein corona on silver nanoparticle stabilization and ion release kinetics in artificial seawater." Environmental Science & Technology 51(3): 1259-1266.

Li, H., C. Liu, Y.-P. Zeng, Y.-H. Hao, J.-W. Huang, Z.-Y. Yang and R. Li (2016). "Nanoceria-mediated drug delivery for targeted photodynamic therapy on drug-resistant breast cancer." ACS Applied Materials & Interfaces 8(46): 31510-31523.

Li, Y. Y., X. He, J. J. Yin, Y. H. Ma, P. Zhang, J. Y. Li, Y. Y. Ding, J. Zhang, Y. L. Zhao, Z. F. Chai and Z. Y. Zhang (2015). "Acquired superoxide-scavenging ability of ceria nanoparticles." Angewandte Chemie-International Edition 54(6): 1832-1835.

Lorenz, M. R., V. Holzapfel, A. Musyanovych, K. Nothelfer, P. Walther, H. Frank, K. Landfester, H. Schrezenmeier and V. Mailänder (2006). "Uptake of functionalized, fluorescent-labeled polymeric particles in different cell lines and stem cells." Biomaterials 27(14): 2820-2828.

Lowry, O., N. Rosebrough, A. L. Farr and R. Randall (1951). "Protein measurement with the Folin phenol reagent." Journal of Biological Chemistry 193(1): 265-275.

Luther, E. M., C. Petters, F. Bulcke, A. Kaltz, K. Thiel, U. Bickmeyer and R. Dringen (2013). "Endocytotic uptake of iron oxide nanoparticles by cultured brain microglial cells." Acta Biomaterialia 9(9): 8454-8465.

Maragakis, N. J. and J. D. Rothstein (2006). "Mechanisms of disease: astrocytes in neurodegenerative disease." Nature Clinical Practice Neurology 2(12): 679-689.

Mathiisen, T. M., K. P. Lehre, N. C. Danbolt and O. P. Ottersen (2010). "The perivascular astroglial sheath provides a complete covering of the brain microvessels: an electron microscopic 3D reconstruction." Glia 58(9): 1094-1103.

Minchenko, D., M. Spivak, R. Herasymenko, V. Ivanov, Y. Tretyakov and O. Minchenko (2013). "Effect of cerium dioxide nanoparticles on the expression of selected growth and transcription factors in human astrocytes." Materialwissenschaft und Werkstofftechnik 44(2-3): 156-160.

Mink, J. W., R. J. Blumenschine and D. B. Adams (1981). "Ratio of central nervous system to body metabolism in vertebrates: its constancy and functional basis." American Journal of Physiology-Regulatory, Integrative and Comparative Physiology 241(3): R203-R212.

Naz, S., J. Beach, B. Heckert, T. Tummala, O. Pashchenko, T. Banerjee and S. Santra (2017). "Cerium oxide nanoparticles: a 'radical'approach to neurodegenerative disease treatment." Nanomedicine: Nanotechnology, Biology, and Medicine 12(5): 545-553.

Nelson, B. C., M. E. Johnson, M. L. Walker, K. R. Riley and C. M. Sims (2016). "Antioxidant cerium oxide nanoparticles in biology and medicine." Antioxidants 5(2): 15.

Parcheta, M., R. Świsłocka, S. Orzechowska, M. Akimowicz, R. Choińska and W. Lewandowski (2021). "Recent developments in effective antioxidants: The structure and antioxidant properties." Materials 14(8): 1984.

Patil, S., S. Reshetnikov, M. K. Haldar, S. Seal and S. Mallik (2007). "Surface-derivatized nanoceria with human carbonic anhydrase II inhibitors and fluorophores: a potential drug delivery device." The Journal of Physical Chemistry C 111(24): 8437-8442.

Patil, S., A. Sandberg, E. Heckert, W. Self and S. Seal (2007). "Protein adsorption and cellular uptake of cerium oxide nanoparticles as a function of zeta potential." Biomaterials 28(31): 4600-4607.

Perez, J. M., A. Asati, S. Nath and C. Kaittanis (2008). "Synthesis of biocompatible dextran-coated nanoceria with pH-dependent antioxidant properties." Small 4(5): 552-556.

Petters, C. and R. Dringen (2015). "Uptake, metabolism and toxicity of iron oxide nanoparticles in cultured microglia, astrocytes and neurons." Springerplus 4(Suppl 1): L32.

Petters, C., E. Irrsack, M. Koch and R. Dringen (2014). "Uptake and metabolism of iron oxide nanoparticles in brain cells." Neurochemical Research 39(9): 1648-1660.

Petters, C., K. Thiel and R. Dringen (2016). "Lysosomal iron liberation is responsible for the vulnerability of brain microglial cells to iron oxide nanoparticles: comparison with neurons and astrocytes." Nanotoxicology 10(3): 332-342.

Phatnani, H. and T. Maniatis (2015). "Astrocytes in neurodegenerative disease." Cold Spring Harbor Perspectives in Biology 7(6): a020628.

Pirmohamed, T., J. M. Dowding, S. Singh, B. Wasserman, E. Heckert, A. S. Karakoti, J. E. S. King, S. Seal and W. T. Self (2010). "Nanoceria exhibit redox state-dependent catalase mimetic activity." Chemical Communications 46(16): 2736-2738.

Rastedt, W., K. Thiel and R. Dringen (2017). "Uptake of fluorescent iron oxide nanoparticles in C6 glioma cells." Biomedical Physics & Engineering Express 3(3): 035007.

Renu, G., V. Rani, S. Nair, K. Subramanian and V.-k. Lakshmanan (2012). "Development of cerium oxide nanoparticles and its cytotoxicity in prostate cancer cells." Advanced Science Letters 6(1): 17-25.

Rzigalinski, B. A., C. S. Carfagna and M. Ehrich (2017). "Cerium oxide nanoparticles in neuroprotection and considerations for efficacy and safety." Wiley Interdisciplinary Reviews: Nanomedicine and Nanobiotechnology 9(4): e1444.

Sack-Zschauer, M., S. Bader and P. Brenneisen (2017). "Cerium oxide nanoparticles as novel tool in glioma treatment: an *in vitro* study." Journal of Nanomedicine & Nanotechnology 8(6): 1000474.

Sack, M., L. Alili, E. Karaman, S. Das, A. Gupta, S. Seal and P. Brenneisen (2014). "Combination of conventional chemotherapeutics with redox-active cerium oxide nanoparticles - a novel aspect in cancer therapy." Molecular Cancer Therapeutics 13(7): 1740-1749.

Sehgal, A., Y. Lalatonne, J.-F. Berret and M. Morvan (2005). "Precipitation– redispersion of cerium oxide nanoparticles with poly (acrylic acid): Toward stable dispersions." Langmuir 21(20): 9359-9364.

Shemirani, F. and S. R. Yousefi (2007). "Selective extraction and preconcentration of cerium (IV) in water samples by cloud point extraction and determination by inductively coupled plasma optical emission spectrometry." Microchimica Acta 157(3): 223-227.

Sies, H., C. Berndt and D. P. Jones (2017). "Oxidative stress." Annual Review of Biochemistry 86: 715-748.

Singh, N., S. K. NaveenKumar, M. Geethika and G. Mugesh (2021). "A cerium vanadate nanozyme with specific superoxide dismutase activity regulates mitochondrial function and ATP synthesis in neuronal cells." Angewandte Chemie International Edition 60(6): 3121-3130.

Singh, S., T. Dosani, A. S. Karakoti, A. Kumar, S. Seal and W. T. Self (2011). "A phosphate-dependent shift in redox state of cerium oxide nanoparticles and its effects on catalytic properties." Biomaterials 32(28): 6745-6753.

Skorodumova, N., S. Simak, B. I. Lundqvist, I. Abrikosov and B. Johansson (2002). "Quantum origin of the oxygen storage capability of ceria." Physical Review Letters 89(16): 166601.

Tian, X., H. Liao, M. Wang, L. Feng, W. Fu and L. Hu (2020). "Highly sensitive chemiluminescent sensing of intracellular Al^{3+} based on the phosphatase mimetic activity of cerium oxide nanoparticles." Biosensors and Bioelectronics 152: 112027.

Tulpule, K., M. C. Hohnholt, J. Hirrlinger and R. Dringen (2014). Primary cultures of astrocytes and neurons as model systems to study the metabolism and metabolite export from brain cells. Brain Energy Metabolism, Springer**:** 45-72.

Vassie, J. A., J. M. Whitelock and M. S. Lord (2017). "Endocytosis of cerium oxide nanoparticles and modulation of reactive oxygen species in human ovarian and colon cancer cells." Acta Biomaterialia 50: 127-141.

Verkhratsky, A., M. Nedergaard and L. Hertz (2015). "Why are astrocytes important?" Neurochemical Research 40(2): 389-401.

Wason, M. S., H. Lu, L. Yu, S. K. Lahiri, D. Mukherjee, C. Shen, S. Das, S. Seal and J. Zhao (2018). "Cerium oxide nanoparticles sensitize pancreatic cancer to radiation therapy through oxidative activation of the JNK apoptotic pathway." Cancers 10(9): 303.

Wason, M. S. and J. Zhao (2013). "Cerium oxide nanoparticles: potential applications for cancer and other diseases." American Journal of Translational Research 5(2): 126.

Wei, H. and E. Wang (2013). "Nanomaterials with enzyme-like characteristics (nanozymes): next-generation artificial enzymes." Chemical Society Reviews 42(14): 6060-6093.

Wilhelm, C., C. Billotey, J. Roger, J. Pons, J.-C. Bacri and F. Gazeau (2003). "Intracellular uptake of anionic superparamagnetic nanoparticles as a function of their surface coating." Biomaterials 24(6): 1001-1011.

Wong, L. L., Q. N. Pye, L. Chen, S. Seal and J. F. McGinnis (2015). "Defining the catalytic activity of nanoceria in the P23H-1 rat, a photoreceptor degeneration model." PloS One 10(3): e0121977.

Wu, J., X. Wang, Q. Wang, Z. Lou, S. Li, Y. Zhu, L. Qin and H. Wei (2019). "Nanomaterials with enzyme-like characteristics (nanozymes): next-generation artificial enzymes (II)." Chemical Society Reviews 48(4): 1004-1076.

Wu, W., Z. Wu, T. Yu, C. Jiang and W.-S. Kim (2015). "Recent progress on magnetic iron oxide nanoparticles: synthesis, surface functional strategies and biomedical applications." Science and Technology of Advanced Materials.

Xia, T., M. Kovochich, M. Liong, L. Madler, B. Gilbert, H. Shi, J. I. Yeh, J. I. Zink and A. E. Nel (2008). "Comparison of the mechanism of toxicity of zinc oxide and cerium oxide nanoparticles based on dissolution and oxidative stress properties." ACS Nano 2(10): 2121-2134.

Xu, M.-X., Y.-F. Zhu, H.-F. Chang and Y. Liang (2016). "Nanoceria restrains PM2. 5-induced metabolic disorder and hypothalamus inflammation by inhibition of astrocytes activation related NF-κB pathway in Nrf2 deficient mice." Free Radical Biology and Medicine 99: 259-272.

Xue, Y., S. R. Balmuri, A. Patel, V. Sant and S. Sant (2018). "Synthesis, physico-chemical characterization, and antioxidant effect of PEGylated cerium oxide nanoparticles." Drug Delivery and Translational Research 8(2): 357-367.

Yen, S. K., P. Padmanabhan and S. T. Selvan (2013). "Multifunctional iron oxide nanoparticles for diagnostics, therapy and macromolecule delivery." Theranostics 3(12): 986.

Zhang, S.-X., S.-F. Xue, J. Deng, M. Zhang, G. Shi and T. Zhou (2016). "Polyacrylic acid-coated cerium oxide nanoparticles: An oxidase mimic applied for colorimetric assay to organophosphorus pesticides." Biosensors and Bioelectronics 85: 457-463.

Zhou, X., B. Wang, Y. Chen, Z. Mao and C. Gao (2013). "Uptake of cerium oxide nanoparticles and their influences on functions of A549 cells." Journal of Nanoscience and Nanotechnology 13(1): 204-215.

2.2 Cerium oxide nanoparticles and CeCl$_3$ stimulates the glycolytic flux in astrocyte-rich primary cultures.

Abstract

Cerium oxide nanoparticles (CeONPs) are considered a solid candidate for the new generation of antioxidants due to their protective potential against oxidative stress demonstrated *in vitro* and *in vivo* and their self-regeneration potential. Cellular or systemic CeONPs protection against radical-induced toxicity is based on their redox cycling capacity coupled with oxygen buffering. However, little is known about potential metabolic consequences of an exposure of healthy brain cells to such particles. Therefore, dimercaptosuccinate-coated cerium oxide nanoparticles (DMSA-CeONPs) or two different cerium salts, $CeCl_3$ or $Ce(SO_4)_2$, were applied to cultured primary rat astrocytes and investigated whether such treatments may alter cell viability and/or glucose metabolism. Astrocytes remained viable during an incubation for up to four days with concentrations of up to 1000 μM cerium. The cellular content of cerium was determined after three days of incubation and showed a concentration-dependent pattern. The intracellular cerium content was 16-fold greater in cells treated with 300 μM DMSA-CeONPs for 3 days compared to cells exposed to $CeCl_3$ or $Ce(SO_4)_2$. The incubation with 300 μM DMSA-CeONPs induced a significant increase in lactate release and glucose consumption from the second day on. A comparable increase was observed when the cells were treated with 300 μM $CeCl_3$ or $Ce(SO_4)_2$, suggesting that the ionic cerium leaked from the NPs might be the responsible for the stimulation of the glycolytic flux. The cerium-induced lactate production persisted after removal of extracellular DMSA-CeONPs. Furthermore, after 72 h such stimulation of the glycolytic flux showed similarities to the stimulation observed when astrocytes had been incubated with hypoxia inducible factor 1 α (Hif-1α) stabilizers. These data demonstrate that cerium upregulates glycolysis after 48 h incubation in cultured astrocytes and the effects persist over time, suggesting that the treatment with the redox active DMSA-CeONPs interfere with brain glucose metabolism and oxygen availability.

Introduction

CeONPs are being intensively studied and are considered solid candidates as therapeutics against oxidative stress in various organs (Alili et al., 2011; Giri et al., 2013; Sack et al., 2014; Hijaz et al., 2016; Das et al., 2017; Fernández-Varo et al., 2020), including the brain (Estevez et al., 2011; Kwon et al., 2016). The radical scavenging potential of CeONPs relies in the flip-flop between Ce^{4+} and Ce^{3+} that occurs at the surface of the NPs and is mediated by the generation of a neutral oxygen vacancy ($O^{2-} \rightarrow 1/2\ O_2\ (g)$), which donates two electrons for the reduction of two Ce^{4+} atoms to Ce^{3+} (Skorodumova et al., 2002). Due to this redox potential, CeONPs can exhibit superoxidase dismutase or catalase mimicking behavior in the presence of reactive oxygen species (ROS) in cells (Korsvik et al., 2007; Pirmohamed et al., 2010).

In this line, previous studies have demonstrated protective effects of CeONPs against neuro-pathologies with a strong background of oxidative stress, such as, AD (Cimini et al., 2012; Dowding et al., 2014; Guan et al., 2016), Parkinson´s disease (Dillon et al., 2011; Pinna et al., 2015) or ischemia (Estevez et al., 2011; Chen and Gao, 2017). Furthermore, the use of CeONPs is thought to be relatively safe as, overall, CeONPs are considered to have no or very low cytotoxicity (Asati et al., 2010; Dhall and Self, 2018; Li et al., 2018).

CeONPs have also been reported to act as oxidants in diverse biological applications. Indeed, CeONPs-induced increase in ROS has been linked to some of the deleterious effects observed *in vitro* (Gagnon and Fromm, 2015). Even such negative effects on cells have been turned into a strength by investigating oxidative-CeONPs as potential anticancer tools. For example, Mittal and Pandey (2014) showed that the treatment of lung adenocarcinoma cells with CeONPs caused DNA damage and apoptotic cell death, which correlated with an increase in ROS. Similarly, CeONPs caused oxidative stress in human hepatoma cells, reducing their viability, causing morphological damage and apoptosis (Cheng et al., 2013). CeONPs also increase ROS generation and subsequently DNA damage in human neuroblastoma cells (Kumari et al., 2014).

However, despite the growing scientific interest in CeONPs and their effects on biological systems, the non-acute and/or long-term effects of CeONPs in healthy cells remain a vast unexplored area of research.

NPs present many advantages over their bulk counterpart, most notably enhanced reactivity due to the larger surface area per unit mass (Sannino, 2021). However, it is worth

noting, that bulk cerium was widely used in medicine, in the past, long before nanoceria (Jakupec et al., 2005; Shcherbakov et al., 2020). Initially, Ce (III) oxalate was prescribed as an antiemetic during pregnancy although its therapeutic effect was never tested in clinical trials (Simpson, 1854; Böhm, 1915; Wilcox, 1917). Later, various formulations of Ce^{3+} were reported and used as antiseptics (Burkes and McCleskey, 1947; Muroma, 1958), as immunomodulators in the treatment of burns (Garner and Heppell, 2005; Garner and Heppell, 2005) or as antitumoral agents in cancer chemotherapy (Lewin, 1924; Sato et al., 1998; Ji et al., 2000; Dai et al., 2002). The mechanisms of action of bulk cerium have not been fully elucidated, but in a very detailed and recent review Shcherbakov et al. (2020) compared the published data on the chemical properties and biological activity of CeONPs and ionic cerium and found that cerium compounds are often reported to have similar catalytic/scavenging properties and to exert similar effects as CeONPs in regenerative medicine, immunomodulation, neuroprotection or cancer. Other studies have also pointed out that the solubility of fine nanoceria i.e. the release of cerium ions, in aqueous solution is calculated to be in the millimolar range (Plakhova et al., 2016), although this aspect is rarely addressed when characterizing CeONPs. Based on these observations Shcherbakov and colleagues (2020) even stated that the ulterior responsible for the biological effect are the cerium ions and not the increased redox potential of the NPs due to the enhanced surface defects caused by the nanoscale, which, on the other hand, constitutes the most extended hypothesis. However, many of the current studies on the effects of CeONPs in biological systems lack of the direct comparison with other cerium compounds, making it very difficult to determine the contribution of the nanomaterials or, in other words, the "NP-effect".

Nevertheless, exposure to ionic cerium has also been shown to have negative effects on cells. Of note, it is its ability to replace Ca^{2+} with Ce^{3+} in calcium channels, enzymes or Ca-binding proteins due to their similar ionic radius (Barker et al., 2022). The substitution of Fe^{2+}, Mg^{2+}, Mn^{2+} and Zn^{2+} by Ce^{3+} in metalloproteins has also been observed (Prejanò et al., 2017; Prejanò et al., 2020). As a consequence, Ce^{3+} interferes with various biological processes for example by blocking the active transport of calcium across mitochondrial membranes (Evans, 2013) or the calcium channels in neurons (Beedle et al., 2002).

Focusing on the brain, astrocytes are the first cells in the brain to encounter NPs or cerium compounds that have crossed the blood-brain barrier (Cupaioli et al., 2014; Kadry et al., 2020). Moreover, these cells are considered as major regulator in the brain as they control the import and export of substances from the plasma (Verkhratsky et al., 2015), supply metabolites and gliotransmitters for neuronal function (Verkhratsky and Nedergaard,

2018) and modulate extracellular ion homeostasis (van Putten et al., 2021). In particular, astrocytes have been shown to accumulate and export ionic copper (Scheiber et al., 2010; Scheiber et al., 2012) and take up DMSA-coated copper- (Bulcke and Dringen, 2016), silver- (Hohnholt et al., 2013) and iron-oxide nanoparticles (Petters et al., 2014). Therefore, astrocytes could be an important target for DMSA-CeONPs when administered as therapeutics for neuroprotection.

Astrocytes also release significant amounts of lactate to the extracellular space. Although its role has not yet been fully elucidated, lactate is thought to serve as energy substrate during high neuronal synaptic activity (Li et al., 2023). Astrocytes exhibit unique metabolic profile in the brain, such as their marked glycolytic phenotype (Almeida et al., 2023), which enables the conversion of glucose via glycolysis four-to fivefold faster than in neurons (Herrero-Mendez et al., 2009). Lactate generation is tightly coupled to the proper functioning of the brain. A significant increase in glycolytic rates in astrocytes has been linked to neurological conditions in which these cells show dysfunction, such as, Alzheimer's disease (AD), Parkinson's disease (PD), or Huntington´s disease (Chen et al., 2023; Shirbandi et al., 2023; Yang et al., 2024).

In addition to trafficking, storing substances and complement the energetic demands of the brain, astrocytes largely regulate the presence of ROS in the brain (Verkhratsky and Nedergaard, 2018). An excess of ROS has been shown to cause astrogliosis (Swanson et al., 2004), which includes cytoplasmic swelling and vacuolation, lipid peroxidation and nuclear alterations leading to apoptosis (Ishii et al., 2017). On the other hand, a strong inhibition of ROS production, can also entail negative consequences on the metabolism of the cells, as ROS exert a signaling function in the regulation of different physiological responses in astrocytes such as glucose metabolism (Vicente-Gutierrez et al., 2019) or oxygen homeostasis (Marrif and Juurlink, 1999; Mansfield et al., 2005; Véga et al., 2006; Allen et al., 2020).

As CeONPs, or the cerium ions leaking from the NPs, have the potential to affect the functioning of brain cells by interfering with ROS balance and ultimately with the metabolism of the cells, it is imperative to test the potential effects of introducing these active redox species into the system. Previously, it was shown that DMSA-CeONPs did not affect the viability of astrocytes, although such NPs were efficiently taken up by the cells. Herein, the consequences on the glucose metabolism of exposing cultured astrocytes to DMSA-CeONPs and ionic cerium were investigated.

Materials and methods

Materials

Cerium oxide nano-powder (<25 nm by Brunauer-Emmet-Teller analysis), cerium (III) chloride heptahydrate, 2, 3-dimercaptosuccinic acid (DMSA), deferoxamine mesylate (DFx), antimycin A (AA), H_2O_2 for ultratrace analysis, sodium chloride and 2-mino-2 (hydroxymethyl)-1,3-propanediol (Trizma base) were purchased from Sigma-Aldrich (Steinheim, Germany). Cerium (IV) sulfate tetrahydrate and $CoCl_2$ were acquired from Merck (Darmstadt, Germany). Dulbecco´s modified Eagle´s medium was (DMEM, containing 25 mM glucose) from Gibco (Karlsruhe, Germany). Fetal calf serum (FCS) and penicillin/streptomycin solution were obtained from Biochrom (Berlin, Germany). Bovine serum albumin (BSA) and nicotinamide adenine dinucleotide (NADH) were purchased from Applichem (Darmstadt, Germany). Cerium dioxide standard (1000 µg mL^{-1}, v/v) for inductively coupled plasma optical emission spectrometry (ICP-OES) analysis was obtained from Inorganic Ventures (Virginia, USA) and dimethyloxalylglycine (DMOG) from Cayman Chemical (Ann Arbor, USA). 24-well cell culture plates and 96-well plates microtiter plates were purchased from Sarstedt (Nümbrecht, Germany).

Coating of CeONPs dispersions with DMSA

A 100 mM dispersion of colloidal uncoated CeONPs (Un-CeONPs) was prepared as stock solution by stirring the nano-powder in pure water for 15 min and ultrasonicated on ice two times in 5 minutes intervals at 50 W with a Branson B-12 sonifier (Danbury, Connecticut, USA). In parallel, a 5 mM DMSA aqueous solution was prepared at 65°C in a covered beaker under stirring for 15 min and left to cool down until reaching room temperature (RT). Afterwards, for the preparation of 20 mM DMSA-CeONPs, 5 mL of the 5 mM DMSA solution was added to 10 mL of a 29 mM dilution in H_2O of the stock CeONPs dispersion. After 15 min of additional stirring at RT the dispersion was collected and centrifuged for 10 min at 1500g and the supernatant was discarded. Subsequently two cycles of washing were completed by washing with 15 mL pure water the pellet containing the DMSA-CeONPs and discarding the washing solution after 10 min centrifugation at 1,500g. The resulting CeONPs pellet was finally dispersed in 15 mL pure H_2O and sonicated twice with the same settings mentioned before. The DMSA-CeONPs dispersion was stored at 4°C and sonicated for 5 min with the above described settings prior to any further use.

Characterization of DMSA-CeONPs

DMSA-CeONPs dispersions (1 mM) in water and different culture media were characterized for their hydrodynamic diameter, polydispersity index and zeta potential (ζ-potential). These parameters were determined by dynamic and electrophoretic light scattering (DLS, ELS) in a Beckman Coulter (Krefeld, Germany) Delsa™ Nano C Particle analyzer at RT as previously described (Bulcke et al., 2014).

Preparation of CeCl$_3$ and Ce(SO4)$_2$ solutions

Two different salts of cerium were also used to test whether the effects observed in the glucose metabolism of astrocyte-rich primary cultures (APCs) were specific to cerium presented in NP form. A 20 mM stock solution of cerium (III) chloride heptahydrate and cerium (IV) sulfate tetrahydrate were prepared in pure water and stored at 4°C until used. Afterwards, they were diluted in culture medium to obtained the desired final concentrations.

Astrocyte cultures

The preparation of the cultures was performed in accordance with the legal regulations dictated by the *Bundesministerium für Ernährung und Landwirtschaft* included in the *Tierschutzgesetz* (reissued on the 18.05.2006) and later modifications. The maintenance of the animals and their utilization with research purposes were approved and supervised by the local animal care committee, *Senatorische Behörde* of Bremen (Germany).

APCs were successfully obtained from the full brains of newborn Wistar rats within the first 24 h after birth and being naturally fed. The cultures were prepared as initially described by Hamprecht and Löffler (1985) using a slight modification (Tulpule et al., 2014). Briefly, the full brains were extracted after decapitation and mechanically dissociated, consecutively, through two nylon meshes of 210 and 132 μm pore diameter to eliminate blood vessels and singularize cells. For seeding, 1 mL culture medium containing approximately 3×10^5 viable cells was transferred into wells of 24-well cell culture plates. The cell culture medium was renewed every 7th day. The age of the cultures used for the experiment described in this manuscript was between 15 and 28 days.

Experimental incubation of cells

For cell experiments, the culture medium was completed aspirated and the cells were washed twice with 1 mL of pre-warmed DMEM + 10% FCS for incubations ≥ 24 h (long

incubations) or they were washed twice with 1 mL physiological incubation buffer (IB; 1.8 mM $CaCl_2$, 1 mM $MgCl_2$, 5.4 mM KCl, 145 mM NaCl, 20 mM HEPES, 5 mM D-glucose; pH 7.4) containing 0.5 mg mL^{-1} bovine serum albumin (IB-BSA) for incubation periods under 24 h (short incubations). Subsequently, the cells were incubated for the indicated time periods at 37°C in the humified atmosphere of an incubator with CO_2 supply for longer incubations and without CO_2 for short incubations. The adequate volume of culture medium or physiological buffer containing the different cerium compounds in the concentrations needed are given in the legends of the figures and tables. To end the incubations, if not stated otherwise, the incubation medium was harvested and the cells were washed twice with 1 mL ice cold (4°C) phosphate-buffered saline (PBS; 10 mM potassium phosphate buffer pH 7.4 containing 150 mM NaCl) and dry cells were lysed as described below for the determination of LDH activity or stored at -20°C until subsequent quantification of cerium and/or protein contents.

To test for potential mitochondrial respiration impairment by DMSA-CeONPs, APCs were pre-incubated for 72 h without or with 1 mL 300 μM DMSA-CeONPs in DMEM + 10% FCS. As the 72-h expired, the pre-incubation media was aspirated and the cells were twice washed with 1 mL pre-warmed (37°C) IB. Subsequently the cells were incubated in the presence or absence of 250 μL 10 μM antimycin A (AA) in IB for 2 and 4 h.

To investigate the potential hypoxia caused by DMSA-CeONPs, APCs were incubated for 4, 24 and 72 h without or with 300 μM DMSA-CeONPs in the absence or the presence of 1 mM deferoxamine (DFx), 1mM dimethyloxaloylglycine (DMOG) or 200 μM $CoCl_2$ in DMEM + 10% FCS. After the completion of the incubation time, the extracellular medium was collected.

Determination of cell viability

Cell vitality was assessed by quantification of the activity of the cellular LDH. Briefly, after the indicated incubation, cells were washed twice with pre-warmed (37°C) DMEM + 10% FCS (longer incubations) or with IB-BSA (short incubations) and lysed with 1% (v/v) Triton x-100 in 1 mL or 200 μL, respectively, of the corresponding incubation medium for 30 min at 37°C. After the lysis, 10 μL of the lysate was diluted with 170 μL LDH buffer (80 mM Tris, 200 mM NaCl, pH 7.2) in a well of a 96-well microtiter plate. The photometric determination of the LDH activity was performed at 340 nm as previously described by Tulpule et al. (2014).

Determination of extracellular glucose and lactate concentrations

Two different coupled enzymatic test systems containing lactate dehydrogenase plus glutamate pyruvate transaminase and hexokinase plus glucose- 6- phosphate dehydrogenase were used to quantify extracellular lactate and glucose concentrations, respectively, as described in detail before (Tulpule et al., 2014). In the particular case of incubations with AA, media samples of 10 µL were taken for each timepoint of the ongoing incubation to quantify the concentration of extracellular lactate and glucose. Glucose consumption was defined as the difference between the glucose concentration determined in the initial medium applied and the glucose concentration in the medium harvested after a given incubation.

Protein content determination

The cells in 24-well plates were lysed in 400 µL 500 mM NaOH, harvested and this lysate was used to determine cellular contents of protein and cerium. The protein contents were analyzed according to the Lowry method (Lowry et al., 1951), using BSA as a standard.

Quantification of cellular cerium content by ICP-OES

For the quantification of cellular cerium content, the NaOH-lysates of the cells were incubated with 1.2 mL of 65% HNO_3 (suprapur) and 0.2 µL of 35% H_2O_2 (suprapur) at 65°C for 240 min and then at 85°C overnight, until the digestion was completed. Digestions were carried out in 2 mL Eppendorf cups which remained open to allow the samples to dry. Dry residues of three replicates were pooled and resuspended in a total volume of 4 mL of 2% HNO_3. The subsequent quantification of cerium was carried out in close collaboration with Dr Fröllje (Geochemistry and Hydrogeology Department, University of Bremen). The cerium content was measured by inductively coupled plasma–optical emission spectrometry (ICP-OES) using a Perkin Elmer Optima 7300 DV instrument (Waltham, Massachusetts, USA). The cerium standards used for the calibration and quality controls were dissolved in extract of cells which had never been exposed to cerium but were digested following the same procedure as the samples obtained for the different treatments. The emission wavelength chosen for cerium determination was 413.764 nm. The specific cellular cerium content was calculated by normalizing the total cellular cerium content per well to the cellular protein content of the respective well.

Statistical analysis and presentation of data

All data are presented as means ± standard deviation (SD) of values obtained in experiments on three independently prepared cultures, if not stated otherwise. Statistical analysis of data from multiple sets of results was carried out by ANOVA followed by the Bonferroni *post-hoc* test, using the software SigmaPlot (version 11.0). Significant differences compared to the control were indicated in the figures by asterisks. The number of asterisks specifies the level of significance with *$p<0.05$, **$p<0.01$ and ***$p<0.001$. Similarly, significant differences between treatments are depicted as hashes in the figures and the number of hashes corresponds with the level of significance (#$p<0.05$; ##$p< 0.01$, ###$p< 0.001$). Values of $p> 0.05$ were considered as not significant.

Results

Characterization of DMSA-CeONPs.

DMSA-CeONPs are agglomerates of crystalline primary NPs. Average size of the primary NPs is approximately 25 nm determined by TEM (see chapter 2.1). Dispersed in DMEM+10% FCS, the DMSA-CeONPs used for the experiments presented here, showed a mean hydrodynamic diameter of 267 ± 12 nm and a ζ-potential of -13.4 mV (Table 1).

Table 1. Characterization of DMSA-CeONPs.

	Hydrodynamic diameter (nm)	Polydispersity index	ζ-potential (mV)	n
H_2O	166 ± 4	0.131 ± 0.02	-28.4 ± 2.3	3
DMEM+10% FCS	267 ± 12	0.175 ± 0.03	-13.4 ± 0.8	3
IB-BSA	220 ±7	0.242 ±0.04	12.7 ±1.1	3

DMSA-CeONPs were synthesized and the hydrodynamic diameter, polydispersity index and ζ-potential of 1 mM dispersions in water, IB-BSA or in DMEM + 10 % FCS were determined. The data represent means ± SD of values obtained in three experiments on *n* independent CeONPs syntheses.

DMSA-CeONPs accelerated the glycolytic flux in APCs.

To investigate whether the exposure to DMSA-CeONPs alters the glucose metabolism of astrocyte-rich primary cultures, a time- and concentration-dependency study was carried

out and the extracellular LDH activity (Fig. 1a,c), lactate release (Fig. 1b,e) and glucose consumption (Fig. 1c,f) were determined.
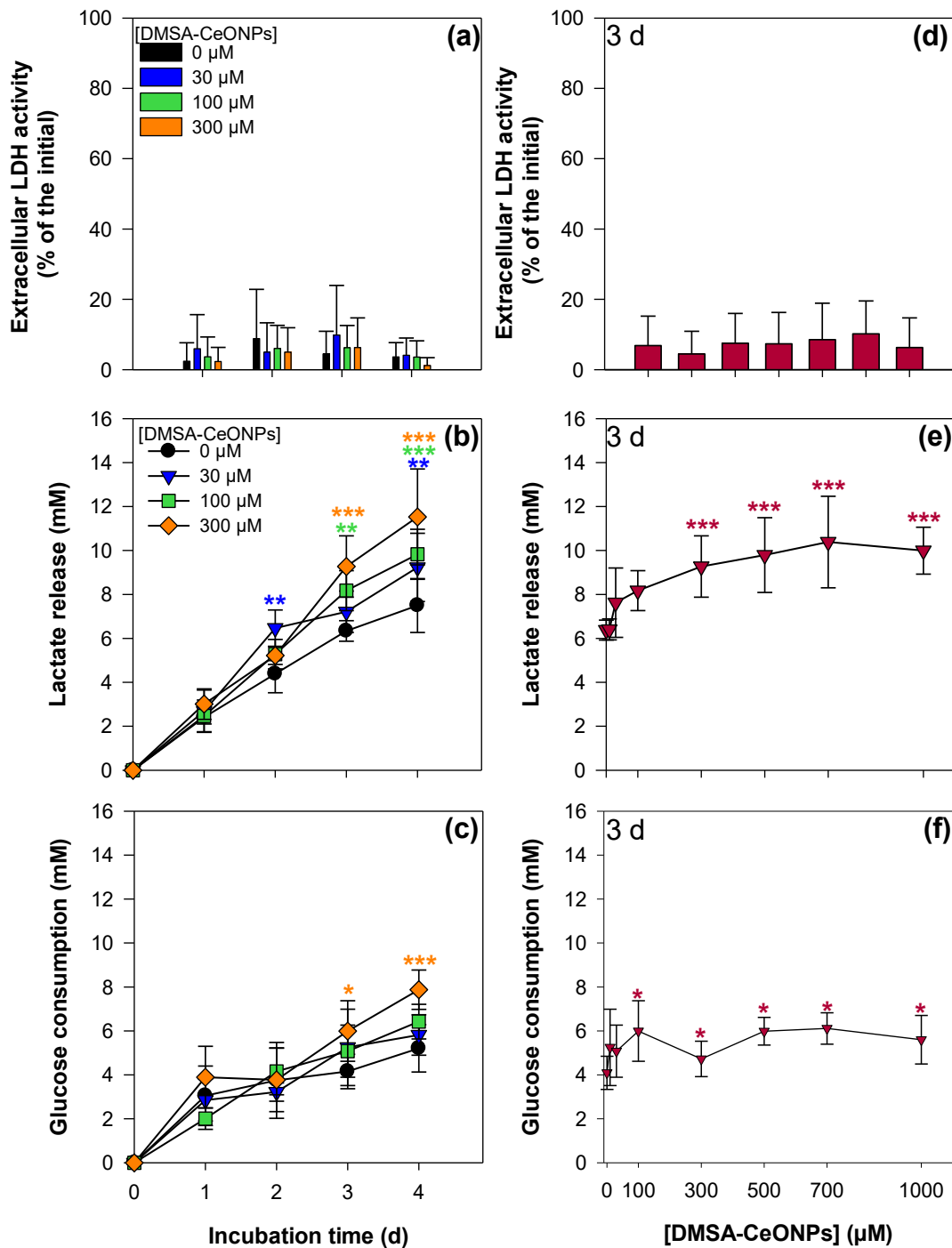
Figure 1. Time and concentration dependent effect of DMSA-CeONPs on the glycolytic flux in cultured astrocytes. The cells were incubated for up to 4 days with or without DMSA-CeONPs in DMEM + 10% FCS. For the indicated timepoints the extracellular LDH **(a, d)**, the extracellular lactate concentration **(b, e)** and the glucose consumption **(c, f)** were determined. The data shown are means ± SD of values obtained in 3 experiments on independently prepared cultures (n=3). The initial cellular LDH activity values correspond

to 125 ±13 nmol min^{-1} well^{-1}. The significance of differences (ANOVA) of data compared to those obtained for incubations in the absence of DMSA-CeONPs (0 µM) is indicated by asterisks in the respective symbol colour (*p<0.05), **p<0.01, ***p<0.001).

The cells were incubated up to four days without (control, 0 µM) or with 30, 100 or 300 µM DMSA-CeONPs (Fig. 1a-c). Additionally, to have a better insight into the concentration dependency, the cells were incubated for three days with a wider range of DMSA-CeONPs concentrations, including also 10, 500, 700 and 1000 µM DMSA-CeONPs for this particular timepoint (Fig. 1d-f). The incubation with DMSA-CeONPs did not cause any significant damage to the cellular membrane for any of the concentrations tested over the four days in comparison to the control. For all the conditions studied, the extracellular LDH activity remained under 20%, ruling out any prominent side effect due to toxicity (Fig. 1 a,d).

The extracellular lactate concentration increased almost linearly over time for all conditions studied (Fig. 1b,e). After three days of incubation, the cells treated with 100 µM or more DMSA-CeONPs had released significantly more lactate to the extracellular space than the control cells, in a concentration-dependent manner (Fig. 1e). The maximal increase in extracellular lactate accumulation was determined after four days of incubation with 300 µM DMSA-CeONPs, showing almost two-times the lactate concentration of cells not exposed to DMSA-CeONPs (Fig. 1e).

An increase in the consumption of glucose compared to the control was also observed after three days of incubation with DMSA-CeONPs and significant differences were found for concentrations of 100 µM and higher (Fig. 1c,f) ~due to analytical reasons, which will be discussed later in the discussion, after three days of incubation only cells incubated with 300 µM consumed significantly more glucose than the cells not exposed to DMSA-CeONPs (Fig. 1c). Cells treated with 300 µM DMSA-CeONPs for four days consumed ~50% more glucose than control cells (Fig. 1c).

Increased glycolytic flux persisted after removing the DMSA-CeONPs by washing

To investigate whether the observed stimulation of glycolytic flux by DMSA-CeONPs required the extracellular presence of DMSA-CeONPs to persist, the cultures were pre-incubated for 3 days in DMEM+ 10% FCS in the absence (control, 0 µM) or the presence of 300 µM DMSA-CeONPs, washed and subsequently main incubated at 37°C for 240 min in a DMSA-CeONPs free-incubation buffer (Fig. 2a, c) or in the presence of 300 µM DMSA-CeONPs (Fig. 2b,d).
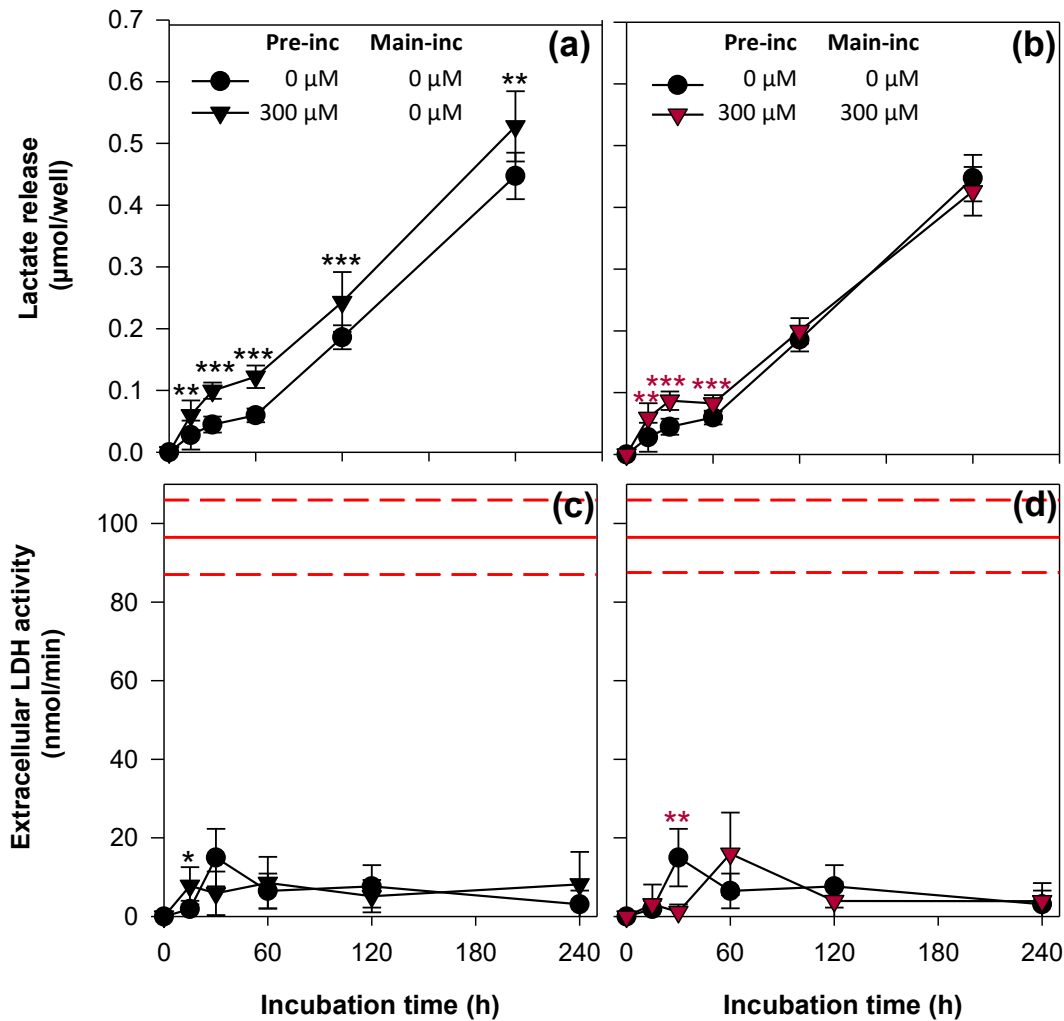
Figure 2. Test for the acute and persistence of the effect of DMSA-CeONPs on the glycolytic flux in cultured astrocytes. The cells were pre-incubated (Pre-inc) without or with 300 μM DMSA-CeONPs in DMEM + 10% FCS for 3 days. Afterwards the cells were washed two times with IB-BSA and further main incubated (Main-inc.) without (black filled triangles) or with 300 μM DMSA-CeONPs (red filled triangles) in IB-BSA for up to 4 h. The cells which had been pre-incubated and subsequently main incubated without DMSA-CeONPs (black filled circles) were considered as the control. The extracellular lactate content **(a, b)** and the extracellular LDH activity **(c, d)** were determined. The data shown are means ± SD of values obtained in 3 experiments on independently prepared cultures (n=3). The significance of differences (t-test) of data compared to those obtained for incubations in the absence of DMSA-CeONPs (0 μM) is indicated by asterisks in the respective symbol colour (*p<0.05, **p<0.01, ***p<0.001). In **(c, d)** the red solid line represents the intracellular LDH activity of non-treated cells at the moment of starting the main incubation (initials) and the red dotted lines are the associated standard deviation.

Already 1 h exposure to DMSA-CeONPs induced later effects in the glycolytic flux.

To test the minimal exposure time to trigger a persistent acceleration in the glycolytic flux in APCs, cells were incubated with 300 μM DMSA-CeONPs for 1, 4, 24 or 72 h, washed (Fig. 3a,c) and subsequently incubated in cerium free DMEM+10% FCS for the remaining time

112

until reaching 72 h after the start of the exposure (Fig. 3b,d,e). After each particular exposure time and after the completion of the 72-h experiment, the extracellular lactate content (Fig. 3a,b) and the glucose consumption (Fig. 3c,d) were determined. The cellular cerium content was determined after 72 h of the start of the exposure (Fig. 3e).

The extracellular lactate concentration right after 1 h exposure of the cells to DMSA-CeONPs was significantly ($p < 0.05$) increased compared to the control (Fig. 3a). However, after 4 h exposure, the extracellular lactate concentration did not significantly differ from the control (Fig. 3a). After 24 of exposure to DMSA-CeONPs the extracellular lactate concentration was again significantly ($p < 0.001$) increased (Fig. 3a). Such exposure resulted in a three-fold increase in lactate release after 24 h and the significant difference persisted until the completion of the 72 h exposure (Fig. 3a). Once the indicated exposure times finished, the cells were washed and incubated in DMSA-CeONPs free fresh DMEM+10%FCS until the completion of 72 h. Remarkably, already 1 h incubation with DMSA-CeONPs, caused a significant increase in lactate release (i.e. 33% over the control) measurable in DMSA-CeONPs free medium after 72 h since the incubation started (Fig. 3b). The same effect was determined when the CeONPs-exposure lasted 4 or 24 h (Fig. 3b).

The increase in extracellular lactate concentration was matched by the correspondent increase in glucose consumption after exposure and at the completion of the 72 h. In this line, the presence of DMSA-CeONPs caused a significant increase to doubling in glucose consumption after 24 h. Incubation times under 24 h did not give any significant difference (Fig. 3c). However, short exposures of 1 or 4 h produced effects in glucose consumption which were detectable after 72 h from the start of the exposure (Fig. 3d). The cells which had been exposed to DMSA-CeONPs and then incubated in NPs-free medium consumed approximately 40% more glucose than cells which had never been exposed to NPs (Fig. 3d). The specific cellular cerium content after completing 72 h experiment was determined (Fig. 3e) and demonstrated a linear increase with exposure time. A specific cellular cerium content of 1.2 ± 0.1 nmol/well, as observed in cells exposed for 1 h, seemed to be sufficient to trigger a stimulation of glycolytic lactate production of APCs (Fig. 3e).
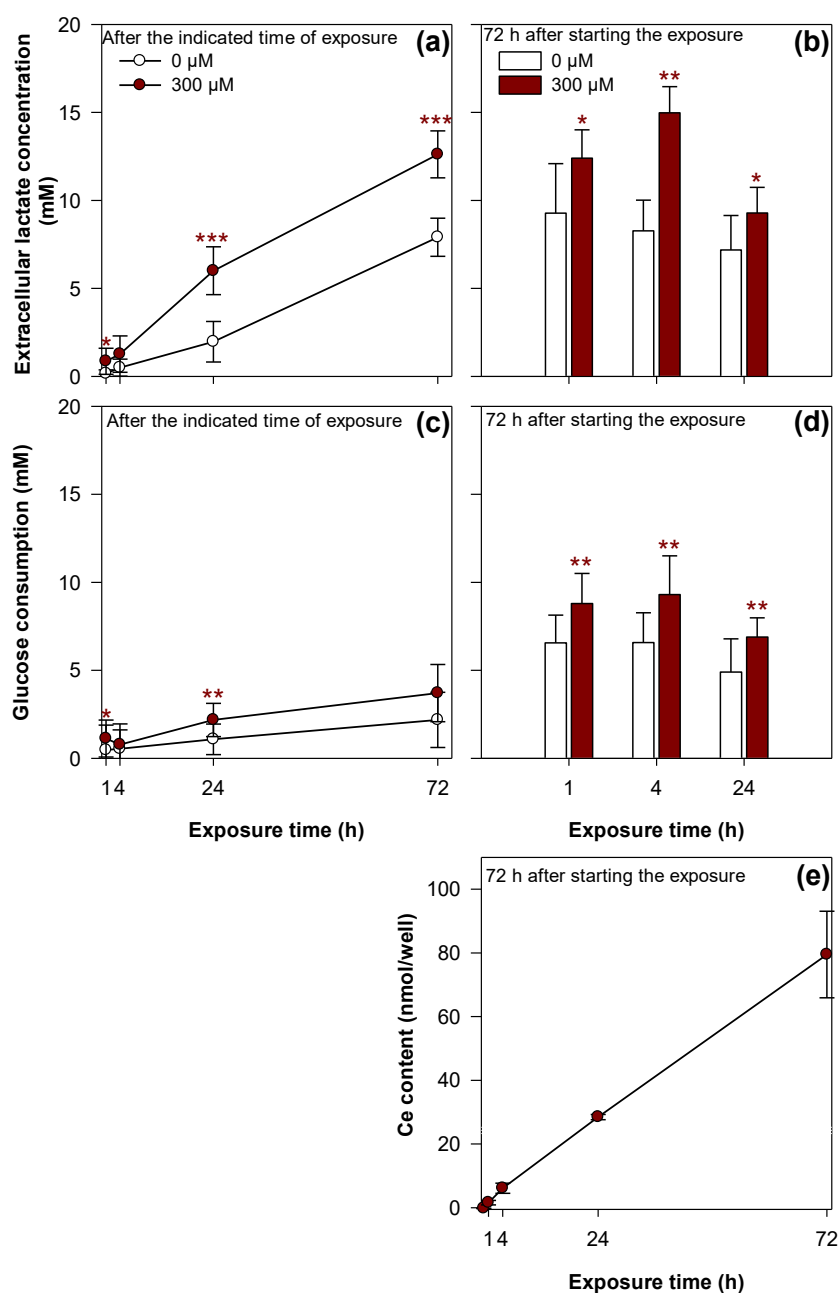
Figure 3. Test for the minimal incubation time required to induce later effects in the glycolytic flux by DMSA-CeONPs. Astrocytes were exposed to none (0 μM) or 300 μM DMSA-CeONPs in DMEM+10% FCS for 1, 4, 24 and 72 h, washed and subsequently incubated for the remaining time until reaching 72 h after the start of the exposure to the NPs. For the exposure timepoints and after completing 72 h after the start of the incubation, the extracellular lactate concentration **(a, b)** and the glucose consumption **(c, d)** were determined. Cellular cerium content **(e)** was determined at the end of the experiment. The data represent mean ± SD of values obtained in 3 experiments on independently prepared cultures (n=3). The significance of differences between data obtained for cultures at the end of the exposition as well as at the completion of the 72 h (calculated by *t-test*) is indicated by asterisks (*p<0.05, **p<0.01, ***p<0.001).

114

CeCl$_3$ accelerated the glycolytic flux in APCs.

To test whether the acceleration in the glycolytic flux only occurs when cerium is applied in the form of NPs, cells were incubated with two different salts of cerium (300 µM CeCl$_3$ or Ce(SO$_4$)$_2$), in which cerium exhibits a different oxidation state (Ce^{3+} or Ce^{4+} respectively) or with 300 µM DMSA-CeONPs as positive control. A negative control was also included (none), where no cerium was added to the incubation medium (Fig. 4).

Extracellular lactate (Fig. 4a) and glucose consumption (Fig. 4c) were determined for 1, 2, 3 or 4 days of incubation. To discard any side effect due to toxicity, the extracellular LDH activity was monitored (Fig. 4e). Additionally, and to obtain a better insight into the concentration dependency, cells were incubated for three days with 0, 100, 300, 500, 700 or 1000 µM of the respective cerium compounds and the extracellular lactate and the glucose consumption were determined (Fig. 4b,d). The specific cellular cerium content after three days was quantified for the treatments without or with 300 and 700 µM cerium (Fig. 4f).

Treatment of APCs with different cerium compounds for up to four days did not compromise cells membrane integrity, as indicated by the extracellular LDH activity that remained comparable to the one of cultures not exposed to cerium (Fig. 4e). Consistent with the results shown previously, after 48 h of incubation in the presence of 300 µM DMSA-CeONPs, the extracellular lactate accumulation was increased by ~24% compared to the control (Fig. 4a). A 48 h incubation with 300 µM CeCl$_3$ produced an identical up-regulation in lactate release (~25%) (Fig. 4a). In contrast, incubation with 300 µM Ce(SO$_4$)$_2$ for two days produced a significant reduction (~16%) in extracellular lactate accumulation. The increase in extracellular lactate after three days was of 22% and 28% for CeCl$_3$ and DMSA-CeONPs, respectively, and after four days a slight decline was recorded (15% for both compounds) (Fig. 4a). Glucose consumption was not significantly altered with the different treatments (Fig. 4c).
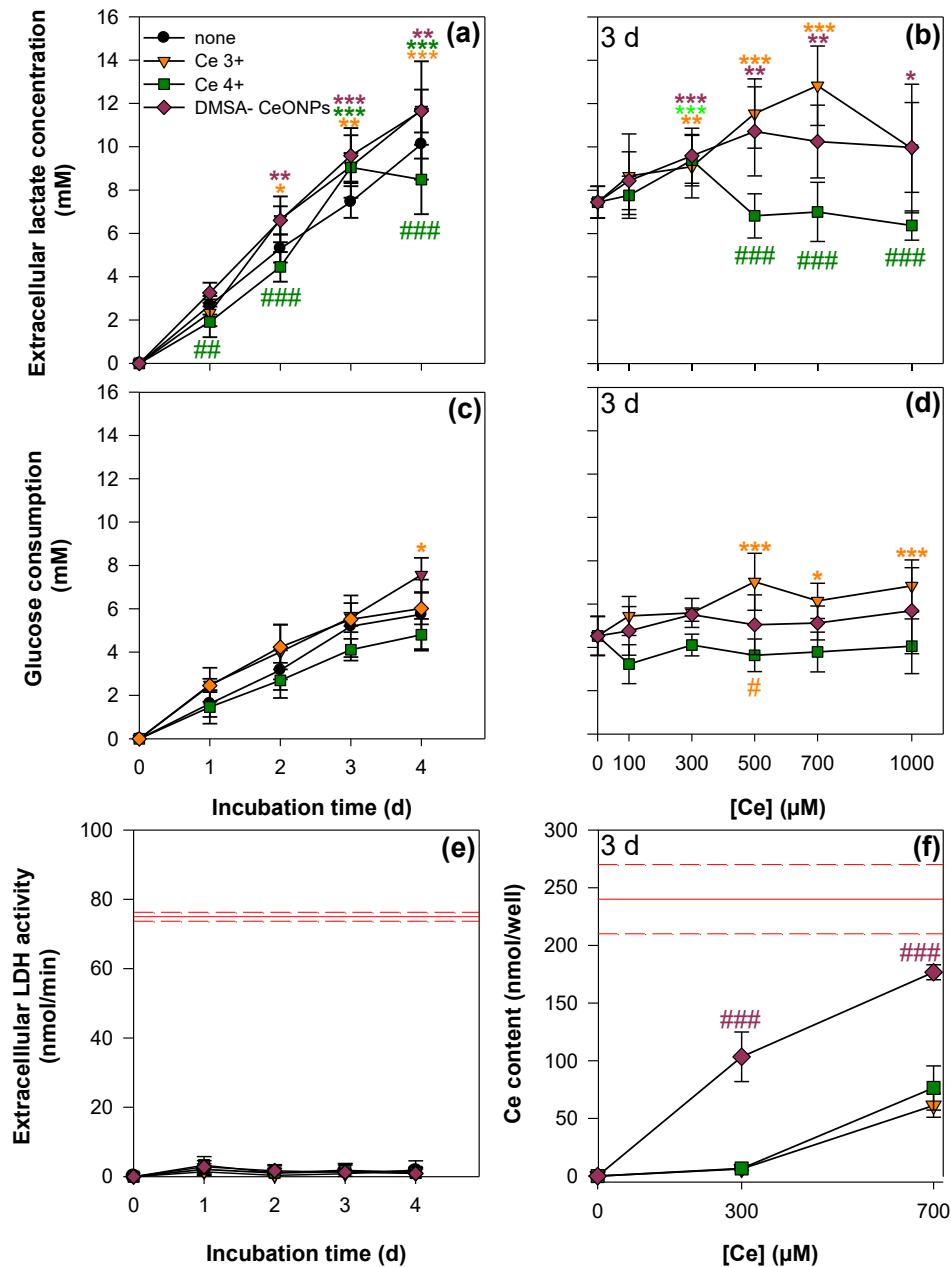
Figure 4. Comparison between the glycolysis stimulating effect of DMSA-CeONPs and cerium salts. Astrocytes were incubated without or with 300 μM CeCl$_3$, Ce(SO$_4$)$_2$ or DMSA-CeONPs in DMEM +10% FCS for up to 4 days **(a, c, e)** or with the indicated concentration of the respective compounds for 3 days **(b, d, e).** The extracellular lactate concentration **(a, b)**, the glucose consumption **(c, d)**, the viability **(e)** and the cerium content **(f)** were determined. The data represent mean ± SD of values obtained in 3 experiments on independently prepared cultures (n=3). The significance of differences (ANOVA) of data compared to those obtained for incubations in the absence of cerium (0 μM) is indicated by asterisks in the respective symbol colour (*p<0.05, **p<0.01, ***p<0.001). Differences between the salts and the DMSA-CeONPs were determined by Bonferroni post-hoc analysis and are depicted as hashes in the respective symbol colour (#p<0.05; ##p< 0.01, ###p< 0.001) **(a, c, f)**. In **(c)** the red solid line represents the intracellular LDH activity of non-treated cells at the moment of starting the incubation (initials) and the red dotted lines are the associated standard deviation.

Regarding three days incubations with higher concentrations of cerium, a significant increase in extracellular lactate concentration was observed (Fig. 4b). For DMSA-CeONPs and CeCl$_3$ a further increase in concentration led to an increase in the extracellular lactate concentration (Fig. 4b). In contrast, Ce(SO$_4$)$_2$ in a concentration above 300 µM did not lead to any significant change in lactate release compared to the control (Fig. 4b). An increase in glucose consumption took place for incubations with 500 µM CeCl$_3$ or more but the results did not reveal any sustained difference compared to cells incubated with DMSA-CeONPs or Ce(SO$_4$)$_2$ (Fig. 4d). The specific cellular content of cerium after three days of incubation with DMSA-CeONPs showed a strong and more effective ($p<0.001$) accumulation of cerium compared to cells exposed to CeCl$_3$ or Ce(SO$_4$)$_2$. (Fig. 4f). In detail, exposure to DMSA-CeONPs caused an approximately 16-fold increase in specific cellular cerium content in comparison to incubations with cerium salts when 300 µM were added. This difference was reduced to ~ 3-fold when the cells were treated with 700 µM cerium salts (Fig. 4f).

Study of the potential impairment of the mitochondrial respiratory chain by DMSA-CeONPs.

An increase in lactate release and glucose consumption in astrocytes has been previously reported for conditions where the respiratory chain was inhibited or blocked (Slater, 1973; Pauwels et al., 1985; Scheiber and Dringen, 2011). Therefore, the inhibition of the respiratory chain in astrocytes preincubated with 300 µM DMSA-CeONPs over three days was investigated. Cells were preincubated as previously described and then washed twice with IB and incubated in 200 µL IB in the absence (-AA) or presence (+AA) of 10 µM AA for 2 and 4 h. After the completion of each timepoint, extracellular lactate concentration, glucose consumption and extracellular LDH activity were determined. Inhibition of the oxidative phosphorylation by AA, increased lactate release and glucose consumption approximately 2-fold ($p<0.001$) (Fig. 5a, b). Cells which had been pre-incubated with DMSA-CeONPs and incubated in IB in the absence or presence of AA, did not show increased extracellular lactate concentration (Fig. 5a) after 4 h and no alteration in glucose consumption (Fig. 5b). Extracellular LDH activity was below 20% compared to the intracellular LDH activity of non-treated cells at the moment of starting the incubation with AA (initials) for the conditions tested (Fig. 5c).
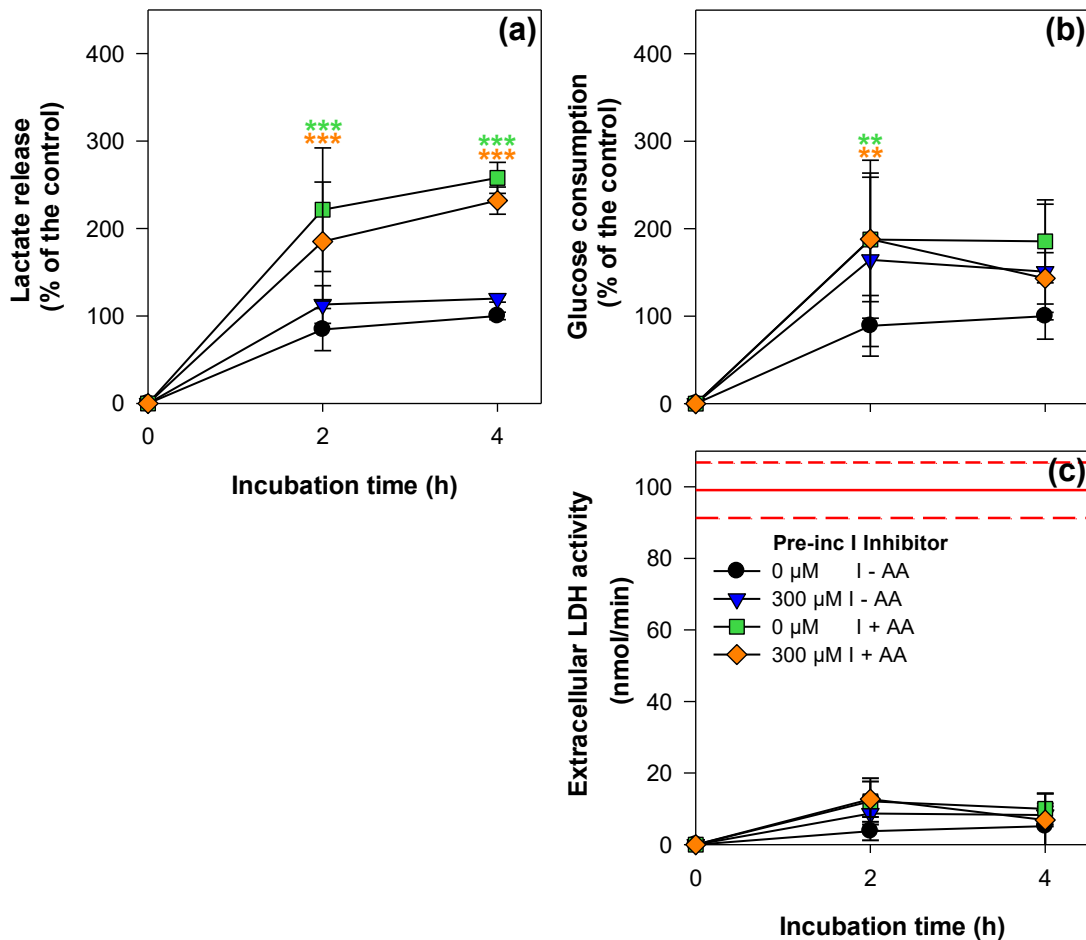
Figure 5. Effects of the mitochondrial respiration chain inhibitor AA on the induced DMSA-CeONPs stimulation of lactate release (a) and glucose consumption (b). Cultured astrocytes were pre-incubated without or with 300 µM DMSA-CeONPs for 72 h. The extracellular lactate content and glucose consumption were determined after washing the DMSA-CeONPs away and after incubation of the cells in the absence or presence of 10 µM AA for 2 and 4 h respectively. The difference of the data for AA-treated cells compared to the respective controls (absence of AA) was highly significant for all the conditions (p<0.001, not depicted in the figure). There was not significance of differences in the data between cells treated with or without DMSA-CeONPs. The data represent mean ± SD of values obtained in three experiments on independently prepared cultures (n=3). The significance of differences of data were investigated by ANOVA and *post-hoc* test Bonferroni. Values of p> 0.05 were considered as not significant. In **(c)** the red solid line represents the intracellular LDH activity of non-treated cells at the moment of starting the incubation with AA (initials) and the red dotted lines are the associated standard deviation.

Study of potential hypoxia caused by DMSA-CeONPs in APCs

Another possible explanation for acceleration of the glycolytic flux in APCs caused by DMSA-CeONPs, is the stabilization of the transcription factor Hif-1α, which induces increased expression of genes that are involved in glucose uptake and glycolysis during episodes of local hypoxia (Mansfield et al., 2005). To investigate whether DMSA-CeONPs might have

caused local hypoxia or directly stabilized Hif-1α, cultured astrocytes were incubated for 4, 24 or 72 h without or with 300 μM DMSA-CeONPs in the presence of compounds, which have been previously reported to stabilize Hif-1α (i.e. DFx, DMOG or $CoCl_2$) (Epstein et al., 2001; Mole et al., 2003; Hirota and Semenza, 2005; Rosafio and Pellerin, 2014). The incubations without or with DMSA-CeONPs in combination with the different Hif-1α stabilizing compounds did not caused any significant disruption of cells membrane for any of the timepoints studied (Fig. 6a-c). DMSA-CeONPs caused a significant increase in extracellular lactate concentration after 72 h of incubation compared to cells not exposed to cerium and stabilizing factors (control) (Fig. 6e,f). After 4 h incubation no effect in the extracellular lactate concentration was recorded for any of the treatments applied (Fig. 6d). In contrast, 24 incubation with DFx caused a significant increase in extracellular lactate in the absence and in the presence of DMSA-CeONPs compared to the control. Similarly, astrocytes incubated with DMOG also increased the extracellular lactate significantly (Fig. 6e). However, cells treated with DMOG and DMSA-CeONPs released less lactate to the extracellular space compared to their controls (Fig. 6e). After 72 h incubation, the presence of stabilizing factors increased significantly the extracellular lactate concentration compared to the control (Fig. 6f). Cells incubated with DMSA-CeONPs and stabilizing factors also showed a statistical difference with the control but not compared with cells incubated only in the presence of NPs (Fig. 6f). Moreover, the increase in extracellular lactate concentration was similar among cells incubated only in the presence of stabilizing factors and those with stabilizing factors plus DMSA-CeONPs (Fig. 6f). Therefore, the increase in extracellular lactate caused by DMSA-CeONPs was not additive to that caused by Hif-1α stabilizing factors (Fig. 6f).
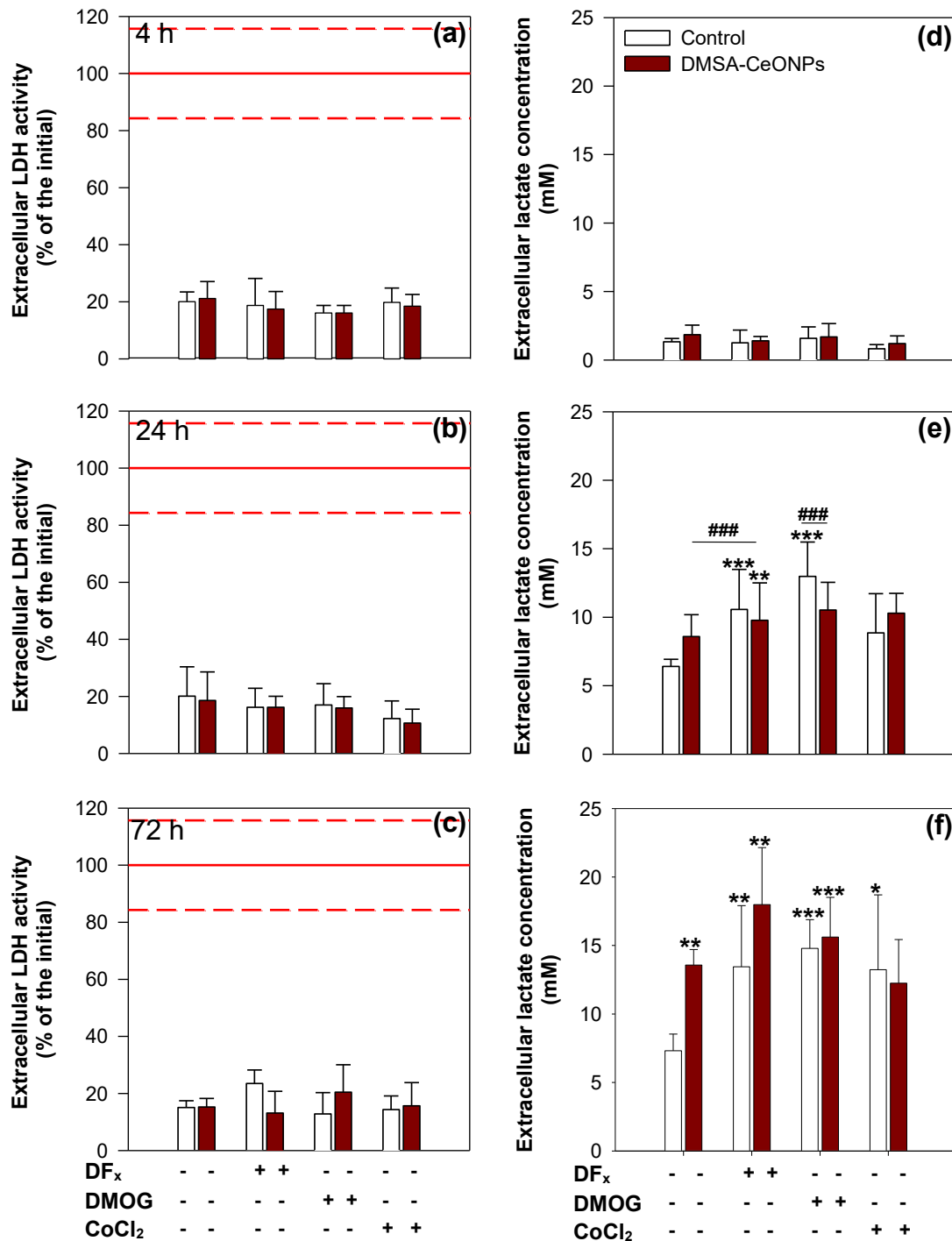
Figure 6. Effects in lactate release caused by DMSA-CeONPs and different stabilisers of Hif-1α in cultures astrocytes. Cells were incubated for 4 **(a, d)**, 24 **(b, e)** and 72 h **(c, f)** without (control) or with 300 µM DMSA-CeONPs in the absence or the presence of 1 mM DFx, 1 mM DMOG or 200 µM CoCl₂ in DMEM +10% FCS. After the completion of the incubation time, the extracellular LDH activity **(a, b, c)** and the extracellular lactate concentration **(d, e, f)** were determined. The data represent mean ± SD of values obtained in three experiments on independently prepared cultures (n=3). The significance of differences (ANOVA) of data compared to those obtained for incubations in the absence of DMSA-CeONPs (control) is indicated by asterisks ($*p<0.05$), ($**p<0.01$), ($***p<0.001$).

Differences among treatments are indicated by hash marks (###p<0.001) In **(a, b, c)** the red solid line represents the intracellular LDH activity of non-treated cells at the moment of starting the incubation (initials) and the red dotted lines are their associated standard deviation.

Discussion

DMSA-CeONPs upregulated glucose metabolism in cultured rat astrocytes in a time- and concentration-dependent manner. Exposure to 300 µM of DMSA-CeONPs for three days consistently stimulated the glycolytic flux. In fact, lactate release was consistently upregulated in cultured astrocytes after three or four days of incubation with concentrations of DMSA-CeONPs of 30 µM or higher, in contrast, increased glucose consumption was only detected when the concentration of DMSA-CeONPs was 300 µM or higher. The discrepancy between the minimal concentration of DMSA-CeONPs that caused a detectable stimulation of lactate release and glucose consumption may be explained by an analytical limitation. The culture media contained 25 mM of glucose and therefore, the samples had to be diluted 1:5 prior to glucose determination. The differences between the initial and final glucose concentrations in the culture medium for the control and the lowest DMSA-CeONPs concentration tested were relatively small and therefore subject to a large variation, which may have hindered the establishment of statistical differences for such values.

Cultured astrocytes incubated with DMSA-CeONPs showed an increase in extracellular lactate concentration even after removal of the NPs from the medium, suggesting that the effect is persistent and may be exerted by the internalized DMSA-CeONPs. This observation excludes a major contribution from extracellular NPs or cell surface phenomena. Incubation times as short as 1 h were sufficient to elicit a significant and sustained stimulation of lactate release, detectable even 72 h after the start of incubation.

Whether the stimulation of the glycolytic flux was attributable to the "NP-effect" or to the presence of cerium was also investigated. $CeCl_3$ also stimulated astrocytic glycolysis in a time- and concentration-dependent manner, as indicated by the approximately 1.75-fold increase in extracellular lactate concentration after three days of incubation compared to the control. $Ce(SO_4)_2$ significantly increased extracellular lactate only after 3 d incubation with 300 µM.

Cerium caused a shift in the ratio of lactate production to glucose consumption in cultured astrocytes. The cells showed a high ratio of extracellular lactate concentration to glucose

consumption i.e. 1.8 for the cells treated with DMSA-CeONPs, 1.6 for $CeCl_3$ and 2.0 for $Ce(SO_4)_2$, after three days of incubation in the presence of 300 µM of the respective cerium compounds. In the absence of cerium, the ratio showed a value of 1.3. Such increase of the ratio usually indicates a mitochondrial impairment and predominant ATP production via glycolysis (Scheiber and Dringen, 2011; Westhaus et al., 2017). In the case of 300 µM DMSA-CeONPs, the concentration-dependent increase in extracellular lactate correlated well with the increase in cellular specific cerium content, indicating that an elevated cellular cerium content (103.4 ± 21.5 nmol well^{-1}) is connected with the stimulation of the glycolytic flux in cultured astrocytes. In the case of $CeCl_3$ and $Ce(SO_4)_2$, cerium internalization was significantly reduced compared to DMSA-CeONPs (6.2 ± 1.3 and 6.6 ± 1.4 nmol well^{-1}, respectively). Therefore, $CeCl_3$, despite the lower uptake, induced the same effect as DMSA-CeONPs, suggesting that the stimulation of the glycolytic flux could be due to the Ce^{3+} ions released from the NPs and not to the cerium presented in the form of NPs. This is consistent with the observation that a treatment with 100 µM copper oxide NPs (CuONPs) in cultured astrocytes stimulated the glycolytic flux, and simultaneously caused a significant elevation in cellular glutathione and metallothionein synthesis (Bulcke and Dringen, 2015). The authors pointed out that copper ions released from the NPs were most likely responsible for these alterations, however, the ultimate mechanism was not elucidated. Interestingly, in the present study, 700 µM of $Ce(SO_4)_2$ was taken up by the cells at a similar or even slightly higher rate than 700 µM $CeCl_3$ after three days of incubation. However, the extracellular lactate concentration decreased sharply when cells were incubated with $Ce(SO_4)_2$ at 500 µM or higher concentrations. Ce^{4+}, when dissolved in aqueous solutions, tends to undergo hydrolysis when it is not dissolved in acidic conditions and/or at high concentrations (Jakupec et al., 2005; Williams and Grant, 2019). Therefore, although a similar uptake was observed, the absence of stimulation of the glycolytic flux could be explained by the chemical modification of the media.

Recent studies, under similar experimental conditions to the presented herein, have also reported a stimulation of the glycolytic flux in cultured astrocytes by a wide spectrum of xenobiotic compounds e.g. formaldehyde (Tulpule et al., 2013), arsenicals (Dringen et al., 2016), metformin (Hohnholt et al., 2017; Westhaus et al., 2017), 8-hydroxy efavirenz (Arend et al., 2016), $CuCl_2$ (Scheiber and Dringen, 2011). Two main causes have been hypothesized to explain the metabolic up-regulation of glycolytic flux in cultured astrocytes: Inactivation of the mitochondrial respiratory chain (Tulpule et al., 2013; Arend et al., 2016; Dringen et al., 2016; Hohnholt et al., 2017; Westhaus et al., 2017) or inactivation of the pyruvate dehydrogenase α-subunit (Scheiber and Dringen, 2011).

Pre-incubation of cultured astrocytes with DMSA-CeONPs followed by the incubation with AA, an inhibitor of the respiratory complex III, aimed at elucidating the potential inactivation of the mitochondrial respiratory chain by DMSA-CeONPs. While treatment with AA resulted in a doubling in extracellular lactate concentration, pre-incubation without or with DMSA-CeONPs had no further effect. These results could not reproduce the persistent increase in extracellular lactate concentration observed in cells preincubated for 72 h with DMSA-CeONPs and incubated for up to 4 h in NPs-free IB-BSA. The absence of BSA in the incubation with AA was the only difference in the conditions compared to the test for the persistence of the effects induced by DMSA-CeONPs. Albumin has been known to cause the disinhibition of pyruvate dehydrogenase (Tabernero et al., 1999), and therefore, increase lactate release. Furthermore, albumin is present at very low concentrations in cells of the adult brain (Ahn et al., 2008) and only increases during pathological conditions, including hypoxic episodes (Plateel et al., 1997). A possible explanation is that internalized DMSA-CeONPs may facilitate the uptake of albumin, if present in the medium, by causing local hypoxia and may at least partly account for the persistent increase in extracellular lactate. However, the inability to reproduce the mentioned increase in extracellular lactate concentration due to DMSA-CeONPs under these experimental conditions prevented an accurate assessment of the potential inhibition of the mitochondrial respiration.

Contradictory results concerning the effect of CeONPs on mitochondrial respiration in different cell types have been reported: CeONPs have been described to reduce (Datta et al., 2020; Gutiérrez-Carcedo et al., 2020) or, on the contrary, to maintain or increase (Chen et al., 2013; Arya et al., 2014) mitochondrial membrane potential. In a recent study, human primary fibroblasts were incubated with 100 µg mL^{-1} of CeONPs for 24 and 72 h and the single contribution of glycolytic ATP generation and oxidative ATP production were investigated. A significant increase of the total amount of ATP, and remarkably of both glycolytic and mitochondrial ATP-specific contributions was recorded (Pezzini et al., 2017). The mechanism for the observed increase in the overall respiratory activity also remained unclear but the authors hypothesized that the ROS scavenging activity of the CeONPs led to a decrease in cardiolipin and cytochrome c oxidase which was translated in an enhancement of respiration after 24 h incubation. The incubation time needed to observe a significant increase in glycolytic ATP generation correlates well with the incubation time needed to record an increase in lactate release in the present study (48 h). However, DMSA-CeONPs seem, if at all, to inhibit the mitochondrial activity rather than up-regulate it, as it can be inferred from the ratio lactate/glucose obtained in the time-dependency experiments. Some explanation for this disparity could be due to differences in the nominal size of the CeONPs

(Ma et al., 2021), the type of cell studied (Chen et al., 2013; Datta et al., 2020) or the absence of ROS scavenging activity by DMSA-CeONPs (Arya et al., 2014; Pezzini et al., 2017) (see section 2.3).

An alternative explanation for the observed stimulation of glycolytic flux was also assessed, namely the possibility that DMSA-CeONPs caused local hypoxia in cultured astrocytes. Stabilization of Hif-1α under normoxic conditions induces the transcription of genes involved on glucose uptake and glycolysis in astrocytes and stimulates the glycolytic flux (Bruick and McKnight, 2001; Epstein et al., 2001; Jaakkola et al., 2001). Local hypoxia and oxidative stress have been identified as stabilizers of Hif-1α (Jung et al., 2008; Movafagh et al., 2015; Li et al., 2019). Both, ROS scavenging activity and the pro-oxidant activities of DMSA-CeONPs are closely linked to the surface exchange with oxygen (Datta et al., 2020; Lord et al., 2021; Dutta et al., 2022). Different chemical Hif-1α stabilizers have been investigated in the past. DFx stabilizes Hif-1α by chelating the iron present and thus avoiding the interaction with the von Hippel-Lindau protein (VHL), which role is the ubiquitylation of Hif-1α for its degradation (Hirota and Semenza, 2005). For cobalt, two mechanisms for the stabilization of Hif-1α have been determined. In the first, cobalt inactivates prolyl hydroxylase domain containing enzymes (PHDs) by occupying an iron-binding site (Epstein et al., 2001) and in the second, cobalt impedes the interaction with VHL by occupying the VHL-binding domain of Hif-1α and hence preventing its degradation (Yuan et al., 2003). In the case of dimethyloxalylglycine (DMOG), the stabilization of Hif-1α is also achieved by inhibition of PHDs (Mole et al., 2003; Rosafio and Pellerin, 2014).

In the present study, incubations for 24 and 72 h of cultured astrocytes with the mentioned chemical stabilizers of Hif-1α caused a significant increase in lactate release in comparison to the control, indicating an enhancement of the glycolysis. The co-incubation of these stabilizers with DMSA-CeONPs resulted in a similar increase of extracellular lactate concentration. Additive effects were not observed, suggesting that DMSA-CeONPs may also trigger the stabilization of Hif-1α. Astrocytes cope with hypoxia by increasing their glycolytic capacity and downregulating ATP requirements (Marrif and Juurlink, 1999; Véga et al., 2006; Allen et al., 2020). Upon hypoxia, astrocytes can double their capacity to perform glycolysis. In this sense, a rise in extracellular lactate, may reflect an oxygen deprivation (Dienel and Hertz, 2005). Shorter incubations (4 h) did not recorded any increase in lactate release. It has been reported that stabilization of Hif-1α mediates the upregulation of specific isoforms of the glycolytic enzymes i.e. LDH4, LDH5 and pyruvate kinase (Marrif and Juurlink, 1999) for what protein synthesis is required, a process that may

need of longer incubation times. Additionally, in a preliminary study, the inhibition of protein synthesis, assessed by co-incubations with cycloheximide and DMSA-CeONPs, abolished the stimulation of lactate release (data not shown), which also points out to the involvement of synthesis of proteins for the up-regulation of glycolysis.

CeONPs have previously been investigated for causing local hypoxia in cells. For example, Das et al. (2012) demonstrated that 1 µM CeONPs, with a nominal size between 3-5 nm and with an elevated Ce^{3+}/Ce^{4+}, stabilized Hif-1α in endothelial cells. In this study, the nuclear expression of Hif-1α was significantly increased after only 2 h of incubation with CeONPs. Differences in exposition times, which caused a significant increase in lactate or in protein expression, can be explained by the different analytical indicators employed, lactate release requiring further cellular processes and therefore, more time to be detected. Another reason, which seems to play a role, is the difference in the type of cells used. In this line, (Varlamova et al., 2023) investigated the effects of CeONPs on cortical astrocytes cultured under oxygen-glucose deprivation. The authors reported, already prior to the insult, a two-fold increase in genes regulating Hif-1α expression in astrocytes pre-incubated for 24 h with CeONPs. Remarkably, Rosafio and Pellerin (2014) observed that cultured astrocytes incubated upon hypoxia with only 1 or 0% of oxygen needed 48 h to significantly increase the expression of Hif-1α and 72 h to reach its maximum. These incubation times highly correlate with the observations presented herein.

Das and colleagues (2012) postulated that the elevated presence of Ce^{3+} in the surface of the NPs is associated with a higher number of oxygen vacancies and therefore, caused the NPs to act as an oxygen buffer, which first possibly retrieved the cellular oxygen, causing local hypoxia. This argument might point out that DMSA-CeONPs contained a high presence of Ce^{3+} ions in their surface and acted as an oxygen buffer too. However, in the case of DMSA-CeONPs such explanation may require an initial flip-flop from Ce^{4+} to Ce^{3+}, as DMSA-CeONPs were functionalized from commercial CeONPs labeled by the manufacturer as Ce(IV) oxide NPs. he fact that $CeCl_3$ elicited the same increase in lactate release as DMSA-CeONPs (Fig. 4c,d) also questions the suggested mechanism.

Based on the present results, it is hypothesized that DMSA-CeONPs or most likely cerium ions released from the NPs, caused a local hypoxia which lead to an increase in the intracellular ROS and, in this way, induced a stabilization of Hif-1α, stimulating the glycolysis to assure cell survival. ROS levels are known to rise as a consequence of a fall in oxygen availability (Dienel and Hertz, 2005) and are essential for oxygen sensing and stabilization of Hif-1α upon moderate hypoxia (Mansfield et al., 2005). It can also be that

DMSA-CeONPs acted as an oxidant, generated ROS and stabilized Hif-1α, thereby, stimulating the glycolysis. Further and more detailed experiments are needed to clarify whether DMSA-CeONPs stabilize Hif-1α. However, if this hypothesis is confirmed, it is highly likely that cerium is also involved in translation-dependent pathways for Hif-1α stabilization.

Other possible scenario is that DMSA-CeONPs did not generate a significant increase in cellular ROS but cerium ions released from the NPs substituted the iron located at the active center of the PHDs, impeding the degradation of Hif-1α (Ma et al., 2021). Other metals e.g. Cu^{2+}, Co^{2+} or Cd^{2+} have been identified as competitors for the iron-binding site in the active center of Hif-PHDs (Martin et al., 2005; Osipyants et al., 2018). This other explanation might also imply the synthesis of proteins as Hif-1α would migrate to the nucleus, bind to Hif-1β and activate the synthesis of proteins.

As iron chelators have been also observed to inhibit Hif-1α degradation (Wang and Semenza, 1993; Weinreb et al., 2013), the DMSA, coating the NPs, could be argued to be the cause behind the suggested Hif-1α stabilization. Although DMSA is used as chelator in lead poisoning its capacity to chelate iron is very limited (Haust et al., 1989). Moreover, $CeCl_3$ samples did not contain DMSA, which definitely rules out its participation and points out to cerium involvement.

In summary, DMSA-CeONPs were effectively taken up and caused a severe increase in lactate production in cultured astrocytes in a time- and concentration-dependent manner. Concerning the incubation time, the effects seem to appear after 48 h incubation. $CeCl_3$ exerted the same effect although the internalized cerium content was significantly lowered in comparison to DMSA-CeONPs-treatments. Two main causes, which justified such upregulation in lactate release, were investigated: mitochondrial respiration inhibition and local hypoxia. Studies about the inhibition of mitochondrial respiration by DMSA-CeONPs were not conclusive. In contrast, DMSA-CeONPs caused a similar lactate release as cells treated with stabilizers of Hif-1α. However, the present study lacks the demonstration of the specific cellular mechanism involved.

As CeONPs are being investigated as nanotherapeutics against illnesses causing oxidative stress in the brain e.g. AD (Cimini et al., 2012; Dowding et al., 2014; Guan et al., 2016), PD (Dillon et al., 2011; Pinna et al., 2015) or ischemia (Estevez et al., 2011; Chen and Gao, 2017), this stimulation of the glycolytic flux needs to be further studied and understood. Ultimately, an increased lactate production from astrocytes could lead to brain lactic acidosis, which

has been linked to impairments of synaptic transmissions and cognitive functions (Kaufmann et al., 2004).

References

Ahn, S.-M., K. Byun, K. Cho, J. Y. Kim, J. S. Yoo, D. Kim, S. H. Paek, S. U. Kim, R. J. Simpson and B. Lee (2008). "Human microglial cells synthesize albumin in brain." PloS One 3(7): e2829.

Alili, L., M. Sack, A. S. Karakoti, S. Teuber, K. Puschmann, S. M. Hirst, C. M. Reilly, K. Zanger, W. Stahl and S. Das (2011). "Combined cytotoxic and anti-invasive properties of redox-active nanoparticles in tumor–stroma interactions." Biomaterials 32(11): 2918-2929.

Allen, S. P., R. S. Seehra, P. R. Heath, B. P. Hall, J. Bates, C. J. Garwood, M. M. Matuszyk, S. B. Wharton and J. E. Simpson (2020). "Transcriptomic analysis of human astrocytes in vitro reveals hypoxia-induced mitochondrial dysfunction, modulation of metabolism, and dysregulation of the immune response." International Journal of Molecular Sciences 21(21): 8028.

Almeida, A., D. Jimenez-Blasco and J. P. Bolaños (2023). "Cross-talk between energy and redox metabolism in astrocyte-neuron functional cooperation." Essays in Biochemistry 67(1): 17-26.

Arend, C., A. Rother, S. Stolte and R. Dringen (2016). "Consequences of a chronic exposure of cultured brain astrocytes to the anti-retroviral drug efavirenz and its primary metabolite 8-hydroxy efavirenz." Neurochemical Research 41(12): 3278-3288.

Arya, A., N. Sethy, M. Das, S. Singh, A. Das, S. Ujjain, R. Sharma, M. Sharma and K. Bhargava (2014). "Cerium oxide nanoparticles prevent apoptosis in primary cortical culture by stabilizing mitochondrial membrane potential." Free Radical Research 48(7): 784-793.

Asati, A., S. Santra, C. Kaittanis and J. M. Perez (2010). "Surface-charge-dependent cell localization and cytotoxicity of cerium oxide nanoparticles." ACS Nano 4(9): 5321-5331.

Barker, E., J. Shepherd and I. O. Asencio (2022). "The use of cerium compounds as antimicrobials for biomedical applications." Molecules 27(9): 2678.

Beedle, A., J. Hamid and G. Zamponi (2002). "Inhibition of transiently expressed low-and high-voltage-activated calcium channels by trivalent metal cations." The Journal of Membrane Biology 187(3): 225-238.

Böhm, C. R. (1915). "Die Seltenen Erden in der Therapie." Angewandte Chemie 28(62): 333-348.

Bruick, R. K. and S. L. McKnight (2001). "A conserved family of prolyl-4-hydroxylases that modify HIF." Science 294(5545): 1337-1340.

Bulcke, F. and R. Dringen (2015). "Copper oxide nanoparticles stimulate glycolytic flux and increase the cellular contents of glutathione and metallothioneins in cultured astrocytes." Neurochemical Research 40(1): 15-26.

Bulcke, F. and R. Dringen (2016). "Handling of copper and copper oxide nanoparticles by astrocytes." Neurochemical Research 41(1): 33-43.

Bulcke, F., K. Thiel and R. Dringen (2014). "Uptake and toxicity of copper oxide nanoparticles in cultured primary brain astrocytes." Nanotoxicology 8(7): 775-785.

Burkes, S. and C. McCleskey (1947). "The bacteriostatic activity of cerium, lanthanum, and thallium." Journal of Bacteriology 54(4): 417-424.

Chen, L. and X. Gao (2017). "The application of nanoparticles for neuroprotection in acute ischemic stroke." Therapeutic Delivery 8(10): 915-928.

Chen, S., Y. Hou, G. Cheng, C. Zhang, S. Wang and J. Zhang (2013). "Cerium oxide nanoparticles protect endothelial cells from apoptosis induced by oxidative stress." Biological Trace Element Research 154(1): 156-166.

Chen, Z., Z. Yuan, S. Yang, Y. Zhu, M. Xue, J. Zhang and L. Leng (2023). "Brain energy metabolism: astrocytes in neurodegenerative diseases." CNS Neuroscience & Therapeutics 29(1): 24-36.

Cheng, G., W. Guo, L. Han, E. Chen, L. Kong, L. Wang, W. Ai, N. Song, H. Li and H. Chen (2013). "Cerium oxide nanoparticles induce cytotoxicity in human hepatoma SMMC-7721 cells via oxidative stress and the activation of MAPK signaling pathways." Toxicology In Vitro 27(3): 1082-1088.

Cimini, A., B. D'Angelo, S. Das, R. Gentile, E. Benedetti, V. Singh, A. M. Monaco, S. Santucci and S. Seal (2012). "Antibody-conjugated PEGylated cerium oxide nanoparticles for specific targeting of Aβ aggregates modulate neuronal survival pathways." Acta Biomaterialia 8(6): 2056-2067.

Cupaioli, F. A., F. A. Zucca, D. Boraschi and L. Zecca (2014). "Engineered nanoparticles. How brain friendly is this new guest?" Progress in Neurobiology 119: 20-38.

Dai, Y., J. Li, J. Li, L. Yu, G. Dai, A. Hu, L. Yuan and Z. Wen (2002). "Effects of rare earth compounds on growth and apoptosis of leukemic cell lines." In Vitro Cellular & Developmental Biology-Animal 38(7): 373-375.

Das, J., Y.-J. Choi, J. W. Han, A. M. M. T. Reza and J.-H. Kim (2017). "Nanoceria-mediated delivery of doxorubicin enhances the anti-tumour efficiency in ovarian cancer cells via apoptosis." Scientific Reports 7(1): 1-12.

Das, S., S. Singh, J. M. Dowding, S. Oommen, A. Kumar, T. X. Sayle, S. Saraf, C. R. Patra, N. E. Vlahakis and D. C. Sayle (2012). "The induction of angiogenesis by cerium oxide nanoparticles through the modulation of oxygen in intracellular environments." Biomaterials 33(31): 7746-7755.

Datta, A., S. Mishra, K. Manna, K. D. Saha, S. Mukherjee and S. Roy (2020). "Pro-oxidant therapeutic activities of cerium oxide nanoparticles in colorectal carcinoma cells." ACS Omega 5(17): 9714-9723.

Dhall, A. and W. Self (2018). "Cerium oxide nanoparticles: a brief review of their synthesis methods and biomedical applications." Antioxidants 7(8): 97.

Dienel, G. A. and L. Hertz (2005). "Astrocytic contributions to bioenergetics of cerebral ischemia." Glia 50(4): 362-388.

Dillon, C., M. Billings, K. Hockey, L. DeLaGarza and B. Rzigalinski (2011). "Cerium oxide nanoparticles protect against MPTP-induced dopaminergic neurodegeneration in a mouse model for Parkinson's disease." Nanotechnology 3: 451-454.

Dowding, J., W. Song, K. Bossy, A. Karakoti, A. Kumar, A. Kim, B. Bossy, S. Seal, M. Ellisman and G. Perkins (2014). "Cerium oxide nanoparticles protect against Aβ-induced mitochondrial fragmentation and neuronal cell death." Cell Death and Differentiation 21(10): 1622-1632.

Dringen, R., S. Spiller, S. Neumann and Y. Koehler (2016). "Uptake, metabolic effects and toxicity of arsenate and arsenite in astrocytes." Neurochemical Research 41(3): 465-475.

Dutta, D., R. Mukherjee, S. Ghosh, M. Patra, M. Mukherjee and T. Basu (2022). "Cerium oxide nanoparticles as antioxidant or pro-oxidant agents." ACS Applied Nano Materials 5(1): 1690-1701.

Epstein, A. C., J. M. Gleadle, L. A. McNeill, K. S. Hewitson, J. O'Rourke, D. R. Mole, M. Mukherji, E. Metzen, M. I. Wilson and A. Dhanda (2001). "*C. elegans* EGL-9 and mammalian homologs define a family of dioxygenases that regulate HIF by prolyl hydroxylation." Cell 107(1): 43-54.

Estevez, A., S. Pritchard, K. Harper, J. Aston, A. Lynch, J. Lucky, J. Ludington, P. Chatani, W. Mosenthal and J. Leiter (2011). "Neuroprotective mechanisms of cerium oxide nanoparticles in a mouse hippocampal brain slice model of ischemia." Free Radical Biology and Medicine 51(6): 1155-1163.

Evans, C. H. (2013). Biochemistry of the Lanthanides, Springer Science & Business Media.

Fernández-Varo, G., M. Perramón, S. Carvajal, D. Oró, E. Casals, L. Boix, L. Oller, L. Macías-Muñoz, S. Marfà and G. Casals (2020). "Bespoken nanoceria: An effective treatment in experimental hepatocellular carcinoma." Hepatology 72(4): 1267-1282.

Gagnon, J. and K. M. Fromm (2015). "Toxicity and protective effects of cerium oxide nanoparticles (nanoceria) depending on their preparation method, particle size, cell type, and exposure route." European Journal of Inorganic Chemistry 2015(27): 4510-4517.

Garner, J. and P. Heppell (2005). "Cerium nitrate in the management of burns." Burns 31(5): 539-547.

Garner, J. and P. Heppell (2005). "The use of Flammacerium in British burns units." Burns 31(3): 379-382.

Giri, S., A. Karakoti, R. P. Graham, J. L. Maguire, C. M. Reilly, S. Seal, R. Rattan and V. Shridhar (2013). "Nanoceria: a rare-earth nanoparticle as a novel anti-angiogenic therapeutic agent in ovarian cancer." PloS One 8(1): e54578.

Guan, Y., M. Li, K. Dong, N. Gao, J. Ren, Y. Zheng and X. Qu (2016). "Ceria/POMs hybrid nanoparticles as a mimicking metallopeptidase for treatment of neurotoxicity of amyloid-β peptide." Biomaterials 98: 92-102.

Gutiérrez-Carcedo, P., S. Navalón, R. Simó, X. Setoain, C. Aparicio-Gómez, I. Abasolo, V. M. Victor, H. García and J. R. Herance (2020). "Alteration of the mitochondrial effects of ceria nanoparticles by gold: An approach for the mitochondrial modulation of cells based on nanomedicine." Nanomaterials 10(4): 744.

Hamprecht, B. and F. Löffler (1985). [27] Primary glial cultures as a model for studying hormone action. Methods in Enzymology, Elsevier. 109: 341-345.

Haust, H. L., M. Inwood, J. D. Spence, H. C. Poon and F. Peter (1989). "Intramuscular administration of iron during long-term chelation therapy with 2, 3-dimercaptosuccinic acid in a man with severe lead poisoning." Clinical Biochemistry 22(3): 189-196.

Herrero-Mendez, A., A. Almeida, E. Fernández, C. Maestre, S. Moncada and J. P. Bolaños (2009). "The bioenergetic and antioxidant status of neurons is controlled by continuous degradation of a key glycolytic enzyme by APC/C–Cdh1." Nature Cell Biology 11(6): 747-752.

Hijaz, M., S. Das, I. Mert, A. Gupta, Z. Al-Wahab, C. Tebbe, S. Dar, J. Chhina, S. Giri and A. Munkarah (2016). "Folic acid tagged nanoceria as a novel therapeutic agent in ovarian cancer." BMC Cancer 16(1): 1-14.

Hirota, K. and G. L. Semenza (2005). "Regulation of hypoxia-inducible factor 1 by prolyl and asparaginyl hydroxylases." Biochemical and Biophysical Research Communications 338(1): 610-616.

Hohnholt, M. C., E. M. Blumrich*, H. S. Waagepetersen and R. Dringen (2017). "The antidiabetic drug metformin decreases mitochondrial respiration and tricarboxylic acid cycle activity in cultured primary rat astrocytes." Journal of Neuroscience Research 95(11): 2307-2320.

Hohnholt, M. C., M. Geppert, E. M. Luther, C. Petters, F. Bulcke and R. Dringen (2013). "Handling of iron oxide and silver nanoparticles by astrocytes." Neurochemical Research 38(2): 227-239.

Ishii, T., Y. Takanashi, K. Sugita, M. Miyazawa, R. Yanagihara, K. Yasuda, H. Onouchi, N. Kawabe, M. Nakata and Y. Yamamoto (2017). "Endogenous reactive oxygen species cause astrocyte defects and neuronal dysfunctions in the hippocampus: a new model for aging brain." Aging Cell 16(1): 39-51.

Jaakkola, P., D. R. Mole, Y.-M. Tian, M. I. Wilson, J. Gielbert, S. J. Gaskell, A. v. Kriegsheim, H. F. Hebestreit, M. Mukherji and C. J. Schofield (2001). "Targeting of HIF-α to the von Hippel-Lindau ubiquitylation complex by O_2-regulated prolyl hydroxylation." Science 292(5516): 468-472.

Jakupec, M., P. Unfried and B. Keppler (2005). "Pharmacological properties of cerium compounds." Reviews of Physiology, Biochemistry and Pharmacology 153: 101-111.

Ji, Y., B. Xiao, Z. Wang, M. Cui and Y. Lu (2000). "The suppression effect of light rare earth elements on proliferation of two cancer cell lines." Biomedical and Environmental Sciences: BES 13(4): 287-292.

Jung, S.-N., W. K. Yang, J. Kim, H. S. Kim, E. J. Kim, H. Yun, H. Park, S. S. Kim, W. Choe and I. Kang (2008). "Reactive oxygen species stabilize hypoxia-inducible factor-1 alpha protein

and stimulate transcriptional activity via AMP-activated protein kinase in DU145 human prostate cancer cells." Carcinogenesis 29(4): 713-721.

Kadry, H., B. Noorani and L. Cucullo (2020). "A blood–brain barrier overview on structure, function, impairment, and biomarkers of integrity." Fluids and Barriers of the CNS 17(1): 1-24.

Kaufmann, P., D. C. Shungu, M. Sano, S. Jhung, K. Engelstad, E. Mitsis, X. Mao, S. Shanske, M. Hirano and S. DiMauro (2004). "Cerebral lactic acidosis correlates with neurological impairment in MELAS." Neurology 62(8): 1297-1302.

Korsvik, C., S. Patil, S. Seal and W. T. Self (2007). "Superoxide dismutase mimetic properties exhibited by vacancy engineered ceria nanoparticles." Chemical Communications(10): 1056-1058.

Kumari, M., S. P. Singh, S. Chinde, M. F. Rahman, M. Mahboob and P. Grover (2014). "Toxicity study of cerium oxide nanoparticles in human neuroblastoma cells." International Journal of Toxicology 33(2): 86-97.

Kwon, H. J., M.-Y. Cha, D. Kim, D. K. Kim, M. Soh, K. Shin, T. Hyeon and I. Mook-Jung (2016). "Mitochondria-targeting ceria nanoparticles as antioxidants for Alzheimer's disease." ACS Nano 10(2): 2860-2870.

Lewin, C. (1924). "Über die Verwendung einer Cerium-Jodverbindung (Introcid) in der Therapie der Geschwulstbildungen." Medizinische Klinik 20: 1319-1323.

Li, C., X. Shi, Q. Shen, C. Guo, Z. Hou and J. Zhang (2018). "Hot topics and challenges of regenerative nanoceria in application of antioxidant therapy." Journal of Nanomaterials 2018.

Li, H.-S., Y.-N. Zhou, L. Li, S.-F. Li, D. Long, X.-L. Chen, J.-B. Zhang, L. Feng and Y.-P. Li (2019). "HIF-1α protects against oxidative stress by directly targeting mitochondria." Redox Biology 25: 101109.

Li, R., Y. Yang, H. Wang, T. Zhang, F. Duan, K. Wu, S. Yang, K. Xu, X. Jiang and X. Sun (2023). "Lactate and lactylation in the brain: current progress and perspectives." Cellular and Molecular Neurobiology 43: 2541-2555.

Lord, M. S., J. F. Berret, S. Singh, A. Vinu and A. S. Karakoti (2021). "Redox Active Cerium Oxide Nanoparticles: Current Status and Burning Issues." Small 17(51).

Lowry, O., N. Rosebrough, A. L. Farr and R. Randall (1951). "Protein measurement with the Folin phenol reagent." Journal of Biological Chemistry 193(1): 265-275.

Ma, Y., P. Li, L. Zhao, J. Liu, J. Yu, Y. Huang, Y. Zhu, Z. Li, R. Zhao and S. Hua (2021). "Size-dependent cytotoxicity and reactive oxygen species of cerium oxide nanoparticles in human retinal pigment epithelia cells." International Journal of Nanomedicine 16: 5333.

Mansfield, K. D., R. D. Guzy, Y. Pan, R. M. Young, T. P. Cash, P. T. Schumacker and M. C. Simon (2005). "Mitochondrial dysfunction resulting from loss of cytochrome c impairs cellular oxygen sensing and hypoxic HIF-α activation." Cell Metabolism 1(6): 393-399.

Marrif, H. and B. H. Juurlink (1999). "Astrocytes respond to hypoxia by increasing glycolytic capacity." Journal of Neuroscience Research 57(2): 255-260.

Martin, F., T. Linden, D. r. M. Katschinski, F. Oehme, I. Flamme, C. K. Mukhopadhyay, K. Eckhardt, J. Tröger, S. Barth and G. Camenisch (2005). "Copper-dependent activation of hypoxia-inducible factor (HIF)-1: implications for ceruloplasmin regulation." Blood 105(12): 4613-4619.

Mittal, S. and A. K. Pandey (2014). "Cerium oxide nanoparticles induced toxicity in human lung cells: role of ROS mediated DNA damage and apoptosis." BioMed research international 2014.

Mole, D. R., I. Schlemminger, L. A. McNeill, K. S. Hewitson, C. W. Pugh, P. J. Ratcliffe and C. J. Schofield (2003). "2-oxoglutarate analogue inhibitors of HIF prolyl hydroxylase." Bioorganic & Medicinal Chemistry Letters 13(16): 2677-2680.

Movafagh, S., S. Crook and K. Vo (2015). "Regulation of hypoxia-inducible factor-1a by reactive oxygen species: new developments in an old debate." Journal of Cellular Biochemistry 116(5): 696-703.

Muroma, A. (1958). "Studies in the bactericidal action of salts of certain rare earth metals." Ann, Med. Exper. et Biol. Fenniae 36(Suppl. 6).

Osipyants, A., N. Smirnova, A. Y. Khristichenko, S. Nikulin, A. Zakhariants, V. Tishkov, I. Gazaryan and A. Poloznikov (2018). "Metal ions as activators of hypoxia inducible factor." Moscow University Chemistry Bulletin 73(1): 13-18.

Pauwels, P. J., F. R. Opperdoes and A. Trouet (1985). "Effects of antimycin, glucose deprivation, and serum on cultures of neurons, astrocytes, and neuroblastoma cells." Journal of Neurochemistry 44(1): 143-148.

Petters, C., E. Irrsack, M. Koch and R. Dringen (2014). "Uptake and metabolism of iron oxide nanoparticles in brain cells." Neurochemical Research 39(9): 1648-1660.

Pezzini, I., A. Marino, S. Del Turco, C. Nesti, S. Doccini, V. Cappello, M. Gemmi, P. Parlanti, F. M. Santorelli and V. Mattoli (2017). "Cerium oxide nanoparticles: the regenerative redox machine in bioenergetic imbalance." Nanomedicine: Nanotechnology, Biology, and Medicine 12(4): 403-416.

Pinna, A., L. Malfatti, G. Galleri, R. Manetti, S. Cossu, G. Rocchitta, R. Migheli, P. A. Serra and P. Innocenzi (2015). "Ceria nanoparticles for the treatment of Parkinson-like diseases induced by chronic manganese intoxication." RSC Advances 5(26): 20432-20439.

Pirmohamed, T., J. M. Dowding, S. Singh, B. Wasserman, E. Heckert, A. S. Karakoti, J. E. S. King, S. Seal and W. T. Self (2010). "Nanoceria exhibit redox state-dependent catalase mimetic activity." Chemical Communications 46(16): 2736-2738.

Plakhova, T. V., A. Y. Romanchuk, S. N. Yakunin, T. Dumas, S. Demir, S. Wang, S. G. Minasian, D. K. Shuh, T. Tyliszczak and A. A. Shiryaev (2016). "Solubility of nanocrystalline cerium dioxide: Experimental data and thermodynamic modeling." The Journal of Physical Chemistry C 120(39): 22615-22626.

Plateel, M., E. Teissier and R. Cecchelli (1997). "Hypoxia dramatically increases the nonspecific transport of blood-borne proteins to the brain." Journal of Neurochemistry 68(2): 874-877.

Prejanò, M., M. E. Alberto, N. Russo, M. Toscano and T. Marino (2020). "The effects of the metal ion substitution into the active site of metalloenzymes: A theoretical insight on some selected cases." Catalysts 10(9): 1038.

Prejanò, M., T. Marino and N. Russo (2017). "How can methanol dehydrogenase from *Methylacidiphilum fumariolicum* work with the alien Ce[III] ion in the active center? A theoretical study." Chemistry–A European Journal 23(36): 8652-8657.

Rosafio, K. and L. Pellerin (2014). "Oxygen tension controls the expression of the monocarboxylate transporter MCT4 in cultured mouse cortical astrocytes via a hypoxia-inducible factor-1α-mediated transcriptional regulation." Glia 62(3): 477-490.

Sack, M., L. Alili, E. Karaman, S. Das, A. Gupta, S. Seal and P. Brenneisen (2014). "Combination of conventional chemotherapeutics with redox-active cerium oxide nanoparticles - a novel aspect in cancer therapy." Molecular Cancer Therapeutics 13(7): 1740-1749.

Sannino, D. (2021). Types and Classification of Nanomaterials. Nanotechnology, Springer: 15-38.

Sato, T., M. Hashizume, Y. Hotta and Y. Okahata (1998). "Morphology and proliferation of B16 melanoma cells in the presence of lanthanoid and Al^{3+} ions." BioMetals 11(2): 107-112.

Scheiber, I. F. and R. Dringen (2011). "Copper accelerates glycolytic flux in cultured astrocytes." Neurochemical Research 36(5): 894-903.

Scheiber, I. F., J. F. Mercer and R. Dringen (2010). "Copper accumulation by cultured astrocytes." Neurochemistry International 56(3): 451-460.

Scheiber, I. F., M. M. Schmidt and R. Dringen (2012). "Copper export from cultured astrocytes." Neurochemistry International 60(3): 292-300.

Shcherbakov, A. B., N. M. Zholobak and V. K. Ivanov (2020). Biological, biomedical and pharmaceutical applications of cerium oxide. Cerium oxide (CeO_2): Synthesis, Properties and Applications, Elsevier: 279-358.

Shirbandi, K., R. Rikhtegar, M. Khalafi, M. M. A. Attari, F. Rahmani, P. Javanmardi, S. Iraji, Z. B. Aghdam and A. M. R. Rashnoudi (2023). "Functional magnetic resonance spectroscopy of lactate in Alzheimer disease: A comprehensive review of Alzheimer disease pathology and the role of lactate." Topics in Magnetic Resonance Imaging 32(2): 15.

Simpson, J. (1854). "Note on the therapeutic action of the salts of cerium." Monthly Journal of Medical Science 19: 564.

Skorodumova, N., S. Simak, B. I. Lundqvist, I. Abrikosov and B. Johansson (2002). "Quantum origin of the oxygen storage capability of ceria." Physical Review Letters 89(16): 166601.

Slater, E. (1973). "The mechanism of action of the respiratory inhibitor, antimycin." Biochimica et Biophysica Acta (BBA)-Reviews on Bioenergetics 301(2): 129-154.

Swanson, R. A., W. Ying and T. M. Kauppinen (2004). "Astrocyte influences on ischemic neuronal death." Current Molecular Medicine 4(2): 193-205.

Tabernero, A., A. Medina, L. I. Sánchez-Abarca, E. Lavado and J. M. Medina (1999). "The effect of albumin on astrocyte energy metabolism is not brought about through the control of cytosolic Ca^{2+} concentrations but by free-fatty acid sequestration." Glia 25(1): 1-9.

Tulpule, K., M. C. Hohnholt and R. Dringen (2013). "Formaldehyde metabolism and formaldehyde-induced stimulation of lactate production and glutathione export in cultured neurons." Journal of Neurochemistry 125(2): 260-272.

Tulpule, K., M. C. Hohnholt, J. Hirrlinger and R. Dringen (2014). Primary cultures of astrocytes and neurons as model systems to study the metabolism and metabolite export from brain cells. Brain Energy Metabolism, Springer**: 45-72.

van Putten, M. J., C. Fahlke, K. W. Kafitz, J. Hofmeijer and C. R. Rose (2021). "Dysregulation of astrocyte ion homeostasis and its relevance for stroke-induced brain damage." International Journal of Molecular Sciences 22(11): 5679.

Varlamova, E. G., A. S. Baryshev, S. V. Gudkov, V. A. Babenko, E. Y. Plotnikov and E. A. Turovsky (2023). "Cerium oxide nanoparticles protect cortical astrocytes from oxygen–glucose deprivation through activation of the Ca^{2+} signaling system." International Journal of Molecular Sciences 24(18): 14305.

Véga, C., L. R. Sachleben Jr, D. Gozal and E. Gozal (2006). "Differential metabolic adaptation to acute and long-term hypoxia in rat primary cortical astrocytes." Journal of Neurochemistry 97(3): 872-883.

Verkhratsky, A. and M. Nedergaard (2018). "Physiology of astroglia." Physiological Reviews 98(1): 239-389.

Verkhratsky, A., M. Nedergaard and L. Hertz (2015). "Why are astrocytes important?" Neurochemical Research 40(2): 389-401.

Vicente-Gutierrez, C., N. Bonora, V. Bobo-Jimenez, D. Jimenez-Blasco, I. Lopez-Fabuel, E. Fernandez, C. Josephine, G. Bonvento, J. A. Enriquez and A. Almeida (2019). "Astrocytic mitochondrial ROS modulate brain metabolism and mouse behaviour." Nature Metabolism 1(2): 201-211.

Wang, G. L. and G. L. Semenza (1993). "Desferrioxamine induces erythropoietin gene expression and hypoxia-inducible factor 1 DNA-binding activity: implications for models of hypoxia signal transduction." Blood 82(12): 3610-3615.

Weinreb, O., S. Mandel, M. B. Youdim and T. Amit (2013). "Targeting dysregulation of brain iron homeostasis in Parkinson's disease by iron chelators." Free Radical Biology and Medicine 62: 52-64.

Westhaus, A., E. M. Blumrich and R. Dringen (2017). "The antidiabetic drug metformin stimulates glycolytic lactate production in cultured primary rat astrocytes." Neurochemical Research 42(1): 294-305.

Wilcox, R. W. (1917). "The therapeutics of cerium." Transactions of the American Therapeutic Society: 68.

Williams, D. E. and K. B. Grant (2019). "Metal-assisted hydrolysis reactions involving lipids: a review." Frontiers in Chemistry 7: 14.

Yang, C., R.-Y. Pan, F. Guan and Z. Yuan (2024). "Lactate metabolism in neurodegenerative diseases." Neural Regeneration Research 19(1): 69-74.

Yuan, Y., G. Hilliard, T. Ferguson and D. E. Millhorn (2003). "Cobalt inhibits the interaction between hypoxia-inducible factor-α and von Hippel-Lindau protein by direct binding to hypoxia-inducible factor-α." Journal of Biological Chemistry 278(18): 15911-15916.

2.3 Scavenging of Reactive Oxygen Species by DMSA-coated Cerium Oxide Nanoparticles and Ionic Cerium in Cultured Glial Cells

<u>Contributions of M. Carmen Osorio Navarro:</u>

- All experimental work
- Preparation of all tables and figures panels
- Writing of the chapter

Abstract

To investigate the antioxidative potential of cerium oxide nanoparticles (CeONPs), commercial CeONPs were coated with dimercaptosuccinate acid (DMSA) and were characterized. DMSA-CeONPs had a mean hydrodynamic diameter in aqueous dispersion of 171 ± 6 nm. Dispersion in incubation buffer containing 0.5 mg L^{-1} of bovine serum albumin (IB-BSA) increased the hydrodynamic diameter to 234 ± 8 nm and changed the zeta potential from -27.4 ± 2.1 mV in water to -13.2 ± 0.9 mV. DMSA-CeONPs remained stable in dispersion for the time and the conditions tested. The extracellular H_2O_2 scavenging potential of DMSA-CeONPs was determined by incubating the NPs in IB containing 0.5 mg ml^{-1} BSA (IB-BSA) in the presence or absence of 100 μM H_2O_2 for up to 24 h. Presence of DMSA-CeONPs significantly removed H_2O_2 from the media in a concentration- and time-dependent manner with a half-time of 12 h. DMSA coating did not affect the antioxidant activity of CeONPs, as identical results were obtained for uncoated CeONPs (Un-CeONPs). However, ionic cerium reacted more effectively with H_2O_2, as Ce^{4+} removed H_2O_2 completely already within 1 h and the H_2O_2 removal rates (nmol min^{-1}) of Ce^{3+} or Ce^{4+} were approximately ten-times higher than those found for DMSA-CeONPs.

DMSA-CeONPs also scavenged superoxide from the extracellular space of cultured rat astrocytes in a concentration- and time-dependent manner. The generation of superoxide was established by incubating the cells with the electron cycler β-lapacho. 700 μM DMSA-CeONPs lowered by 11% the superoxide-induced WST1 formazan formation within 60 min, whereas the addition of superoxide dismutase (SOD) reduced it by 63% compared to the control. Ionic cerium showed an enhanced superoxide scavenging activity compared to its NP counterpart, as 150 μM of cerium salts caused a 53% depletion of WST1 formazan formation. The data obtained suggests that the reaction of DMSA-CeONPs with H_2O_2 or superoxide did not follow a catalytic or enzymatic-like reaction but rather represents a stoichiometric reaction with these reactive oxygen species (ROS).

To assess the potential neuroprotective effect of cellular DMSA-CeONPs against oxidative stress, glial cells were pre-incubated with these NPs and then incubated in the presence of exogenous H_2O_2 or under the β-lapachone formation of superoxide. Loading of C6 glioma cells or astrocytes with up to 1 mM DMSA-CeONPs did not compromised cell viability. However, the presence of internalized DMSA-CeONPs did not prevent H_2O_2-induced cytotoxicity in C6 glioma cells. In addition, DMSA-CeONPs internalized by cultured astrocytes did not scavenge superoxide nor rescue cultured astrocytes from acute oxidative

stress induced by 20 µM β-lapachone. These results demonstrate that DMSA-CeONPs have only a limited ROS scavenging capacity, and that internalized DMSA-CeONPs did not act as antioxidants in glial cells nor show nanozyme activities under the conditions tested.

Introduction

Brain cells have an extraordinarily high energy demand, mainly required to maintain brain intrinsic functional activity (Raichle, 2006). To meet this demand, the brain consumes approximately 20% of the inhaled O_2, ten times more than predicted by its weight alone (Bolaños, 2016). Under pathological conditions, this consumption of O_2, leads to the appearance of oxidative stress. Indeed, ageing, stroke and major brain disorders (i.e. Alzheimer´s disease (AD), Parkinson´s disease (PD), amyotrophic lateral sclerosis (ALS) and multiple sclerosis show oxidative stress as a concomitant symptom (Emerit et al., 2004; Puspita et al., 2017; Liguori et al., 2018; Cunha-Oliveira et al., 2020; Orellana-Urzúa et al., 2020; Jelinek et al., 2021).

For decades, much effort has been devoted to finding exogenous antioxidants that protect the brain from such oxidative stress (Floyd, 1999; Gilgun-Sherki et al., 2001; Neves Carvalho et al., 2017). In this line, CeONPs have gained great interest and have been extensively investigated due to their demonstrated ability to act as scavengers of ROS, such as superoxide (Korsvik et al., 2007) or H_2O_2 (Pirmohamed et al., 2010). Their low cytotoxicity (Fisichella et al., 2014; Urner et al., 2014; Forest et al., 2017), high reducibility (Skorodumova et al., 2002; Spadaro et al., 2016) and the possibility to be functionalized to cross the blood-brain barrier (Heckman et al., 2013; Bao et al., 2018) make them potential therapeutics (Celardo et al., 2011; Nelson et al., 2016; Feng et al., 2022). The mechanism of ROS scavenging by CeONPs is commonly assumed to be based on the flip-flop between Ce^{4+} and Ce^{3+} on the surface of the NPs, facilitated by the formation of oxygen vacancies and the consequent lattice expansion of the crystal (Skorodumova et al., 2002; Zhang et al., 2002; Wu et al., 2004).

The removal of H_2O_2 by CeONPs has been reported extracellularly (Rzigalinski, 2005; Pirmohamed et al., 2010; Baldim et al., 2018; Estevez et al., 2019; Seminko et al., 2021) and intracellularly (Zhou et al., 2013; Singh and Singh, 2019; Wei et al., 2021) in different cell lines. These reports, sometimes also indirectly measured H_2O_2 scavenging and showed some evidence of NP cycling over time. In this line, Pirmohamed et al. (2010) determined the removal of H_2O_2 by CeONPs in media by using UV-Vis spectrophotometry and, indirectly, by monitoring O_2 formation. Another recent study shows that CeONPs catalyzed the decomposition of H_2O_2 according to a Langmuir adsorption isotherm, concluding that the catalysis of H_2O_2 occurs at the surface of the CeONPs according to adsorption/desorption kinetics (Baldim et al., 2018). However, other reports demonstrated the removal of H_2O_2 by

CeONPs but suggested that cerium catalyzes the decomposition of H_2O_2 via the Fenton/Haber-Weiss reaction (Heckert et al., 2008; Karakoti et al., 2010; Lee et al., 2013). Focusing on the removal of H_2O_2 by CeONPs in the intracellular space of nervous cells, Chen et al. (2006) showed in an early *in vitro* study, that preincubation of retinal neurons with CeONPs significantly inhibited the formation of intracellular ROS induced by the application of H_2O_2. The authors hypothesized that the auto-regeneration of the antioxidant capacity of CeONPs explains the enhanced neuronal viability. At the same time, another line of investigation also showed a higher survival rate of spinal cord neurons insulted with H_2O_2 when treated with CeONPs (Das et al., 2007). Subsequent studies have also demonstrated neuroprotection against H_2O_2. For example, an *in vitro* study found a concentration-dependent decrease in intracellular ROS in PC12 neuron-like cells, which had been preincubated for three days in the presence of CeONPs and then insulted with H_2O_2 (Ciofani et al., 2013).

CeONPs have also been shown to scavenge superoxide from media. Korsvik et al. (2007) were the first to show the generation of H_2O_2 from the degradation of superoxide by CeONPs. Subsequent studies have focused on finding the conditions that enhance superoxide scavenging (Baldim et al., 2018; Estevez et al., 2019) and elucidating the cycling between Ce^{4+} and Ce^{3+} in the presence of superoxide (Heckert et al., 2008; Celardo et al., 2011). In addition, CeONPs have been reported to scavenge superoxide intracellularly. In particular, CeONPs were shown to significantly reduce the superoxide generation in an *in vitro* model of ischemia (Estevez et al., 2011). In a follow-up experiment, Estevez et al. (2019) also showed *in vivo* a reduction to the half of the total amount of superoxide produced during ischemia and reperfusion of the hippocampus of rats pretreated with CeONPs. Also, in an *in vivo* ALS model using transgenic mice overexpressing a mutation in the SOD^{G93A}, CeONPs were shown to significantly prolong the lifespan of the animals due to their ROS scavenging (DeCoteau et al., 2016).

Based on these observations and many other studies in other cell lines (see review by Dhall and Self (2018)), it has been stated that CeONPs possess catalase (CAT) (Pirmohamed et al., 2010; Estevez et al., 2019; Seminko et al., 2021) and SOD mimetic activity (Korsvik et al., 2007; Heckert et al., 2008; Estevez et al., 2019) and are therefore, generally considered to be nanozymes (Wei and Wang, 2013; Seminko et al., 2021; Singh et al., 2023). The first reports attributing CAT and SOD mimic activities to CeONPs argued that, similar to the action of the native enzymes, an electron transfer occurs in the reaction of CeONPs with H_2O_2 or superoxide, and that such a reaction is catalyzed by the redox cycling of the cerium.

Recently, (Seminko et al., 2021) monitored via luminescence the decomposition of H_2O_2 on the surface of CeONPs and recorded the redox cycling between Ce^{3+} and Ce^{4+} taking place. These authors demonstrated that the surface defects of CeONPs act similar to active sites in enzyme molecules and that the decomposition of H_2O_2 followed the Michaelis-Menten equation. For all that, CeONPs are considered extraordinarily promising and more efficient as their counterpart bulk cerium (Herper et al., 2020). The so called "NP effect" i.e. the combination of their enhanced antioxidant capacity, due to their large specific surface area with the simultaneous presence of Ce^{3+} and Ce^{4+} coupled with their self-regeneration accounts for such greater antioxidant capacity (Rzigalinski et al., 2017).

A major concern in the advance on the use of CeONPs as antioxidant is the lack of standardization of the NPs, meaning that each new line of investigation has the obligation to start from the basics, slowing down and driving up progress on the field. To overcome the variability introduced by the different synthesis of CeONPs, in our study, the antioxidant capacity of commercial CeONPs functionalized with DMSA was investigated. Previous reports have shown that coating various metal NPs with DMSA facilitates the study of their fate and effect on mammalian brain cells (Geppert et al., 2011; Geppert et al., 2013; Luther et al., 2013; Bulcke et al., 2014; Petters et al., 2014; Petters et al., 2016). This coating improves colloidal stability in physiological media (Bulcke et al., 2014; Joshi et al., 2016) and allows the fluorescent labelling of the NPs for later microscopic observation (Rastedt et al., 2017; Willmann and Dringen, 2018). Therefore, the antioxidant potential of this new functionalized DMSA-CeONPs was determined and compared to Un-CeONPs and ionic cerium in Ce^{3+} and Ce^{4+} oxidation states. Moreover, DMSA-CeONPs were tested extracellularly and once internalized by astrocytes or C6 glioma cells.

The neuroprotective effect of CeONPs has attracted a large body of research, with enormous basic science and clinical efforts devoted to find treatments that are effective in neuronal cultures or disease models. Despite the accumulated evidence of the involvement of glial cells in neurodegeneration (Pöyhönen et al., 2019; Huang et al., 2022), there are few studies approaching the effect of CeONPs on astrocytes or similar cellular models (Varlamova et al., 2023). Therefore, in order to explore the possibilities of DMSA-CeONPs as neuroprotective tools and to substantially extend the knowledge on their effect on glial cells, the antioxidant potential of DMSA-CeONPs on C6 glioma cells insulted with H_2O_2 and in astrocytes after addition of the electron cycler β-lapachone was investigated in detail. Hydrogen peroxide is the simplest peroxide and often used as a model to investigate mechanisms that are involved in antioxidative defense (Hohnholt et al., 2015) and WST1 formazan formation

with β-lapachone as electron cycler has been recently proposed as a suitable experimental paradigm to study the consequences of oxidative stress caused by superoxide (Steinmeier et al., 2020; Watermann and Dringen, 2023). The present data show that DMSA-CeONPs possessed some but limited extracellular antioxidant capacity, especially in the presence of superoxide. However, the scavenging of superoxide did not mimic SOD activity but a chemical stoichiometric reaction. In addition, loading glial cells with DMSA-CeONPs did not prevent later H_2O_2 or superoxide-induced oxidative stress *in vitro* in cultured glial cells.

Materials and Methods

Materials

Cerium oxide nano-powder (<25 nm by Brunauer-Emmet-Teller analysis), cerium (III) chloride heptahydrate, cerium (IV) sulfate tetrahydrate, 2, 3-dimercaptosuccinic acid (DMSA), hydrogen peroxide 35% (95299), sodium chloride and 2-mino-2 (hydroxymethyl)-1,3-propanediol (Trizma base), dicoumarol (M1390), iodoacetate (16375), 2′-7-dichlorofluorescin diacetate (DCFH$_2$-DA) and Xylenol orange were purchased from Sigma-Aldrich (Steinheim, Germany). Cerium (IV) sulfate tetrahydrate were acquired from Merck (Darmstadt, Germany). Dulbecco′s modified Eagle′s medium (DMEM, containing 25 mM glucose) was from Gibco (Karlsruhe, Germany). Fetal calf serum (FCS), trypsin solution and penicillin/streptomycin solution were obtained from Biochrom (Berlin, Germany). Bovine serum albumin (BSA) and nicotinamide adenine dinucleotide (NADH) were purchased from Applichem (Darmstadt, Germany). WST1 (W201) was from Dojindo (Munich, Germany). β-lapachone (ab 141097) was obtained from Abcam (Berlin, Germany). The native enzymes CAT and SOD were purchased from Roche Diagnostics (Mannheim, Germany). Sterile 24-well cell culture plates and 96-well microtiter plates were purchased from Sarstedt (Nümbrecht, Germany) and black 96-well plates were purchased from VWR (Darmstadt, Germany).

Dispersion and coating of CeONPs

A 100 mM dispersion of colloidal uncoated CeONPs (Un-CeONPs) was prepared as stock solution by stirring the nano-powder in pure water for 15 min and ultrasonicated on ice two times in 5 minutes intervals at 50 W with a Branson B-12 sonifier (Danbury, Connecticut, USA). In parallel, a 5 mM DMSA aqueous solution was prepared at 65°C in a covered beaker under stirring for 15 min and left to cool down until reaching room temperature (RT). Afterwards, for the preparation of 20 mM DMSA-CeONPs, 5 mL of the 5 mM DMSA solution

was added to 10 mL of a 29 mM dilution in H_2O of the stock CeONPs dispersion. After 15 min of additional stirring at RT the dispersion was collected and centrifuged for 10 min at 1,500g and the supernatant was discarded. Subsequently two cycles of washing were completed by washing with 15 mL distilled H_2O the pellet containing the DMSA-CeONPs and discarding the washing solution after 10 min centrifugation at 1,500g respectively. The resulting CeONPs pellet was finally dispersed in 15 mL distilled H_2O and sonicated twice with the same settings mentioned before. The DMSA-CeONPs dispersion was stored at 4°C and sonicated for 5 min with the above described settings prior to any further use.

Characterization of CeONPs

The hydrodynamic diameter (D_H), the polydispersity index (Pi) and the ζ-potential of 1 mM commercial CeONPs in different media were determined by DLS and electrophoretic (ELS) light scattering techniques in a Beckman Coulter (Krefeld, Germany) Delsa Nano C Particle Analyzer at 25 °C, as previously described (Bulcke et al., 2014).

Preparation of $CeCl_3$ and $Ce(SO4)_2$ solutions

Two different salts of cerium were also used to test whether the ROS scavenging capacity of cerium was enhanced when presented as NP. A 20 mM stock solution of cerium (III) chloride heptahydrate and cerium (IV) sulfate tetrahydrate were prepared in pure water respectively and stored at 4°C until used. Afterwards, they were diluted in culture medium to obtained the desired concentrations.

C6 glioma cell cultures

The C6 cell line was cultured as previously described (Joshi et al., 2016). Briefly, C6 glioma cells (passage numbers between 3 and 14) were cultured in 175 cm² flasks in cell culture medium (DMEM+10% FCS; 90% DMEM, 10% fetal calf serum (FCS), 1 mM pyruvate, 18 U mL^{-1} penicillin G, 18 μg mL^{-1} streptomycin sulfate) and preserved at 37°C in an humified atmosphere enriched with 10% CO_2 inside a Sanyo incubator (Osaka, Japan). The cultures used in the presented experiments were obtained from 80% of confluent cultures. In short, the cultures were washed twice with 10 mL of pre-warmed (37°C) sterile phosphate-buffered saline (PBS; 10 mM potassium phosphate buffer, 150 mM NaCl; pH 7.4) and treated with 10 mL 0.05% (w/v) trypsin in pre-warmed (37°C) PBS for 5 min at 37°C. The activity of trypsin was terminated by the addition of 10 mL cultured medium. The resulting 20 mL cell suspension was centrifuged for 5 min at 400g. Subsequently, the supernatant was discarded and the cell pellet resuspended in 10 mL DMEM +10% FCS. The cell density was

then determined by nigrosine staining (0.25%, w/v) using a Neubauer-counting chamber as described earlier (Hohnholt et al., 2011) stated otherwise, cells were seeded in 1 mL DMEM + 10% FCS at a seeding density of $1x10^5$ viable cells well^{-1}, into wells of 24-well plates and used for experimental incubations 24 h after seeding.

Astrocyte-rich primary cultures

The preparation of the cultures was performed in accordance with the legal regulations dictated by the University of Bremen and of the State of Bremen (Germany). Astrocyte-rich primary cultures (APCs) were successfully obtained from the whole brain of newborn Wistar rats within the first 24 h after birth and being naturally fed. The cultures were prepared as initially described by Hamprecht and Löffler (1985) and later slightly modified (Tulpule et al., 2014). Briefly, the full brains were extracted after decapitation and mechanically dissociated, consecutively, through two nylon meshes of 210 and 132 μm pore diameter respectively to eliminate blood vessels and singularize cells. For seeding, 1 mL culture medium containing approximately 300,000 viable cells was transferred into wells of 24-well cell culture plates. The cell culture medium was renewed every 7th day. The age of the cultures used for the experiment described in this manuscript was between 15 and 30 days.

Extracellular removal of H_2O_2

To investigate the removal of extracellular H_2O_2 by DMSA-CeONPs and Un-CeONPs, UV-Vis absorption spectra of the NPs dispersions in the presence or absence of 10 mM H_2O_2 were recorded. Different concentrations of DMSA-CeONPs and Un-CeONPs were dispersed in the media indicated in the legend of the figures and the absorbance was monitored in a wavelength range from 220 to 500 nm. Variations in the absorbance were also recorded at 240 nm over time, for up to 90 min. All these measurements were performed at RT in a Varian Cary 50 UV-Vis spectrophotometer (Melbourne, Australia).

Determination of extracellular H_2O_2 contents by Xylenol orange assay

The extracellular concentration of H_2O_2 was measured by an adaptation of a colorimetric assay, previously established by Dringen et al. (1998). Briefly, samples were centrifuged at 12,300g for 75 s to precipitate and therefore, stop the reaction between CeONPs and H_2O_2. Samples containing cerium salts, although the reaction could not be stopped by centrifugation, were also spun for reproducibility. Afterwards, 10 μL of media samples were added to wells of a 96-well microtiter plate containing 180 μL of the reaction mixture (100

mM sorbitol, 25 mM H_2SO_4, 250 µM $(NH4)_2Fe(SO_4)_2$, 100 µM Xylenol orange in pure water) and 170 µL H_2SO_4 (25 mM) and allowed to react for 45 min at RT. This reaction mixture contains Fe^{2+} which is oxidised to Fe^{3+} by the remaining H_2O_2 present in solution. The generated Fe^{3+} ions then form a complex with the dye Xylenol orange, which absorbance was measured at 540 nm, indirectly informing on the amount of H_2O_2 present. To quantify the corresponding H_2O_2 concentration, eight standards ranging from 0-200 µM were simultaneously prepared and measured in duplicate. The concentration of H_2O_2 in the samples was calculated from the linear regression of the absorbance obtained for the standards.

The rate of H_2O_2 removal (nmol min^{-1}) was calculated by subtracting the content of H_2O_2 (nmol) present in the media after 24 h incubation with the different cerium compounds to the initial amount present (nmol) and dividing it by the time lapse (min). Besides that, the half-times of the peroxide for incubations with 200 µM Un-CeONPs and DMSA-CeONPs were calculated assuming that the reaction followed a first order kinetic, and therefore defined as half-time (h)= Ln (2)/k. The reaction constants (k) were obtained from the graphical representation of the semi-logarithmic representation of clearance of H_2O_2 by Sigmaplot 11.0.

Extracellular scavenging of superoxide

For the study of the extracellular scavenging of superoxide by the different cerium compounds, confluent astrocyte cultures were incubated as previously described in Watermann and Dringen (2023). Briefly, cultures were washed twice with 1 mL pre-warmed (37°C) incubation buffer (IB; 20 mM HEPES, 145 mM NaCl, 5.4 mM KCl, 1.8 mM $CaCl_2$, 1 mM $MgCl_2$, pH 7.4) and incubated up to 1 h at 37°C with 400 µL IB that contained 400 µM WST1 and the indicated concentration of the electron cycler β-lapachone in the presence or absence of DMSA-CeONPs, $CeCl_3$ or $Ce(SO_4)_2$, dicoumarol (30 µM) and/or the native enzymes 260 U CAT or 25 U SOD, as indicated in the respective figure legends. Media samples were collected at the specified timepoints for the determination of the extracellular contents of WST1 formazan and the activity of extracellular LDH.

Pre-incubation of C6 glioma cells or astrocyte-rich cultures with DMSA-CeONPs

To load the cells with DMSA-CeONPs, twenty-four hours after the seeding in the case of C6 glioma cells or at least 15 days old confluent astrocytes in 24-well cell culture plates were washed twice with 1 mL pre-warmed (37°C) DMEM + 10% FCS. Subsequently, the cells were incubated for the time periods stated in the legends of the figures at 37°C in the humified

atmosphere of an incubator, with 10% CO_2 supply, with the adequate volume of DMEM + 10% FCS, containing DMSA-CeONPs at the concentrations given in the legends of the figures. To end the incubations, the cells were washed twice with 1 mL ice-cold (4°C) phosphate buffer saline (PBS). Media samples were collected for the determination of the extracellular LDH activity.

H_2O_2 insult on C6 glioma cells

To establish the optimal experimental conditions to cause a loss of ∼50% of viability in C6 glioma cells, $2x10^5$ C6 glioma cells/well were seeded in 24-well plates and twenty-four hours after the cells were washed twice with 1 mL pre-warmed IB containing 0.5 mg ml^{-1} BSA (IB-BSA) and incubated with 200 µL IB-BSA containing different concentrations of H_2O_2 as indicated in the figures for up to 4 h. When the incubation ended, cells were washed twice with ice-cold PBS and then harvested for the determination of intracellular LDH activity or prepared for propidium iodide (PI) staining.

To investigate a potential neuroprotection by DMSA-CeONPs, C6 glioma cells were challenged with H_2O_2, immediately after the end of the pre-incubation with the NPs. In this case, C6 glioma cells loaded with DMSA-CeONPs for up to 24 h in 24-well plates, were washed twice with pre-warmed IB-BSA and incubated with 200 µL of IB-BSA containing 100 µM H_2O_2 for 3 h. After the incubation period, media samples were collected to determine the concentration of H_2O_2 still present. Then, the cells were washed twice with ice-cold PBS and harvested to determine the intracellular LDH activity. Cells for the determination of the protein content were stored directly in the 24-well plates at -20°C until its assessment.

Viability assays and determination of protein content

Cell vitality was assessed by quantification of the correspondent LDH activity and by visualizing the cell membrane integrity by PI staining as described previously (Bulcke et al., 2014; Tulpule et al., 2014; Joshi et al., 2016).

LDH activity determination

For the intracellular determination of LDH activity, the cells were washed twice with pre-warmed IB-BSA after the indicated incubation. After completely aspirate the washing, the cells were lysed with 1% (v/v) Triton X-100 in 200 µL IB-BSA for 30 min at 37°C. When the lysis was completed, 10 µL of the lysate was harvested and diluted with 170 µL LDH buffer (80 mM Tris, 200 mM NaCl, pH 7.2) in a well of a 96-well microtiter plate.

If the extracellular LDH activity was to be determined, 20 µL of the collected media after incubation of the cells was added to 160 µL LDH buffer in a well of a 96-well microtiter plate. The photometric determination of the LDH activity was performed at 340 nm as previously described (Dringen et al., 1998; Tulpule et al., 2014).

Prior to the determination of the extracellular LDH activity, if the samples contained H_2O_2, it was removed from the incubation medium by addition of 2 µL IB-BSA containing 50 U CAT.

Propidium iodide staining (PI)

The integrity of the cellular membrane was used as an indicator of cell viability and was determined by staining the cells with the membrane impermeable fluorescent dye PI as described previously by Tulpule et al. (2014). In addition, the membrane permeable dye Hoechst H33342 was applied to visualize all cell nuclei present. Images of the stained cells were captured using a fluorescence microscope (Eclipse TE-2000-U with a DS-QiMc camera and imaging software NIS-Elements BR, Nikon, Düsseldorf, Germany). For monitoring the different fluorescence signals the following filter settings were used: PI (λ_{ex}: 510-560 nm; λ_{em}: 590 nm; dichromatic mirror: 505 nm) and H33342 (λ_{ex}: 330-380 nm; λ_{em}: 435-485 nm; dichromatic mirror: 400 nm).

Protein determination

For the determination of protein contents, cells in 24-well dishes were lysed in 400 µL 0.05 M NaOH for 60 min at RT in a humidified atmosphere. The protein content of the cultures was determined based on the Lowry method (Lowry et al., 1951), using BSA as standard protein.

Determination of ROS production

Cellular ROS production was quantified by adding of non-fluorescent dihydrochlorofluorescein-diacetate (DCFH2-DA) to cultured astrocytes as previously reported (Steinmeier et al., 2020). In principle, when cells internalize DCFH2-DA, it undergoes enzymatic deacetylation and is converted to DCFH2, which in turn, can be oxidized to the fluorescent dichlorofluorescein (DCF) by the presence of ROS in the cytosol. In this experimental setup, cultured astrocytes were washed twice with 1 mL of pre-warmed DMEM+10% FCS and pre-incubated with 1 mL DMEM+10% FCS in the presence or absence of 700 µM DMSA-CeONPs for 4 h. Subsequently, the cells were washed twice with pre-warmed IB and incubated with 200 µL IB containing 50 µM DCFH2-DA at 37°C for 30

min. At the end of the incubation with the non-fluorescent dye, the cells were again washed twice with 1 mL IB to eliminate the rests of the non-internalized substance, and were incubated in 200 μL IB in the presence or absence of 20 μM β-lapachone, 1 mM H_2O_2 and/or 30 μM NQO1 inhibitor dicoumarol, as indicated in the correspondent legend of the figure. Finally, the cells were washed and lysed in 400 μL ice-cold (4°C) hypotonic potassium phosphate buffer (20 mM, pH 7.4) on ice for 10 min in the dark. The lysates were harvested and centrifuged for 1 min at 12.300g. 200 μL of lysate supernatant were collected and quantified in a fluorescence plate and used to determine DCF fluorescence (λ_{ex}: 485 nm; λ_{em}: 520 nm) present in the samples (Fluoroskan Ascent FL, Thermo Fischer Scientific, Schwerte, Germany).

Presentation of data

All data are presented as means ± standard deviation of values obtained in experiments on three independently prepared cultures, if not stated otherwise. Statistical analysis of multiple sets of data was carried out by ANOVA followed by the Bonferroni *post-hoc* test, using the software SigmaPlot (version 11.0). Significant differences compared to the control were indicated in the figures by asterisks while significant differences compared to other conditions were indicated in the figures by hash marks. The number of asterisks specifies the level of significance with *p<0.05, **p<0.01 and ***p<0.001. Analogously, the number of hash marks specifies the level of significance with #p<0.05, ##p<0.01 and ###p<0.001. Values of p> 0.05 were considered as not significant.

Results

Characterization of DMSA-CeONPs

Dispersions of DMSA-CeONPs in water or IB were characterized by DLS (Table 1). DMSA-CeONPs dispersed in water possessed a hydrodynamic diameter of 171 nm, a narrow size distribution as indicated by a polydispersity index (Pi) of 0.13 and a ζ-potential of -27.4 mV. When DMSA-CeONPs were dispersed in IB containing 0.5 mg L^{-1} BSA, the hydrodynamic diameter increased to up to 234 nm, while the size distribution in the dispersion remained homogeneous (Pi= 0.22) and the ζ-potential turned less negative (-13 mV).

Table 1. Characterization of DMSA-CeONPs.

	Hydrodynamic diameter (nm)	Pi	ζ-potential (mV)
H₂O	171 ± 6	0.13 ± 0.02	-27.4 ± 2.1
IB-BSA	234 ± 8	0.22± 0.03	-13.2± 0.9

DMSA-CeONPs were synthesized and the hydrodynamic diameter, Pi and ζ-potential of 1 mM dispersions in pure water or in IB-BSA were determined. The data represent means ± SD of values obtained on NPs from three independent syntheses.

Test for H_2O_2 removal by DMSA-CeONPs in the absence of cells

Literature data demonstrated catalase mimic activity of CeONPs using a spectrophotometric method and measuring the variation in absorbance at 240 (nm), when CeONPs and H_2O_2 were present (Pirmohamed et al., 2010). The decrease in absorbance was interpreted as decomposition of H_2O_2 by CeONPs. Therefore, to test whether DMSA-CeONPs decomposed H_2O_2, a similar spectrophotometric approach was applied. The spectra of 10, 50, 100 and 150 µM DMSA-CeONPs suspended in IB or IB-BSA were recorded (Fig. 1a,b). In addition, the spectra of 10 mM H_2O_2 (Fig. 1a,b), IB and IB-BSA (Fig. 1c) were also obtained.

DMSA-CeONPs suspended in IB and IB-BSA respectively showed a concentration-dependent absorption at 240 nm, being higher for all the concentrations tested when the NPs were suspended in IB-BSA (Fig. 1a,b). For Un-CeONPs, similar spectra were obtained (data not shown). DMSA-CeONPs suspended in IB (Fig. 1a) additionally presented a peak in absorption at 320 nm, which also displayed a concentration-dependency. In the case of DMSA-CeONPs in IB-BSA (Fig. 1b), a maximum in absorbance at 280 nm preceded and overlapped the peak recorded at 320 nm. At both wavelengths the absorption increased with increasing concentration. The presence of BSA explained the maximum at 280 nm, as it can be clearly observed in Fig. 1c. The presence of BSA was mandatory for further experiments on cells as DMSA-CeONPs agglomerate over time, when suspended only in IB (see Chapter 2.1). Therefore, the initial absorption value under these conditions was the result of ∼ 1 a.u. for 150 µM DMSA-CeONPs in IB-BSA plus the absorption of 10 mM H_2O_2 (∼0.5 a.u). Absorption spectrophotometry works rather precisely with values up to 2 a. u. (Mäntele and Deniz, 2017). Therefore, high absorption shown under these experimental conditions prevented the use of higher concentrations of DMSA-CeONPs, hindering the investigation of the removal of H_2O_2 by DMSA-CeONPs.
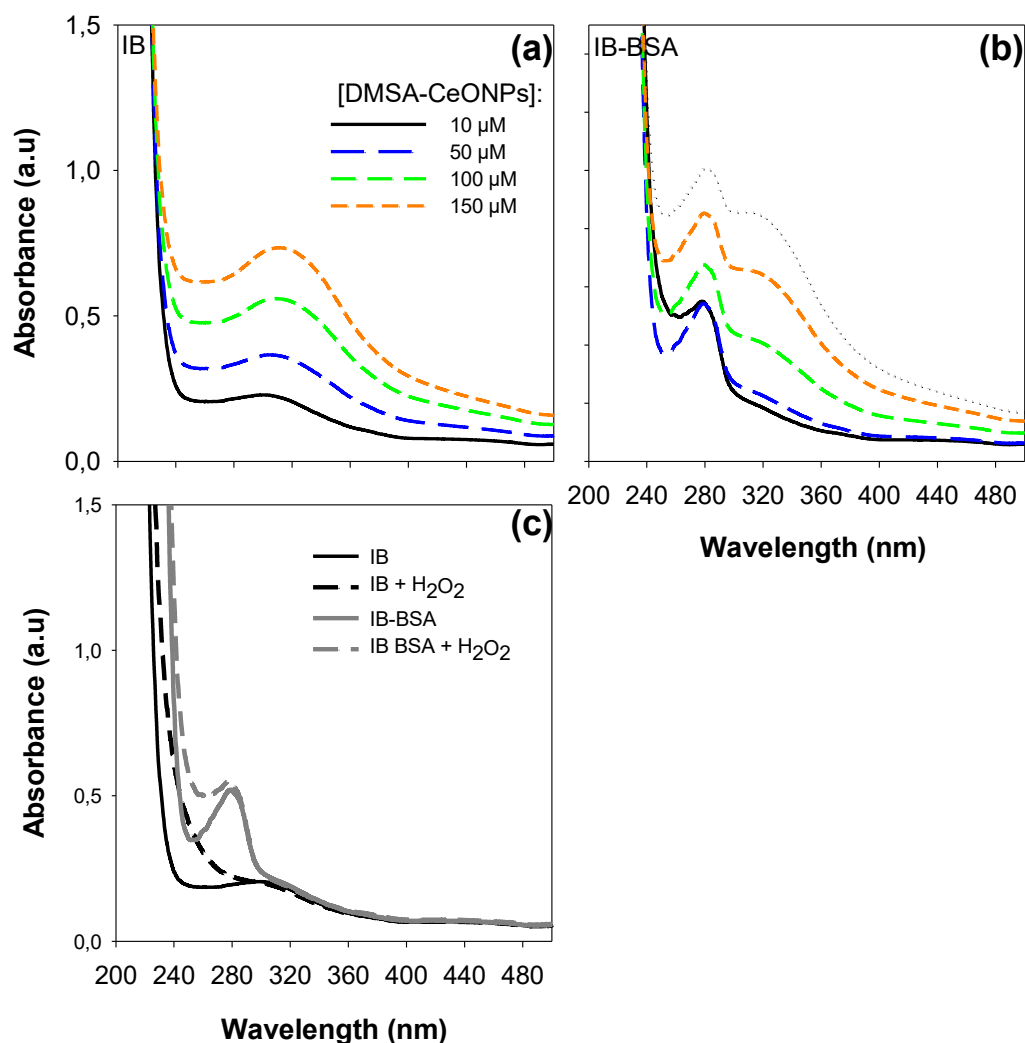
Figure 1. Absorption spectra for the study of H₂O₂ removal by DMSA-CeONPs. DMSA-CeONPs were dispersed at concentrations of 10, 50, 100 or 150 μM in IB **(a)** or IB-BSA **(b)** and the absorption spectra were recorded. The spectra of 10 mM H₂O₂ diluted in IB **(a)** and IB-BSA **(b)** were also determined**.** To complete the study and as a control the absorption spectra of IB and IB-BSA alone **(c)** were measured. All determinations were performed at RT.

To overcome these limitations, Un-CeONPs suspended in a 1:5 dilution of IB-BSA in pure water (IB-BSA (1:5)) were used. Un-CeONPs were chosen to further test the removal of H₂O₂ to avoid interference in the determination caused by precipitation and agglomeration of DMSA-CeONPs when dispersed in a diluted IB-BSA. Un-CeONPs dispersed in IB-BSA (1:5) did not precipitate or agglomerate over 90 min (Fig. 2a) and a decrease in absorbance occurred when 10 mM H₂O₂ was added (Fig. 2b).

After this initial test, time-dependent decline of H₂O₂ at more realistic concentrations (100 μM) was tested. The decline in absorbance at 240 nm was determined over 40 min for 100

and 300 µM Un-CeONPs dispersed in IB-BSA (1:5) (Fig. 2c). During the 40 min interval, the absorbance at 240 nm of 10 mM H_2O_2 remained stable (Fig. 2c) in absence of CeONPs. 300 µM Un-CeONPs showed a discretely higher loss in H_2O_2 absorbance within the first 2 min compared to 100 µM Un-CeONPs. Afterwards, both concentrations had a parallel decline in absorbance. The total loss in absorbance after 40 min was 0.05 and 0.06 for 100 and 300 µM Un-CeONPs, respectively (Fig. 2c).
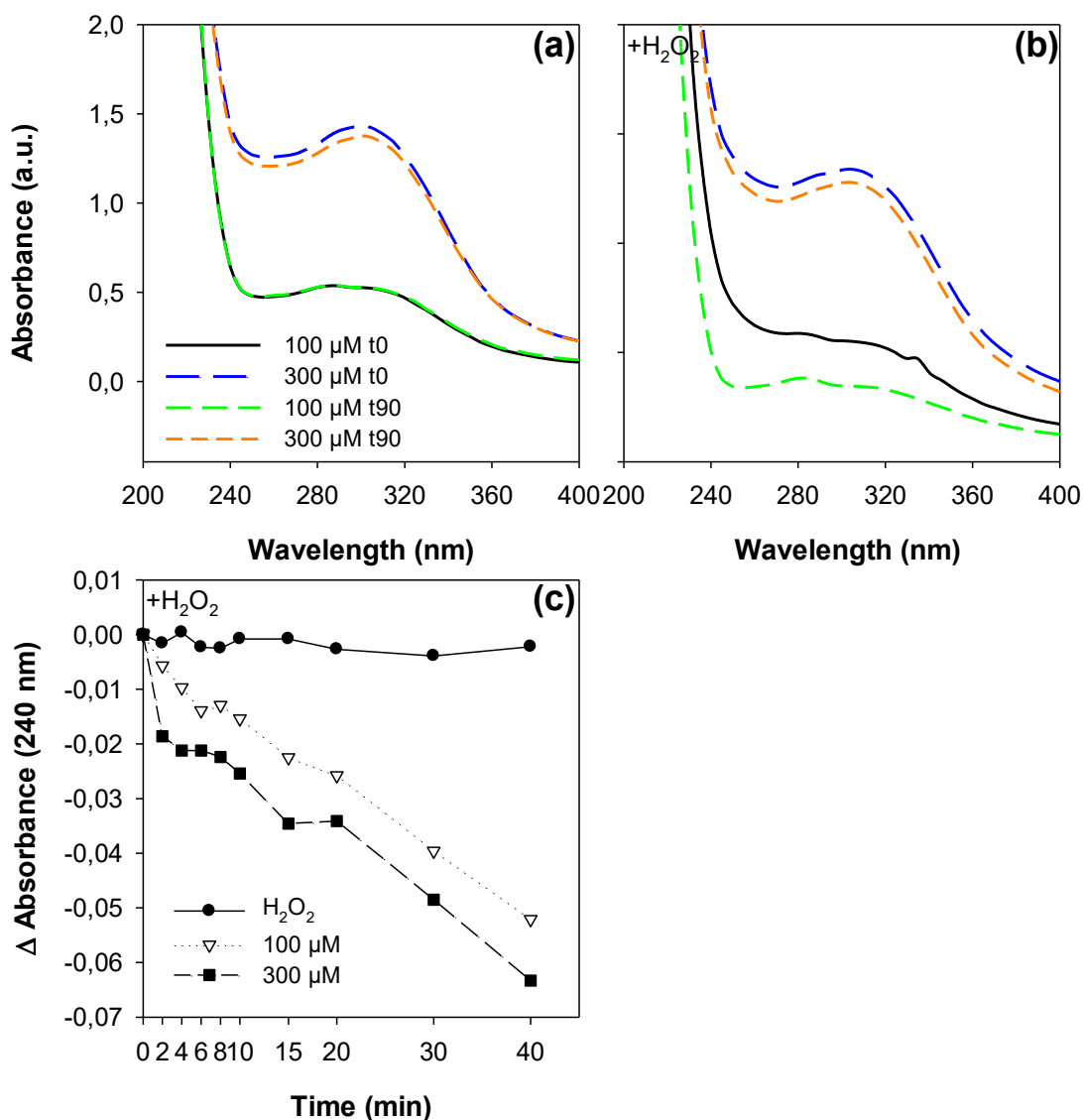
Figure 2. Un-CeONPs removal of H_2O_2 in the absence of cells. 100 and 300 µM Un-CeONPs were suspended in IB-BSA, diluted 1:5 in pure water. Absorbance spectra were obtained at the start (t0) and after 90 min (t90) in absence of 10 mM H_2O_2 **(a)** and in the presence of 10 mM H_2O_2 **(b)**. 100 µM and 300 µM Un-CeONPs were diluted in IB-BSA (1:5) in the presence of 100 µM H_2O_2 and the variation in absorbance at 240 nm was studied over time **(c)**.

As an alternative to investigate the potential ability of DMSA-CeONPs to remove H_2O_2, the formation of the complex Fe^{3+}-Xylenol orange (540 nm) was monitored and interpreted as an indicator of the residual amount H_2O_2 present (Fig. 3). 0, 10, 50, 100 and 200 µM Un-CeONPs, DMSA-CeONPs, $CeCl_3$ or $Ce(SO_4)_2$ were added to IB-BSA containing 100 µM H_2O_2. The samples were incubated for 0, 1, 3, 5 and 24 h. At 540 nm the absorption for IB-BSA alone was on average 0.316± 0.024 a. u. (n=3) and for 100 µM H_2O_2 diluted in IB-BSA 0.940 ± 0.018 a. u. (n=3) (data not shown). DMSA-CeONPs at all concentrations tested stayed stable in dispersion over the time tested (data not shown).
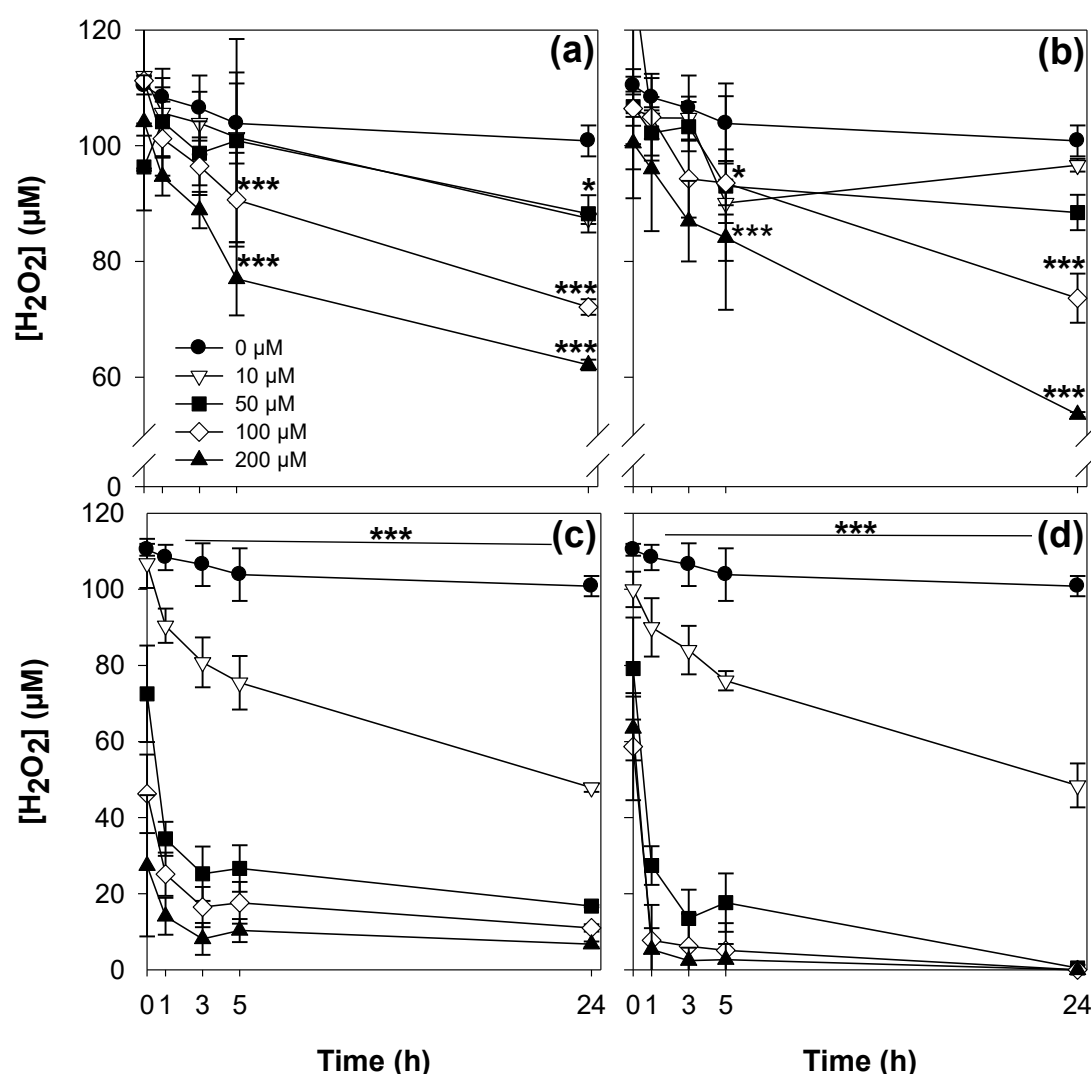
Figure 3. Time-dependent removal of H_2O_2 by CeONPs and ionic cerium in the absence of cells. The presence of H_2O_2 was monitored after 0, 1, 3, 5 and 24 h in the absence (0 µM) or the presence of 10, 50, 100 and 200 µM of **(a)** Un-CeONPs **(b)** DMSA-CeONPs, **(c)** $CeCl_3$ or **(d)** $Ce(SO_4)_2$ in IB-BSA by the Xylenol orange assay. Average values and ± SD of data from three independent experiments are shown (n=3). The significance of differences compared to the values obtained for the control condition (treatment without cerium) was analysed by Two-Way ANOVA followed by Tukey Multiple Comparison Test and is indicated by asterisks (*p< 0.05, ***p < 0.001). Note that the y-scale changes between experiments.

In the absence of cerium, the concentration of H_2O_2 remained stable over time. Increasing concentration of Un-CeONPs or DMSA-CeONPs led to a significant decrease in the detectable concentration of H_2O_2 (Fig. 3a,b). Both types of CeONPs showed a slow scavenging, needing up to 5 h to significantly decrease the concentration of H_2O_2. No difference in the H_2O_2 removal was found between Un-CeONPs and DMSA-CeONPs. In contrast, dissolved $CeCl_3$ and $Ce(SO_4)_2$ reacted instantly with H_2O_2 and already after 3 h incubation with 50 µM of either cerium ions, the concentration of H_2O_2 was reduced by 80% (Fig. 3c,d). As shown in Fig. 3c and d for t=0 h, the reaction between H_2O_2 and the salts of cerium was so fast that within the minute it took to mix the cerium salts with the H_2O_2 in an Eppendorf cup and to combine this sample with the reaction mixture in a 96 well plate, a significant and concentration-dependent clearance had occurred. To investigate this rapid reaction in more detail, an assay was performed where the addition of cerium, H_2O_2 and the reaction mix occurred directly in wells of a 96-well plate. The Un-CeONPs and DMSA-CeONPs did not show any significant difference to the standard procedure. However, for $CeCl_3$ and $Ce(SO_4)_2$ a significant decrease in absorbance occurred when they were previously mixed in an Eppendorf cup (data not shown).

A period of 24 h was not sufficient for Un-CeONPs or DMSA-CeONPs to clear all the H_2O_2 present under the experimental conditions applied. However, the decrease in H_2O_2 increased linearly with increasing concentration and time when Un-CeONPs (Fig. 3a) or DMSA-CeONPs (Fig. 3b) were present, suggesting that the reaction could continue over a prolonged time, potentially until exhausting the H_2O_2 pool. In contrast, 50 µM $Ce(SO_4)_2$ was sufficient to consume rapidly all the H_2O_2 present in the medium (Fig. 3d).

The removal rate for H_2O_2 (nmol min^{-1}) was calculated for the first hour. The rates calculated for cerium salts were approximately 10-times higher than those observed for CeONPs under these experimental conditions (Table 2). Since the removal of H_2O_2 followed a first order kinetics (data not shown), half-times for 200 µM Un-CeONPs and DMSA-CeONPs could also be calculated. Un-CeONPs needed 11 h and DMSA-CeONPs 12 h to clear half of the initial concentration of H_2O_2.

Table 2. Removal rate of H_2O_2 by different cerium compounds.

	H_2O_2 removal rate (nmol min^{-1})	
	100 μM	**200 μM**
Un-CeONPs	0.119 ± 0.062	0.228 ± 0.029
DMSA-CeONPs	0.057 ± 0.069	0.207 ± 0.063
CeCl$_3$	1.677 ± 0.003	1.718 ± 0.002
Ce(SO$_4$)$_2$	1.388 ± 0.009	1.720 ± 0.004

Rate of change in H_2O_2 levels after incubation with different cerium compounds for the first hour. The initial concentration of H_2O_2 was 100 μM for all the cases. The rates are given as nmol min^{-1}. Average values ± SD from three independent experiments are shown (n=3).

Test for superoxide scavenging by DMSA-CeONPs in cultured astrocytes

The electron cycler β–lapachone induces oxidative stress mediated by NQO1 in cultured astrocytes (Steinmeier et al., 2020). Inside the cell, NQO1 reduces β-lapachone into β-lapachol by transferring two electrons (Ross and Siegel, 2021). β-lapachol is highly unstable under physiological conditions and rapidly auto-oxidise first to β-lapachone-semiquinone and then back to β-lapachone, producing two molecules of superoxide as by-products (Zhang et al., 2018). WST1 is added in the assay as it is a membrane impermeable compound that can be reduced in cell cultures by membrane permeable electron cyclers, e.g. β-lapachone, to form a yellow water-soluble formazan product (WST1 formazan) (Stapelfeldt et al., 2017) and can be used as an indirect indicator of NQO1 activity and therefore, superoxide formation (Watermann and Dringen, 2023). Dicoumarol is an NQO1 inhibitor and it has been observed to prevent ROS formation when cultured astrocytes are co-treated with β–lapachone and dicoumarol (Steinmeier et al., 2020).

Increasing concentrations of DMSA-CeONPs reduced the WST1 formazan formation in cultured astrocytes

Based on this paradigm and to stablish a suitable test to assess the potential SOD-like activity of DMSA-CeONPs, cultured astrocytes were incubated with 1, 2, 3 or 5 μM β-lapachone in the absence (0 μM) or presence of 300, 700 or 1000 μM of DMSA-CeONPs in IB for up to 1 h. This experiment aimed at finding optimal concentrations of the electron cycler, β-lapachone, in combination with DMSA-CeONPs for further investigations.

The reduction of WST1 to WST1 formazan increased with an increasing amount of β-lapachone and showed an inverse correlation with the concentration of DMSA-CeONPs (Fig. 4). For all the conditions tested, a DMSA-CeONPs concentration of 700 μM or higher significantly lowered (p<0.001) the reduction of extracellular WST1. A concentration of 3

µM β-lapachone led to a WST1 formazan formation of 21 ± 1 nmol after 1 h incubation (Fig. 4c). The presence of 700 µM and 1000 µM DMSA-CeONPs significantly reduced this amount by 38±0.2% and 36±0.2% respectively. Previous studies showed that concentrations of β-lapachone of 3 µM or less did not alter vitality or glucose metabolism in astrocytes (Watermann and Dringen, 2023). Therefore, subsequent analysis of superoxide scavenging potential of DMSA-CeONPs was carried out with 3 µM β-lapachone and 700 µM DMSA-CeONPs.
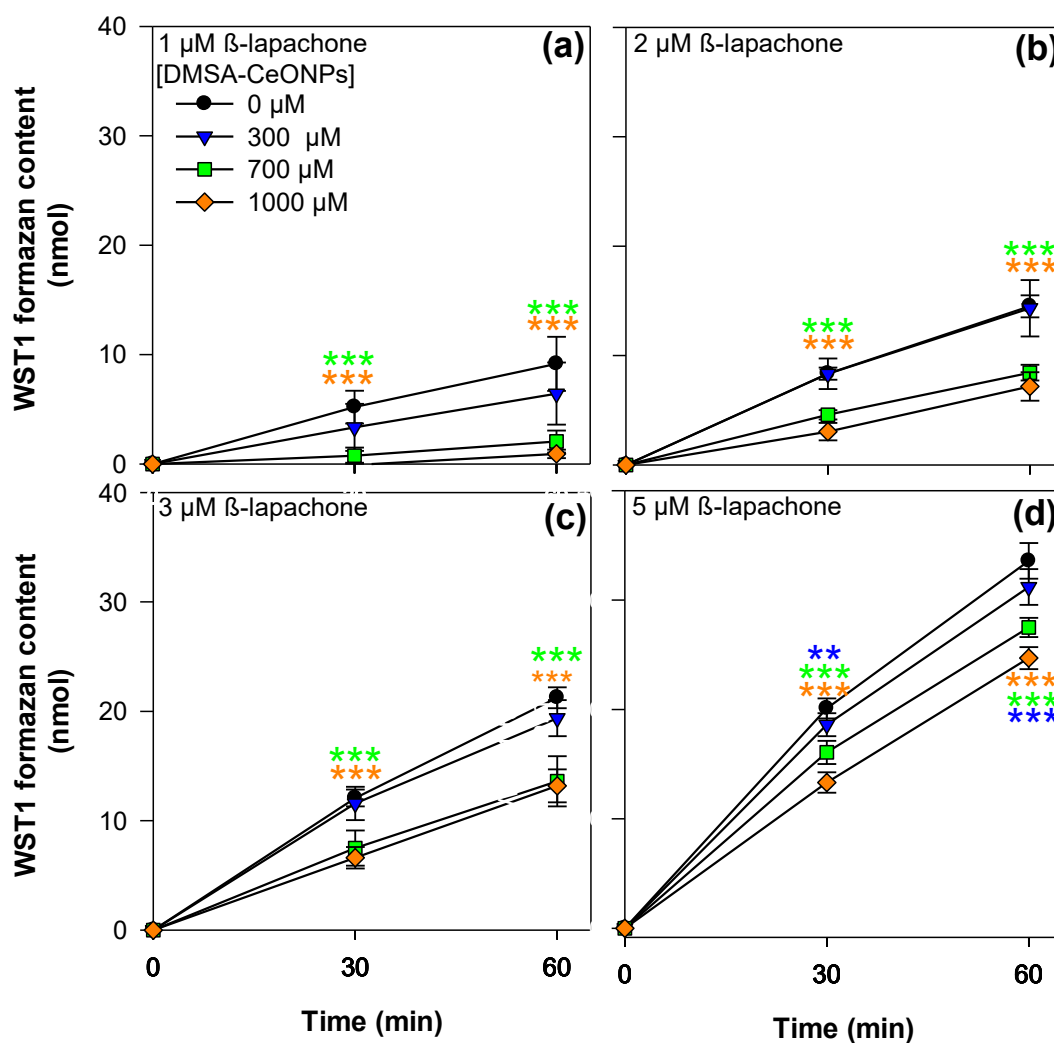
Figure 4. Time and concentration dependent effect of DMSA-CeONPs on the WST1 formazan formation in cultured astrocytes. The cells were incubated up to 60 min without (0 µM) or with the indicated concentration of DMSA-CeONPs in IB containing WST1. β–lapachone was applied as electron cycler in different concentrations: 1 µM **(a)**, 2 µM **(b)**, 3 µM **(c)** and 5 µM **(d)**. The data shown are means ± SD of values obtained in three experiments on independently prepared cultures (n=3). The significance of differences (ANOVA) of data compared to those obtained for incubations in the absence of DMSA-CeONPs (0 µM) is indicated by asterisks in the respective symbol colour ($*p<0.05$), $**p<0.01$, $***p<0.001$).

DMSA-CeONPs scavenged superoxide from the extracellular space

To confirm the potential scavenging of superoxide by DMSA-CeONPs, the detoxifying enzymes catalase and/or SOD were applied as a comparison. Moreover, the NQO1-inhibitor, dicoumarol (Ernster et al., 1960; Hollander and Ernster, 1975) was also included as a control for the involvement of NQO1 in astrocytic WST1 formazan formation. (Fig. 5).
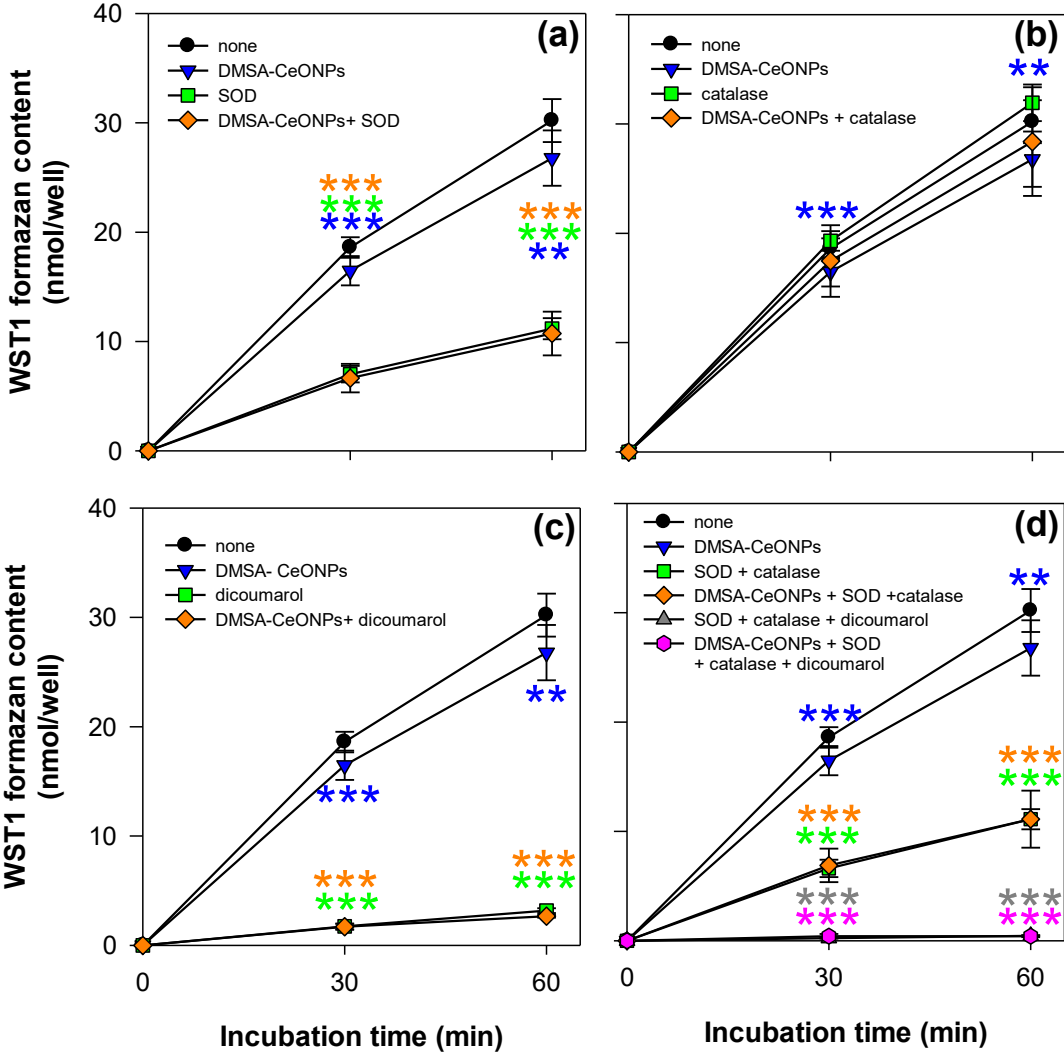
Figure 5. Extracellular superoxide scavenging activity of DMSA-CeONPs. The cells were incubated with 400 μM WST1 and 3 μM β-lapachone in the absence (control) or the presence of 700 μM DMSA-CeONPs, SOD (25 U), catalase (260 U) and/or 30 μM dicoumarol. The data shown are means ± SD of values obtained in three experiments on independently prepared cultures (n=3). Significant differences (ANOVA) of data compared to the data obtained for the control condition are indicated by asterisks depicted in the colours of the respective symbols (**p<0.01, ***p<0.001).

In this experiment, incubation of cultured astrocytes with 3 μM β-lapachone and 700 μM DMSA-CeONPs led to a significant (**p<0.01) 11.4±0.1% decrease in WST1 formazan

formation in comparison to the control (none) after 60 min (Fig. 5a). If exogenous SOD was present during the incubation of cells with β-lapachone, the WST1 formazan after 60 min was reduced by 63±0.2% compared to the control (Fig. 5a) and was identical to the reduction obtained when the treatment containing SOD and DMSA-CeONPs (Fig. 5a). On the contrary, the presence of catalase did not have any effect on the total amount of WST1 formazan determined (Fig. 5b). Dicoumarol, as expected, almost completely inhibited the reduction of WST1, independently of the presence or absence of DMSA-CeONPs (Fig. 5c). The decrease in WST1 formazan formation caused by DMSA-CeONPs, SOD and catalase together (Fig. 5d) resulted in values identical to those obtained with SOD alone (Fig. 5a) or SOD plus catalase (Fig. 5d). Complete prevention of WST1 formazan formation was achieved by application of a combination of dicoumarol, SOD and catalase and DMSA-CeONPs (Fig. 5d).

DMSA-CeONPs did not react as a catalyst

In a further analysis of the data, the delta WST1 formazan content (%) due to the presence of DMSA-CeONPs was calculated. For this, the amount of WST1 formazan produced in the presence of 300, 700 or 1000 μM DMSA-CeONPs was first subtracted from the total amount of WST1 formazan produced by the cells in the absence of DMSA-CeONPs (control) for each condition. To normalize the data of the three independent experiments (n=3), the average delta WST1 formazan for each concentration of DMSA-CeONPs was divided by the respective average WST1 formazan of the control and multiplied by 100. This value was calculated for each concentration of β-lapachone and for each time point measured (30 and 60 min) (Fig. 6).

The reduction in WST1 formazan content increased with increasing concentration of DMSA-CeONPs for all the individual concentrations of β-lapachone. However, an increase in β-lapachone, and therefore, in superoxide, resulted in a decrease in the percentage removed by each concentration of DMSA-CeONPs tested. These data indicate that the maximum scavenging capacity was already reached at a β-lapachone concentration of 1 μM. Statistical analysis confirmed that any increase in β-lapachone resulted in a significant loss of relative superoxide scavenging capacity of DMSA-CeONPs at 700 and 1000 μM concentrations (Fig. 6b).
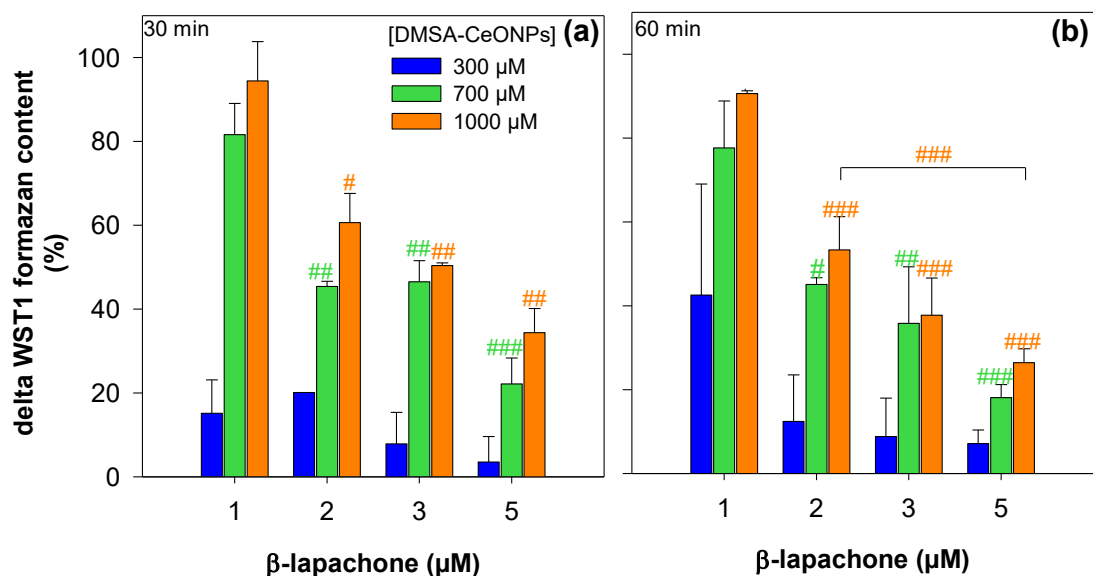
Figure 6. Analysis of the catalytic properties of DMSA-CeONPs. The cells were incubated without (0 µM) or with 300, 700 or 1000 µM DMSA-CeONPs in IB for up to 60 min. β-lapachone was used as electron cycler at different concentrations: from 1 µM to 5 µM to reduce WST1 to WST1 formazan. Samples for the analysis were taken after 30 min **(a)** and 60 min **(b)** respectively. The delta WST1 formazan content (%) was calculated by subtracting the WST1 formazan produced in the presence of DMSA-CeONPs from the WST1 formazan content found in the absence of DMSA-CeONPs (control) and then, divided by the WST1 formazan content of the control and multiplied by 100 to obtain the percentage. Data shown are mean ± SD of values obtained in three experiments on independently prepared cultures (n=3). The significance of the differences (ANOVA) of the data between the different concentrations of β-lapachone is indicated by hashes depicted in the colours of the respective bars ($\#p<0.05$; $\#\#p<0.01$; $\#\#\#p<0.001$). For graphical reasons, the hashes right above the respective bars represent the statistical difference obtained for 1 µM β-lapachone compared to the other conditions.

Ionic cerium effectively reduced the WST1 formazan formation in cultured astrocytes

To investigate whether the superoxide scavenging was limited to the presence of cerium in NPs, cultured astrocytes were incubated with 30, 150 or 300 µM $Ce(SO_4)_2$ or $CeCl_3$ respectively in an identical setup as the one used for DMSA-CeONPs. The β-lapachone dependent WST1 reduction was reduced to 53% by 150 µM Ce^{3+} compared to the control (none) (***$p<0.001$) (Fig. 7). This decrease was 1.5-times higher than the one caused by DMSA-CeONPs (Fig. 7b and 5a, respectively). Of note, the concentration of Ce^{3+} was 4.7 times lower than the calculated cerium concentration of DMSA-CeONPs previously applied (Fig. 5).
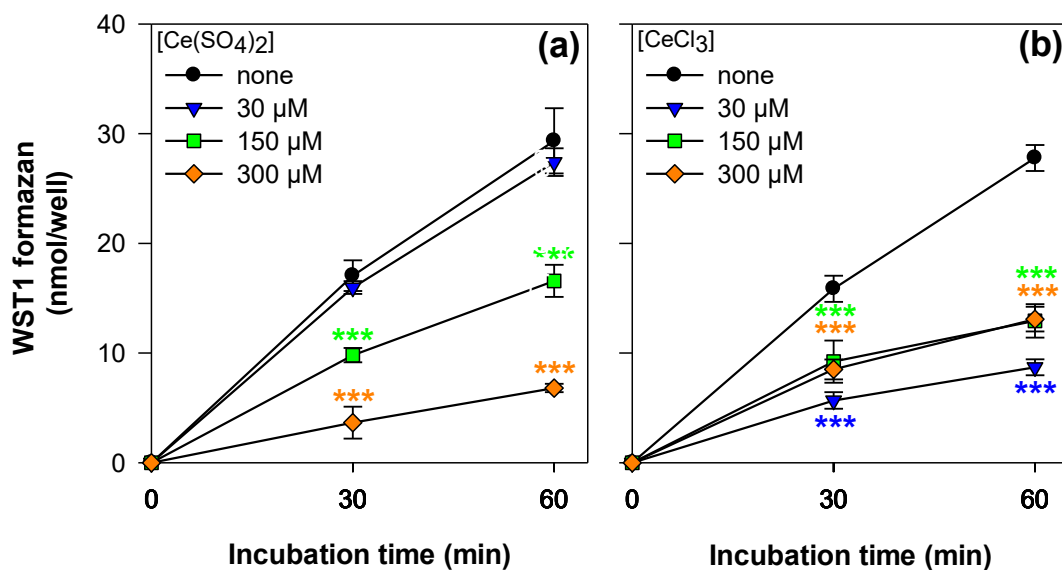
Figure 7. Assay to determine the extracellular superoxide scavenging activity of ionic cerium. Cultured astrocytes were incubated with 400 µM WST1 and 3 µM β-lapachone in the absence (control) or the presence of $Ce(SO_4)_2$ **(a)** or $CeCl_3$ **(b)** for up to 60 min. The data shown are means ± SD of values obtained in three experiments on independently prepared cultures (n=3). Significant differences (ANOVA) of data compared to the data obtained for the control condition are indicated by asterisks depicted in the colours of the respective symbols (***p<0.001).

Assessment of the antioxidant potential of DMSA-CeONPs in glial cells

The potential protection of DMSA-CeONPs and ionic cerium against oxidative stress was also investigated intracellularly. In these experimental setups (see below), glial cells were exposed to these compounds prior to the oxidative insult.

C6 glioma cell viability after oxidative insult with H_2O_2

Prior to investigate the potential antioxidative protection of CeONPs in glial cells, suitable experimental conditions for the oxidative insult needed to be established. For this purpose, the C6 glioma cells were incubated for up to 4 h in the absence or presence of 50, 100, 200 or 500 µM of H_2O_2. The cell viability was monitored by determining the intracellular LDH (Fig. 8) and the microscopical inspection of the PI staining and morphology of the cells (Fig. 9). A significant loss in intracellular LDH occurred in H_2O_2 treated cells, showing a concentration and time dependency. After 2 h incubation the percentage of intracellular LDH activity for C6 glioma cells treated with more than 50 µM was around 75%, whereas after 3 h it was around 50%. Treatments of cells with 200 µM or 500 µM H_2O_2 for more than 3 h did not further increase toxicity (Fig. 8).

161
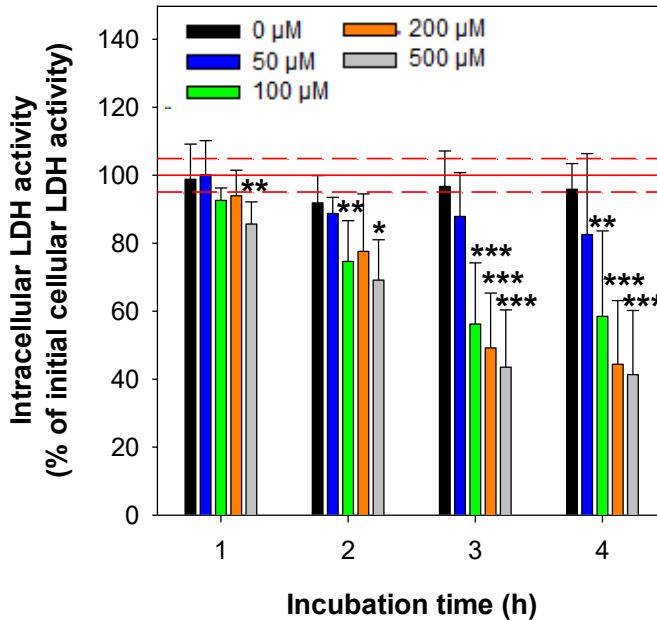
Figure 8. Effect on viability of C6 glioma cells after application of H_2O_2. Cellular LDH activity was determined on C6 glioma cells that had been exposed to H_2O_2 in the indicated concentrations for 1, 2, 3 or 4 h. Average values +/- SD of data obtained in three independent experiments are shown (n=3). Statistical differences were calculated by a One-way ANOVA. *p< 0.05, **p < 0.01, ***p < 0.001 indicate differences compared with the control condition (0 μM).

The PI staining confirmed the results obtained with the LDH measurements. Remarkable changes in cells morphology and a prominent reduction in cell processes were observed after 3 h incubation for concentrations of 100 μM H_2O_2 or greater (Fig. 9). The treatment with 200 μM H_2O_2 seemed to cause a slightly increased number of dead cells in comparison to 100 μM and the changes in morphology were more prominent (Figure 9l,b). The toxic effect of 500 μM H_2O_2 was similar to the damage caused by $AgNO_3$, and thus, most likely not suitable for rescue experiments (Figure 9d,n;e,o).
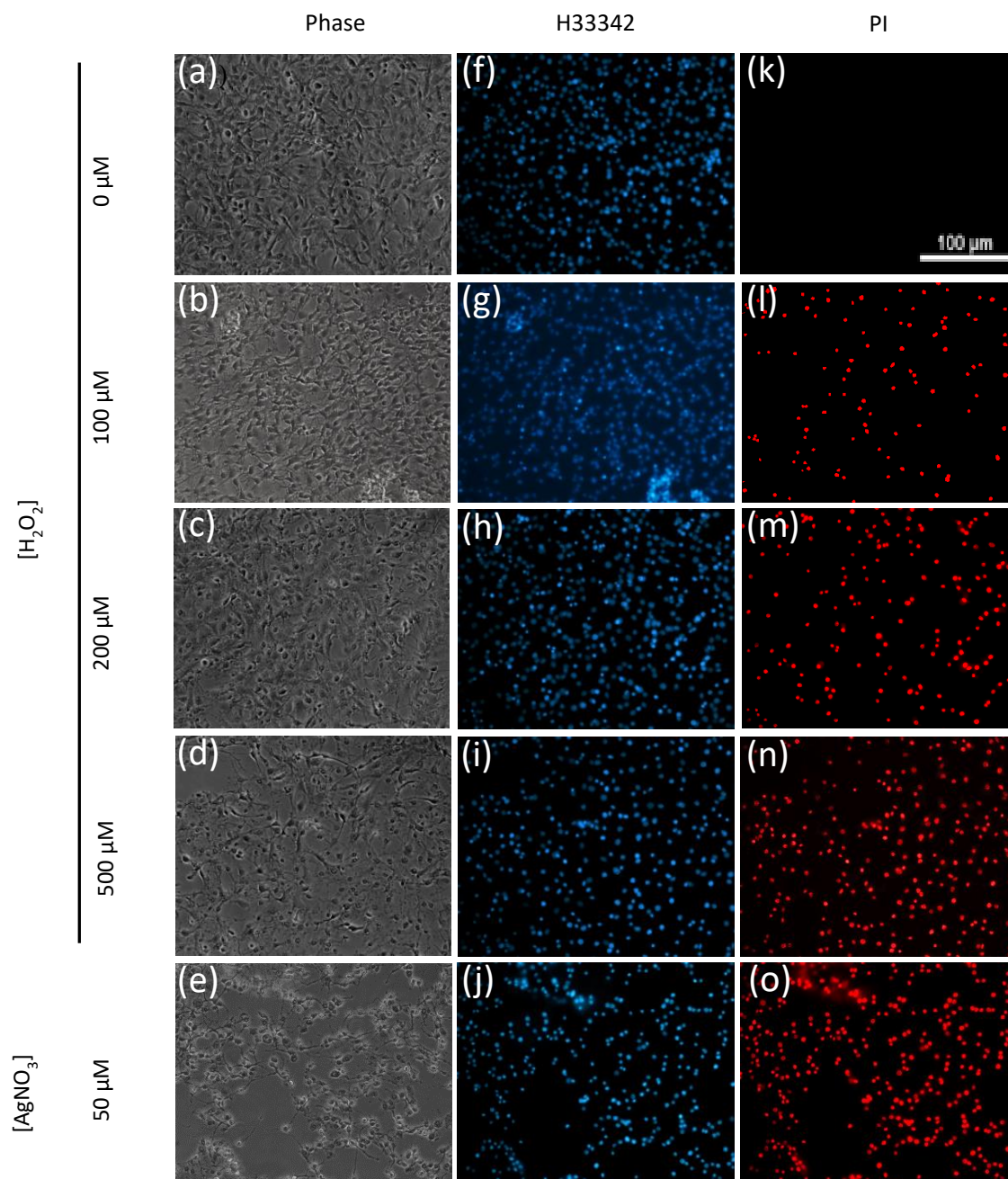
Figure 9. Morphology and membrane integrity of C6 glioma cells exposed to H_2O_2. Cells were incubated with H_2O_2 in the indicated concentrations for 3 h, and the morphology was assessed **(a-d).** Subsequently, the cell nuclei were stained with H33342 to stain all cell nuclei present **(f–i)** and PI to visualize the nuclei of cells with compromised membrane integrity **(k–n)**. As positive control for toxicity, the cells were incubated with 50 µM AgNO$_3$ **(e, j, o)** for 3 h prior to the incubation with H33342 and PI. The data shown are from a representative experiment that was replicate twice on independent prepared cultures with equivalent results. The scale bar in panel **(k)** represents 100 µm and applies to all panels

163

Investigation of H_2O_2 removal by CeONPs pre-treated C6 glioma cells

To assess the potential antioxidative properties of CeONPs against H_2O_2 toxicity, C6 glioma cells were pre-incubated with CeONPs or ionic cerium. The effect of the pre-incubations on the viability of the cells was determined (Fig. 10a).
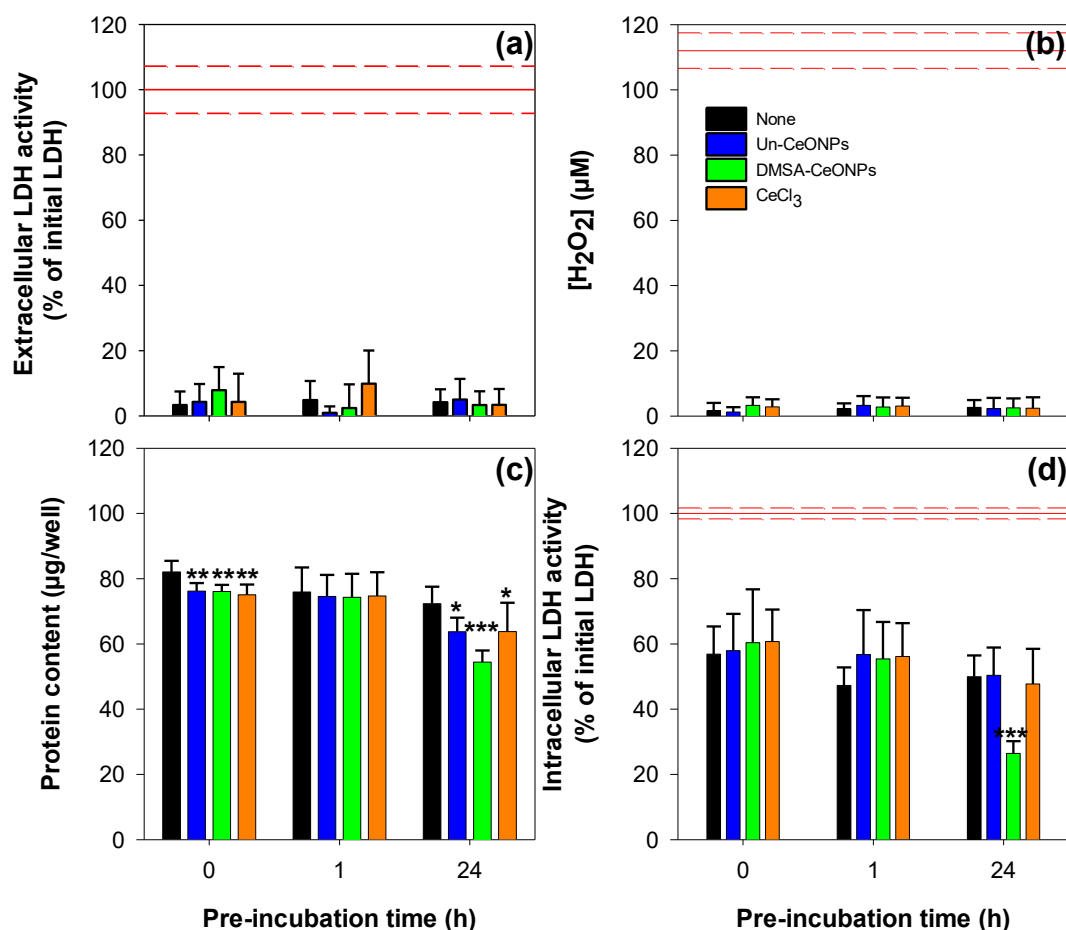
Figure 10. **Effect of CeONPs pre-incubation on the resistance of C6 glioma cells to oxidative stress.** C6 glioma cells were pre-incubated with or without 1 mM cerium applied as Un-CeONPs, DMSA-CeONPs or CeCl$_3$ at 37°C for 0, 1 or 24 h. **(a)** Extracellular LDH activity (% of initial LDH) was determined just after each pre-incubation time was over. Afterwards a 3 h incubation with 100 μM H_2O_2 was started and at its end **(b)** the concentration (μM) of H_2O_2 in the medium, **(c)** the cellular protein content (μg/well) and (**d**) the intracellular LDH activity were determined. Average values and standard deviations of data from three independent experiments are shown (n=3). Each condition was performed in triplicates in every single experiment. Statistical differences were calculated by a Two-way ANOVA *p< 0.05, **p<0.01, ***p < 0.001, indicates differences compared with the control condition (none) and were obtained by Tukey Multiple Comparison Test.

The pre-incubation of cells with 1 mM Un-CeONPs or DMSA-CeONPs or ionic cerium for 1 or 24 h did not significantly impair the cell integrity in comparison to the controls. Afterwards, cells were incubated for 3 h with 100 μM H_2O_2 in IB-BSA. After 3 h incubation,

the remaining extracellular H_2O_2 was less than 10 µM for all conditions and did not show any significant difference among treatments (Fig. 10b). Untreated C6 cells had on average 113 ± 12 µg protein per well before the 3 h incubation with IB-BSA containing H_2O_2 started. In comparison to these initial values, the cells which were preincubated without cerium showed an average loss of 32.7% in protein content. The oxidative stress caused by the incubation with H_2O_2 led to a loss in proteins that ultimately can be interpreted as a reduction in the number of viable cells. Pre-incubations with Un-CeONPs or DMSA-coated CeONPs or ionic cerium for 0 or 1 h did not prevent the reduction in the amount of proteins significantly. Moreover, a 24 h pre-incubation with both kinds of CeONPs and $CeCl_3$ significantly lowered the protein content of the C6 glioma cells compared to the cultures which had not been exposed to cerium (Fig. 10c). Based on the protein content, the cerium treatments thus did not seem to prevent the toxic effect of the H_2O_2 insult and might even decrease the viability when the pre-incubation is held for 24 h.

As expected from previous results (Fig. 8), when no cerium was added to the cells, the membrane integrity was compromised by the H_2O_2 treatment by ~50% (Fig. 9d,n). Taking a high intracellular LDH as an indicator of cell viability, Un-CeONPs and DMSA-CeONPs, as well as $CeCl_3$, did not show any neuroprotective effect (Fig. 10). In fact, pre-incubation with DMSA-CeONPs for 24 h caused a significant loss in intracellular LDH compared to the control (Fig. 10d). As such an effect was not observed for Un-CeONPs, DMSA-coating seems to allow for a stronger accumulation of cerium in the cell interior, ultimately leading to concentrations which, paired with the H_2O_2 challenge, might be responsible for significant cell damage.

Investigation of antioxidant protective effect of DMSA-CeONPs in cultured astrocytes

To test whether DMSA-CeONPs scavenge the superoxide formed by the auto-oxidation of β-lapachol to β-lapachone intracellularly (Steinmeier et al., 2020), cultured astrocytes were pre-incubated without or with DMSA-CeONPs up to 4 h in DMEM+10% FCS. Afterwards, cells were incubated with 400 µM WST1, 3 µM β-lapachone in the absence or presence of 30 µM dicoumarol in NP-free physiological medium. None of the concentrations of tested DMSA-CeONPs were able to reduce WST1 formazan formation under these experimental conditions. In contrast, the presence of dicoumarol alone or in combination with DMSA-CeONPs strongly prevented the WST1 reduction (p<0.001) (data not shown).

Pre-treatment with DMSA-CeONPs did not prevent oxidative stress by H_2O_2 in APCs

To test the capacity of DMSA-CeONPs to protect cultured astrocytes from an oxidative insult, the cells were pre-incubated without or with DMSA-CeONPs for 4 h. Once the NPs were washed away, ROS formation was assessed after treating cells with or without H_2O_2 in the absence or presence of β-lapachone and/or dicoumarol (Fig. 11).
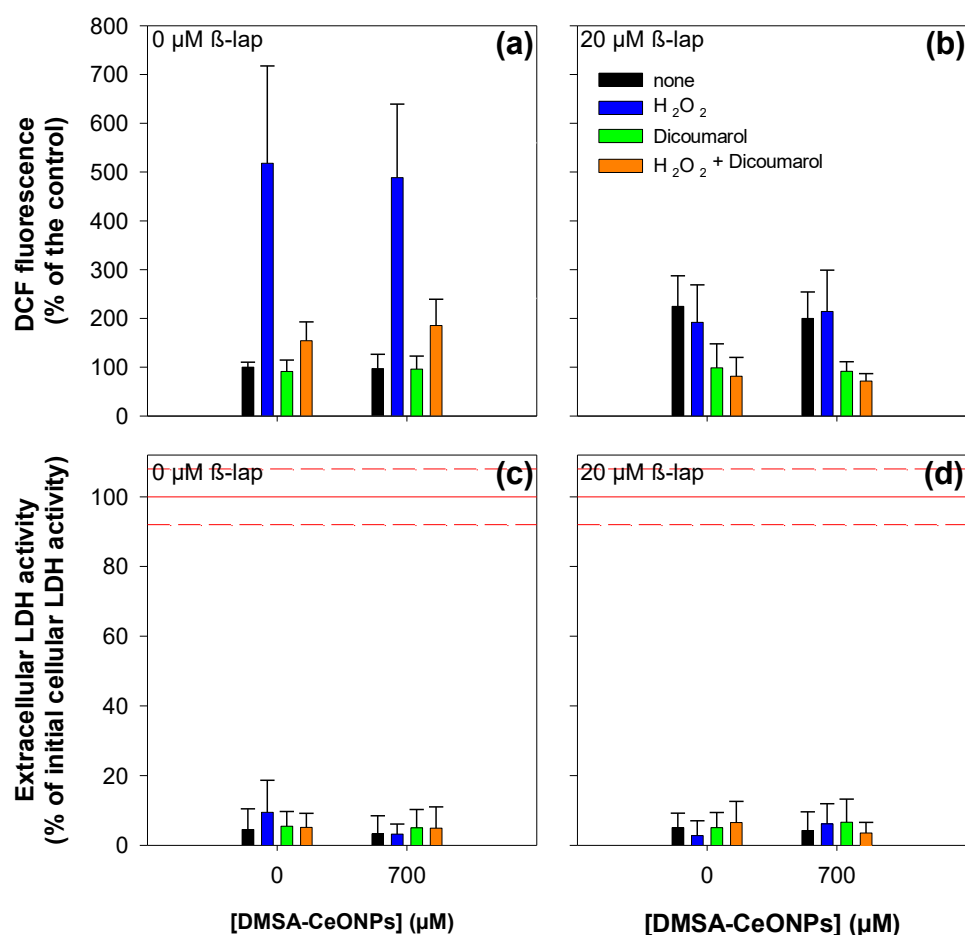
Figure 11. Pre-treatment with DMSA-CeONPs did not prevent oxidative stress by superoxide or H_2O_2. The cells were pre-incubated in the absence (0 μM) or the presence of 700 μM DMSA-CeONPs for 4 h in DMEM+10% FCS. Subsequently the cells were washed and loaded with 50 μM DCFH$_2$-DA in IB for 30 min. Afterwards the cells were treated without or with 20 μM β-lapachone, 1 mM H_2O_2 and/or 30 μM dicoumarol up to 5 min. Finally, the cells were washed and lysed in hypotonic lysis buffer for 10 min. The lysates were harvested and centrifuge at 12,300g for 60 s. The presence of ROS was measured by fluorometry (λ_{ex}: 485 nm and λ_{em}: 520 nm) **(a, b).** The viability of the cells after the treatment was also determined **(c, d).** DCF-fluorescence is expressed as percentage compared to cells not pre-incubated with DMSA-CeONPs and without the addition of β-lapachone, H_2O_2 or dicoumarol. The data shown are means ± SD of values obtained in three experiments on independently prepared cultures (n=3). No significant differences (ANOVA) were observed between cells pre-incubated with DMSA-CeONPs and not pre-incubated under the same conditions.

Loading cells with DCFH$_2$-DA and 5 min treatment in the presence or absence of β-lapachone, H$_2$O$_2$ and/or dicoumarol did not impair cells membrane integrity under experimental conditions (Fig. 11c,d). In the absence of β-lapachone, pre-incubation of cultured astrocytes with 700 µM DMSA-CeONPs did not increase ROS formation (Fig. 11a). However, incubation with H$_2$O$_2$ led to a significant increase in ROS (Fig. 11a). The presence of dicoumarol did not elevate ROS formation and when co-incubated with H$_2$O$_2$ prevented their formation (Fig. 11a). On the contrary, addition of 20 µM β-lapachone increased basal ROS formation to ~200% of the control, independently if the cells were pre-incubated with or without DMSA-CeONPs (Fig 11a, b). Remarkably, the presence of β-lapachone decreased DCF fluorescence in the presence of H$_2$O$_2$ ~50% in comparison to incubations in the absence of β-lapachone (Fig. 11a,b). The presence of dicoumarol under these experimental conditions kept ROS formation at the same level as found for the control (Fig. 11b).

Discussion

DMSA-CeONPs scavenged H$_2$O$_2$ and superoxide when present in biological media, but did not exert an antioxidant effect in glial cells when internalised. Furthermore, in the present study, the removal of H$_2$O$_2$ and the scavenging of superoxide by DMSA-CeONPs followed a chemical stoichiometric reaction pattern rather than an enzymatic reaction. As a proof of concept, it was demonstrated that incubation of Un-CeONPs with a relatively high concentration of H$_2$O$_2$, caused a reduction in absorbance that can be attributed to the removal of H$_2$O$_2$ by Un-CeONPs. Such results were consistent with those reported by (Pirmohamed et al., 2010) in their seminal work demonstrating the catalase-like activity of CeONPs. Later, in a different experimental setup with a concentration of H$_2$O$_2$ closer to biological values, the present study shows that DMSA-CeONPs were also able to remove H$_2$O$_2$ in the absence of cells. The decrease in H$_2$O$_2$ in the medium increased linearly with increasing concentration and time when Un-CeONPs or DMSA-coated CeONPs were present, suggesting that the reaction could continue over a prolonged time, potentially until exhausting the H$_2$O$_2$ pool. The calculated rates of extracellular H$_2$O$_2$ disappearance are in the same order of magnitude as those reported previously (Pirmohamed et al., 2010). However, their CeONPs showed a rate equivalent to that calculated for CeCl$_3$ (1.677 ± 0.003 nmol min^{-1}) in the present study and 10 times higher than those presented by DMSA-CeONPs.

It was also demonstrated that DMSA-CeONPs scavenge extracellular superoxide. Exposure of cultured astrocytes to β-lapachone caused a rapid concentration-dependent increase in WST1 formazan formation, consistent with literature data (Watermann and Dringen, 2023).

A concentration of 3 µM β-lapachone was found to be sufficient to test the ability of DMSA-CeONPs to scavenge superoxide from the extracellular space. This experimental setup potentially avoided stress signals, such as the increase in lactate release and glutathione disulfide, derived from the use of β-lapachone in higher concentrations (Steinmeier et al., 2020; Watermann and Dringen, 2023) and therefore, the observations could be exclusively attributed to the uptake of DMSA-CeONPs.

Application of DMSA-CeONPs to cultured astrocytes significantly reduced the formation of WST1 formazan in a concentration-dependent manner. DMSA-CeONPs showed a significant antioxidant capacity in the extracellular space. An extracellular concentration of 700 µM DMSA-CeONPs was able to reduce WST1 formazan formation by 11% compared to the control. However, the reducing power of DMSA-CeONPs was approximately 2.4 times lower than that of exogenous SOD (25 U). The effects observed when combined DMSA-CeONPs and SOD and DMSA-CeONPs plus SOD plus catalase were not additive, what may corroborate that DMSA-CeONPs scavenge extracellular superoxide and that the effect observed was not due to other reactions. The results are consistent with literature data. SOD-mimetics as for example Cu^{2+}, Zn, Mn^{2+}, Co^{2+} and Co^{3+} complexes have two to four orders of magnitude less activity than the native SOD (Zhidkova et al., 2011; Sozarukova et al., 2020). These observations support the view that DMSA-CeONPs may constitute an interesting tool against oxidative stress.

The commonly advocated mechanism explaining the scavenging of ROS by CeONPs is considered to be redox-state dependent, where CeONPs act as a catalyst or, in other words, a nanozyme if applied in a biological system (Wei and Wang, 2013; Seminko et al., 2021; Singh et al., 2023). Nanozymes are able to increase the rate of a chemical reaction, convert a substantial amount of substrate with a reduce amount of catalyst and regenerate, which means that after the completion of the catalytic cycle the reagents are regenerated to their initial state (Kozuch and Martin, 2012; Popov et al., 2017). CeONPs have been long used as catalysts in industrial applications (Scirè and Palmisano, 2020). Moreover, CeONPs can mimic different enzymes as they possess oxidoreductase (Hayat et al., 2015; Singh, 2016), phosphatase (Dhall et al., 2017), catalase (Pirmohamed et al., 2010) and SOD activities (Korsvik et al., 2007).

However, the DMSA-CeONPs used in the current study did not act as nanozymes under the experimental conditions tested. The removal of H_2O_2 occurred with a slow reaction rate, far from that of native catalase. In addition, double of concentration of DMSA-CeONPs compared to the subtract was needed to remove 100 µM H_2O_2. Application of 200 µM Un-

CeONPs and DMSA-CeONPs needed 11 and 12 h respectively (data not shown) to reach their half time for the removal of 100 μM extracellular H_2O_2. Putting it into context, Hirrlinger et al. (2002) estimated a half-time of decomposition of 100 μM H_2O_2 by cultured astrocytes of 4.8 min. Thus, the extracellular clearance of H_2O_2 by extracellular DMSA-CeONPs in the medium of cell cultures seems negligible compared to the cell-dependent H_2O_2 clearance under non-pathological conditions. In addition, there was no evidence of regeneration of DMSA-CeONPs within the time frame studied, or it may have occurred at a very slow rate. These facts may indicate that DMSA-CeONPs reacted stoichiometrically with H_2O_2 rather than act as a catalyst on its removal.

Similarly, the capacity of DMSA-CeONPs to scavenge superoxide was already saturated in the presence of only 1 μM β-lapachone (Fig. 4), i.e. when the concentration of DMSA-CeONPs was kept constant, increasing β-lapachone concentration resulted in a decrease in the percentage of reduction in WST1 formazan. Moreover, when the concentration of β-lapachone was approximately doubled, the percentage of reduction in WST1 formazan by the same amount of DMSA-CeONPs was approximately 50% (Fig. 6). This observation indicates that the reaction was strongly limited by the amount of DMSA-CeONPs present and therefore, suggests a stoichiometric chemical reaction rather than a catalytic reaction.

The present study did not directly address the mechanism behind the reactions of DMSA-CeONPs with H_2O_2 or superoxide. Nevertheless, it can be assumed that the reactivity of DMSA-CeONPs was due to the flip-flop between Ce^{3+} and Ce^{4+} on the surface (Heckert et al., 2008; Singh et al., 2021). For the removal of H_2O_2, many authors have suggested that Ce^{4+} could be reduced to Ce^{3+} by the electrons left behind by oxygen vacancy formation (Fig. 12a) (Pirmohamed et al., 2010; Celardo et al., 2011; Singh et al., 2011; Thakur et al., 2019). Celardo et al., 2010; Thakur et al., 2019) and recently, Popov et al. (2017) provided further insight by demonstrating that Ce^{3+} also participates in the catalase-like reaction (Fig. 12b). In the dismutation of superoxide, Ce^{3+} reduces superoxide to H_2O_2, and is itself oxidised to Ce^{4+}, which in turn disproportionates H_2O_2 to molecular O_2 and H_2O (Korsvik et al., 2007; Heckert et al., 2008; Celardo et al., 2011; Corsi et al., 2018). For all that, it is likely that DMSA-CeONPs presented a similar amount of Ce^{4+} and Ce^{3+} on the surface, as they scavenged both, H_2O_2 and superoxide. In terms of regeneration, the flip-flop may be extremely slow or may not have occurred under our experimental conditions.

169
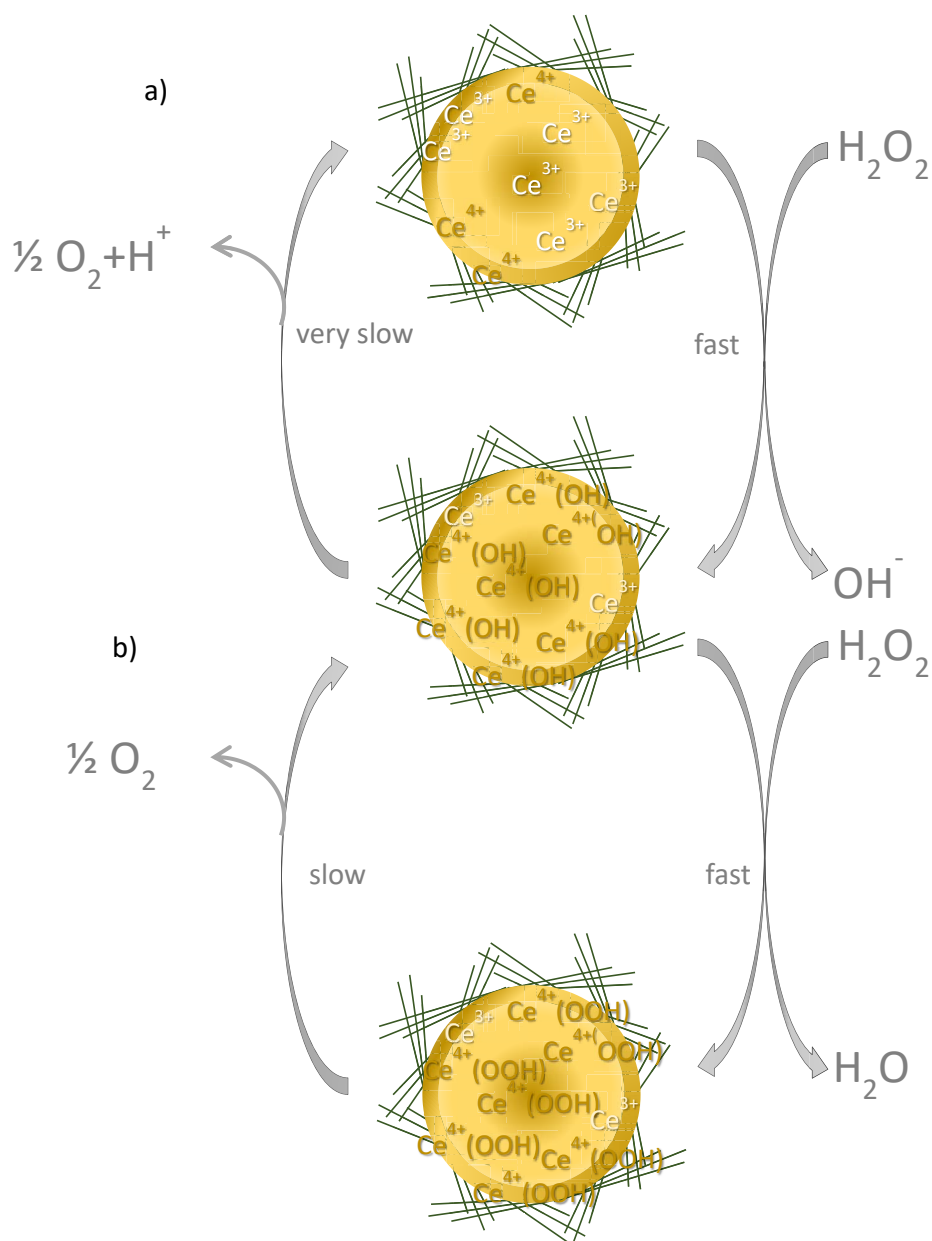
Figure 12. Schematic theoretical model of catalase activity by DMSA-CeONPs. The disproportionation of H_2O_2 may occurred in two stages. DMSA-CeONPs when having a predominance in Ce^{3+} on the surface show a fast flip-flop to Ce^{4+} as convert H_2O_2 to OH^- **(a)** Consecutively, cerium hydroperoxide would be formed on the surface while it further decomposes to water and with the formation of oxygen **(b)**. DMSA-CeONPs could return to a state of predominance of Ce^{3+} to Ce^{4+}. Modified from Popov et al., 2017.

Surface functionalization influences the enzymatic activity of CeONPs (Hanafy et al., 2019; Bhushan et al., 2023). The here presented results demonstrate that the coating with DMSA did not affect the scavenging of H_2O_2 of the NPs or was not responsible of the depletion of their regeneration, as Un-CeONPs showed no significant differences in the removal of H_2O_2 compared to DMSA-CeONPs. This, together with the high biocompatibility with brain cells already described for the DMSA coating (Geppert et al., 2011; Bulcke et al., 2014; Joshi et al.,

2016; Rastedt et al., 2017), the possibility of further functionalization with fluorescent dyes (see Chapter 2.1) and the enhanced uptake of DMSA-CeONPs compared to Un-CeONPs (data not shown) suggests that DMSA coating still constitutes a great alternative for CeONPs.

However, other parameters could still be revisited to achieve DMSA-CeONPs act as a nanozyme. For instance, DMSA-CeONPs had a nominal size of about 25 nm, measured by transmission electron microscopy (see Chapter 2.1). It is commonly accepted that CeONPs shows enhanced catalytic activity when presented in 3-9 nm size (Xue et al., 2011; Cafun et al., 2013; Lee et al., 2013; Baldim et al., 2018). Such a reduction in size has been demonstrated to ease the formation of oxygen vacancies (Tsunekawa et al., 1999; Deshpande et al., 2005; Naganuma, 2017) and therefore, to favour the flip-flop/number of active sites and consequently increase the removal of H_2O_2 or the scavenging of superoxide (Thao et al., 2023). Although examples on the contrary can also be found in the literature (Li et al., 2015), these might suggest that a reduction in the size could increase the disproportionation of H_2O_2 and the superoxide scavenging potential by DMSA-CeONPs.

Dissolved $CeCl_3$ and $Ce(SO_4)_2$ were included in the present study to test for the "NP-effect". CeONPs have been thoroughly investigated under the premise to be a more powerful antioxidant as their bulk counterpart, based on the simultaneous presence of different oxidation states in the lattices of the NPs and their auto-regeneration (cycling) (Herper et al., 2020). However, in the present study ionic cerium showed a much stronger potential than the NPs tested to remove H_2O_2. Studies from the late 1950's already established the reduction of Ce^{4+} aqueous solutions by H_2O_2 into Ce^{3+} but of note, with the formation of hydroperoxyl radicals (OOH·) (Baer and Stein, 1953; Sigler and Masters, 1957; Bielski and Saito, 1962; Heckert et al., 2008). Over the last two decades, it has been argued that CeONPs has also the advantage to strongly limit the formation/release of such radicals (Heckert et al., 2008) and therefore, being less toxic to the cell. However, recent studies have questioned it as the appearance of stable intermediate species, such as peroxyl or hydroperoxyl bound to the NPs surface were observed (Scholes et al., 2006; Damatov and Mayer, 2016). In the present investigation, under the conditions tested, the "NP-effect" did not result in any advantage. The removal of exogenous H_2O_2 was significantly faster with ionic cerium compared to DMSA-CeONPs. Similarly, bulk cerium scavenged more efficiently superoxide than DMSA-CeONPs. In fact, after 60 min, bulk cerium reduced WST1 formazan formation 54% compared to the control (none). This reduction was even slightly higher than the one shown by SOD (47%) compared to the control.

The lack of nanozyme behaviour under these experimental conditions may have prevented the "NP effect". Nevertheless, as reviewed by Shcherbakov et al. (2020), cerium salts share the same properties and beneficial biological activities attributed to CeONPs. For example, long before CeONPs, cerium salts were shown to exhibit catalase (Van Noorden and Frederiks, 1993; Ivanov et al., 2009), SOD (Wang et al., 1997; Kostova and Traykova, 2006; Kostova et al., 2008) and peroxidase(Tian et al., 2015) activities, as well as hydroxyl radical scavenging (Yu et al., 1993). In fact, based on these observations, the authors argue that, cerium ions leaking into the media are primarily responsible for these activities, and as such CeONPs have to be considered only as an effective carrier. For DMSA-CeONPs, further studies on cerium ion leakage may be required.

Ultimately, this study aimed to elucidate the antioxidant potential of DMSA-CeONPs on glial cells under oxidative stress. C6 glioma cells were loaded with cerium in the form of NPs or bulk and then stressed by incubation in the presence of 100 μM H_2O_2. Preincubation with Un-CeONPs, DMSA-CeONPs or $CeCl_3$ did not prevent the observed loss of LDH activity and even accelerated the loss of protein compared to the control. Thus, cerium did not show any neuroprotective effect against acute oxidative stress induced by an exogenous H_2O_2-insult. It can be indirectly concluded that Un-CeONPs, DMSA-CeONPs or bulk cerium, once inside the cell, did not effectively protect C6 glioma cells. In particular, DMSA-CeONPs further inhibited the proliferation of C6 glioma cells when loaded for 24 hours. The uptake of DMSA-CeONPs alone did not show any effect on extracellular LDH activity, but only after the 3 h of exposure to H_2O_2. The question is whether DMSA-CeONPs showed a pro-oxidant behaviour, that together with the H_2O_2 insult, damaged the C6 glioma cells, or whether the accumulation of DMSA-CeONPs over 24 h alone made the cells to be more susceptible to oxidative stress.

As there was no difference in the amount of H_2O_2 left in the media, it is hypothesized that DMSA-CeONPs did not affect the native antioxidant mechanisms of the C6 glioma cells. On the other hand, previous results on the uptake of DMSA-CeONPs by C6 cells (data not shown) may support that DMSA-CeONPs are internalised more rapidly and to a greater extent. Additionally, in a previous study, it was shown that the internalization of DMSA-CeONPs in primary astrocytes is significantly higher (16 to 3-fold depending on the conditions) than that of bulk cerium (see Chapter 2.2). These considerations may suggest that an overload of DMSA-CeONPs prior to the insult may sensitize cells, making them more susceptible to oxidative stress. In order to narrow down the trigger of the decrease in cellular vitality, other assays may be of interest. For example, Hohnholt et al. (2015)

observed that the LDH assay was a late predictor of cell damage on cerebellar granule neurons, subjected to acute and transient exposure to H_2O_2. In contrast, 3-(4,5-dimethylthiazol-2-yl)-2,5-diphenyltertrazolium bromide (MTT) reduction or neutral red accumulation were able to predict the consequences of oxidative stress earlier. In further studies, it may be of interest to analyse whether C6 glioma cells show a decrease in MTT reduction or increased neutral red accumulation after uptake of DMSA-CeONPs.

Similarly, loading primary astrocytes with DMSA-CeONPs did not reduce the WST1 formazan formation in the presence of β-lapachone. The scavenging capacity of DMSA-CeONPs was not detectable when internalized. Some superoxide is expected to be generated when 3 μM of β-lapachone is added, as indicated by the 50% reduction of WST1 formazan in the presence of SOD. This lack of reactivity of DMSA-CeONPs can be attributed to several causes. First, the amount of internalization of DMSA-CeONPs within 1 h may be insufficient to observe a significant effect. Previously, it was showed that incubation of astrocytes with 300 μM DMSA-CeONPs for 1 h resulted in internalization of 1.59 μM (see Chapter 2.2). Extracellularly, a concentration of 30 μM DMSA-CeONPs did not significantly reduce the formation of WST1 formazan, so once internalized, it is very unlikely that a significant scavenging effect would be detected. In the case of ionic cerium, the accumulation may have been even less, as showed in a previous section as well (see Chapter 2.2). Secondly, the fate of the NPs once internalised may prevent their activity. Internalization and subcellular localization strongly depend on many factors such as size, shape, coating, oxidation state, concentration, time and type of cell (reviewed by Chen and Stephen Inbaraj (2018)). Many authors experimenting with different CeONPs, cell lines and conditions have reported accumulation of CeONPs in lysosomes among other possibilities. Previous studies from Dringen's laboratory have established that glial cells accumulate iron oxide NPs (Petters and Dringen, 2015) and copper oxide NPs (Joshi et al., 2019) in lysosomes. Furthermore, the accumulation of CeONPs in lysosomes appears to induce autophagy/apoptosis (Song et al., 2014; Qiu et al., 2015; Lord et al., 2016), which may also explain why DMSA-CeONPs did not prevent oxidative stress in glial cells. Lastly, in this particular experimental setup the likelihood of DMSA-CeONPs being placed in the same cellular space and at the same time, where the superoxide is generated by the auto-oxidation of β-lapachol is reduced, and even more so considering that 3 μM β-lapachone induces a limited oxidative stress in cultured astrocytes (Watermann and Dringen, 2023).

Therefore, an increase in β-lapachone might be useful to study the acute oxidative effect and the potential of DMSA-CeONPs to scavenge superoxide. In line with this, it was previously

noted that CeONPs might be more effective in pathological conditions (Rzigalinski et al., 2017). For the aforementioned reasons in a different experimental setup, the amount of β-lapachone (20 μM) was increased to study the presence of ROS in cells loaded with DMSA-CeONPs. Under such conditions, the production of superoxide is thought to cause oxidative stress in cultures astrocytes. Indeed, the addition of 20 μM β-lapachone doubled the presence of ROS compared to the 0 μM β-lapachone condition, replicating previous results (Steinmeier et al., 2020). However, loading of cultured astrocytes with DMSA-CeONPs did not reduce ROS formation in this experimental setup either. In absence of β-lapachone, DMSA-CeONPs did not reduce the amount of intracellular ROS produced by exogenous H_2O_2. Moreover, when 20 μM β-lapachone was added, the amount of ROS without and with DMSA-CeONPs was also doubled. Thus, DMSA-CeONPs did not reduce oxidative stress in the cells. Interestingly, the addition of exogenous H_2O_2 to primary astrocytes containing 20 μM β-lapachone did not further increase the amount of ROS, independently of the presence or not of DMSA-CeONPs. These results remain unexplained, however, the simultaneous presence of superoxide and H_2O_2 may produce some side reaction leading to a lower signal. Little is still known about the use of β-lapachone in conditions with an external addition of ROS.

In conclusion, DMSA-CeONPs showed a limited extracellular capacity to scavenge H_2O_2 and superoxide. Under the experimental conditions used, DMSA-CeONPs did not act as nanozymes and, therefore, did not catalyse such reactions. There was also no evidence of auto-regeneration. Loading glial cells with DMSA-CeONPs did not prevent oxidative stress induced by exogenous H_2O_2 or the electron cycler β-lapachone. As DMSA-CeONPs are biocompatible with cultured brain cells at relatively high concentrations, further studies to increase their scavenging activity may be advisable. In this direction, it may be of interest to functionalize smaller CeONPs with DMSA and to test for their scavenging activity. Although the design of the DMSA-CeONPs failed to show an optimal antioxidative potential, the experimental setups could still be useful to study other CeONPs with different physico-chemical properties. Regarding their application as neuroprotectors, further investigation of their effect and fate on glial cells is necessary. Moreover, it needs to be considered the extension of the study to other types of cells less robust to oxidative stress and metals, such as neurons (Herrero-Mendez et al., 2009).

References

Baer, S. and G. Stein (1953). "633. The decomposition of hydrgen peroxide by ceric salts. Part I. The action of ceric sulphate." Journal of the Chemical Society (Resumed): 3176-3179.

Baldim, V., F. Bedioui, N. Mignet, I. Margaill and J.-F. Berret (2018). "The enzyme-like catalytic activity of cerium oxide nanoparticles and its dependency on Ce^{3+} surface area concentration." Nanoscale 10(15): 6971-6980.

Bao, Q., P. Hu, Y. Xu, T. Cheng, C. Wei, L. Pan and J. Shi (2018). "Simultaneous blood–brain barrier crossing and protection for stroke treatment based on edaravone-loaded ceria nanoparticles." ACS Nano 12(7): 6794-6805.

Bhushan, S., S. Singh, T. K. Maiti, A. Das, A. Barui, L. R. Chaudhari, M. G. Joshi and D. Dutt (2023). "Cerium oxide nanoparticles disseminated chitosan gelatin scaffold for bone tissue engineering applications." International Journal of Biological Macromolecules 236: 123813.

Bielski, B. H. and E. Saito (1962). "The activation energy for the disproportionation of the HO_2 radical in acid solutions1." The Journal of Physical Chemistry 66(11): 2266-2268.

Bolaños, J. P. (2016). "Bioenergetics and redox adaptations of astrocytes to neuronal activity." Journal of Neurochemistry 139: 115-125.

Bulcke, F., K. Thiel and R. Dringen (2014). "Uptake and toxicity of copper oxide nanoparticles in cultured primary brain astrocytes." Nanotoxicology 8(7): 775-785.

Cafun, J.-D., K. O. Kvashnina, E. Casals, V. F. Puntes and P. Glatzel (2013). "Absence of Ce^{3+} sites in chemically active colloidal ceria nanoparticles." ACS Nano 7(12): 10726-10732.

Celardo, I., J. Z. Pedersen, E. Traversa and L. Ghibelli (2011). "Pharmacological potential of cerium oxide nanoparticles." Nanoscale 3(4): 1411-1420.

Chen, B.-H. and B. Stephen Inbaraj (2018). "Various physicochemical and surface properties controlling the bioactivity of cerium oxide nanoparticles." Critical Reviews in Biotechnology 38(7): 1003-1024.

Chen, J., S. Patil, S. Seal and J. F. McGinnis (2006). "Rare earth nanoparticles prevent retinal degeneration induced by intracellular peroxides." Nature Nanotechnology 1(2): 142-150.

Ciofani, G., G. G. Genchi, I. Liakos, V. Cappello, M. Gemmi, A. Athanassiou, B. Mazzolai and V. Mattoli (2013). "Effects of cerium oxide nanoparticles on PC12 neuronal-like cells: proliferation, differentiation, and dopamine secretion." Pharmaceutical Research 30: 2133-2145.

Corsi, F., F. Caputo, E. Traversa and L. Ghibelli (2018). "Not only redox: the multifaceted activity of cerium oxide nanoparticles in cancer prevention and therapy." Frontiers in Oncology 8: 309.

Cunha-Oliveira, T., L. Montezinho, C. Mendes, O. Firuzi, L. Saso, P. J. Oliveira and F. S. Silva (2020). "Oxidative stress in amyotrophic lateral sclerosis: pathophysiology and opportunities for pharmacological intervention." Oxidative Medicine and Cellular Longevity 2020.

Damatov, D. and J. M. Mayer (2016). "(Hydro) peroxide ligands on colloidal cerium oxide nanoparticles." Chemical Communications 52(67): 10281-10284.

Das, M., S. Patil, N. Bhargava, J. F. Kang, L. M. Riedel, S. Seal and J. J. Hickman (2007). "Auto-catalytic ceria nanoparticles offer neuroprotection to adult rat spinal cord neurons." Biomaterials 28(10): 1918-1925.

DeCoteau, W., K. L. Heckman, A. Y. Estevez, K. J. Reed, W. Costanzo, D. Sandford, P. Studlack, J. Clauss, E. Nichols and J. Lipps (2016). "Cerium oxide nanoparticles with antioxidant properties ameliorate strength and prolong life in mouse model of amyotrophic lateral sclerosis." Nanomedicine: Nanotechnology, Biology and Medicine 12(8): 2311-2320.

Deshpande, S., S. Patil, S. V. Kuchibhatla and S. Seal (2005). "Size dependency variation in lattice parameter and valency states in nanocrystalline cerium oxide." Applied Physics Letters 87(13).

Dhall, A., A. Burns, J. Dowding, S. Das, S. Seal and W. Self (2017). "Characterizing the phosphatase mimetic activity of cerium oxide nanoparticles and distinguishing its active site from that for catalase mimetic activity using anionic inhibitors." Environmental Science: Nano 4(8): 1742-1749.

Dhall, A. and W. Self (2018). "Cerium oxide nanoparticles: a brief review of their synthesis methods and biomedical applications." Antioxidants 7(8): 97.

Dringen, R., L. Kussmaul and B. Hamprecht (1998). "Detoxification of exogenous hydrogen peroxide and organic hydroperoxides by cultured astroglial cells assessed by microtiter plate assay." Brain Research Protocols 2(3): 223-228.

Emerit, J., M. Edeas and F. Bricaire (2004). "Neurodegenerative diseases and oxidative stress." Biomedicine and Pharmacotherapy 58(1): 39-46.

Ernster, L., M. Ljunggren and L. Danielson (1960). "Purification and some properties of a highly dicumarol-sensitive liver diaphorase." Biochemical and Biophysical Research Communications 2(2): 88-92.

Estevez, A., S. Pritchard, K. Harper, J. Aston, A. Lynch, J. Lucky, J. Ludington, P. Chatani, W. Mosenthal and J. Leiter (2011). "Neuroprotective mechanisms of cerium oxide nanoparticles in a mouse hippocampal brain slice model of ischemia." Free Radical Biology and Medicine 51(6): 1155-1163.

Estevez, A. Y., M. Ganesana, J. F. Trentini, J. E. Olson, G. Li, Y. O. Boateng, J. M. Lipps, S. E. Yablonski, W. T. Donnelly and J. C. Leiter (2019). "Antioxidant enzyme-mimetic activity and neuroprotective effects of cerium oxide nanoparticles stabilized with various ratios of citric acid and EDTA." Biomolecules 9(10): 562.

Feng, N., Y. Liu, X. Dai, Y. Wang, Q. Guo and Q. Li (2022). "Advanced applications of cerium oxide based nanozymes in cancer." RSC Advances 12(3): 1486-1493.

Fisichella, M., F. Berenguer, G. Steinmetz, M. Auffan, J. Rose and O. Prat (2014). "Toxicity evaluation of manufactured CeO_2 nanoparticles before and after alteration: combined physicochemical and whole-genome expression analysis in Caco-2 cells." BMC Genomics 15(1): 1-15.

Floyd, R. A. (1999). "Antioxidants, oxidative stress, and degenerative neurological disorders." Proceedings of the Society for Experimental Biology and Medicine 222(3): 236-245.

Forest, V., L. Leclerc, J.-F. Hochepied, A. Trouvé, G. Sarry and J. Pourchez (2017). "Impact of cerium oxide nanoparticles shape on their in vitro cellular toxicity." Toxicology In Vitro 38: 136-141.

Geppert, M., M. C. Hohnholt, K. Thiel, S. Nürnberger, I. Grunwald, K. Rezwan and R. Dringen (2011). "Uptake of dimercaptosuccinate-coated magnetic iron oxide nanoparticles by cultured brain astrocytes." Nanotechnology 22(14): 145101.

Geppert, M., C. Petters, K. Thiel and R. Dringen (2013). "The presence of serum alters the properties of iron oxide nanoparticles and lowers their accumulation by cultured brain astrocytes." Journal of Nanoparticle Research 15: 1-15.

Gilgun-Sherki, Y., E. Melamed and D. Offen (2001). "Oxidative stress induced-neurodegenerative diseases: the need for antioxidants that penetrate the blood brain barrier." Neuropharmacology 40(8): 959-975.

Hamprecht, B. and F. Löffler (1985). [27] Primary glial cultures as a model for studying hormone action. Methods in Enzymology, Elsevier. 109**:** 341-345.

Hanafy, B. I., G. W. Cave, Y. Barnett and B. Pierscionek (2019). "Ethylene glycol coated nanoceria protects against oxidative stress in human lens epithelium." RSC Advances 9(29): 16596-16605.

Hayat, A., J. Cunningham, G. Bulbul and S. Andreescu (2015). "Evaluation of the oxidase like activity of nanoceria and its application in colorimetric assays." Analytica Chimica Acta 885: 140-147.

Heckert, E. G., A. S. Karakoti, S. Seal and W. T. Self (2008). "The role of cerium redox state in the SOD mimetic activity of nanoceria." Biomaterials 29(18): 2705-2709.

Heckert, E. G., S. Seal and W. T. Self (2008). "Fenton-like reaction catalyzed by the rare earth inner transition metal cerium." Environmental Science & Technology 42(13): 5014-5019.

Heckman, K. L., W. DeCoteau, A. Estevez, K. J. Reed, W. Costanzo, D. Sanford, J. C. Leiter, J. Clauss, K. Knapp and C. Gomez (2013). "Custom cerium oxide nanoparticles protect against a free radical mediated autoimmune degenerative disease in the brain." ACS Nano 7(12): 10582-10596.

Herper, H. C., O. Y. Vekilova, S. I. Simak, I. Di Marco and O. Eriksson (2020). "Localized versus itinerant character of 4f-states in cerium oxides." Journal of Physics: Condensed Matter 32(21): 215502.

Herrero-Mendez, A., A. Almeida, E. Fernández, C. Maestre, S. Moncada and J. P. Bolaños (2009). "The bioenergetic and antioxidant status of neurons is controlled by continuous degradation of a key glycolytic enzyme by APC/C–Cdh1." Nature Cell Biology 11(6): 747-752.

Hirrlinger, J., A. Resch, J. M. Gutterer and R. Dringen (2002). "Oligodendroglial cells in culture effectively dispose of exogenous hydrogen peroxide: comparison with cultured neurones, astroglial and microglial cells." Journal of Neurochemistry 82(3): 635-644.

Hohnholt, M. C., E. M. Blumrich and R. Dringen (2015). "Multiassay analysis of the toxic potential of hydrogen peroxide on cultured neurons." Journal of Neuroscience Research 93(7): 1127-1137.

Hohnholt, M. C., M. Geppert and R. Dringen (2011). "Treatment with iron oxide nanoparticles induces ferritin synthesis but not oxidative stress in oligodendroglial cells." Acta Biomaterialia 7(11): 3946-3954.

Hollander, P. M. and L. Ernster (1975). "Studies on the reaction mechanism of DT diaphorase: action of dead-end inhibitors and effects of phospholipids." Archives of Biochemistry and Biophysics 169(2): 560-567.

Huang, J., C. Li and H. Shang (2022). "Astrocytes in neurodegeneration: inspiration from genetics." Frontiers in Neuroscience 16: 882316.

Ivanov, V. K., A. B. Shcherbakov and A. Usatenko (2009). "Structure-sensitive properties and biomedical applications of nanodispersed cerium dioxide." Russian Chemical Reviews 78(9): 855.

Jelinek, M., M. Jurajda and K. Duris (2021). "Oxidative stress in the brain: basic concepts and treatment strategies in stroke." Antioxidants 10(12): 1886.

Joshi, A., W. Rastedt, K. Faber, A. G. Schultz, F. Bulcke and R. Dringen (2016). "Uptake and toxicity of copper oxide nanoparticles in C6 glioma cells." Neurochemical Research 41(11): 3004-3019.

Joshi, A., K. Thiel, K. Jog and R. Dringen (2019). "Uptake of intact copper oxide nanoparticles causes acute toxicity in cultured glial cells." Neurochemical Research 44(9): 2156-2169.

Karakoti, A., S. Singh, J. M. Dowding, S. Seal and W. T. Self (2010). "Redox-active radical scavenging nanomaterials." Chemical Society Reviews 39(11): 4422-4432.

Korsvik, C., S. Patil, S. Seal and W. T. Self (2007). "Superoxide dismutase mimetic properties exhibited by vacancy engineered ceria nanoparticles." Chemical Communications(10): 1056-1058.

Kostova, I. and M. Traykova (2006). "Cerium (III) and Neodymium (III) Complexes as Scavengers of X/XODerived Superoxide Radical." Medicinal Chemistry 2(5): 463-470.

Kostova, I., M. Traykova and V. K. Rastogi (2008). "New lanthanide complexes with antioxidant activity." Medicinal Chemistry 4(4): 371-378.

Kozuch, S. and J. M. Martin (2012). ""Turning over" definitions in catalytic cycles." ACS Catalysis 2(12): 2787-2794.

Lee, S. S., W. Song, M. Cho, H. L. Puppala, P. Nguyen, H. Zhu, L. Segatori and V. L. Colvin (2013). "Antioxidant properties of cerium oxide nanocrystals as a function of nanocrystal diameter and surface coating." ACS Nano 7(11): 9693-9703.

Li, Y., X. He, J. J. Yin, Y. Ma, P. Zhang, J. Li, Y. Ding, J. Zhang, Y. Zhao and Z. Chai (2015). "Acquired superoxide-scavenging ability of ceria nanoparticles." Angewandte Chemie 127(6): 1852-1855.

Liguori, I., G. Russo, F. Curcio, G. Bulli, L. Aran, D. Della-Morte, G. Gargiulo, G. Testa, F. Cacciatore, D. Bonaduce and P. Abete (2018). "Oxidative stress, aging, and diseases." Clinical Interventions in Aging 13: 757-772.

Lord, M. S., B. L. Farrugia, C. M. Yan, J. A. Vassie and J. M. Whitelock (2016). "Hyaluronan coated cerium oxide nanoparticles modulate CD44 and reactive oxygen species expression in human fibroblasts." Journal of Biomedical Materials Research Part A 104(7): 1736-1746.

Lowry, O., N. Rosebrough, A. L. Farr and R. Randall (1951). "Protein measurement with the Folin phenol reagent." Journal of Biological Chemistry 193(1): 265-275.

Luther, E. M., C. Petters, F. Bulcke, A. Kaltz, K. Thiel, U. Bickmeyer and R. Dringen (2013). "Endocytotic uptake of iron oxide nanoparticles by cultured brain microglial cells." Acta Biomaterialia 9(9): 8454-8465.

Mäntele, W. and E. Deniz (2017). "UV–VIS absorption spectroscopy: Lambert-Beer reloaded." Spectrochimica Acta Part A: Molecular and Biomolecular Spectroscopy 173: 965-968.

Naganuma, T. (2017). "Shape design of cerium oxide nanoparticles for enhancement of enzyme mimetic activity in therapeutic applications." Nano Research 10: 199-217.

Nelson, B. C., M. E. Johnson, M. L. Walker, K. R. Riley and C. M. Sims (2016). "Antioxidant cerium oxide nanoparticles in biology and medicine." Antioxidants 5(2): 15.

Neves Carvalho, A., O. Firuzi, M. Joao Gama, J. van Horssen and L. Saso (2017). "Oxidative stress and antioxidants in neurological diseases: is there still hope?" Current Drug Targets 18(6): 705-718.

Orellana-Urzúa, S., I. Rojas, L. Líbano and R. Rodrigo (2020). "Pathophysiology of ischemic stroke: role of oxidative stress." Current Pharmaceutical Design 26(34): 4246-4260.

Petters, C. and R. Dringen (2015). "Uptake, metabolism and toxicity of iron oxide nanoparticles in cultured microglia, astrocytes and neurons." Springerplus 4(Suppl 1): L32.

Petters, C., E. Irrsack, M. Koch and R. Dringen (2014). "Uptake and metabolism of iron oxide nanoparticles in brain cells." Neurochemical Research 39(9): 1648-1660.

Petters, C., K. Thiel and R. Dringen (2016). "Lysosomal iron liberation is responsible for the vulnerability of brain microglial cells to iron oxide nanoparticles: comparison with neurons and astrocytes." Nanotoxicology 10(3): 332-342.

Pirmohamed, T., J. M. Dowding, S. Singh, B. Wasserman, E. Heckert, A. S. Karakoti, J. E. S. King, S. Seal and W. T. Self (2010). "Nanoceria exhibit redox state-dependent catalase mimetic activity." Chemical Communications 46(16): 2736-2738.

Popov, A. L., A. B. Shcherbakov, N. Zholobak, A. Y. Baranchikov and V. K. Ivanov (2017). "Cerium dioxide nanoparticles as third-generation enzymes (nanozymes)." Наносистемы: физика, химия, математика 8(6): 760-781.

Pöyhönen, S., S. Er, A. Domanskyi and M. Airavaara (2019). "Effects of neurotrophic factors in glial cells in the central nervous system: expression and properties in neurodegeneration and injury." Frontiers in Physiology 10: 486.

Puspita, L., S. Y. Chung and J.-w. Shim (2017). "Oxidative stress and cellular pathologies in Parkinson's disease." Molecular Brain 10: 1-12.

Qiu, Y., E. Rojas, R. A. Murray, J. Irigoyen, D. Gregurec, P. Castro-Hartmann, J. Fledderman, I. Estrela-Lopis, E. Donath and S. E. Moya (2015). "Cell uptake, intracellular distribution, fate and reactive oxygen species generation of polymer brush engineered CeO_{2-x} NPs." Nanoscale 7(15): 6588-6598.

Raichle, M. E. (2006). "The brain's dark energy." Science 314(5803): 1249-1250.

Rastedt, W., K. Thiel and R. Dringen (2017). "Uptake of fluorescent iron oxide nanoparticles in C6 glioma cells." Biomedical Physics & Engineering Express 3(3): 035007.

Ross, D. and D. Siegel (2021). "The diverse functionality of NQO1 and its roles in redox control." Redox Biology 41: 101950.

Rzigalinski, B. A. (2005). "Nanoparticles and cell longevity." Technology in Cancer Research & Treatment 4(6): 651-659.

Rzigalinski, B. A., C. S. Carfagna and M. Ehrich (2017). "Cerium oxide nanoparticles in neuroprotection and considerations for efficacy and safety." Wiley Interdisciplinary Reviews: Nanomedicine and Nanobiotechnology 9(4): e1444.

Scholes, F., C. Soste, A. Hughes, S. Hardin and P. Curtis (2006). "The role of hydrogen peroxide in the deposition of cerium-based conversion coatings." Applied Surface Science 253(4): 1770-1780.

Scirè, S. and L. Palmisano (2020). Cerium and cerium oxide: a brief introduction. Cerium Oxide (CeO_2): Synthesis, Properties and Applications, Elsevier: 1-12.

Seminko, V., P. Maksimchuk, G. Grygorova, E. Okrushko, O. Avrunin, V. Semenets and Y. Malyukin (2021). "Mechanism and dynamics of fast redox cycling in cerium oxide nanoparticles at high oxidant concentration." The Journal of Physical Chemistry C 125(8): 4743-4749.

Shcherbakov, A. B., N. M. Zholobak and V. K. Ivanov (2020). Biological, biomedical and pharmaceutical applications of cerium oxide. Cerium oxide (CeO_2): Synthesis, Properties and Applications, Elsevier: 279-358.

Sigler, P. B. and B. Masters (1957). "The hydrogen peroxide-induced Ce*(III)-Ce (IV) exchange System1." Journal of the American Chemical Society 79(24): 6353-6357.

Singh, N., S. K. NaveenKumar, M. Geethika and G. Mugesh (2021). "A cerium vanadate nanozyme with specific superoxide dismutase activity regulates mitochondrial function and ATP synthesis in neuronal cells." Angewandte Chemie International Edition 60(6): 3121-3130.

Singh, N., G. Sherin and G. Mugesh (2023). "Antioxidant and prooxidant nanozymes: from cellular redox regulation to next-generation therapeutics." Angewandte Chemie: e202301232.

Singh, R. and S. Singh (2019). "Redox-dependent catalase mimetic cerium oxide-based nanozyme protect human hepatic cells from 3-AT induced acatalasemia." Colloids and Surfaces B: Biointerfaces 175: 625-635.

Singh, S. (2016). "Cerium oxide based nanozymes: Redox phenomenon at biointerfaces." Biointerphases 11(4): 04B202.

Singh, S., T. Dosani, A. S. Karakoti, A. Kumar, S. Seal and W. T. Self (2011). "A phosphate-dependent shift in redox state of cerium oxide nanoparticles and its effects on catalytic properties." Biomaterials 32(28): 6745-6753.

Skorodumova, N., S. Simak, B. I. Lundqvist, I. Abrikosov and B. Johansson (2002). "Quantum origin of the oxygen storage capability of ceria." Physical Review Letters 89(16): 166601.

Song, W., S. Soo Lee, M. Savini, L. Popp, V. L. Colvin and L. Segatori (2014). "Ceria nanoparticles stabilized by organic surface coatings activate the lysosome-autophagy system and enhance autophagic clearance." ACS Nano 8(10): 10328-10342.

Sozarukova, M., M. Shestakova, M. Teplonogova, D. Y. Izmailov, E. Proskurnina and V. Ivanov (2020). "Quantification of free radical scavenging properties and SOD-like activity of cerium dioxide nanoparticles in biochemical models." Russian Journal of Inorganic Chemistry 65: 597-605.

Spadaro, M. C., P. Luches, G. Bertoni, V. Grillo, S. Turner, G. Van Tendeloo, S. Valeri and S. D'Addato (2016). "Influence of defect distribution on the reducibility of CeO_{2-x} nanoparticles." Nanotechnology 27(42): 425705.

Stapelfeldt, K., E. Ehrke, J. Steinmeier, W. Rastedt and R. Dringen (2017). "Menadione-mediated WST1 reduction assay for the determination of metabolic activity of cultured neural cells." Analytical Biochemistry 538: 42-52.

Steinmeier, J., S. Kube, G. Karger, E. Ehrke and R. Dringen (2020). "β-lapachone induces acute oxidative stress in rat primary astrocyte cultures that is terminated by the NQO1-inhibitor dicoumarol." Neurochemical Research 45(10): 2442-2455.

Thakur, N., P. Manna and J. Das (2019). "Synthesis and biomedical applications of nanoceria, a redox active nanoparticle." Journal of Nanobiotechnology 17(1): 1-27.

Thao, N. T. M., H. D. K. Do, N. N. Nam, N. K. S. Tran, T. T. Dan and K. T. L. Trinh (2023). "Antioxidant Nanozymes: Mechanisms, Activity Manipulation, and Applications." Micromachines 14(5): 1017.

Tian, Z., J. Li, Z. Zhang, W. Gao, X. Zhou and Y. Qu (2015). "Highly sensitive and robust peroxidase-like activity of porous nanorods of ceria and their application for breast cancer detection." Biomaterials 59: 116-124.

Tsunekawa, S., R. Sivamohan, S. Ito, A. Kasuya and T. Fukuda (1999). "Structural study on monosize CeO_{2-x} nano-particles." Nanostructured Materials 11(1): 141-147.

Tulpule, K., M. C. Hohnholt, J. Hirrlinger and R. Dringen (2014). Primary cultures of astrocytes and neurons as model systems to study the metabolism and metabolite export from brain cells. Brain Energy Metabolism, Springer: 45-72.

Urner, M., A. Schlicker, B. R. Z'graggen, A. Stepuk, C. Booy, K. P. Buehler, L. Limbach, C. Chmiel, W. J. Stark and B. Beck-Schimmer (2014). "Inflammatory response of lung macrophages and epithelial cells after exposure to redox active nanoparticles: effect of solubility and antioxidant treatment." Environmental Science & Technology 48(23): 13960-13968.

Van Noorden, C. and W. Frederiks (1993). "Cerium methods for light and electron microscopical histochemistry." Journal of Microscopy 171(1): 3-16.

Varlamova, E. G., A. S. Baryshev, S. V. Gudkov, V. A. Babenko, E. Y. Plotnikov and E. A. Turovsky (2023). "Cerium oxide nanoparticles protect cortical astrocytes from oxygen–glucose deprivation through activation of the Ca^{2+} signaling system." International Journal of Molecular Sciences 24(18): 14305.

Wang, J., C. Guo and Y. Cheng (1997). "Mechanism of cerium ion clearing superoxide radical." Journal of the Chinese Society of Rare Earths 15(2): 151-154.

Watermann, P. and R. Dringen (2023). "β-lapachone-mediated WST1 reduction as indicator for the cytosolic redox metabolism of cultured primary astrocytes." Neurochemical Research 48(7): 2148-2160.

Wei, F., C. J. Neal, T. S. Sakthivel, T. Kean, S. Seal and M. J. Coathup (2021). "Multi-functional cerium oxide nanoparticles regulate inflammation and enhance osteogenesis." Materials Science and Engineering: C 124: 112041.

Wei, H. and E. Wang (2013). "Nanomaterials with enzyme-like characteristics (nanozymes): next-generation artificial enzymes." Chemical Society Reviews 42(14): 6060-6093.

Willmann, W. and R. Dringen (2018). "Monitoring of the cytoskeleton-dependent intracellular trafficking of fluorescent iron oxide nanoparticles by nanoparticle pulse-chase experiments in C6 glioma cells." Neurochemical Research 43: 2055-2071.

Wu, L., H. Wiesmann, A. Moodenbaugh, R. Klie, Y. Zhu, D. Welch and M. Suenaga (2004). "Oxidation state and lattice expansion of CeO_{2-x} nanoparticles as a function of particle size." Physical Review B 69(12): 125415.

Xue, Y., Q. Luan, D. Yang, X. Yao and K. Zhou (2011). "Direct evidence for hydroxyl radical scavenging activity of cerium oxide nanoparticles." The Journal of Physical Chemistry C 115(11): 4433-4438.

Yu, S., S. Wang, Q. Luo, L. Wang, Z. Peng and X. Gao (1993). "Synthesis, characterization and scavenger effects of $OH^{\bullet}$ and $O^{-\bullet 2}$ radicals of lanthanide (III) complexes with pyruvic acid semicarbazone." Polyhedron 12(9): 1093-1096.

Zhang, F., S.-W. Chan, J. E. Spanier, E. Apak, Q. Jin, R. D. Robinson and I. P. Herman (2002). "Cerium oxide nanoparticles: size-selective formation and structure analysis." Applied Physics Letters 80(1): 127-129.

Zhang, K., D. Chen, K. Ma, X. Wu, H. Hao and S. Jiang (2018). "NAD(P)H: quinone oxidoreductase 1 (NQO1) as a therapeutic and diagnostic target in cancer." Journal of Medicinal Chemistry 61(16): 6983-7003.

Zhidkova, T., E. Proskurnina, E. Parfenov and Y. A. Vladimirov (2011). "Determination of superoxide dismutase and SOD-mimetic activities by a chemical system: Co_2/H_2O_2/lucigenin." Analytical and Bioanalytical Chemistry 401: 381-386.

Zhou, X., B. Wang, Y. Chen, Z. Mao and C. Gao (2013). "Uptake of cerium oxide nanoparticles and their influences on functions of A549 cells." Journal of Nanoscience and Nanotechnology 13(1): 204-215.

3 Summarizing Discussion

3.1 Coating, functionalization and physicochemical properties of cerium oxide nanoparticles

The CeONPs used in this study were commercially available from Sigma-Aldrich and were labeled as cerium (IV) nanoparticles with an average nominal size of 25 nm, as confirmed by TEM analysis (Chapter 2.1). The physicochemical characteristics of CeONPs dramatically influence their properties and, consequently, their behavior in biological systems (Lord et al., 2021). These properties stem from the precursor used and the method of synthesis (Nyoka et al., 2020). One of the major problems in translating research results into clinical advances is the lack of standardization of CeONPs (Zhao et al., 2017). To overcome this problem, the above-mentioned CeONPs were chosen as a standard alternative, since they are commercially available in many countries, are not influenced by the particular synthesis conditions of each investigation laboratory, and are tested for quality standards.

CeONPs were coated with dimercaptosuccinic acid (DMSA) by the initial binding of the negatively charged carboxyl groups of DMSA to the surface of CeONPs (Fig. 3.1), as previously described for iron oxide NPs (IONPs) (Geppert et al., 2011; Hohnholt et al., 2011; Petters et al., 2014) and copper oxide NPs (CuONPs) (Bulcke et al., 2014; Joshi et al., 2019). It has also been reported that DMSA forms a cage-like structure around the individual NPs. Such a cage-like structure results from the oxidation of the thiol groups, which then form intermolecular disulfide bridges between the DMSA molecules (Fauconnier et al., 1997; Geppert et al., 2011). This coating offers several advantages, that have already been described for IONPs (Rastedt et al., 2017) and CuONPs (Bulcke et al., 2014; Joshi et al., 2019). Due to its properties, DMSA has been used in heavy metal chelation therapy and shows high biocompatibility (Miller, 1998; Sevinç et al., 2012; Silva et al., 2016; Kim et al., 2019). Furthermore, coating with DMSA expands the use of the NPs, as its SH group allows the formation of a thioether bound to e.g. drugs (Kossatz et al., 2015), nucleic acids (Galli et al., 2017) or fluorescent dyes (Fig. 3.1) (Luther et al., 2013; Petters et al., 2014; Rastedt et al., 2017) as adapted for OG-DMSA-CeONPs within this thesis (Chapter 2.1).
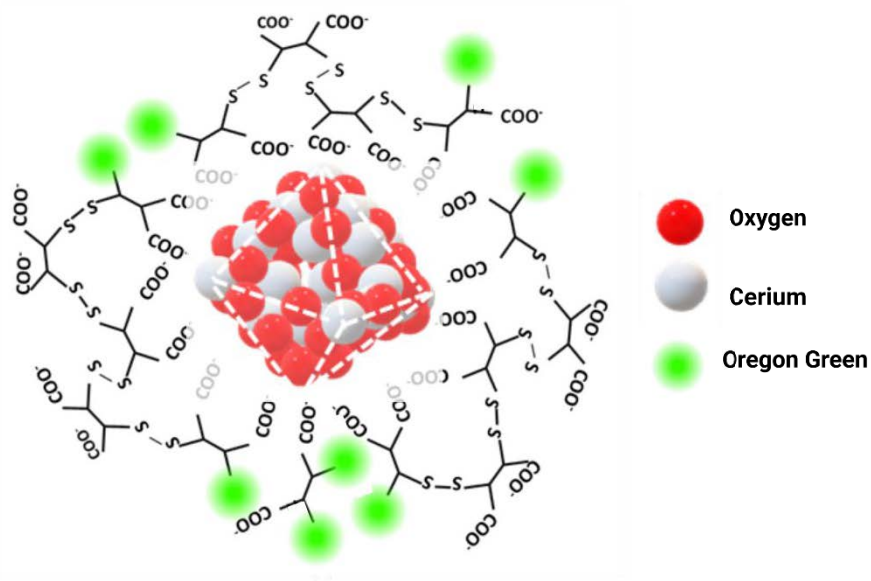
Figure 3.1. Fluorescent labeled CeONPs. CeONPs were first dispersed in H_2O and immediately after, coated with a solution containing DMSA and the fluorescent dye Oregon Green (OG). The adsorption of the coating to the surface is achieved by the binding of the negatively charged carboxyl groups and the positive surface of the CeONPs. The OG dye is attached to the coating by the formation of thioether bindings. Created using Biorender.

The DMSA coating did not significantly affect the hydrodynamic diameter of the CeONPs when dispersed in H_2O, nor the size distribution, as indicated by similar polydispersity indices for Un-CeONPs and DMSA-CeONPs (see Chapter 2.1). However, coating with DMSA shifted the zeta potential (ζ-potential) from positive to negative (see Chapter 2.1). Such a shift was not relevant for the colloidal stability in H_2O_2, as the strength of the surface repulsive forces was sufficient to avoid aggregation of the NPs. On the other hand, the shift in the ζ-potential and the presence of sulfur detected by energy dispersive X-ray spectroscopy for DMSA-CeONPs confirmed the successful coating of the NPs (Chapter 2.1).

Dejarguin-Landau-Verwey-Overbeek (DLVO) theory classically postulates that colloidal stability occurs when electrostatic repulsive forces counterbalance the van der Waals attractive forces (Derjaguin, 1941; Verwey and Overbeek, 1947). Afterwards, non-DLVO forces such as hydration, steric or magnetic forces have been added to more accurately describe the complexity of colloidal stability of dispersions and have been used to model the behavior of colloids in different solutions (Van Oss, 1989; Yotsumoto and Yoon, 1993; Boström et al., 2006). In the thesis presented here, Un-CeONPs and DMSA-CeONPs remained

stable and dispersed in pure H_2O after short ultrasonication, but after dispersion in protein-free physiological buffer, the NPs agglomerated and settled. DMSA-CeONPs, although also subject to sedimentation, exhibited a hydrodynamic diameter half that of Un-CeONPs under these conditions. Two main factors may contribute to this effect: a change in pH and the ionic strength of the media. The pH increases to 7.4 in the media and it approaches the isoelectric point or point of zero charge, where the ζ-potential reaches 0 mV and therefore, the electrostatic forces become negligible and cannot counterbalance the van der Waals attractive forces, leading to agglomeration and sedimentation. For Un-CeONPs, such an isoelectric point has been reported at around pH 8 (Baalousha et al., 2012) and this may explain the strong aggregation observed. Un-CeONPs and DMSA-CeONPs are affected by variations in the pH and therefore, steric forces do not seem to play a role in their colloidal stability. At the same time, the ionic strength of the solution was remarkably increased. Dispersion of NPs in ion-rich media but in the absence of proteins has been reported to significantly increase the hydrodynamic diameter of NPs showing an absolute value of ζ-potential greater than 15 mV (Saptarshi et al., 2013; Aires et al., 2017), as it was the case for Un-CeONPs and DMSA-CeONPs (Chapter 2.1). Explained in terms of the extended DLVO theory, such an increase in ionic strength exerts a certain compression on the electric double layer formed by the ions with opposite charge to that of the NPs at the surface which are distributed in a diffuse layer around the NPs, thus reducing the colloidal stability of the suspension. It has also been described that NPs, whose colloidal behavior is determined by electrostatic forces, tend to aggregate more frequently in the presence of multivalent electrolytes due to shielding of the electrostatic forces (Allen and Matijević, 1969; Galli et al., 2020).

The addition of protein, in the form of bovine serum albumin (BSA) or fetal calf serum (FCS) prevented agglomeration. This phenomenon has also been reported for gold NPs (Mahl et al., 2010), ZnONPs (Tantra et al., 2010), IONPs (Geppert et al., 2011) or CuONPs (Bulcke et al., 2014). However, a contradictory destabilization of the NPs when introduced into a medium containing serum have also been described (Mahmoudi et al., 2011). In this thesis, BSA or FCS are likely to improve the stability of NPs in ion-rich media by forming a protein corona of albumin. It is hypothesized that such an albumin-corona avoids an uncontrolled and non-uniform protein adsorption and therefore, leads to an increase in the colloidal stability of the NPs. The specific adsorption mechanisms of the protein to Un-CeONPs or DMSA-CeONPs were not the focus of this study, but previous reports have found that albumin most likely binds to the NPs surface via electrostatic interactions (Treuel et al.,

2015). Despite the importance of the protein corona and its interaction with the NPs, the knowledge in this field is still limited, more likely due to the complexity of its analysis.

The addition of BSA or FCS may also facilitate the uptake of DMSA-CeONPs by astrocytes or C6 glioma cells (Walkey et al., 2015). Furthermore, it has been observed *in vivo* that intraperitoneal injections of NPs form a spontaneous protein corona, the main component of which is albumin (Konduru et al., 2017; Simon et al., 2021), as albumin is found in high concentration in blood (Moman et al., 2017). Along this line, the *in vitro* study of DMSA-CeONPs in the presence of albumin or FCS may better mimic *in vivo* conditions. However, the presence of BSA and FCS presents also disadvantages. The physicochemical properties of the NPs are strongly influenced by the properties of the protein corona. Moreover, factors such as the thickness of the protein adsorption, the full or patched cover of the NPs and the stability of the corona can hinder the catalytic activities of the NPs. For example, Ju et al. (2020) observed that commercial CeONPs lost almost all of their antioxidant activity when fetal bovine serum was added to the medium compared to serum free medium.

The colloidal stability of Un-CeONPs and DMSA-CeONPs was strongly reduced in the presence of phosphate. In PBS, which contains 20 mM phosphate, the NPs strongly agglomerated. Similarly, when dispersed in IB-BSA containing phosphate (0.8 mM), their hydrodynamic diameter tended to increase significantly. In this thesis, phosphate was left out in the preparation of IB or IB-BSA to avoid interfering with the colloidal stability of the NPs and PBS was not used to disperse them. Interestingly, DMEM contains ~1 mM phosphate but in this case, no effects on the hydrodynamic diameter or polydispersity index were observed. Previous reports have described that CeONPs also agglomerate in the presence of high concentrations of phosphate (Singh et al., 2011). Some other investigations have pointed out that Ce^{3+}, but not Ce^{4+}, on the surface of the NPs interacts with the phosphate anion and even lead to the depletion of the superoxide dismutase mimic activity of such NPs (Singh et al., 2011; McCormack et al., 2014; Singh and Singh, 2015).

Taken together, DMSA-CeONPs dispersed in IB-BSA in the absence of phosphate or in DMEM containing 10% FCS, possessed high stability and were considered as suitable tool to further investigate their biocompatibility, uptake and accumulation by glial cells and their potential as reactive oxidant species (ROS) scavengers.

3.2 Uptake and accumulation of cerium in glial cells

Data on the uptake of CeONPs are scattered and highly subjected to specific CeONPs and cell lines. Furthermore, the internalization and fate of CeONPs by glial cells has not been investigated in detail. Most of the publications focus on the investigation of the biological activity of CeONPs and the uptake is only confirmed by the quantification of the cerium content, thus overlooking the specific mechanism or the kinetics of uptake. In this thesis, two different methods were adapted to investigate their internalization. DMSA-CeONPs were successfully functionalized with the fluorescent dye Oregon Green (OG) and their uptake, by C6 glioma cells and astrocytes, was monitored microscopically. Cerium uptake was also quantitatively assessed by ICP-OES. DMSA-CeONPs did not simply diffuse across the cell membrane of glial cells, but were actively internalized as indicated by the increase in intracellular cerium detected by fluorescence microscopy and ICP-OES when cells were incubated in the presence of DMSA-CeONPs at 37°C compared to 4°C. At 4°C, the fluorescence signal was weak and diffuse and can be interpreted as the signal from the fluorescent NPs adsorbed extracellularly to the cell membrane. Indeed, glial cells accumulated DMSA-CeONPs in a time- and temperature-dependent manner (Chapter 2.1). The accumulation of DMSA-CeONPs was rapid and after only 15 min OG-DMSA-CeONPs were already visible intracellularly. Furthermore, from the observations presented in this thesis, it can be concluded that astrocytes and C6 glioma cells appear to have similar mechanisms and kinetics for the internalization of DMSA-CeONPs, at least when exposed to a high concentration (1 mM) and for short incubation times. This is consistent with the findings of Asati et al. (2011) on the internalization of CeONPs in healthy versus cancer cells (Table 3.1). These authors did not find differences in the uptake due to the type of cell investigated but due to the surface charge of the CeONPs applied.

It is hypothesized that DMSA-CeONPs are taken up by glial cells by endocytosis, as has been described for CeONPs in several cell lines (Singh et al., 2010; Chen et al., 2013; Vassie et al., 2017; Wang et al., 2021). This is in line with previous findings that show that metal oxide NPs are generally internalized by endocytic pathways irrespective of the cell line studied (Iversen et al., 2011; Chen et al., 2017; Rennick et al., 2021). Such uptake of DMSA-CeONPs is proposed to follow several steps: (1) adhesion to the cell surface membrane, (2) vesicle formation by deformation of the plasma membrane (3) detachment of the vesicle from the membrane (4) migration of the vesicles to specific subcellular targets and finally (5) storage in endosomes or lysosomes for digestion or degradation. The accumulation of OG-DMSA-CeONPs in endosomes is suggested by the observation of a dotted intense fluorescence

signal after 30 min, which appears to migrate to perinuclear locations over time. Such a signal is thought to be generated by the accumulation of many OG-DMSA-CeONPs at this site. Lysosomal formation has been shown to require ~30 min (Canton and Battaglia, 2012; Thimiri Govinda Raj and Khan, 2016), which is consistent with the microscopic observations of this thesis. In this line, CeONPs have been reported to accumulate in different compartments of the endocytic pathway, as summarized below (Table 3.1). Such accumulation has been shown to be cell- and NP-dependent (Canton and Battaglia, 2012; Rennick et al., 2021).

Glial cells have been studied for the internalization of other types of NPs, such as DMSA-IONPs and DMSA-CuONPs under conditions similar to those presented here. Indeed, these NPs share, some hallmarks with DMSA-CeONPs. Uptake by C6 glioma cells and astrocytes occurs in a time-, concentration and temperature-dependent manner (Geppert et al., 2011; Bulcke et al., 2014; Petters et al., 2014; Petters and Dringen, 2015; Joshi et al., 2019) and the accumulation of these NPs shows no differences between C6 glioma cells or cultured astrocytes (Geppert et al., 2011; Rastedt et al., 2017; Willmann and Dringen, 2018; Joshi et al., 2019). However, the amount of DMSA-IONPs taken up by the cells is clearly higher than the amount of DMSA-CuONPs (Rastedt et al., 2017; Joshi et al., 2019). The intracellular content of cerium observed in this thesis after incubation at 37°C for 1 h is much more similar to that of DMSA-CuONPs (Joshi et al., 2019). Interestingly, the incubations of DMSA-CuONPs and DMSA-CeONPs, were performed in the presence of BSA. Previous studies have also shown that absolute uptake, both in C6 glioma cells and cultured astrocytes, is reduced by 80-90% in serum enriched medium. This observation has also been reported for other neural cells (Geppert et al., 2013; Petters et al., 2014; Petters and Dringen, 2015) and for other types of NPs (Ju et al., 2020). Such a decrease in accumulation, compared to DMSA-IONPs, can therefore be attributed to the protein corona, which may limit the adsorption of the NPs to the cell membrane. In the case of DMSA-CeONPs, as mentioned above, the addition of serum to the incubation medium was mandatory to avoid agglomeration and sedimentation. Also, considering their potential use as nanotherapeutics, the presence of a protein corona mimics more realistic *in vivo* conditions, and therefore, the study of the uptake under these conditions provides a better understanding of the accumulation.

Table 3.1. Trafficking of fluorescent CeONPs reported in diverse mammalian cell types

Labeling dye	Size[a] (nm)	ζ-potential[b] (mV)	Cell organelle[c]	Cell type	Reference
FITC[1]	8	-10*	Endosomes, lysosomes	Macrophage and epithelial cells	Xia et al. (2008)
Carboxyfluorescein	50	-18.2***	Cytoplasm, mitochondria, lysosome nucleus	Human keratinocytes	Singh et al. (2010)
DiI[2]	3±0.5	~+25[N/A]	Lysosome	Cardiac myocites, embryonic kidney cells, lung carcinoma cells	Asati et al. (2011)
		~0[N/A]	Cytoplasm	Cardiac myocytes, embryonic kidney cells, lung and breast carcinoma cells	
		~-43[N/A]	Lysosome	Lung carcinoma cells	
ATTO 647 N-APS	18± 5	-24.0 ± 0.3**	Endosome, secondary lysosome and cytoplasm	Microvascular endothelial cells	Strobel et al. (2015)
FITC[1]	7	+4.82****	Cytoplasm, endosome, caveolae and lysosome	Human ovarian and colon cancer cells	Vassie et al. (2017)
	94	N/A[3]			
Cy5	7,8	-1.1***** +5.8*****	Endosome	Brain endothelial cells	Goujon et al. (2021)
Cy5.5	5	-3.9	Lysosome	Brain microvascular endothelial cells and hippocampal neurons	Li et al. (2022)

Abbreviations: [1]FITC: fluorescein isothiocyanate; [2]DiI: Dioctadecyl-3,3,3′,3′-tetramethylindocarbocyanine perchlorate, [3]N/A: not available
(a) Size and form determined by TEM
(b) ζ-potential determined by ELS: in *cell medium, ** cell medium enriched with serum, ***pBS, **** water, ***** acetate buffer
(c) Cell organelles in which CeONPs were determined to be localized once internalized by the cells

Further comparison shows that the cellular uptake of NPs is also limited by another factor, which may be independent of the nature or the physicochemical properties of the different DMSA-NPs and is more likely conditioned by the cell type. Adsorption of the DMSA-IONPs, DMSA-CuONPs and DMSA-CeONPs to the cell membrane resulted in 70% of the total metal detected when the cells were incubated at 37°C (Bulcke et al., 2014; Rastedt et al., 2017; Joshi et al., 2019)(Chapter 2.1). These data may indicate that the maximum uptake rate is reached under these conditions, and thus, the adsorption process or the endocytic mechanisms in glial cells actually limit internalization rather than the nature or the physicochemical conditions of the different NPs in glial cells.

The uptake of ionic cerium into cells is more difficult to elucidate than that of CeONPs because it cannot be tracked by fluorescent labelling and observed under the microscope. In fact, no specific studies on the uptake and the possible transporters involved in cerium uptake in mammalian cells could be found in the literature. However, in the present thesis, it was observed by ICP-OES that the amount of ionic cerium internalized by astrocytes after 3 days of incubation is 16 times lower than if presented as NPs (Chapter 2.2). This suggests that NPs presenting a protein corona are more effectively taken up by cultured astrocytes *via* endocytosis than cerium ions. However, another possibility that cannot be ruled out is that the aforementioned adsorption of DMSA-CeONPs to the cell membrane occurs to a greater extent and is accounted for as internalized cerium when quantified by ICP-OES, whereas non-internalized ionic cerium is effectively washed away.

3.3   Cell viability and proliferation of glial cells treated with cerium

CeONPs are considered to be biocompatible as thoroughly demonstrated *in vitro* with different cell types (Fisichella et al., 2014; Urner et al., 2014; Forest et al., 2017) and even *in vivo* (reviewed in Dhall and Self (2018). However, several reports pointing out some toxicity can also be found in the literature (Yokel et al., 2014; Gagnon and Fromm, 2015; Rosário et al., 2020; García-Salvador et al., 2021). The redox activity of CeONPs has been identified as a determining factor for their toxicity (Datta et al., 2020). As an important first step, results showed that incubation with DMSA-CeONPs or ionic cerium did not affect cell viability of glial cells under the conditions tested, and therefore, these compounds can be considered as biocompatible (Chapter 2.1, 2.2 and 2.3).

However, the investigation of antioxidants aims at identifying compounds that increase the lifespan of cells (Gulcin, 2020), usually demonstrated by a reduction in apoptotic cells (Kahl et al., 2004; Park et al., 2020). Cell death is the result of a very complex mechanism that can be triggered by the activation of different signalling cascades (Ryter et al., 2007). Exogenous H_2O_2 is widely used to activate the apoptotic pathway. In a pioneering study concerning biomedical applications of CeONPs, Rzigalinski (2005) observed an increase in lifespan in cells treated with CeONPs. Furthermore, CeONPs have also been reported to reduce the proportion of apoptotic cells induced by H_2O_2 in a concentration-dependent manner (Chen et al., 2013; Arya et al., 2014; Zhou et al., 2014). These studies have shown that CeONPs reduce several signals of apoptosis, such as DNA fragmentation and loss of mitochondrial membrane potential (Ryter et al., 2007) and these effects had been seen to be intrinsically linked to their antioxidant behaviour (Celardo et al., 2011; Chen et al., 2013; Arya et al., 2014). However, in the presented thesis, the loss of $\sim 50\%$ of the viability by application of H_2O_2 could not be prevented. The experimental setup presented here (Chapter 2.3) simulated an acute episode of oxidative stress. However, under these conditions neither DMSA-CeONPs nor cerium ions acted as ROS scavengers (Chapter 2.3) nor were able to reduce the extend of cell death in C6 glioma cells. Interestingly, CeONPs and ionic cerium did not act as antiproliferative compounds either. C6 glioma cells pre-incubated with cerium did not show a further increase in the loss of intracellular LDH activity or protein content (Chapter 2.3).

Based on the literature, other possible scenario may have been that DMSA-CeONPs showed antiproliferative effects in C6 glioma cells. Indeed, CeONPs have been suggested as anticancer agents. Many studies have already reported that they cause selective apoptosis in cancer cells and even suppress the proliferation of tumour cells (reviewed by Gao et al. (2014)). DMSA-CeONPs caused a significant loss in proliferation only in C6 glioma cells preincubated with 1 mM DMSA-CeONPs for 24 h and incubated with 100 µM H_2O_2 (Chapter 2.3; Fig. 10). This observation may account for a synergistic effect and not only due to the presence of DMSA-CeONPs *per se* because, as shown in previous results (Chapter 2.1), DMSA-CeONPs at this concentration and incubation time showed no cytotoxicity in either astrocytes or glioma cells.

An interesting, and not thoroughly investigated question regarding proliferation, is how CeONPs are distributed in dividing cells and what are the consequences of the mitosis on the possible therapeutic effect of the NPs, particularly in cancer cells. In the case of CeONPs, there are no reports addressing this issue, and even the influence of CeONPs exposure on

the cell cycle remains controversial (Mittal and Pandey, 2014; Rosário et al., 2020). In this thesis, C6 glioma cells presented a rapid duplication rate (~20 h) (Joshi et al., 2016), and their microscopic observation revealed the presence of numerous cells in different phases of the mitosis (data not shown). Twenty-four hours preincubation with DMSA-CeONPs exceeds such doubling time, so all cells should have completed at least one division cycle during this time. However, how the different cell phases interfere with the uptake and how the cellular partitioning of the NPs occurred needs to be further investigated.

Regarding other types of NPs, Kim et al. (2012) showed that the rate of uptake of carboxylated polysterene NPs by human lung carcinoma cells was not affected by the cellular phase, but the total accumulation presented differed from cells entering the cell cycle as they could accumulate NPs longer than cells just dividing. In addition, Summers et al. (2011) showed that the partitioning of vesicles containing CdTe/ZnS quantum dots in human osteosarcoma cells was asymmetric and their dilution over generations was random but biased as it is the mitotic division of endosomes (Bergeland et al., 2001; Daeden and Gonzalez-Gaitan, 2018). Such asymmetry in vesicle partitioning may confer an adaptative advantage to cells, reducing the potential damage of an externally delivered toxin. This knowledge impacts on the future use of NPs as therapeutics, as it can be inferred that cancer cells experience greater dilution of the NP load than healthy cells, which replicate significantly less. Furthermore, the time required for glial to wash away CeONPs is also unknown, but it has been reported that human endothelial cells actively exocytose 70% of CeONPs within the first 48 h of incubation (Strobel et al., 2015). Although no data are available, some of this extrusion may also occur within the first 24 h. Taken together, these facts add additional uncertainty to any future pharmacodynamic prediction of the treatment with CeONPs against cancer.

3.4   Stimulation of astrocytic metabolism by cerium

As mentioned in the previous section, DMSA-CeONPs were not toxic to glial cells. In the present thesis, loss in cell viability was only observed in cells, which were subjected to an acute episode of oxidative stress after incubation with DMSA-CeONPs at a relatively high concentration (Chapter 2.3). However, DMSA-CeONPs caused an up-regulation of glucose metabolism in cultured astrocytes (Chapter 2.2), thus altering the metabolic homeostasis of the cells. Interestingly, the increase in extracellular lactate was similar to that caused by chemical stabilizers of the hypoxia inducible factor 1α (Hif-1α). Furthermore, cells preincubated with DMSA-CeONPs and main incubated with stabilizers of Hif-1α showed the

same acceleration in the glycolytic flux. The proposed stabilization of Hif-1α by DMSA-CeONPs could be caused by two different mechanisms: (1) DMSA-CeONPs caused local hypoxia and/or oxidative stress or (2) DMSA-CeONPs chemically interfered with the degradation of Hif-1α by, for example by inhibiting the prolyl hydroxylase domain-containing enzymes (PHDs). Similar stimulatory effects on the glycolysis were recorded for ionic cerium (Chapter 2.2). These observations seem to point out that cerium, regardless whether it is presented as NPs or in its ionic form, stabilized Hif-1α. It is therefore hypothesized that the cerium ions leaking from the NPs are ultimately responsible for the observed alterations.

To understand the likelihood that DMSA-CeONPs and/or ionic cerium stabilize Hif-1α, it may be noted that Hif-1α pathway is activated by oxygen-independent factors such as transition metals (Li et al., 2006; Aschner et al., 2023), nitric oxide (Sandau et al., 2001; Yang et al., 2023), ROS (Galanis et al., 2008; Movafagh et al., 2015), growth factors (Lee et al., 2004) or mechanical stress (Feng et al., 2017; Shimomura et al., 2021) (Fig. 3.2). Such stimuli typically trigger a complex cascade of responses in the cell leading to Hif-1α stabilization (Lee, 2021). Recent research has also included NPs as a potential stabilizer of Hif-1α (Aschner et al., 2023). In fact, CeONPs were previously suspected of causing hypoxic conditions in cells (Das et al., 2012). The authors reported that CeONPs activate Hif-1α by first sequestering intracellular oxygen and then releasing it when the flip-flop between Ce^{3+} and Ce^{4+} occurred. In a recent report, CeONPs were observed to significantly upregulate Hif-1α in human bone marrow-derived mesenchymal stem cells after irradiation (Wei et al., 2023). However, in this study the mechanism remains unknown. Other NPs have been found to stabilize Hif-1α. Similar to the results presented in this thesis, nickel oxide NPs were reported to leak nickel (II) ions after 24 h in human lung epithelial cells, causing the stabilization of Hif-1α by competing with iron sites on PHD (Pietruska et al., 2011). However, nickel oxide NPs caused a more potent and sustained activation of the Hif-1α signaling pathway. The authors conclude that the delivery of the nickel ions by ion transporters was less efficient than the endocytosis and release of ions after dissolution of the NPs (Pietruska et al., 2011). In the case of DMSA-CeONPs, it is thought that the NPs began to dissolve and release ions after accumulating in lysosomes as shown for nickel release from nickel oxide NPs, however, the mechanism for stabilizing Hif-1α may be the reaction of cerium with oxygen, leading to local hypoxia, as previously suggested by Das et al. (2012).

Ion leakage from CeONPs has not been systematically approached, much less in biomedical research. However, some ecological studies have assessed the dissolution of the NPs as an

indicator of toxicity. Dahle et al. (2015) showed that above pH 5, dissolved ions from CeONPs were not detected, while at more acidic values, the ions in solution increased inversely with pH. Similarly, Galyamin et al. (2022) showed that CeONPs dissolved over time at acidic pH, as Ce^{3+} ions remain in solution at this pH, they cannot be re-oxidized to Ce^{4+} and therefore, cannot regain the oxygen into their crystal fluorite structure. It was also determined that the dissolution rate increased with increasing acidification of the solution and decreasing size of the NPs (Galyamin et al., 2022). For example, at pH 4.4, 3 nm CeONPs dissolved in ~60 hours while at pH 1.7 it took less than 3 hours. Dissolution of NPs has also been observed for other metal NPs such as CuONPs or ZnONPs (Wang et al., 2013; Fatehah et al., 2014; Odzak et al., 2014; Wang et al., 2020). In the case of DMSA-CuONPs, the leakage of copper ions led to a significant increase in toxicity in cultured astrocytes and C6 glioma cells. Interestingly, the glycolytic flux was also accelerated under these conditions and correlated with the presence of ions (Bulcke and Dringen, 2015; Joshi et al., 2019). Furthermore, incubation of C6 glioma cells with DMSA-CuONPs and a copper chelator significantly reduced toxicity and extracellular lactate accumulation (Joshi et al., 2019).

The conditions for the dissolution of DMSA-CeONPs can be explained by their accumulation in lysosomes within the cells, as mentioned above. The characteristic pH in lysosomes is 4.5-5.0. In the present thesis, the time for the observation of an increase in the glycolytic flux was ~ 48 hours, which is also consistent with the time required for the engulfment and distribution of CeONPs within lysosomes of glial cells, and also with the dissolution rate shown by Galyamin et al (2022). However, an equivalent time was also required to stimulate the glycolytic flux of cultured astrocytes incubated with Ce^{3+} (Chapter 2.2). Therefore, the delay in the stimulation of the glycolytic flux cannot solely be explained by the time required for the dissolution of the DMSA-CeONPs inside the lysosomes or the time required for the internalization of ionic cerium, but also may depend on the time required for the stabilization of the Hif-1α factor, the start of transcription and the synthesis of proteins related to its stabilization. The stimulation of the glycolytic flux by copper also requires the synthesis of proteins (Scheiber and Dringen, 2011). In this line, in a preliminary study performed (data not shown), it was observed that cells preincubated with DMSA-CeONPs and then incubated for 3 days with an inhibitor of protein synthesis, cycloheximide, did not stimulate the glycolytic flux. These preliminary results seem to support the hypothesis that DMSA-CeONPs and ionic cerium stimulate the protein synthesis mediated by Hif-1α.
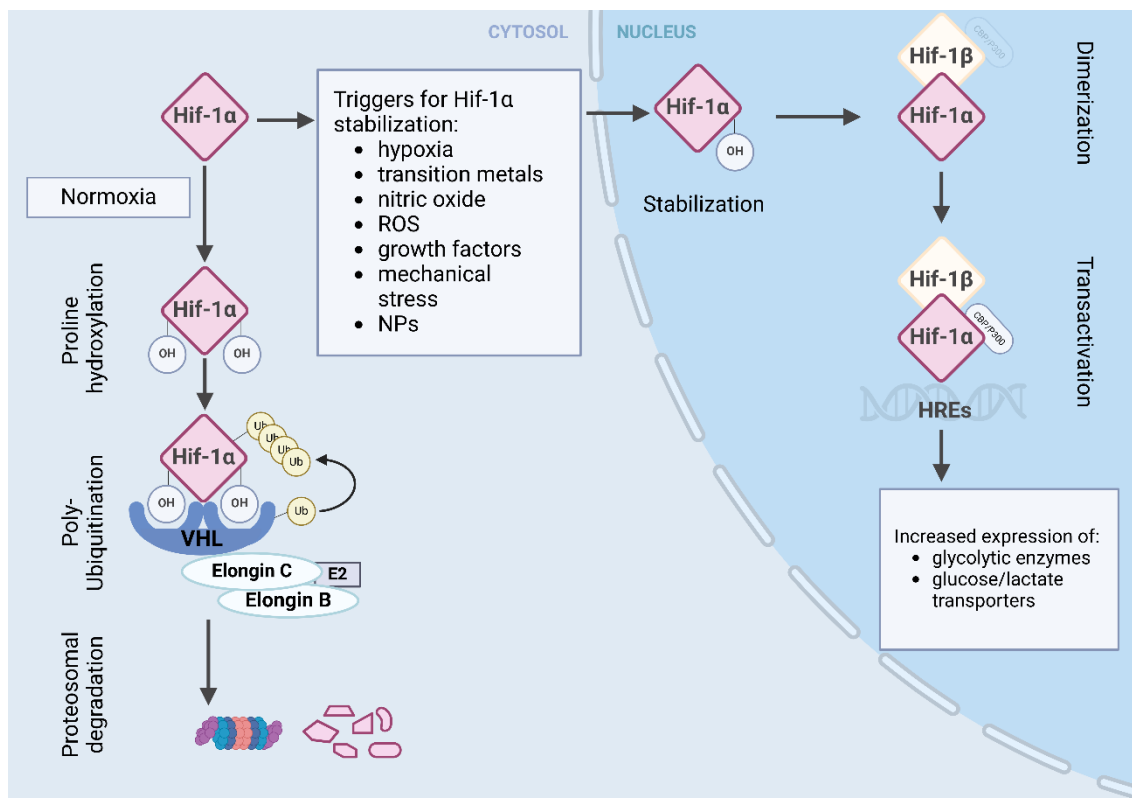
Figure 3.2. Schematic representation of the regulation of hypoxia-inducible factor 1 α (Hif-1α) pathway by the presence or absence of oxygen. Under normoxia, Hif-1α is hydroxylated by prolyl hydroxylase domain proteins. This allows the binding of von Hippel Landau (VHL) proteins which via Elongin C, recruits a ubiquitin ligase complex, leading to Hif-1α ubiquitination and proteosomal degradation. In the absence of oxygen or due to other stimuli, Hif-1α is stabilized and subsequently dimerize with a hypoxia-inducible factor 1 β (Hif-1β) subunit, enabling the interaction with hypoxia-responsive elements (HREs) in a wide range of gene promoters in the nucleus. This transactivation drives cellular responses to hypoxia which also involve the expression of genes codifying for glycolytic enzymes and glucose and lactate transporters. Created as an adaptation from Koyasu et al. (2018) using Biorender..

3.5 ROS scavenging potential of DMSA-CeONPs

The results shown in this thesis provide evidence for the ROS scavenging capacity of DMSA-CeONPs. However, this capacity was only detectable in the extracellular space (Chapter 2.3) as no proof for a potential scavenging of ROS in cells was observed when DMSA-CeONPs had been internalized.

The ROS scavenging capacity of CeONPs have accumulated a strong scientific evidence along the last two decades (Casals et al., 2020). Many studies have reported the scavenging of H_2O_2 and superoxide by CeONPs (Table 3.2) and have additionally attempted to infer intrinsic features that optimize such capacities. In this line, and as already discussed extensively in this thesis, the size, the shape, the ζ-potential, the Ce^{3+}/Ce^{4+} ratio, the coating, the protein corona or the synthesis method have been investigated (Lee et al., 2013; Gupta et al., 2016;

Naganuma, 2017; Dhall and Self, 2018; Singh et al., 2021; Wu and Ta, 2021). Similarly, the cell line, the uptake pathway or the subcellular environment have been tested to determine their influence on the ROS scavenging potential of CeONPs (De Marzi et al., 2013; Walkey et al., 2015; Nelson et al., 2016). This wealth of literature data seems to indicate that all these factors contribute to the effective scavenging of ROS by CeONPs, with size, Ce^{3+}/Ce^{4+} ratio, the protein corona and the subcellular environment being prominent limiting factors.

From the results obtained in the presented thesis, it can be stated that the coating and the protein corona do not limit the ROS scavenging capacity, since the experiments within this thesis included Un-CeONPs or ionic cerium as controls and showed similar results. However, from literature analysis, the limited scavenging activity of DMSA-CeONPs may be explained by its size. A reduction in their nominal size to 5 nm or less may result in an enhancement of its scavenging capacity. Cafun et al. (2013) observed that CeONPs with a nominal size of 25 nm did not react significantly with extracellular H_2O_2 compared to 3 and 10 nm CeONPs. This observation can be explained by the quantum confinement effect, which correlates a decreasing size with the presence of Ce^{3+} and oxygen vacancies (Skorodumova et al., 2002) and is consistent with other experimental reports where smaller NPs showed an enhanced scavenging activity (see references in Table 3.2). While DMSA-CeONPs did show extracellular scavenging capacity, these arguments may explain why 25 nm DMSA-CeONPs did not show catalase or SOD mimic behaviour but rather reacted stoichiometrically with H_2O_2 and superoxide.

The observation that DMSA-CeONPs did not act as a catalyst in ROS clearance had a major impact on the results presented here. Firstly, it lowers their potential relevance as nanotherapeutics as there are other antioxidant compounds that are also easily consumed during their interaction with ROS (i.e. ionic cerium, vitamins C, E or A) and may not present the risks of working in the nanoscale (Lee et al., 2020). In addition, the lack of catalytic activity, together with the influence of the subcellular environment, also limited to some extent the experiments to test their intracellular antioxidant capacity. Initially, it was hypothesized that DMSA-CeONPs would act as catalase and/or SOD nanozymes, and therefore, the experimental design envisaged loading the cells with such catalysts prior to the oxidative challenge. The pre-incubation times (1 and 24 h for the H_2O_2 incubation or 4 h for the superoxide test) and the different concentrations used were set up from uptake observations.

Direct incubation with ionic cerium was expected to reduce cell loss in a greater extent than DMSA-CeONPs, as extracellular $CeCl_3$ was shown to extracellularly scavenge significantly

more H_2O_2 than DMSA-CeONPs. However, after internalization, no protective effect was observed.

Table 3.2. Selected studies demonstrating CeONPs scavenging of ROS extracellularly (E) and/or intracellularly (I) in mammalian cells.

Size[a] (nm)	(E)/ (I)	Cell type	Pre-incubation time (h)	Reference
		H₂O₂		
				Rzigalinski (2005)
5	I	Retinal neurons	12, 24, 96	Chen et al. (2006)
2-5	E/I	Spinal cord neurons	30 days	Das et al. (2007)
10-15	E	-	-	Pirmohamed et al. (2010)
3, 10	E	-	-	Cafun et al. (2013)
5-80	I	PC12 neuronal-like cells	7, 2	Ciofani et al. (2013)
20	I	Endothelial cells		Chen et al. (2013)
9-11	E	-	-	Naganuma (2017)
2-3	E	-	-	Gil et al. (2017)
4.5, 8, 23, 28	E	-	-	Baldim et al. (2018)
2-2.5	E/I	Hippocampal brain slice	72	Estevez et al. (2019)
12	E/ I	Skin keratinocytes	3	Singh et al. (2021)
2	E/I	Osteoblastic cells	1	Ju et al. (2021)
4, 14	I	Kidney and bone marrow cells	24	Shlapa et al. (2022)
5, 8, 23, 28	E	-	-	Finocchiaro et al. (2023)
		Superoxide		
3-5	E			Korsvik et al. (2007)
16	E	-	-	Clark et al. (2011)
2-3	E	-	-	Gil et al. (2017)
4.5, 8, 23, 28	E	-	-	Baldim et al. (2018)
2-2.5	E/I	Hippocampal brain slice	72	Estevez et al. (2019)
82	I	Macrophage RAW 264.7	24	Khurana et al. (2019)
3	E	-	-	Sozarukova et al. (2020)
3-5	I	Retinal tissue	-	Shin et al. (2022)
12-18	E	-	-	Baranchikov et al. (2023)

[a]: determined by TEM

Further analysis of the data revealed that the H_2O_2 concentration in the media after 3 h incubation was minimal and independent of the presence or absence of cerium prior or not to the insult (Chapter 2.3). It demonstrates that the endogenous ROS detoxification mechanisms effectively removed exogenous H_2O_2 from the media. However, the ~50% loss of viability within 3 h could not be prevented. The experimental setup presented here simulates an acute episode of oxidative stress. C6 glioma cells had been seen to dispose 100 µM of exogenous H_2O_2 dissolved in 2 mL medium with a half-time of 15 min for a cell number of $4x10^5$ (Gülden et al., 2010). In addition, Gülden et al. (2010) also established that the viability of $4x10^5$ C6 glioma cells after 24 h of treating cells with 1 mL well^{-1} medium containing 100 µM H_2O_2 were reduced to the 50% compared to not treated cells. These results are very similar to the presented in this thesis. Differences on the amount of time required to observe the effects can be explained from the experimental setup and especially due to the volume of incubation used (Gülden et al., 2010). Wiese et al. (1995) pointed out that cell density may account for differences in H_2O_2-induced damages *in vitro*, however Gülden et al. (2010) only found statistical differences depending on cell concentration and incubation volume in the H_2O_2-detoxification by C6 glioma cells.

Different antioxidative systems are involved in the detoxification of H_2O_2 in glial cells (see Chapter 1, Fig. 1.2). Catalase activity in C6 glioma cells has been shown to be relatively high (Makino et al., 2008) but on the contrary, cells present a low glutathione peroxidase (GPx) activity (Makino et al 2008), at least when compared to astrocytes. These findings result in an antioxidant profile of C6 glioma cells based preferentially on catalase disproportionation. Astrocytes, in contrast, rely on a combined H_2O_2-detoxification driven by GPx and catalase. Other cell types, as for example human umbilical vein endothelial cells, presented an enhanced activity of glucose-6-phosphate dehydrogenase, involving that H_2O_2-detoxification first implies a strong activation of the oxidative step of the pentose phosphate pathway (Gülden et al., 2010).

CeONPs have previously been reported to efficiently mitigate the damage in acute episodes of oxidative stress (Table 3.2 and references therein). To significantly contribute to the intracellular detoxification of H_2O_2, CeONPs require access to H_2O_2 and need to present a low ratio Ce^{3+}/Ce^{4+} (Pirmohamed et al., 2010). Data from the presented thesis suggest that DMSA-CeONPs seem to accumulate in lysosomes and due to the pH probably favour a high Ce^{3+}/Ce^{4+} ratio. In the case of ionic cerium, $CeCl_3$, is presented as Ce^{3+}. These factors may account for the absence of cell protection against H_2O_2.

The superoxide dismutase (SOD) mimic activity of DMSA-CeONPs was also investigated by exploiting the endogenous generation of superoxide in the reduction of the electron cycler ß-lapachone. Such a reaction is coupled to the reduction of the extracellular water-soluble tetrazolium salt 1 (WST1) into the yellow WST1 formazan (Steinmeier et al., 2020), which it is then, measured by spectrophotometry. NQO1 seems to be the only responsible for the reduction of ß-lapachone and, therefore, when it is inhibited by dicoumarol, superoxide production is abolished (Steinmeier et al., 2020). This paradigm has recently been proposed as an indicator of the cytosolic redox metabolism of cultured primary astrocytes (Watermann and Dringen, 2023) and provides the framework to investigate the contribution of DMSA-CeONPs as extracellular redox scavengers. In this thesis, DMSA-CeONPs, and ionic cerium efficiently scavenged superoxide from the extracellular space under these conditions, but when cultured astrocytes were pre-incubated for 4 h with DMSA-CeONPs, no decrease of superoxide was recorded (Chapter 2.3).

Recently, Boey et al. (2021) reported that human hepatic stellate cells LX2 significantly reduced NQO1 expression when incubated for 24 h in the presence of 500 μM CeONPs. It should be noted that CeONPs were purchased from Sigma-Aldrich and were therefore identical to those used in the present thesis, except that they were not further coated with DMSA. A decrease in ROS generation was also observed by Boey et al (2021). As a result, the total activity of nuclear factor erythroid 2-related factor 2 (Nrf2) was also significantly reduced. Nrf2 is a key regulator that controls the cellular response to oxidative stress (Vomund et al., 2017; He et al., 2020). It controls the expression of phase II detoxification enzymes such as glutathione S-transferase (Chanas et al., 2002; Jaganjac et al., 2020), and enzymes directly involved in the detoxification of electrophiles such as NQO1 (Nioi et al., 2003; Dinkova-Kostova and Talalay, 2010).

As listed in Table 3.2, many reports have effectively determined the catalysis of H_2O_2 and/or superoxide removal by CeONPs. These and many other capabilities have earned them the name of nanozymes. This name was first time used in 2004 (Manea et al., 2004) for an assembly of triazacyclonane/Zn^{2+} in gold NPs and its use was expanded after the review of Wei and Wang (2013). However, some experts in the field of catalysis and enzymology are deliberately against this term (Scott et al., 2020). Indeed, their arguments were presented in the quoted ACS Catalysis editorial entitled "*Nano-apples and orange-zymes*" (Scott et al., 2020). It is argued that the principles that rule the ability of NPs to catalyse e.g. H_2O_2 disproportionation are not related to the principles of biochemistry or enzymatic catalysis. In this line, it is also observed that artificial enzymes preserve the essential features of the

original active site, which implies some structural and/or functional similarity to the native enzyme. Furthermore, the authors remark that the quantitative comparison between the scavenging potential of NPs and a specific enzymatic activity is misleading, since in many cases the number of active sites of the NPs is unknown. On the contrary, experts in the field of the nanomaterials (NMs) defend the use of the term nanozyme because these NMs catalyse the conversion of enzyme substrates into products and follow enzymatic kinetics (e.g. Michaelis Menten) although the ultimate mechanism differs from the corresponding native enzyme (Wei et al., 2021). In addition, there have been remarkable efforts to mimic the structural design of natural enzymes (Zhang et al., 2017; Benedetti et al., 2018; Li et al., 2020). Nanomaterials have also been proved to mimic enzymes *in vitro* and *in vivo*. For example, in a neuronal model of SOD deficiency, $CeVO_4$-NPs successfully replaced the function of SOD1 and SOD2 (Singh et al., 2021). After reviewing the literature on CeONPs, it is fair to say that there is some misuse of the term nanozyme. Not all CeONPs catalyse or even mimic enzymatic reactions. Nevertheless, authors may refer to them as nanozymes in their manuscripts. In the present thesis, DMSA-CeONPs reacted with H_2O_2 and superoxide under the conditions tested, but analysis of the data showed that the reaction was stoichiometric rather than enzymatic. Nevertheless, major advances have been made by the fusion of nanotechnology and enzymology and some NMs take credit for such "fuzzy" definition (Lehn, 1995; Wei et al., 2021). Therefore, NPs research has been and continues to be worth the effort, regardless of the term nanozyme, as it brings new knowledge and solutions in very different fields.

3.6   Reflections on the *in vivo*: relevance of the data obtained

CeONPs have been under investigation as antioxidants for approximately two decades and have yet to reach the clinical phase (Casals et al., 2020). Despite numerous *in vivo* studies being conducted, the potential adverse effects of CeONPs on the brain have not been the primary focus of this research. Recently, Mundekkad and Cho (2022) reviewed the clinical translation of different types of NPs for cancer therapy. The study highlighted several reasons why certain formulations approved by the Food and Drug Administration (USA) were never commercialized. For example, the unpredictable immunological reaction is mentioned, but the possibilities to interfere with brain functioning were not included (Mundekkad and Cho, 2022).

Of note, exposure to CeONPs may also occur unintentionally or even accidentally. Major sources of exposure to CeONPs arise from daily activities like exhaust fume from vehicles

or their use in agriculture (Li et al., 2016; You et al., 2021; Bathi et al., 2022). As a result, whether CeONPs are used for therapeutic purposes or are unintentionally inhaled or consumed, they pose a risk to health. Therefore, a risk/benefit assessment should be conducted prior to their regulation.

The presented DMSA-CeONPs showed no cytotoxicity. Nevertheless, incubation with ionic cerium and DMSA-CeONPs had an impact on the metabolism of healthy, cultured astrocytes. Cultured astrocytes serve as a commonly model system to investigate adverse effects of different compounds on the brain (Tulpule et al., 2014; Galland et al., 2019). This thesis empirically demonstrates that DMSA-CeONPs are biocompatible with glial cells, however, they increase lactate production in cultured astrocytes. Certain concern may arise as a disruption in lactic acid homeostasis in the brain is linked to alterations in neuronal energy supply and brain functioning (Chen et al., 2022). For example, an increase in lactate levels in the precuneus had also recently been correlated with mild cognitive impairment (Wang et al., 2017) or the accumulation of lactate in the dorsomedial hypothalamic nucleus had been shown to contribute to panic attack symptoms (Chen et al., 2022). Moreover, a severe accumulation of lactate may lead to a decrease in brain pH or acidosis (Li et al., 2023). Brain acidosis has been observed in ageing (Cunnane et al., 2020), cancer (Schwartz et al., 2020) and neurodegenerative diseases as Alzheimer's Disease or Parkinson's Disease (Yang et al., 2024). Therefore, the significance of this work translates to *in vivo* studies by remarking the potential side effects on the brain´s homeostasis that may occur following administration of CeONPs. It is hypothesized that the rise in extracellular lactate was due to cerium ions inducing local hypoxia, and it remains uncertain whether this oxygen sequestration would be mitigated when CeONPs actually catalyzes the intracellular ROS removal or exacerbated by their role as active scavengers. It may also have implications for the length of the exposure/treatment due to potential accumulation.

3.7 References

Aires, A., D. Cabrera, L. C. Alonso-Pardo, A. L. Cortajarena and F. J. Teran (2017). "Elucidation of the physicochemical properties ruling the colloidal stability of iron oxide nanoparticles under physiological conditions." ChemNanoMat 3(3): 183-189.

Allen, L. H. and E. Matijević (1969). "Stability of colloidal silica: I. Effect of simple electrolytes." Journal of Colloid and Interface Science 31(3): 287-296.

Arya, A., N. Sethy, M. Das, S. Singh, A. Das, S. Ujjain, R. Sharma, M. Sharma and K. Bhargava (2014). "Cerium oxide nanoparticles prevent apoptosis in primary cortical culture by stabilizing mitochondrial membrane potential." Free Radical Research 48(7): 784-793.

Asati, A., C. Kaittanis, S. Santra and J. M. Perez (2011). "pH-tunable oxidase-like activity of cerium oxide nanoparticles achieving sensitive fluorigenic detection of cancer biomarkers at neutral pH." Analytical hemistry 83(7): 2547-2553.

Aschner, M., A. V. Skalny, R. Lu, A. Santamaria, J.-C. Zhou, T. Ke, M. Y. Karganov, A. Tsatsakis, K. S. Golokhvast and A. B. Bowman (2023). "The role of hypoxia-inducible factor 1 alpha (HIF-1α) modulation in heavy metal toxicity." Archives of Toxicology 97(5): 1299-1318.

Baalousha, M., Y. Ju-Nam, P. A. Cole, B. Gaiser, T. F. Fernandes, J. A. Hriljac, M. A. Jepson, V. Stone, C. R. Tyler and J. R. Lead (2012). "Characterization of cerium oxide nanoparticles - Part 1: Size measurements." Environmental Toxicology and Chemistry 31(5): 983-993.

Baldim, V., F. Bedioui, N. Mignet, I. Margaill and J.-F. Berret (2018). "The enzyme-like catalytic activity of cerium oxide nanoparticles and its dependency on Ce^{3+} surface area concentration." Nanoscale 10(15): 6971-6980.

Baranchikov, A. E., M. Sozarukova, I. V. Mikheev, A. Egorova, E. Proskurnina, I. Poimenova, S. Krasnova, A. D. Filippova and V. Ivanov (2023). "Biocompatible ligands modulate nanozyme activity of CeO_2 nanoparticles." New Journal of Chemistry.

Bathi, J. R., L. Wright and E. Khan (2022). "Critical review of engineered nanoparticles: Environmental concentrations and toxicity." Current Pollution Reports 8(4): 498-518.

Benedetti, T. M., C. Andronescu, S. Cheong, P. Wilde, J. Wordsworth, M. Kientz, R. D. Tilley, W. Schuhmann and J. J. Gooding (2018). "Electrocatalytic nanoparticles that mimic the three-dimensional geometric architecture of enzymes: Nanozymes." Journal of the American Chemical Society 140(41): 13449-13455.

Bergeland, T., J. Widerberg, O. Bakke and T. W. Nordeng (2001). "Mitotic partitioning of endosomes and lysosomes." Current Biology 11(9): 644-651.

Boey, A., S. Q. Leong, S. Bhave and H. K. Ho (2021). "Cerium oxide nanoparticles alleviate hepatic fibrosis phenotypes in vitro." International Journal of Molecular Sciences 22(21): 11777.

Boström, M., V. Deniz, G. Franks and B. Ninham (2006). "Extended DLVO theory: Electrostatic and non-electrostatic forces in oxide suspensions." Advances in Colloid and Interface Science 123: 5-15.

Bulcke, F. and R. Dringen (2015). "Copper oxide nanoparticles stimulate glycolytic flux and increase the cellular contents of glutathione and metallothioneins in cultured astrocytes." Neurochemical Research 40(1): 15-26.

Bulcke, F., K. Thiel and R. Dringen (2014). "Uptake and toxicity of copper oxide nanoparticles in cultured primary brain astrocytes." Nanotoxicology 8(7): 775-785.

Cafun, J.-D., K. O. Kvashnina, E. Casals, V. F. Puntes and P. Glatzel (2013). "Absence of Ce^{3+} sites in chemically active colloidal ceria nanoparticles." ACS Nano 7(12): 10726-10732.

Canton, I. and G. Battaglia (2012). "Endocytosis at the nanoscale." Chemical Society Reviews 41(7): 2718-2739.

Casals, E., M. Zeng, M. Parra-Robert, G. Fernández-Varo, M. Morales-Ruiz, W. Jimenez, V. Puntes and G. Casals (2020). "Cerium oxide nanoparticles: advances in biodistribution, toxicity, and preclinical exploration." Small 16(20): 1907322.

Casals, E., M. Zeng, M. Parra-Robert, G. Fernández-Varo, M. Morales-Ruiz, W. Jiménez, V. Puntes and G. Casals (2020). "Cerium oxide nanoparticles: advances in biodistribution, toxicity, and preclinical exploration." Small 16(20): 1907322.

Celardo, I., M. De Nicola, C. Mandoli, J. Z. Pedersen, E. Traversa and L. Ghibelli (2011). "Ce^{3+} ions determine redox-dependent anti-apoptotic effect of cerium oxide nanoparticles." ACS Nano 5(6): 4537-4549.

Chanas, S. A., Q. Jiang, M. McMahon, G. K. McWalter, L. I. McLellan, C. R. Elcombe, C. J. Henderson, C. R. Wolf, G. J. Moffat and K. Itoh (2002). "Loss of the Nrf2 transcription factor causes a marked reduction in constitutive and inducible expression of the glutathione S-transferase Gsta1, Gsta2, Gstm1, Gstm2, Gstm3 and Gstm4 genes in the livers of male and female mice." Biochemical Journal 365(2): 405-416.

Chen, D., N. A. Monteiro-Riviere and L. W. Zhang (2017). "Intracellular imaging of quantum dots, gold, and iron oxide nanoparticles with associated endocytic pathways." Wiley Interdisciplinary Reviews: Nanomedicine and Nanobiotechnology 9(2): e1419.

Chen, J., S. Patil, S. Seal and J. F. McGinnis (2006). "Rare earth nanoparticles prevent retinal degeneration induced by intracellular peroxides." Nature Nanotechnology 1(2): 142-150.

Chen, S., Y. Hou, G. Cheng, C. Zhang, S. Wang and J. Zhang (2013). "Cerium oxide nanoparticles protect endothelial cells from apoptosis induced by oxidative stress." Biological Trace Element Research 154(1): 156-166.

Chen, S., Y. Hou, G. Cheng, C. Zhang, S. Wang and J. Zhang (2013). "Cerium oxide nanoparticles protect endothelial cells from apoptosis induced by oxidative stress." Biological Trace Element Research 154: 156-166.

Chen, X., Y. Zhang, H. Wang, L. Liu, W. Li and P. Xie (2022). "The regulatory effects of lactic acid on neuropsychiatric disorders." Discover Mental Health 2(1): 8.

Ciofani, G., G. G. Genchi, I. Liakos, V. Cappello, M. Gemmi, A. Athanassiou, B. Mazzolai and V. Mattoli (2013). "Effects of cerium oxide nanoparticles on PC12 neuronal-like cells: proliferation, differentiation, and dopamine secretion." Pharmaceutical Research 30: 2133-2145.

Cunnane, S. C., E. Trushina, C. Morland, A. Prigione, G. Casadesus, Z. B. Andrews, M. F. Beal, L. H. Bergersen, R. D. Brinton and S. de la Monte (2020). "Brain energy rescue: an emerging therapeutic concept for neurodegenerative disorders of ageing." Nature Reviews Drug Discovery 19(9): 609-633.

Daeden, A. and M. Gonzalez-Gaitan (2018). "Endosomal trafficking during mitosis and notch-dependent asymmetric division." Endocytosis and Signaling: 301-329.

Dahle, J. T., K. Livi and Y. Arai (2015). "Effects of pH and phosphate on CeO_2 nanoparticle dissolution." Chemosphere 119: 1365-1371.

Das, M., S. Patil, N. Bhargava, J. F. Kang, L. M. Riedel, S. Seal and J. J. Hickman (2007). "Auto-catalytic ceria nanoparticles offer neuroprotection to adult rat spinal cord neurons." Biomaterials 28(10): 1918-1925.

Das, S., S. Singh, J. M. Dowding, S. Oommen, A. Kumar, T. X. Sayle, S. Saraf, C. R. Patra, N. E. Vlahakis and D. C. Sayle (2012). "The induction of angiogenesis by cerium oxide nanoparticles through the modulation of oxygen in intracellular environments." Biomaterials 33(31): 7746-7755.

Datta, A., S. Mishra, K. Manna, K. D. Saha, S. Mukherjee and S. Roy (2020). "Pro-oxidant therapeutic activities of cerium oxide nanoparticles in colorectal carcinoma cells." ACS Omega 5(17): 9714-9723.

De Marzi, L., A. Monaco, J. De Lapuente, D. Ramos, M. Borras, M. Di Gioacchino, S. Santucci and A. Poma (2013). "Cytotoxicity and genotoxicity of ceria nanoparticles on different cell lines in vitro." International Journal of Molecular Sciences 14(2): 3065-3077.

Derjaguin, B. V. (1941). "Theory of the stability of strongly charged lyophobic sol and of the adhesion of strongly charged particles in solutions of electrolytes." Acta Physicochimica URSS 14: 633.

Dhall, A. and W. Self (2018). "Cerium oxide nanoparticles: a brief review of their synthesis methods and biomedical applications." Antioxidants 7(8): 97.

Dinkova-Kostova, A. T. and P. Talalay (2010). "NAD(P)H: quinone acceptor oxidoreductase 1 (NQO1), a multifunctional antioxidant enzyme and exceptionally versatile cytoprotector." Archives of Biochemistry and Biophysics 501(1): 116-123.

Estevez, A. Y., M. Ganesana, J. F. Trentini, J. E. Olson, G. Li, Y. O. Boateng, J. M. Lipps, S. E. Yablonski, W. T. Donnelly and J. C. Leiter (2019). "Antioxidant enzyme-mimetic activity and neuroprotective effects of cerium oxide nanoparticles stabilized with various ratios of citric acid and EDTA." Biomolecules 9(10): 562.

Fatehah, M. O., H. A. Aziz and S. Stoll (2014). "Stability of ZnO nanoparticles in solution. Influence of pH, dissolution, aggregation and disaggregation effects." Journal of Colloid Science and Biotechnology 3(1): 75-84.

Fauconnier, N., J. Pons, J. Roger and A. Bee (1997). "Thiolation of maghemite nanoparticles by dimercaptosuccinic acid." Journal of Colloid and Interface Science 194(2): 427-433.

Feng, S., N. Bowden, M. Fragiadaki, C. Souilhol, S. Hsiao, M. Mahmoud, S. Allen, D. Pirri, B. T. Ayllon and S. Akhtar (2017). "Mechanical activation of hypoxia-inducible factor 1α drives endothelial dysfunction at atheroprone sites." Arteriosclerosis, Thrombosis, and Vascular Biology 37(11): 2087-2101.

Finocchiaro, G., X. Ju, B. Mezghrani and J.-F. Berret (2023). "Cerium oxide catalyzed disproportionation of hydrogen peroxide: a closer look at the reaction intermediate." Chemistry–A European Journal: e202304012.

Fisichella, M., F. Berenguer, G. Steinmetz, M. Auffan, J. Rose and O. Prat (2014). "Toxicity evaluation of manufactured CeO_2 nanoparticles before and after alteration: combined physicochemical and whole-genome expression analysis in Caco-2 cells." BMC Genomics 15(1): 1-15.

Forest, V., L. Leclerc, J.-F. Hochepied, A. Trouvé, G. Sarry and J. Pourchez (2017). "Impact of cerium oxide nanoparticles shape on their in vitro cellular toxicity." Toxicology In Vitro 38: 136-141.

Gagnon, J. and K. M. Fromm (2015). "Toxicity and protective effects of cerium oxide nanoparticles (nanoceria) depending on their preparation method, particle size, cell type, and exposure route." European Journal of Inorganic Chemistry 2015(27): 4510-4517.

Galanis, A., A. Pappa, A. Giannakakis, E. Lanitis, D. Dangaj and R. Sandaltzopoulos (2008). "Reactive oxygen species and HIF-1 signalling in cancer." Cancer Letters 266(1): 12-20.

Galland, F., M. Seady, J. Taday, S. S. Smaili, C. A. Gonçalves and M. C. Leite (2019). "Astrocyte culture models: Molecular and function characterization of primary culture, immortalized astrocytes and C6 glioma cells." Neurochemistry International 131: 104538.

Galli, M., A. Guerrini, S. Cauteruccio, P. Thakare, D. Dova, F. Orsini, P. Arosio, C. Carrara, C. Sangregorio and A. Lascialfari (2017). "Superparamagnetic iron oxide nanoparticles functionalized by peptide nucleic acids." RSC Advances 7(25): 15500-15512.

Galli, M., S. Sáringer, I. Szilágyi and G. Trefalt (2020). "A simple method to determine critical coagulation concentration from electrophoretic mobility." Colloids and Interfaces 4(2): 20.

Galyamin, D., L. M. Ernst, A. Fitó-Parera, G. Mira-Vidal, N. G. Bastús, N. Sabaté and V. Puntes (2022). "Nanoceria dissolution at acidic pH by breaking off the catalytic loop." Nanoscale 14(38): 14223-14230.

Gao, Y., K. Chen, J.-l. Ma and F. Gao (2014). "Cerium oxide nanoparticles in cancer." OncoTargets and Therapy 7: 835-840.

García-Salvador, A., A. Katsumiti, E. Rojas, C. Aristimuño, M. Betanzos, M. Martínez-Moro, S. E. Moya and F. Goñi-de-Cerio (2021). "A complete in vitro toxicological assessment of the biological effects of cerium oxide nanoparticles: From acute toxicity to multi-dose subchronic cytotoxicity study." Nanomaterials 11(6): 1577.

Geppert, M., M. C. Hohnholt, K. Thiel, S. Nürnberger, I. Grunwald, K. Rezwan and R. Dringen (2011). "Uptake of dimercaptosuccinate-coated magnetic iron oxide nanoparticles by cultured brain astrocytes." Nanotechnology 22(14): 145101.

Geppert, M., C. Petters, K. Thiel and R. Dringen (2013). "The presence of serum alters the properties of iron oxide nanoparticles and lowers their accumulation by cultured brain astrocytes." Journal of Nanoparticle Research 15: 1-15.

Gil, D., J. Rodriguez, B. Ward, A. Vertegel, V. Ivanov and V. Reukov (2017). "Antioxidant activity of SOD and catalase conjugated with nanocrystalline ceria." Bioengineering 4(1): 18.

Goujon, G., V. Baldim, C. Roques, N. Bia, J. Seguin, B. Palmier, A. Graillot, C. Loubat, N. Mignet and I. Margaill (2021). "Antioxidant activity and toxicity study of cerium oxide nanoparticles stabilized with innovative functional copolymers." Advanced Healthcare Materials 10(11): 2100059.

Gulcin, İ. (2020). "Antioxidants and antioxidant methods: An updated overview." Archives of Toxicology 94(3): 651-715.

Gülden, M., A. Jess, J. Kammann, E. Maser and H. Seibert (2010). "Cytotoxic potency of H_2O_2 in cell cultures: impact of cell concentration and exposure time." Free Radical Biology and Medicine 49(8): 1298-1305.

Gupta, A., S. Das, C. J. Neal and S. Seal (2016). "Controlling the surface chemistry of cerium oxide nanoparticles for biological applications." Journal of Materials Chemistry B 4(19): 3195-3202.

He, F., X. Ru and T. Wen (2020). "NRF2, a transcription factor for stress response and beyond." International Journal of Molecular Sciences 21(13): 4777.

Hohnholt, M. C., M. Geppert and R. Dringen (2011). "Treatment with iron oxide nanoparticles induces ferritin synthesis but not oxidative stress in oligodendroglial cells." Acta Biomaterialia 7(11): 3946-3954.

Iversen, T.-G., T. Skotland and K. Sandvig (2011). "Endocytosis and intracellular transport of nanoparticles: Present knowledge and need for future studies." Nano Today 6(2): 176-185.

Jaganjac, M., L. Milkovic, S. B. Sunjic and N. Zarkovic (2020). "The NRF2, thioredoxin, and glutathione system in tumorigenesis and anticancer therapies." Antioxidants 9(11): 1151.

Joshi, A., W. Rastedt, K. Faber, A. G. Schultz, F. Bulcke and R. Dringen (2016). "Uptake and toxicity of copper oxide nanoparticles in C6 glioma cells." Neurochemical Research 41(11): 3004-3019.

Joshi, A., K. Thiel, K. Jog and R. Dringen (2019). "Uptake of intact copper oxide nanoparticles causes acute toxicity in cultured glial cells." Neurochemical Research 44(9): 2156-2169.

Ju, X., A. Fučíková, B. Šmíd, J. Nováková, I. Matolínová, V. Matolín, M. Janata, T. Bělinová and M. H. Kalbáčová (2020). "Colloidal stability and catalytic activity of cerium oxide nanoparticles in cell culture media." RSC Advances 10(65): 39373-39384.

Ju, X., M. H. Kalbacova, B. Šmíd, V. Johánek, M. Janata, T. N. Dinhová, T. Bělinová, M. Mazur, M. Vorokhta and L. Strnad (2021). "Poly (acrylic acid)-mediated synthesis of cerium oxide nanoparticles with variable oxidation states and their effect on regulating the intracellular ROS level." Journal of Materials Chemistry B 9(36): 7386-7400.

Kahl, R., A. Kampkötter, W. Wätjen and Y. Chovolou (2004). "Antioxidant enzymes and apoptosis." Drug Metabolism Reviews 36(3-4): 747-762.

Khurana, A., P. Anchi, P. Allawadhi, V. Kumar, N. Sayed, G. Packirisamy and C. Godugu (2019). "Superoxide dismutase mimetic nanoceria restrains cerulein induced acute pancreatitis." Nanomedicine: Nanotechnology, Biology, and Medicine 14(14): 1805-1825.

Kim, G. E., J. H. Park, J. S. Kim, K. S. Won and H. W. Kim (2019). "Comparison of Tc-99m DMSA renal planar scan and SPECT for detection of cortical defects in infants with suspected acute pyelonephritis." The Indian Journal of Pediatrics 86(9): 797-802.

Kim, J. A., C. Åberg, A. Salvati and K. A. Dawson (2012). "Role of cell cycle on the cellular uptake and dilution of nanoparticles in a cell population." Nature Nanotechnology 7(1): 62-68.

Konduru, N. V., R. M. Molina, A. Swami, F. Damiani, G. Pyrgiotakis, P. Lin, P. Andreozzi, T. C. Donaghey, P. Demokritou and S. Krol (2017). "Protein corona: implications for nanoparticle interactions with pulmonary cells." Particle and Fibre Toxicology 14: 1-12.

Korsvik, C., S. Patil, S. Seal and W. T. Self (2007). "Superoxide dismutase mimetic properties exhibited by vacancy engineered ceria nanoparticles." Chemical Communications(10): 1056-1058.

Kossatz, S., J. Grandke, P. Couleaud, A. Latorre, A. Aires, K. Crosbie-Staunton, R. Ludwig, H. Dähring, V. Ettelt and A. Lazaro-Carrillo (2015). "Efficient treatment of breast cancer xenografts with multifunctionalized iron oxide nanoparticles combining magnetic hyperthermia and anti-cancer drug delivery." Breast Cancer Research 17: 1-17.

Koyasu, S., M. Kobayashi, Y. Goto, M. Hiraoka and H. Harada (2018). "Regulatory mechanisms of hypoxia-inducible factor 1 activity: Two decades of knowledge." Cancer Science 109(3): 560-571.

Lee, J.-W., S.-H. Bae, J.-W. Jeong, S.-H. Kim and K.-W. Kim (2004). "Hypoxia-inducible factor (HIF-1) α: its protein stability and biological functions." Experimental and Molecular Medicine 36(1): 1-12.

Lee, K. H., M. Cha and B. H. Lee (2020). "Neuroprotective effect of antioxidants in the brain." International Journal of Molecular Sciences 21(19): 7152.

Lee, S. S., W. Song, M. Cho, H. L. Puppala, P. Nguyen, H. Zhu, L. Segatori and V. L. Colvin (2013). "Antioxidant properties of cerium oxide nanocrystals as a function of nanocrystal diameter and surface coating." ACS Nano 7(11): 9693-9703.

Lee, T.-Y. (2021). "Lactate: a multifunctional signaling molecule." Yeungnam University Journal of Medicine 38(3): 183.

Lehn, J.-M. (1995). Supramolecular Chemistry. Weinheim, Germany, VCH.

Li, M., J. Chen, W. Wu, Y. Fang and S. Dong (2020). "Oxidase-like MOF-818 nanozyme with high specificity for catalysis of catechol oxidation." Journal of the American Chemical Society 142(36): 15569-15574.

Li, Q., H. Chen, X. Huang and M. Costa (2006). "Effects of 12 metal ions on iron regulatory protein 1 (IRP-1) and hypoxia-inducible factor-1 alpha (HIF-1α) and HIF-regulated genes." Toxicology and Applied Pharmacology 213(3): 245-255.

Li, R., Y. Yang, H. Wang, T. Zhang, F. Duan, K. Wu, S. Yang, K. Xu, X. Jiang and X. Sun (2023). "Lactate and lactylation in the brain: current progress and perspectives." Cellular and Molecular Neurobiology 43: 2541-2555.

Li, X., Z. Han, T. Wang, C. Ma, H. Li, H. Lei, Y. Yang, Y. Wang, Z. Pei and Z. Liu (2022). "Cerium oxide nanoparticles with antioxidative neurorestoration for ischemic stroke." Biomaterials 291: 121904.

Li, Y., P. Li, H. Yu and Y. Bian (2016). "Recent advances (2010–2015) in studies of cerium oxide nanoparticles' health effects." Environmental Toxicology and Pharmacology 44: 25-29.

Lord, M. S., J. F. Berret, S. Singh, A. Vinu and A. S. Karakoti (2021). "Redox Active Cerium Oxide Nanoparticles: Current Status and Burning Issues." Small 17(51).

Luther, E. M., C. Petters, F. Bulcke, A. Kaltz, K. Thiel, U. Bickmeyer and R. Dringen (2013). "Endocytotic uptake of iron oxide nanoparticles by cultured brain microglial cells." Acta Biomaterialia 9(9): 8454-8465.

Mahl, D., C. Greulich, W. Meyer-Zaika, M. Köller and M. Epple (2010). "Gold nanoparticles: dispersibility in biological media and cell-biological effect." Journal of Materials Chemistry 20(29): 6176-6181.

Mahmoudi, M., I. Lynch, M. R. Ejtehadi, M. P. Monopoli, F. B. Bombelli and S. Laurent (2011). "Protein– nanoparticle interactions: opportunities and challenges." Chemical Reviews 111(9): 5610-5637.

Manea, F., F. B. Houillon, L. Pasquato and P. Scrimin (2004). "Nanozymes: Gold-nanoparticle-based transphosphorylation catalysts." Angewandte Chemie International Edition 43(45): 6165-6169.

McCormack, R. N., P. Mendez, S. Barkam, C. J. Neal, S. Das and S. Seal (2014). "Inhibition of nanoceria's catalytic activity due to Ce^{3+} site-specific interaction with phosphate ions." The Journal of Physical Chemistry C 118(33): 18992-19006.

Miller, A. L. (1998). "Dimercaptosuccinic acid (DMSA), a non-toxic, water-soluble treatment for heavy metal toxicity." Alternative Medicine Review: A Journal of Clinical Therapeutic 3(3): 199-207.

Mittal, S. and A. K. Pandey (2014). "Cerium oxide nanoparticles induced toxicity in human lung cells: role of ROS mediated DNA damage and apoptosis." BioMed research international 2014.

Moman, R. N., N. Gupta and M. Varacallo (2017). Physiology, Albumin. Treasure Island (FL), StatPearls Publishing.

Movafagh, S., S. Crook and K. Vo (2015). "Regulation of hypoxia-inducible factor-1a by reactive oxygen species: new developments in an old debate." Journal of Cellular Biochemistry 116(5): 696-703.

Mundekkad, D. and W. C. Cho (2022). "Nanoparticles in clinical translation for cancer therapy." International Journal of Molecular Sciences 23(3): 1685.

Naganuma, T. (2017). "Shape design of cerium oxide nanoparticles for enhancement of enzyme mimetic activity in therapeutic applications." Nano Research 10: 199-217.

Nelson, B. C., M. E. Johnson, M. L. Walker, K. R. Riley and C. M. Sims (2016). "Antioxidant cerium oxide nanoparticles in biology and medicine." Antioxidants 5(2): 15.

Nioi, P., M. McMahon, K. Itoh, M. Yamamoto and J. D. Hayes (2003). "Identification of a novel Nrf2-regulated antioxidant response element (ARE) in the mouse NAD (P) H: quinone oxidoreductase 1 gene: reassessment of the ARE consensus sequence." Biochemical Journal 374(2): 337-348.

Nyoka, M., Y. E. Choonara, P. Kumar, P. P. Kondiah and V. Pillay (2020). "Synthesis of cerium oxide nanoparticles using various methods: implications for biomedical applications." Nanomaterials 10(2): 242.

Odzak, N., D. Kistler, R. Behra and L. Sigg (2014). "Dissolution of metal and metal oxide nanoparticles under natural freshwater conditions." Environmental Chemistry 12(2): 138-148.

Park, H.-A., M. M. Hayden, S. Bannerman, J. Jansen and K. M. Crowe-White (2020). "Anti-apoptotic effects of carotenoids in neurodegeneration." Molecules 25(15): 3453.

Petters, C. and R. Dringen (2015). "Uptake, metabolism and toxicity of iron oxide nanoparticles in cultured microglia, astrocytes and neurons." Springerplus 4(Suppl 1): L32.

Petters, C., E. Irrsack, M. Koch and R. Dringen (2014). "Uptake and metabolism of iron oxide nanoparticles in brain cells." Neurochemical Research 39(9): 1648-1660.

Pietruska, J. R., X. Liu, A. Smith, K. McNeil, P. Weston, A. Zhitkovich, R. Hurt and A. B. Kane (2011). "Bioavailability, intracellular mobilization of nickel, and HIF-1α activation in human lung epithelial cells exposed to metallic nickel and nickel oxide nanoparticles." Toxicological Sciences 124(1): 138-148.

Pirmohamed, T., J. M. Dowding, S. Singh, B. Wasserman, E. Heckert, A. S. Karakoti, J. E. S. King, S. Seal and W. T. Self (2010). "Nanoceria exhibit redox state-dependent catalase mimetic activity." Chemical Communications 46(16): 2736-2738.

Rastedt, W., K. Thiel and R. Dringen (2017). "Uptake of fluorescent iron oxide nanoparticles in C6 glioma cells." Biomedical Physics & Engineering Express 3(3): 035007.

Rennick, J. J., A. P. Johnston and R. G. Parton (2021). "Key principles and methods for studying the endocytosis of biological and nanoparticle therapeutics." Nature Nanotechnology 16(3): 266-276.

Rosário, F., M. J. Bessa, F. Brandão, C. Costa, C. B. Lopes, A. C. Estrada, D. S. Tavares, J. P. Teixeira and A. T. Reis (2020). "Unravelling the potential cytotoxic effects of metal oxide nanoparticles and metal (Loid) mixtures on a549 human cell line." Nanomaterials 10(3): 447.

Ryter, S. W., H. P. Kim, A. Hoetzel, J. W. Park, K. Nakahira, X. Wang and A. M. Choi (2007). "Mechanisms of cell death in oxidative stress." Antioxidants & Redox Signaling 9(1): 49-89.

Rzigalinski, B. A. (2005). "Nanoparticles and cell longevity." Technology in Cancer Research & Treatment 4(6): 651-659.

Sandau, K. B., J. Fandrey and B. Brüne (2001). "Accumulation of HIF-1α under the influence of nitric oxide." Blood, The Journal of the American Society of Hematology 97(4): 1009-1015.

Saptarshi, S. R., A. Duschl and A. L. Lopata (2013). "Interaction of nanoparticles with proteins: relation to bio-reactivity of the nanoparticle." Journal of Nanobiotechnology 11(1): 1-12.

Scheiber, I. F. and R. Dringen (2011). "Copper accelerates glycolytic flux in cultured astrocytes." Neurochemical Research 36(5): 894-903.

Schwartz, L., S. Peres, M. Jolicoeur and J. da Veiga Moreira (2020). "Cancer and Alzheimer's disease: intracellular pH scales the metabolic disorders." Biogerontology 21: 683-694.

Scott, S., H. Zhao, A. Dey and T. B. Gunnoe (2020). "Nano-apples and orange-zymes." ACS Catalysis 10(23): 14315-14317.

Sevinç, E., F. S. Ertas, G. Ulusoy, C. Ozen and H. Y. Acar (2012). "Meso-2, 3-dimercaptosuccinic acid: from heavy metal chelation to CdS quantum dots." Journal of Materials Chemistry 22(11): 5137-5144.

Shimomura, S., H. Inoue, Y. Arai, S. Nakagawa, Y. Fujii, T. Kishida, M. Shin-Ya, S. Ichimaru, S. Tsuchida and O. Mazda (2021). "Mechanical stimulation of chondrocytes regulates HIF-1α under hypoxic conditions." Tissue and Cell 71: 101574.

Shin, C. S., R. A. Veettil, T. S. Sakthivel, A. Adumbumkulath, R. Lee, M. Zaheer, E. Kolanthai, S. Seal and G. Acharya (2022). "Noninvasive Delivery of Self-Regenerating Cerium Oxide Nanoparticles to Modulate Oxidative Stress in the Retina." ACS Applied Bio Materials 5(12): 5816-5825.

Shlapa, Y., S. Solopan, V. Sarnatskaya, K. Siposova, I. Garcarova, K. Veltruska, I. Timashkov, O. Lykhova, D. Kolesnik and A. Musatov (2022). "Cerium dioxide nanoparticles synthesized via precipitation at constant pH: Synthesis, physical-chemical and antioxidant properties." Colloids and Surfaces B: Biointerfaces 220: 112960.

Silva, L. H., J. R. da Silva, G. A. Ferreira, R. C. Silva, E. C. Lima, R. B. Azevedo and D. M. Oliveira (2016). "Labeling mesenchymal cells with DMSA-coated gold and iron oxide nanoparticles: assessment of biocompatibility and potential applications." Journal of Nanobiotechnology 14(1): 1-15.

Simon, J., G. Kuhn, M. Fichter, S. Gehring, K. Landfester and V. Mailänder (2021). "Unraveling the in vivo protein corona." Cells 10(1): 132.

Singh, N., S. K. NaveenKumar, M. Geethika and G. Mugesh (2021). "A cerium vanadate nanozyme with specific superoxide dismutase activity regulates mitochondrial function and ATP synthesis in neuronal cells." Angewandte Chemie International Edition 60(6): 3121-3130.

Singh, R. and S. Singh (2015). "Role of phosphate on stability and catalase mimetic activity of cerium oxide nanoparticles." Colloids and Surfaces B: Biointerfaces 132: 78-84.

Singh, S., T. Dosani, A. S. Karakoti, A. Kumar, S. Seal and W. T. Self (2011). "A phosphate-dependent shift in redox state of cerium oxide nanoparticles and its effects on catalytic properties." Biomaterials 32(28): 6745-6753.

Singh, S., A. Kumar, A. Karakoti, S. Seal and W. T. Self (2010). "Unveiling the mechanism of uptake and sub-cellular distribution of cerium oxide nanoparticles." Molecular Biosystems 6(10): 1813-1820.

Singh, S., U. Kumar, D. Gittess, T. S. Sakthivel, B. Babu and S. Seal (2021). "Cerium oxide nanomaterial with dual antioxidative scavenging potential: Synthesis and characterization." Journal of Biomaterials Applications 36(5): 834-842.

Skorodumova, N., S. Simak, B. I. Lundqvist, I. Abrikosov and B. Johansson (2002). "Quantum origin of the oxygen storage capability of ceria." Physical Review Letters 89(16): 166601.

Sozarukova, M., M. Shestakova, M. Teplonogova, D. Y. Izmailov, E. Proskurnina and V. Ivanov (2020). "Quantification of free radical scavenging properties and SOD-like activity of cerium dioxide nanoparticles in biochemical models." Russian Journal of Inorganic Chemistry 65: 597-605.

Steinmeier, J., S. Kube, G. Karger, E. Ehrke and R. Dringen (2020). "β-lapachone induces acute oxidative stress in rat primary astrocyte cultures that is terminated by the NQO1-inhibitor dicoumarol." Neurochemical Research 45(10): 2442-2455.

Strobel, C., H. Oehring, R. Herrmann, M. Förster, A. Reller and I. Hilger (2015). "Fate of cerium dioxide nanoparticles in endothelial cells: exocytosis." Journal of Nanoparticle Research 17: 1-14.

Summers, H. D., P. Rees, M. D. Holton, M. Rowan Brown, S. C. Chappell, P. J. Smith and R. J. Errington (2011). "Statistical analysis of nanoparticle dosing in a dynamic cellular system." Nature Nanotechnology 6(3): 170-174.

Tantra, R., J. Tompkins and P. Quincey (2010). "Characterisation of the de-agglomeration effects of bovine serum albumin on nanoparticles in aqueous suspension." Colloids and Surfaces B: Biointerfaces 75(1): 275-281.

Thimiri Govinda Raj, D. B. and N. A. Khan (2016). "Designer nanoparticle: nanobiotechnology tool for cell biology." Nano Convergence 3(1): 1-12.

Treuel, L., D. Docter, M. Maskos and R. H. Stauber (2015). "Protein corona–from molecular adsorption to physiological complexity." Beilstein Journal of Nanotechnology 6(1): 857-873.

Tulpule, K., M. C. Hohnholt, J. Hirrlinger and R. Dringen (2014). Primary cultures of astrocytes and neurons as model systems to study the metabolism and metabolite export from brain cells. Brain Energy Metabolism, Springer: 45-72.

Urner, M., A. Schlicker, B. R. Z'graggen, A. Stepuk, C. Booy, K. P. Buehler, L. Limbach, C. Chmiel, W. J. Stark and B. Beck-Schimmer (2014). "Inflammatory response of lung macrophages and epithelial cells after exposure to redox active nanoparticles: effect of solubility and antioxidant treatment." Environmental Science & Technology 48(23): 13960-13968.

Van Oss, C. J. (1989). "Energetics of cell-cell and cell-biopolymer interactions." Cell Biophysics 14: 1-16.

Vassie, J. A., J. M. Whitelock and M. S. Lord (2017). "Endocytosis of cerium oxide nanoparticles and modulation of reactive oxygen species in human ovarian and colon cancer cells." Acta Biomaterialia 50: 127-141.

Verwey, E. and J. T. G. Overbeek (1947). "Theory of the stability of lyophobic colloids." The Journal of Physical and Colloid Chemistry 51(3): 631-636.

Vomund, S., A. Schäfer, M. J. Parnham, B. Brüne and A. Von Knethen (2017). "Nrf2, the master regulator of anti-oxidative responses." International Journal of Molecular Sciences 18(12): 2772.

Walkey, C., S. Das, S. Seal, J. Erlichman, K. Heckman, L. Ghibelli, E. Traversa, J. F. McGinnis and W. T. Self (2015). "Catalytic properties and biomedical applications of cerium oxide nanoparticles." Environmental Science: Nano 2(1): 33-53.

Wang, F., E. Wang, J. Han, Y. Li, Y. Jin, F. Lv, C. Ren, H. Liu and G. Zhou (2021). "Cerium oxide nanoparticles promote proliferation of primary osteoblasts via cell cycle machinery in vitro." Journal of Nanoparticle Research 23: 1-11.

Wang, H., X. Tan, J. Xu, H. Li, M. Wang, S. Chen, X. Yang, Y. Liu and F. Wang (2017). "Negative correlation between CSF lactate levels and MoCA scores in male Chinese subjects." Psychiatry Research 255: 49-51.

Wang, X., T. Sun, H. Zhu, T. Han, J. Wang and H. Dai (2020). "Roles of pH, cation valence, and ionic strength in the stability and aggregation behavior of zinc oxide nanoparticles." Journal of Environmental Management 267: 110656.

Wang, Z., A. Von Dem Bussche, P. K. Kabadi, A. B. Kane and R. H. Hurt (2013). "Biological and environmental transformations of copper-based nanomaterials." ACS Nano 7(10): 8715-8727.

Watermann, P. and R. Dringen (2023). "β-lapachone-mediated WST1 reduction as indicator for the cytosolic redox metabolism of cultured primary astrocytes." Neurochemical Research 48(7): 2148-2160.

Wei, F., C. J. Neal, T. S. Sakthivel, Y. Fu, M. Omer, A. Adhikary, S. Ward, K. M. Ta, S. Moxon and M. Molinari (2023). "A novel approach for the prevention of ionizing radiation-induced bone loss using a designer multifunctional cerium oxide nanozyme." Bioactive Materials 21: 547-565.

Wei, H., L. Gao, K. Fan, J. Liu, J. He, X. Qu, S. Dong, E. Wang and X. Yan (2021). "Nanozymes: A clear definition with fuzzy edges." Nano Today 40: 101269.

Wei, H. and E. Wang (2013). "Nanomaterials with enzyme-like characteristics (nanozymes): next-generation artificial enzymes." Chemical Society Reviews 42(14): 6060-6093.

Wiese, A. G., R. E. Pacifici and K. J. Davies (1995). "Transient adaptation to oxidative stress in mammalian cells." Archives of Biochemistry and Biophysics 318(1): 231-240.

Willmann, W. and R. Dringen (2018). "Monitoring of the cytoskeleton-dependent intracellular trafficking of fluorescent iron oxide nanoparticles by nanoparticle pulse-chase experiments in C6 glioma cells." Neurochemical Research 43: 2055-2071.

Wu, Y. and H. T. Ta (2021). "Different approaches to synthesising cerium oxide nanoparticles and their corresponding physical characteristics, and ROS scavenging and anti-inflammatory capabilities." Journal of Materials Chemistry B 9(36): 7291-7301.

Xia, T., M. Kovochich, M. Liong, L. Madler, B. Gilbert, H. Shi, J. I. Yeh, J. I. Zink and A. E. Nel (2008). "Comparison of the mechanism of toxicity of zinc oxide and cerium oxide nanoparticles based on dissolution and oxidative stress properties." ACS Nano 2(10): 2121-2134.

Yang, C., R.-Y. Pan, F. Guan and Z. Yuan (2024). "Lactate metabolism in neurodegenerative diseases." Neural Regeneration Research 19(1): 69-74.

Yang, N., X. Yang, Y. Fang, Y. Huang, W. Shi, W. Li, M. Ding, Q. An and Y. Zhao (2023). "Nitric oxide promotes cerebral ischemia/reperfusion injury through upregulating hypoxia-inducible factor1-α-associated inflammation and apoptosis in rats." Neuroscience Letters 795: 137034.

Yokel, R. A., S. Hussain, S. Garantziotis, P. Demokritou, V. Castranova and F. R. Cassee (2014). "The yin: an adverse health perspective of nanoceria: uptake, distribution, accumulation, and mechanisms of its toxicity." Environmental Science: Nano 1(5): 406-428.

Yotsumoto, H. and R.-H. Yoon (1993). "Application of extended DLVO theory: I. Stability of rutile suspensions." Journal of Colloid and Interface Science 157(2): 426-433.

You, G., J. Hou, Y. Xu, L. Miao, Y. Ao and B. Xing (2021). "Surface properties and environmental transformations controlling the bioaccumulation and toxicity of cerium oxide nanoparticles: a critical review." Reviews of Environmental Contamination and Toxicology 253: 155-206.

Zhang, Z., X. Zhang, B. Liu and J. Liu (2017). "Molecular imprinting on inorganic nanozymes for hundred-fold enzyme specificity." Journal of the American Chemical Society 139(15): 5412-5419.

Zhao, Y., Y. Wang, F. Ran, Y. Cui, C. Liu, Q. Zhao, Y. Gao, D. Wang and S. Wang (2017). "A comparison between sphere and rod nanoparticles regarding their in vivo biological behavior and pharmacokinetics." Scientific Reports 7(1): 4131.

Zhou, G., Y. Li, B. Zheng, W. Wang, J. Gao, H. Wei, S. Li, S. Wang and J. Zhang (2014). "Cerium oxide nanoparticles protect primary osteoblasts against hydrogen peroxide induced oxidative damage." Micro & Nano Letters 9(2): 91-96.

4 Conclusions

This doctoral dissertation examines the impact of CeONPs on glial cells at the molecular level *in vitro*. The study investigates the interaction between CeONPs and two types of glial cells, providing evidence for the following outcomes:

- DMSA coating and the labelling with Oregon Green fluorescent dye is a cost-effective and straightforward method for functionalizing commercially available CeONPs. The resulting DMSA-CeONPs remain stable on a nanoscale level and exhibit a negative ζ-potential in physiological media. These characteristics make them a useful tool for investigating the *in vivo* interactions between NPs and glial cells. To our knowledge, this is the first study to examine such functionalization of CeONPs.

- The internalization of DMSA-CeONPs by C6 glioma cells and cultured astrocytes depends on active internalization mechanisms, most likely via endocytosis. The uptake is time- and concentration-dependent and rapid. Endosomes and/or lysosomes containing DMSA-CeONPs were present in the cytosol after only 15 min and migrated over time towards perinuclear sites, as demonstrated by the observation of strong fluorescent dots inside the cells.

- DMSA-CeONPs accumulate in cultured astrocytes in a temperature-, concentration- and time-dependent manner. The total cerium content can be assessed using ICP-OES, which is a time and cost-efficient technique.

- DMSA-CeONPs have demonstrated biocompatibility with C6 glioma cells and cultured astrocytes for up to 72 h across a range of concentrations, reaching up to 1 mM. Cell membrane integrity is maintained during uptake and subsequent accumulation of the NPs. Furthermore, ionic cerium has not displayed cytotoxicity towards glial cells under the conditions tested.

- DMSA-CeONPs significantly stimulate the glycolytic flux in cultured astrocytes when incubated for 24 h or longer. Similarly, ionic cerium also causes an acceleration of the glucose metabolism in cultured astrocytes. This study provides the first evidence of such metabolic dysregulation in glial cells.

- The extracellular cerium-induced lactate increase is similar to the one observed when hypoxia-inducible factor 1-alpha (Hif-1α) is chemically stabilized. DMSA-CeONPs are hypothesized to leak cerium ions, which then may react with available oxygen, causing hypoxic conditions in cultured astrocytes.

- DMSA-CeONPs function as extracellular scavengers of H_2O_2 and superoxide. Their scavenging of H_2O_2 is comparable to that of other CeONPs, although still negligible when compared to the endogenous detoxifying system of healthy cultured astrocytes. On the other hand, their superoxide scavenging capabilities are more prominent as tested in a non-acute situation of oxidative stress.

- DMSA-CeONPs react stoichiometrically rather than catalytically with H_2O_2 or superoxide. Ionic cerium is more effective than DMSA-CeONPs in removing H_2O_2 and superoxide from the extracellular space. Its reaction is also dependent on concentration and time.

- After internalization of DMSA-CeONPs by glial cells, no improved ROS scavenging potential was detectable. Thus, acute oxidative stress caused by the exogenous addition of H_2O_2 or mild oxidative stress caused by the endogenous production of superoxide is not ameliorated by pre-incubation with DMSA-CeONPs.

- The ß-lapachone mediated extracellular reduction of the water-soluble tetrazolium salt 1 (WST1) is a reliable method for testing the scavenging of cell-derived superoxide by CeONPs in glial cells. This approach permits the degree of oxidative stress induced in the cells to be determined by modifying the concentration of ß-lapachone. Consequently, the therapeutic potential of CeONPs can be explored.

5 Future Perspectives

DMSA-CeONPs have been demonstrated in this thesis to be a valuable tool for investigating the uptake, accumulation and impact on glial cells in this thesis. However, in order to make further progress in the investigation of their therapeutic potential, several aspects need to be reevaluated and examined in greater depth. The next logical step in this project, is to fine-tune the physico-chemical properties of DMSA-CeONPs. This should be followed by further characterization of the scavenging capacities and completion of the study of the effects on the metabolism and homeostasis of healthy cultured astrocytes. Therefore, the first step will be to enhance the scavenging capacity of reactive oxygen species (ROS), as it was currently limited to the extracellular space and was stoichiometric rather than catalytical. To overcome this limitation, one potential solution is to substantially decrease their nominal size. Previous experimental reports with CeONPs (see references in Table 3.2) and quantum confinement studies (Skorodumova et al., 2002) suggest that NPs of ~5 nm contain an optimal amount of Ce^{3+} atoms and oxygen vacancies on the surface, which allows them to react effectively with the available ROS. Moreover, at this size, the flip-flop between Ce^{3+} and Ce^{4+} also occurs more rapidly and therefore, the nanozyme activity is thought to be substantial. This strategy requires tailoring the coating and labeling procedure, along with the associated physicochemical characterization to obtain ultra-small stable DMSA-CeONPs in dispersion.

The determination of the ratio Ce^{3+}/Ce^{4+} could complete the physico-chemical characterization and aid in predicting the catalytic behavior of NPs in subsequent experiments. Different analytical techniques are available to gain insight into the Ce^{3+}/Ce^{4+} ratios of CeONPs, including x-ray photoelectron spectroscopy (Zhang et al., 2004; Thill et al., 2020), electron energy loss spectroscopy (Baalousha et al., 2012; Jayakumar et al., 2019), x-ray absorption spectroscopy (Cafun et al., 2013; Plakhova et al., 2019; Ghosalya et al., 2021), Raman spectroscopy (Goharshadi et al., 2011; Jayakumar et al., 2019), ultraviolet/visible/infrared spectroscopy (Thill et al., 2020) or scanning transmission x-ray microscopy coupled with super resolution fluorescence structured illumination microscopy (Szymanski et al., 2015). While these techniques demonstrate high reproducibility and sensitivity, they also present certain limitations. The major concern is the lack of materials that can serve as technique-independent standards. It has been also argued that techniques operating in vacuum and/or dry environments may introduce alteration the oxidation state of the cerium, resulting in a biased determination (Ghosalya et al., 2021). An investigation

of the redox state of DMSA-CeONPs can be performed via an experimental confirmation analysis that records oscillations in the luminescence band intensity during interactions with H_2O_2, which have been observed to correspond with the flip-flop between Ce^{3+} and Ce^{4+} (Seminko et al., 2021).

The possible leakage of cerium ions from the DMSA-CeONPs must also be considered in order to differentiate the effects of the NPs from those caused by ionic cerium. This phenomenon has been reported in relation to other metal NPs (Sengul and Asmatulu, 2020). To precisely distinguish the presence of various cerium species in the sample, the use of single particle-inductively coupled mass spectrometry (sp-ICP-MS) has been proved to be useful (Bolea et al., 2021). Huang et al. (2022) recently reported a comprehensive ICP-MS-based analytical method for fractionating and characterizing ionic and nanoparticulate cerium species in the tissues of animals exposed to CeONPs. This procedure consists of determination of the total cerium by ICP-MS, followed by an ultrafiltration and quantification of the fraction containing ionic cerium also by ICP-MS and a final determination of CeONPs by sp-ICP-MS. The costs of these analyses are high, especially considering the large number of replicates required for *in vitro* studies and their limited availability. A recent study by Joshi et al. (2019) used a copper chelator to investigate ion leakage from DMSA-CuONPs. However, in the biomedical field, research into cerium chelation remains unexplored. It is noteworthy that the chelation of f-elements (i.e. lanthanides and actinides) is uniquely challenging due to their electronic configuration, which makes covalent bonding stabilization difficult (Abergel and Kozimor, 2020). In addition, to chemically bind cerium in cells, the chelator must be biocompatible and able to cross the cell membrane. Therefore, as an initial proof of concept, it may be most feasible to coat NPs with another coating material to prevent or delay ion leakage. However, such a modification will also require the characterization of resulting NPs and testing their scavenging capabilities, as the coating can significantly alter these properties.

Further insight into the uptake and fate of DMSA-CeONPs in cells may be useful for future applications. The disquisition between the NPs adhered to the cell membrane compared to the internalized could be addressed by isolating the plasma membrane (Henn and Hamberger, 1976; Mersel et al., 1984; Suski et al., 2014) at different relevant time points during the incubation. Furthermore, the interaction between DMSA-CeONPs and the cell surface could be investigated by atomic force microscopy. As reported by Willmann (2018), the Hybrid Material Interface Group (University of Bremen) has in the past developed a protocol for studying the interaction between the free thiol-groups in OG-DMSA-IONPs and

a maleimide-polyethylenglycol-N-hydroxysuccinimid linker (Klebert, 2017). This protocol could be extended to DMSA-CeONPs to examine their endocytosis by glial cells in greater depth. Based on the knowledge gained from this research, it may be possible to optimize the kinetics of DMSA-CeONPs adsorption and uptake. Utilizing chemical inhibitors of clathrin-mediated endocytosis, micropinocytosis and caveolae-mediated endocytosis combined with flow cytometry could help to understand the cellular mechanism of uptake of DMSA-CeONPs (Singh et al., 2010; Vassie et al., 2017).

The trafficking and fate of DMSA-CeONPs once internalized in cells appears to be the bottleneck of their applicability, as during this process their ROS scavenging capacity turns to be undetectable. According to current literature, cargo undergoes gradual transportation into increasingly acidic environments during endocytosis (Canton and Battaglia, 2012). The redox potential of CeONPs and their dissolution have also been reported to be pH dependent. The use of a pH-dependent fluorescent dye in the coating of the NPs may provide vital information regarding the pH levels at which DMSA-CeONPs may be stored at different times since their application (Zhu et al., 2019; Sabljo et al., 2022). By using such dyes, it is possible to determine whether the coating and the NPs have degraded and/or separated, and to gain insight into the time scale over which these phenomena occur (Szapoczka et al., 2023). Furthermore, chemical lysosomal studies can be employed to supplement the analysis of intracellular storage of DMSA-CeONPS inside cells (Lu et al., 2017). Fluorescent dyes, including lysotracker, or inhibitors like bafilomycin A1, can also provide information on the accumulation of DMSA-CeONPs in lysosomes. A cost-effective approach to test the fate of DMSA-CeONPs inside the cells is the co-incubation and microscopic examination of OG-DMSA-CeONPs alongside chemical inhibitors of actin filaments and microtubules, including cytochalasin D (Spector et al., 1999; Willmann and Dringen, 2018) or colchicine (Weisenberg et al., 1968; Willmann and Dringen, 2018; Sargsyan et al., 2023). This information could help elucidate the role of the cytoskeleton in the cellular trafficking of OG-DMSA-CeONPs. For increased precision and spatial resolution, a more potent method, such as laser scanning microscopy combined with fluorescence lifetime imaging microscopy (Pujals et al., 2019; Datta et al., 2020), could be employed to precisely locate DMSA-CeONPs within glial cells. Additionally, regarding C6 glioma cells, capturing continuous time-lapse images of DMSA-CeONPs could support the comprehension and observation of NP distribution during cells division. These findings could progress the exploration of CeONPs as potential cancer fighting agents. Lastly, the plausible exocytosis of DMSA-CeONPs (Strobel et al., 2015) requires more investigation, as it could impact their applicability as antioxidants.

As previously stated, enhancing the ROS scavenging potential should be a priority for DMSA-CeONPs. To achieve this goal, decreasing their size has been advised as a primary step. Then, additional tests could be implemented to explore their potential in therapeutics. For example, determining the optimal pre-incubation time of cultured astrocytes with DMSA-CeONPs before the exogenous oxidative challenge takes place could offer valuable insights. Furthermore, the study of the effect of DMSA-CeONPs on cultured astrocytes, which exhibit changes in glutathione homeostasis under oxidative stress (Hirrlinger et al., 2001; Dringen et al., 2015) may yield information on their antioxidant properties. To fully elucidate the antioxidant capabilities of DMSA-CeONPs, testing their ability to scavenge superoxide and evaluating alterations in the expression of NQO1 or Nrf2 in cultured astrocytes after incubation with DMSA-CeONPs would be necessary. To expand the characterization of the scavenging potential of DMSA-CeONPs, further assessment on their ability to neutralize other compounds causing oxidative stress is needed. For example, it has also been reported the capacity of CeONPs to scavenge reactive nitrogen species (Dowding et al., 2012). Addition of lipopolysaccharide to cultured astrocytes have been seen to cause an upregulation in extracellular NO (Iwase et al., 2000; Kozuka et al., 2005). It could be determined whether incubation with DMSA-CeONPs reduces its production in cultured astrocytes under these conditions.

Nevertheless, the present thesis also highlights the significance of investigating any potential adverse effect, derived from the exposure to cerium beyond cell viability. Thus, exploring the accelerated flux of the glycolytic pathway outlined in this work becomes an important focus. To reinforce the initial finding that cerium ions leaking from DMSA-CeONPs stabilize hypoxia inducible factor 1 α (Hif-1α), additional testing is required.

References

Abergel, R. J. and S. A. Kozimor (2020). "Innovative f-element chelating strategies." Inorganic Chemistry 59(1): 4-7.

Baalousha, M., Y. Ju-Nam, P. A. Cole, B. Gaiser, T. F. Fernandes, J. A. Hriljac, M. A. Jepson, V. Stone, C. R. Tyler and J. R. Lead (2012). "Characterization of cerium oxide nanoparticles - Part 1: Size measurements." Environmental Toxicology and Chemistry 31(5): 983-993.

Bolea, E., M. S. Jimenez, J. Perez-Arantegui, J. C. Vidal, M. Bakir, K. Ben-Jeddou, A. C. Gimenez-Ingalaturre, D. Ojeda, C. Trujillo and F. Laborda (2021). "Analytical applications of single particle inductively coupled plasma mass spectrometry: A comprehensive and critical review." Analytical Methods 13(25): 2742-2795.

Cafun, J.-D., K. O. Kvashnina, E. Casals, V. F. Puntes and P. Glatzel (2013). "Absence of Ce^{3+} sites in chemically active colloidal ceria nanoparticles." ACS Nano 7(12): 10726-10732.

Canton, I. and G. Battaglia (2012). "Endocytosis at the nanoscale." Chemical Society Reviews 41(7): 2718-2739.

Datta, R., T. M. Heaster, J. T. Sharick, A. A. Gillette and M. C. Skala (2020). "Fluorescence lifetime imaging microscopy: fundamentals and advances in instrumentation, analysis, and applications." Journal of Biomedical Optics 25(7): 071203-071203.

Dowding, J. M., T. Dosani, A. Kumar, S. Seal and W. T. Self (2012). "Cerium oxide nanoparticles scavenge nitric oxide radical (˙NO)." Chemical Communications 48(40): 4896-4898.

Dringen, R., M. Brandmann, M. C. Hohnholt and E.-M. Blumrich (2015). "Glutathione-dependent detoxification processes in astrocytes." Neurochemical Research 40(12): 2570-2582.

Ghosalya, M. K., X. Li, A. Beck, J. A. van Bokhoven and L. Artiglia (2021). "Size of ceria particles influences surface hydroxylation and hydroxyl stability." The Journal of Physical Chemistry C 125(17): 9303-9309.

Goharshadi, E. K., S. Samiee and P. Nancarrow (2011). "Fabrication of cerium oxide nanoparticles: Characterization and optical properties." Journal of Colloid and Interface Science 356(2): 473-480.

Henn, F. A. and A. Hamberger (1976). "Preparation of glial plasma membrane from a cell fraction enriched in astrocytes." Neurochemical Research 1: 261-273.

Hirrlinger, J., J. König, D. Keppler, J. Lindenau, J. B. Schulz and R. Dringen (2001). "The multidrug resistance protein MRP1 mediates the release of glutathione disulfide from rat astrocytes during oxidative stress." Journal of Neurochemistry 76(2): 627-636.

Huang, Y., J. T.-S. Lum and K. S.-Y. Leung (2022). "An integrated ICP-MS-based analytical approach to fractionate and characterize ionic and nanoparticulate Ce species." Analytical and Bioanalytical Chemistry 414(11): 3397-3410.

Iwase, K., K. Miyanaka, A. Shimizu, A. Nagasaki, T. Gotoh, M. Mori and M. Takiguchi (2000). "Induction of endothelial nitric-oxide synthase in rat brain astrocytes by systemic lipopolysaccharide treatment." Journal of Biological Chemistry 275(16): 11929-11933.

Jayakumar, G., A. Albert Irudayaraj and A. Dhayal Raj (2019). "A comprehensive investigation on the properties of nanostructured cerium oxide." Optical and Quantum Electronics 51(9): 312.

Joshi, A., K. Thiel, K. Jog and R. Dringen (2019). "Uptake of intact copper oxide nanoparticles causes acute toxicity in cultured glial cells." Neurochemical Research 44(9): 2156-2169.

Klebert, E. (2017). Untersuchung der zelluläeren Wechselwirkung von mit Dimercaptosuccinat ummnantelten Eiseoxid-Nanopartikeln mithilfe von Kraftspektroscopie. University of Bremen, University of Bremen. Master.

Kozuka, N., R. Itofusa, Y. Kudo and M. Morita (2005). "Lipopolysaccharide and proinflammatory cytokines require different astrocyte states to induce nitric oxide production." Journal of Neuroscience Research 82(5): 717-728.

Lu, S., T. Sung, N. Lin, R. T. Abraham and B. A. Jessen (2017). "Lysosomal adaptation: How cells respond to lysosomotropic compounds." PloS One 12(3): e0173771.

Mersel, M., A. Malviya, C. Hindelang and P. Mandel (1984). "Plasma membrane isolated from astrocytes in primary cultures. Its acceptor oxidoreductase properties." Biochimica et Biophysica Acta (BBA)-Biomembranes 778(1): 144-154.

Plakhova, T. V., A. Y. Romanchuk, S. M. Butorin, A. D. Konyukhova, A. V. Egorov, A. A. Shiryaev, A. E. Baranchikov, P. V. Dorovatovskii, T. Huthwelker and E. Gerber (2019). "Towards the surface hydroxyl species in CeO$_2$ nanoparticles." Nanoscale 11(39): 18142-18149.

Pujals, S., N. Feiner-Gracia, P. Delcanale, I. Voets and L. Albertazzi (2019). "Super-resolution microscopy as a powerful tool to study complex synthetic materials." Nature Reviews Chemistry 3(2): 68-84.

Sabljo, K., J. Napp, F. Alves and C. Feldmann (2022). "pH-Dependent fluorescence of [La (OH) 2]+[ARS]− hybrid nanoparticles for intracellular pH-sensing." Chemical Communications 58(67): 9417-9420.

Sargsyan, A., H. Sahakyan and K. Nazaryan (2023). "Effect of colchicine binding site inhibitors on the tubulin intersubunit interaction." ACS Omega 8(32): 29448-29454.

Seminko, V., P. Maksimchuk, G. Grygorova, E. Okrushko, O. Avrunin, V. Semenets and Y. Malyukin (2021). "Mechanism and dynamics of fast redox cycling in cerium oxide nanoparticles at high oxidant concentration." The Journal of Physical Chemistry C 125(8): 4743-4749.

Sengul, A. B. and E. Asmatulu (2020). "Toxicity of metal and metal oxide nanoparticles: a review." Environmental Chemistry Letters 18: 1659-1683.

Singh, S., A. Kumar, A. Karakoti, S. Seal and W. T. Self (2010). "Unveiling the mechanism of uptake and sub-cellular distribution of cerium oxide nanoparticles." Molecular Biosystems 6(10): 1813-1820.

Skorodumova, N., S. Simak, B. I. Lundqvist, I. Abrikosov and B. Johansson (2002). "Quantum origin of the oxygen storage capability of ceria." Physical Review Letters 89(16): 166601.

Spector, I., F. Braet, N. R. Shochet and M. R. Bubb (1999). "New anti-actin drugs in the study of the organization and function of the actin cytoskeleton." Microscopy Research and Technique 47(1): 18-37.

Strobel, C., H. Oehring, R. Herrmann, M. Förster, A. Reller and I. Hilger (2015). "Fate of cerium dioxide nanoparticles in endothelial cells: exocytosis." Journal of Nanoparticle Research 17: 1-14.

Suski, J. M., M. Lebiedzinska, A. Wojtala, J. Duszynski, C. Giorgi, P. Pinton and M. R. Wieckowski (2014). "Isolation of plasma membrane–associated membranes from rat liver." Nature Protocols 9(2): 312-322.

Szapoczka, W. K., A. L. Truskewycz, T. Skodvin, B. Holst and P. J. Thomas (2023). "Fluorescence intensity and fluorescence lifetime measurements of various carbon dots as a function of pH." Scientific Reports 13(1): 10660.

Szymanski, C. J., P. Munusamy, C. Mihai, Y. Xie, D. Hu, M. K. Gilles, T. Tyliszczak, S. Thevuthasan, D. R. Baer and G. Orr (2015). "Shifts in oxidation states of cerium oxide nanoparticles detected inside intact hydrated cells and organelles." Biomaterials 62: 147-154.

Thill, A. S., F. O. Lobato, M. O. Vaz, W. P. Fernandes, V. E. Carvalho, E. A. Soares, F. Poletto, S. R. Teixeira and F. Bernardi (2020). "Shifting the band gap from UV to visible region in cerium oxide nanoparticles." Applied Surface Science 528: 146860.

Vassie, J. A., J. M. Whitelock and M. S. Lord (2017). "Endocytosis of cerium oxide nanoparticles and modulation of reactive oxygen species in human ovarian and colon cancer cells." Acta Biomaterialia 50: 127-141.

Weisenberg, R. C., G. G. Broisy and E. W. Taylor (1968). "Colchicine-binding protein of mammalian brain and its relation to microtubules." Biochemistry 7(12): 4466-4479.

Willmann, W. (2018). Synthesis and characterization of fluorescent iron oxide nanoparticles to study uptake and intracellular trafficking of nanoparticles in neural cells, Universität Bremen.

Willmann, W. and R. Dringen (2018). "Monitoring of the cytoskeleton-dependent intracellular trafficking of fluorescent iron oxide nanoparticles by nanoparticle pulse-chase experiments in C6 glioma cells." Neurochemical Research 43: 2055-2071.

Zhang, F., P. Wang, J. Koberstein, S. Khalid and S.-W. Chan (2004). "Cerium oxidation state in ceria nanoparticles studied with X-ray photoelectron spectroscopy and absorption near edge spectroscopy." Surface Science 563(1-3): 74-82.

Zhu, J.-L., Z. Xu, Y. Yang and L. Xu (2019). "Small-molecule fluorescent probes for specific detection and imaging of chemical species inside lysosomes." Chemical Communications 55(47): 6629-6671.